

DESICCATION CRACKING

OF

SOILS

A Thesis

Submitted to the Faculty of Graduate Studies

in Partial Fulfilment of the Requirements

for the Degree of

Master of Science

in the Department of Civil Engineering

University of Saskatchewan, Saskatoon, Canada

by

Jacky Tak Kwai Lau

Saskatoon, Saskatchewan

CANADA

April, 1987

The University of Saskatchewan claims copyright in conjunction with the author. Use shall not be made of the material contained herein without proper acknowledgement.

The author has agreed that the Library, University of Saskatchewan, may make this thesis freely available for inspection. Moreover, the author has agreed that permission for extensive copying of this thesis for scholarly purposes may be granted by the professor who supervised the thesis work recorded herein, or in his absence, by the Head of the Department or the Dean of the College in which the thesis work was done. It is understood that due recognition will be given to the author of this thesis and to the University of Saskatchewan in any use of the material in this thesis. Copying or publication or any other use of the thesis for financial gain without approval by the University of Saskatchewan and the author's written permission is prohibited.

Requests for permission to copy or to make any other use of material in this thesis in whole or in part should be addressed to:

Head of Department of Civil Engineering,
University of Saskatchewan,
Saskatoon, Saskatchewan,
CANADA.

UNIVERSITY OF SASKATCHEWAN
College of Graduate Studies and Research
Saskatoon

CERTIFICATION OF THESIS WORK

We, the undersigned, certify that _____

LAU, JACKY (TAK KWAI)
(full name)

B.Sc.
(degrees)

candidate for the degree of M.Sc. at the University of Saskatchewan, has presented
his thesis report with the following title _____

DESICCATION CRACKING OF SOILS

(as it appears on title page)

and that the thesis is acceptable in form and content, and that a satisfactory
knowledge of the field covered by the thesis was demonstrated by the candidate
through an oral examination held on April 8, 1987

External Examiner _____

Prof. E. de Jong 

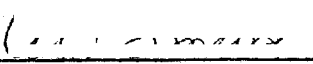
Internal Examiners _____

Prof. S.L. Barbour _____

Prof. D.E. Pufahl _____

Prof. D.G. Fredlund  _____

Chairman _____

Prof. C.D. Smith 

ABSTRACT

The depth of cracking of soils is often required for boundary value and limit equilibrium analyses in geotechnical engineering. At present, the depth of cracking is customarily expressed as a function of shear strength using the Rankine theory of lateral earth pressure. The objectives of this thesis are to study the mechanism of desiccation cracking in soils and to propose a mathematical model for the prediction of crack depth.

Observations obtained from the laboratory program indicated that the locations of desiccation cracks and the crack spacing were highly dependent upon the inhomogeneities in the soils. Based on the experimental results, desiccation cracks were initiated at a matric suction of less than 10 kPa for silty and clayey soils. Silty soils are expected to require a higher matric suction at cracking than do clayey soils. The volumetric shrinkage strain at cracking for Indian Head Till was about 7%. Regina Clay is expected to require a lower volumetric shrinkage strain at cracking than does Indian Head Till.

Two mathematical expressions were derived using the volume change (i.e., elastic equilibrium analysis) and shear strength (i.e., plastic equilibrium analysis) behavior of unsaturated soils for the prediction of crack depth. Based

on the result of a parametric study, it was found that the crack depth predicted by the plastic analysis was almost twice as deep as that predicted by the elastic analysis. Since desiccation cracks are formed as a result of soil volume reduction, the elastic analysis is expected to be more appropriate for the prediction of crack depth, although the validity of the analysis must be confirmed with future studies on the desiccation crack depth in the field.

ACKNOWLEDGEMENTS

The author would like to express his sincere appreciation to Professor D. G. Fredlund, under whose supervision this work was done. His patience, guidance, suggestions and freely available time were invaluable.

Financial support for this study, which was provided in form of a scholarship by the College of Graduate Studies, is gratefully acknowledged.

Special gratitude is extended to Professor E. K. Sauer for his helpful discussions and for supplying the photographs on desiccation cracks in Saskatchewan. To the faculty, staff and fellow graduate students, the author would like to express his thankfulness for their assistance and encouragement. The generous assistance of Mr. Alex Kozlow and Mr. H. Rahardjo are greatly appreciated.

My deepest gratitude is given to my wife, not only for her support, patience, understanding and encouragement, but also for her services as a typist and a proofreader.

Most of all, I would like to thank my Lord Jesus Christ for He has given me health, strength and wisdom throughout the study. To Him be the glory forever and ever.

TABLE OF CONTENTS

	Page
ABSTRACT	i
ACKNOWLEDGEMENTS	iii
TABLE OF CONTENTS	iv
LIST OF SYMBOLS	vii
LIST OF TABLES	ix
LIST OF FIGURES	x
 CHAPTER 1. INTRODUCTION	
1.1 General.....	1
1.2 Significance of Crack Depth in Engineering Problems.....	2
1.3 The Needs.....	8
1.4 The Scope of This Dissertation.....	9
 CHAPTER 2. LITERATURE REVIEW	
2.1 Introduction.....	12
2.2 Shrinkage of Soils.....	12
2.2.1 Other Soil Shrinkage and Cracking Phenomena.....	16
2.3 Desiccation Cracking of Soils	18
2.3.1 Aerial Pattern.....	26
2.3.2 Crack Spacing and Crack Depth.....	28
2.4 Fracture Mechanics and Desiccation Cracking of Soils...	34
2.5 Factors Affecting the Shrinkage and Cracking of Soils.....	38
2.5.1 Observations from Soil-Cement Pavement Studies.....	43
2.5.2 Significance of Soil Suction in Desiccation of Soil.....	45
2.5.2.1 Effect of Evaporation and Vegetation on Soil Suction.....	46
2.5.2.2 Effect of Soil Cracking on Soil Suction.....	47
2.5.3 Tensile Strength of Soils.....	48
2.5.4 Failure Criterion of Soils Under Tension.....	52
2.6 Summary.....	57

TABLE OF CONTENTS (continued)

	Page
CHAPTER 3. THEORY OF CRACKING IN SOILS	
3.1 Introduction.....	61
3.2 Stress State Variables for Unsaturated Soil Mechanics.....	62
3.3 Matric Suction Profiles.....	62
3.4 Elastic Equilibrium Analysis.....	69
3.5 Plastic Equilibrium Analysis.....	74
CHAPTER 4. ANALYTICAL AND EXPERIMENTAL PROGRAM	
4.1 Introduction.....	82
4.2 Analytical Program.....	82
4.3 Experimental Program.....	83
4.3.1 Soils.....	84
4.3.2 Container.....	88
4.3.3 Tensiometer.....	92
4.3.4 Temperature and Humidity.....	94
4.3.5 Experimental Procedures.....	94
CHAPTER 5. RELATIONSHIP BETWEEN ELASTIC MODULI E AND H	
5.1 Introduction.....	102
5.2 Empirical Relationship between E and H moduli.....	102
5.3 Experimental Data on E/H ratio.....	111
CHAPTER 6. PRESENTATION OF RESULTS	
6.1 Introduction.....	119
6.2 Prediction of Crack Depth.....	119
6.2.1 Elastic Equilibrium Analysis.....	120
6.2.2 Plastic Equilibrium Analysis.....	127
6.3 Experimental Results.....	137
6.3.1 Shrinkage Tests.....	137
6.3.2 Cracking Tests.....	144

TABLE OF CONTENTS (continued)

	Page
CHAPTER 7. DISCUSSION OF RESULTS	
7.1 Introduction.....	165
7.2 Characteristics of Cracking of Soil.....	165
7.2.1 Crack Spacing.....	168
7.2.2 Soil Suction.....	170
7.2.3 Shrinkage Strain.....	172
7.3 Prediction of Crack Depth.....	175
7.3.1 Matric Suction Profiles.....	176
7.3.2 Elastic Equilibrium Analysis.....	177
7.3.3 Plastic Equilibrium Analysis.....	180
7.3.4 Comparison of Elastic and Plastic Equilibrium Analyses.....	188
CHAPTER 8. CONCLUSIONS AND RECOMMENDATIONS	
8.1 Conclusions.....	193
8.2 Recommendations for Future Research.....	197
REFERENCES.....	199
APPENDICES.....	209
A. Soil Properties of Indian Head Till and Regina Clay.	
B. Operation Instructions for Flexible Tube Tensiometer.	
C. Tabulated Values on the Predicted Crack Depth Obtained From Elastic Equilibrium and Plastic Equilibrium Analyses.	
D. Experimental Results on Shrinkage Tests and Cracking Tests.	

LIST OF SYMBOLS

B_m	- bulk modulus.
c	- cohesion.
c'	- effective cohesive intercept.
C_t	- compressive index with respect to a change of total stress.
C_m	- compressive index with respect to a change of matric suction.
dc	- predicted crack depth.
δV	- a change in volume.
$\Delta\theta_w$	- change in the amount of water by volume in a given soil element.
D	- constrained modulus.
D_w	- depth between ground surface and the water table.
e_o	- initial void ratio.
e_f	- final void ratio.
E	- elastic modulus with respect to total stress.
ϵ_{vol}	- volumetric strain.
$\epsilon_x, \epsilon_y, \epsilon_z$	- strains in the x, y, and z directions.
ϵ_h	- strain in the horizontal direction.
ϵ_v	- strain in the vertical direction.
F_w	- a factor to describe the matric suction profile.
F_t	- ratio of tensile strength to unconfined compressive strength.
ϕ'	- effective friction angle.
ϕ^b	- friction angle with respect to matric suction.
G	- elastic energy release rate per crack tip.
γ	- unit weight of soils, which is the product of the density of soil and the gravitational acceleration.
γ_w	- unit weight of water, which is the product of the density of water and the gravitational acceleration.
H	- elastic modulus with respect to matric suction.
H_1	- water phase modulus with respect to total stress.
K	- stress intensity factor.
μ	- Poisson's ratio.
Q_u	- unconfined compressive strength.
R	- crack resistance.
R_1	- water phase modulus with respect to matric suction.
σ	- total stress.
σ_1'	- major principal stress.
σ_3'	- minor principal stress.
σ_n'	- effective normal stress.
$\sigma_x, \sigma_y, \sigma_z$	- stresses in the x, y, and z directions.
σ_h	- horizontal stress.
σ_v	- vertical stress.
σ_t	- tensile strength.
pF	- the logarithm to the base 10 of the suction head of water in cm.

LIST OF SYMBOLS (continued)

τ	- shear strength.
τ_f	- shear strength at failure condition.
u_a	- pore air pressure.
u_w	- pore water pressure.
$(\sigma - u_a)$	- stress state variable for total stress.
$(\sigma - u_a)_a$	- average of initial and final total stresses.
$(u_a - u_w)$	- stress state variable for matric suction.
$(u_a - u_w)_a$	- average of initial and final matric suction.
U	- elastic energy release.
V	- original volume.
W	- energy for crack growth.
w	- water content in percentage.
z_c	- depth of tension crack.

LIST OF TABLES

	Page
Table 2.01: Average crack spacing and frequency of occurrence, for some vertisols in Sudan (after Zein El Abedine and Robinson, 1971).....	31
Table 2.02: Frequencies of occurrence percent, and average depths of cracks in Sudan (after Zein El Abedine and Robinson, 1971).....	31
Table 2.03: Crack widths and crack depths in selected clay soil sites in Saskatchewan (after Dasog, 1986).....	32
Table 4.01: Summary of the properties of the soils used in the experimental program.....	87
Table 4.02: Detailed conditions of the shrinkage tests and cracking tests.....	95
Table 5.01: Determination of the elastic modulus E, for the slurried Regina Clay from one-dimensional consolidation test results (data obtained from Fredlund, 1964).....	114
Table 5.02: Determination of the elastic modulus H, for the slurried Regina Clay from suction test results (data obtained from Fredlund, 1964).....	114
Table 6.01: Relationship between X and Y terms and ϕ' angles.....	128
Table 6.02: Minimum X and maximum Y terms and their corresponding ϕ' angles.....	129
Table 6.03: The increase in crack depth due to cohesion intercept c'	136
Table 6.04: A summary of the shrinkage test results during various conditions.....	143
Table 6.05: A summary of the cracking test results.....	145
Table 7.01: A summary of volumetric shrinkage strains for the cracking tests.....	173
Table 7.02: Range of Poisson's ratio for different soils (after Winterkorn and Fang, 1975).....	179
Table 7.03: Some experimental values for ϕ^b (by assuming a constant ϕ^b value with matric suction, Fredlund, 1985).....	187

LIST OF FIGURES

	Page
Fig. 1.01: The length of slip surface is shortened due to the presence of tension cracks.....	3
Fig. 1.02: Critical height of unsupported vertical slope with tension cracks versus depth of water table (after Pufahl et al, 1983).....	4
Fig. 1.03: Installation of a vertical moisture barrier along the edge of a highway pavement (after Picornell, 1985).....	7
Fig. 2.01: Shrinkage curve for typical clay soils.....	14
Fig. 2.02: Shrinkage curve for soils with crumb structure (after Yong and Warkentin, 1966).....	14
Fig. 2.03: Hexagonal mud crack pattern on a playa surface composed of very uniform sediments, Nevada. (after Longwell, 1928, notes: the hammer and handle measured 330 mm (13.0 in.)).....	19
Fig. 2.04: Playa cracks with large polygons of irregular shape in Nevada. The edges are noticeably rounded probably due to slaking and to wind action (after Longwell, 1928).....	20
Fig. 2.05: Giant desiccation cracks on the Black Rock and Smoke Creek Deserts, Nevada. (Note that the fissures are about 61.0 m to 73.1 m (200 ft. to 240 ft.) apart, the highway and the car tracks are visible in the photo) (after Willden and Mabey, 1961).....	20
Fig. 2.06: Orthogonal cracks pattern in till after rain, Univ. of Saskatchewan campus, Saskatoon, Saskatchewan.....	21
Fig. 2.07: Crack pattern in till deposits, located in a highway ditch, near Davidson, Saskatchewan.....	22
Fig. 2.08: Desiccation fractures in varved sequence of clays and silts. Open fractures are confined to fine-grained clay rich layers, in Drumheller areas, Alberta (Note: compass as shown is 75 mm long, after Babcock, 1977).....	23
Fig. 2.09: Desiccation cracking in a dried-out hydraulic fill site in Los Angeles (after Mitchell, 1986).....	24

LIST OF FIGURES (continued)

	Page
Fig. 2.10: A close-up view of the desiccation crack at the hydraulic fill site in Los Angeles (after Mitchell, 1986)	24
Fig. 2.11: Orthogonal crack patterns on frozen ground in permafrost (after Lachenbruch, 1962)	25
Fig. 2.12: Hexagonal cracks patterns on cooling joints in andesite, Mt. Rainer National Park, Washington (after Lachenbruch, 1962)	25
Fig. 2.13: Crack in a finite plate	35
Fig. 2.14: The three modes of cracking	35
Fig. 2.15: Idealized section through soil (after Means and Parcher, 1963)	42
Fig. 2.16: Water pressure and stresses in subsoil under a building on an expansive clay subsoils (after Jennings, 1961)	42
Fig. 2.17: Relationship between tensile strength and plasticity index (after Fang and Chen, 1972)	51
Fig. 2.18: Relationship between unconfined compressive strength - tensile strength ratio to plasticity index (after Fang and Chen, 1972)	51
Fig. 2.19: Mohr-Coulomb failure criterion	53
Fig. 2.20: Failure envelopes accordings to different criteria (after Lee and Ingles, 1968)	53
Fig. 2.21: Modified Mohr-Coulomb criterion (after Fang and Chen, 1972)	56
Fig. 3.01: Stress distribution during desiccation of a soil (after Fredlund, 1981)	64
Fig. 3.02: Effect of various environmental conditions on the matric suction profile (after Peter, 1979)	65
Fig. 3.03: Idealized matric suction profile "A" (i.e., matric suction varies with depth)	66
Fig. 3.04: Idealized matric suction profile "B" (i.e., matric suction is constant with depth)	67

LIST OF FIGURES (continued)

	Page
Fig. 3.05: A typical desiccated soil.....	71
Fig. 3.06: Three dimensional failure surface using stress variable ($\sigma - u_a$) and ($u_a - u_w$) (after Fredlund, 1981).....	75
Fig. 3.07: A typical soil element at the tip of a desiccation crack.....	77
Fig. 3.08: Modified Mohr-Coulomb Failure Criterion (after Fang and Chen, 1971, 1972).....	78
Fig. 4.01: Grain size gradation curve for Indian Head Till.....	85
Fig. 4.02: Grain size gradation curve for Regina Clay.....	86
Fig. 4.03: Brass containers of 61.50 mm I.D. and 22.85 mm deep were used for the shrinkage test.....	89
Fig. 4.04: Dimensions of the wooden container used for the cracking test.....	90
Fig. 4.05: The layout of equipment for the cracking test.....	91
Fig. 4.06: Flexible tube tensiometer (after Soilmoisture Equipment Corp. Model No. 2100F).....	93
Fig. 4.07: The soils for the cracking test was hand-mixed to the desired water content.....	97
Fig. 4.08: After mixing, the soils was placed in the wooden container and was vibrated slightly to reduce occluded air bubbles.....	97
Fig. 4.09: Small amount of soil was sampled to determine the water content during the cracking test. After sampling, the cavity was filled with soils of suitable water content.....	98
Fig. 4.10: Various positions for the installation of the ceramic cup sensors in different cracking tests....	100
Fig. 5.01: Various types of loading conditions and moduli (after Lambe and Whitman, 1969).....	104
Fig. 5.02: Arithmetic representation of stress state variables versus void ratio (after Fredlund, 1979).....	107

LIST OF FIGURES (continued)

	Page
Fig. 5.03: Logarithm of stress state variables versus void ratio (after Fredlund, 1979).....	107
Fig. 5.04: Theoretical C_m/C_t ratio versus E/H ratio.....	110
Fig. 5.05: Logarithm of matric suction versus void ratio, suction tests on slurried Regina Clay, (data obtained from Fredlund, 1964).....	112
Fig. 5.06: Logarithm of effective stress versus void ratio, one-dimensional consolidation tests on Regina Clay, (data obtained from Fredlund, 1964).....	113
Fig. 5.07: Average initial and final stresses versus elastic modulus (data obtained from Fredlund, 1964).....	115
Fig. 5.08: Average initial and final stresses versus E/H ratio (data obtained from Fredlund, 1964).....	116
Fig. 5.09: Logarithm of stress state variables versus void ratio for silt compacted dry of optimum water content (after Ho, 1987).....	117
Fig. 6.01: E/H ratio versus crack depth to the depth to water table ratio (d_c/D_w), using elastic equilibrium analysis, suction profile "A" (i.e., matric suction varies linearly with depth) $F_w = 1.0$, $\gamma = 18.5 \text{ kN/m}^3$	122
Fig. 6.02: E/H ratio versus crack depth to the depth to water table ratio (d_c/D_w), using elastic equilibrium analysis, suction profile "A" (i.e., matric suction varies linearly with depth) $F_w = 1.5$, $\gamma = 18.5 \text{ kN/m}^3$	123
Fig. 6.03: E/H ratio versus crack depth to the depth to water table ratio (d_c/D_w), using elastic equilibrium analysis, suction profile "A" (i.e., matric suction varies linearly with depth) $F_w = 2.0$, $\gamma = 18.5 \text{ kN/m}^3$	124
Fig. 6.04: E/H ratio versus crack depth to the depth to water table ratio (d_c/D_w), using elastic equilibrium analysis, suction profile "B" (i.e., matric suction is constant with depth), $F_w = 1.0$, $\gamma = 18.5 \text{ kN/m}^3$	125

LIST OF FIGURES (continued)

Page

- Fig. 6.05: ϕ^b angles versus crack depth to the depth to water table ratio (dc/D_w), using plastic equilibrium analysis, suction profile "A" (i.e., matric suction varies linearly with depth) $F_w = 0.5$, $c' = 0$, $\gamma = 18.5 \text{ kN/m}^3$ (note: Q_u = unconfined compressive strength T_s = tensile strength).....131
- Fig. 6.06: ϕ^b angles versus crack depth to the depth to water table ratio (dc/D_w), using plastic equilibrium analysis, suction profile "A" (i.e., matric suction varies linearly with depth) $F_w = 1.0$, $c' = 0$, $\gamma = 18.5 \text{ kN/m}^3$. (note: Q_u = unconfined compressive strength T_s = tensile strength).....132
- Fig. 6.07: ϕ^b angles versus crack depth to the depth to water table ratio (dc/D_w), using plastic equilibrium analysis, suction profile "A" (i.e., matric suction varies linearly with depth) $F_w = 1.5$, $c' = 0$, $\gamma = 18.5 \text{ kN/m}^3$. (note: Q_u = unconfined compressive strength T_s = tensile strength).....133
- Fig. 6.08: ϕ^b angles versus crack depth to the depth to water table ratio (dc/D_w), using plastic equilibrium analysis, suction profile "A" (i.e., matric suction varies linearly with depth) $F_w = 2.0$, $c' = 0$, $\gamma = 18.5 \text{ kN/m}^3$. (note: Q_u = unconfined compressive strength T_s = tensile strength).....134
- Fig. 6.09: ϕ^b angles versus crack depth to the depth to water table ratio (dc/D_w), using plastic equilibrium analysis, suction profile "B" (i.e., matric suction is constant with depth), $F_w = 1.0$, $c' = 0$, $\gamma = 18.5 \text{ kN/m}^3$. (note: Q_u = unconfined compressive strength T_s = tensile strength).....135
- Fig. 6.10: Water content versus specific volume for Indian Head Till mixed at water contents of 31.0% and 37.7% and allowed to dry in a brass container (Test Nos. S01 and S02).....138
- Fig. 6.11: Water content versus specific volume for Regina Clay mixed at water content of 80.0% and allowed to dry in a brass container (Test No. S03).....139

LIST OF FIGURES (continued)

	Page
Fig. 6.12: Water content versus shrinkage strain for Indian Head Till mixed at water content of 37.7% and allowed to dry in a brass container (Test No. S01).....	140
Fig. 6.13: Water content versus shrinkage strain for Indian Head Till mixed at water content of 31.0% and allowed to dry in a brass container (Test No. S02).....	141
Fig. 6.14: Water content versus shrinkage strain for Regina Clay mixed at water content of 80.0% and allowed to dry in a brass container (Test No. S03).....	142
Fig. 6.15: Time versus vertical shrinkage strain for Indian Head Till mixed at initial water content of 37.7% and the soil sample was 58.8 mm thick (Test No. T01).....	146
Fig. 6.16: Time versus vertical shrinkage strain for Indian Head Till mixed at initial water content of 38.2% and the soil sample was 54.1 mm thick (Test No. T02).....	147
Fig. 6.17: Time versus vertical shrinkage strain for Indian Head Till mixed at initial water content of 31.1% and the soil sample was 60.4 mm thick (Test No. T03).....	148
Fig. 6.18: Time versus vertical shrinkage strain for Indian Head Till mixed at initial water content of 38.1% and the soil sample was 33.7 mm thick (Test No. T04).....	149
Fig. 6.19: Time versus vertical shrinkage strain for Regina Clay mixed at initial water content of 82.5% and the soil sample was 59.7 mm thick (Test No. T05).....	150
Fig. 6.20: Time versus vertical shrinkage strain for Indian Head Till mixed at initial water content of 37.5% and the soil sample was 60.8 mm thick (Test No. T06).....	151
Fig. 6.21: Cracking test T01 on till after 43.0 hours. The water content of the sample was about 33.0%. All ceramic cup sensors were installed horizontally from the container sidewalls, 150 mm into the soil.....	152

LIST OF FIGURES (continued)

	Page
Fig. 6.22: Cracking test T01 on till after 54.6 hours. The water content of the sample was about 29.0%.....	152
Fig. 6.23: Cracking test T01 on till after 78.2 hours. The water content of the sample was about 27.0%.....	153
Fig. 6.24: Cracking test T01 on till after 138.9 hours. The water content of the sample was about 23.4%.....	153
Fig. 6.25: Cracking test T02 on till after 38.5 hours. The water content of the sample was about 32.0%. All ceramic cup sensors were installed vertically from the bottom of the container, 35 mm into the soil.....	154
Fig. 6.26: Cracking test T02 on till after 54.5 hours. The water content of the sample was about 30.0%.....	154
Fig. 6.27: Cracking test T02 on till after 94.3 hours. The water content of the sample was about 25.8%.....	155
Fig. 6.28: Cracking test T02 on till after 216.0 hours. The water content of the sample was about 9.5%.....	155
Fig. 6.29: Cracking test T03 on till after 6.0 hours. The water content of the sample was about 28.5%. All ceramic cup sensors were installed vertically from the bottom of the container, 35 mm into the soil.....	156
Fig. 6.30: Cracking test T03 on till after 11.0 hours. The water content of the sample was about 28.0%.....	156
Fig. 6.31: Cracking test T03 on till after 40.5 hours. The water content of the sample was about 25.5%.....	157
Fig. 6.32: Cracking test T03 on till after 337.0 hours. The water content of the sample was about 3.3%.....	157
Fig. 6.33: Cracking test T04 on till after 27.5 hours. The water content of the sample was about 32.5%. All ceramic cup sensors were installed horizontally from the container sidewalls, 35 mm into the soil.....	158
Fig. 6.34: Cracking test T04 on till after 47.0 hours. The water content of the sample was about 28.5%.....	158

LIST OF FIGURES (continued)

	Page
Fig. 6.35: Cracking test T04 on till after 56.5 hours. The water content of the sample was about 26.6%.....	159
Fig. 6.36: Cracking test T04 on till after 192.0 hours. The water content of the sample was about 5.7%.....	159
Fig. 6.37: Cracking test T05 on clay after 56.5 hours. The water content of the sample was about 71.0%. All ceramic cup sensors were installed vertically from the bottom of the container, 35 mm into the soil. Container side walls were lined with wax paper and aluminum foils.....	160
Fig. 6.38: Cracking test T05 on clay after 92.0 hours. The water content of the sample was about 66.7%.....	160
Fig. 6.39: Cracking test T05 on clay after 143.0 hours. The water content of the sample was about 57.0%.....	161
Fig. 6.40: Cracking test T05 on clay after 358.0 hours. The water content of the sample was about 23.5%.....	161
Fig. 6.41: Cracking test T06 on till after 78.5 hours. The water content of the sample was about 27.5%. ceramic cup sensors were installed vertically from the bottom of the container, 35 mm into the soil. Container side walls were lined with wax paper and aluminum foils.....	162
Fig. 6.42: Cracking test T06 on till after 127.0 hours. The water content of the sample was about 25.0%.....	162
Fig. 6.43: Cracking test T06 on till after 151.0 hours. The water content of the sample was about 23.0%.....	163
Fig. 6.44: Cracking test T06 on till after 291.0 hours. The water content of the sample was about 7.2%.....	163
Fig. 6.45: Interfacial markings on the cracked soil surface (Test No. T04).....	164
Fig. 6.46: Interfacial markings on the cracked soil surface (Test No. T05).....	164

LIST OF FIGURES (continued)

	Page
Fig. 7.01: A typical orthogonal cracking pattern (after Test No. T06).....	167
Fig. 7.02: Crack pattern in 10mm thick slurried Indian Head Till after desiccation.....	169
Fig. 7.03: No crack was observed in 40mm thick slurried Indian Head Till after desiccation.....	169
Fig. 7.04: Plasticity Index versus ratio of unconfined compressive strength to tensile strength (after Fang and Chen, 1972).....	184
Fig. 7.05: Matric suction versus ϕ^b and shear stresses for compacted Indian Head Till (after Gan, 1986).....	185
Fig. 7.06: Matric suction versus ϕ^b and shear stresses for low density samples of Dhanauri Clay (after Gan, 1986).....	186
Fig. 7.07: The range of predicted crack depth for Indian Head Till, using elastic equilibrium analysis, suction profile "A" (i.e., matric suction varies linearly with depth) $F_w = 1.0$, $\gamma = 18.5 \text{ kN/m}^3$	189
Fig. 7.08: The range of predicted crack depth for Indian Head Till, using plastic equilibrium analysis, suction profile "A" (i.e., matric suction varies linearly with depth) $F_w = 1.0$, $\gamma = 18.5 \text{ kN/m}^3$	190

To Anne,

Sharon and Ryan.

CHAPTER 1

INTRODUCTION

1.1 GENERAL

Large portions of the land surface on earth have been subjected to the influence of desiccation. In nature, desiccation takes place whenever the surface of the soils is not permanently flooded. Most soil deposits when originally laid down are saturated. Lacustrine deposits, for example, are deposited at water contents above the liquid limit and are then consolidated by the weight of the overlying sediments. When the surface of a soil deposit is exposed to the air, desiccation proceeds slowly from the exposed soil surface in a downward direction.

In localities where the soils are continuously below the water table or where evaporation is slow, desiccation will remain near the ground surface. In semi-arid regions, the water table is drawn below the ground surface, particularly during dry periods. The soil loses water and shrinks during desiccation. Consequently, the upper portion of the soil profile becomes unsaturated and desiccation cracks are formed. These cracks extend some distance below the ground surface.

1.2 SIGNIFICANCE OF CRACK DEPTH IN ENGINEERING PROBLEMS

In geotechnical engineering, the depth of cracking is often required for boundary value and limit equilibrium analyses. As an example, cracking due to shrinkage affects the stability of embankments and earth dams. In slope stability computations, the presence of tension cracks affects the analysis in a number of ways (Spencer, 1968):

- a) by shortening the length of the slip surface (as shown in Fig. 1.01), thus reducing the resistance to failure,
- b) the water pressure acting on the crack face constitutes an additional driving force contributing to failure, and
- c) the water in the crack tends to soften the soil, degrading its strength properties.

When designing an open cut in cohesive soils, the presence of tension cracks must be considered. Pufahl et al (1983) showed that the presence of tension cracks substantially reduced the critical height of an unsupported vertical slope. The effect of the tension cracks on the

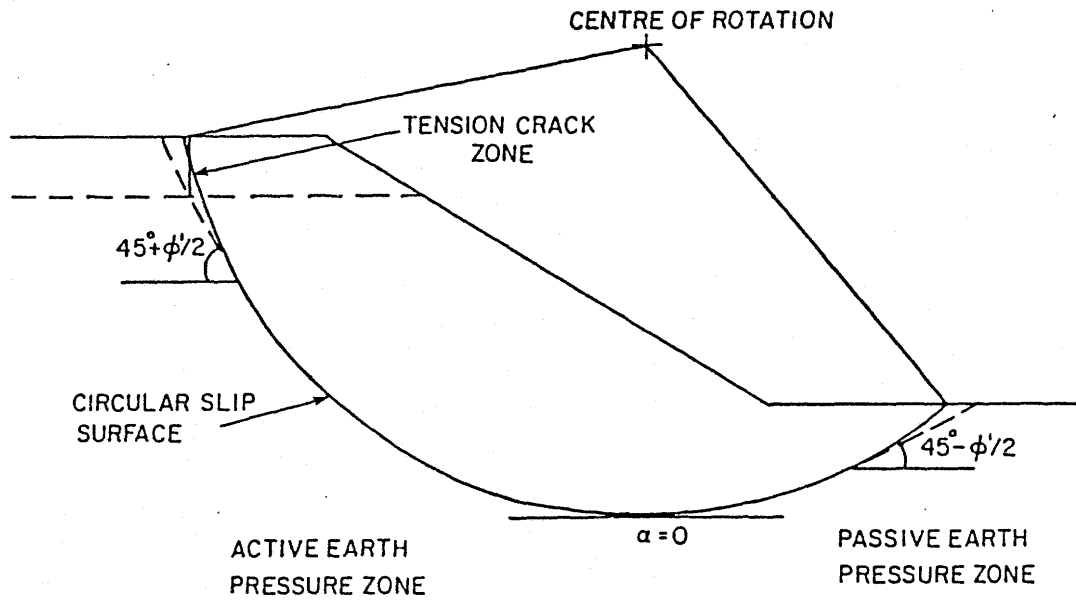
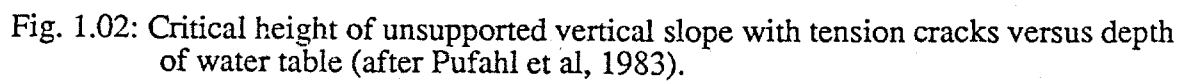
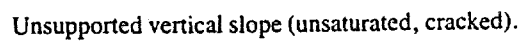


Fig. 1.01: The length of slip surface is shortened due to the presence of tension cracks.



critical height of an unsupported excavation is illustrated in Fig. 1.02.

Compacted cohesive soils are often used as "impermeable" barriers to retain various types of industrial waste products. Compacted clay liners are prone to crack due to desiccation. A cracked clay liner has a permeability many orders of magnitude greater than does an uncracked liner. Desiccation cracking has been known to cause problem in the field (Kleppe and Olson, 1985). Excessive water loss in an exploratory borehole was partially blamed on desiccation cracking in the clay core of Lovewell Dam (Sherard, 1973). The clay core had been exposed to desiccation in dry weather during a construction stoppage.

The infiltration rate in fractured soils depends on the configuration and the extent of cracking. From a computer study on the infiltration in an fractured soil, Moore and Ali (1982) found that the depth of cracking played a significant role, whereas the cracking frequency was less important.

When a desiccated soil is soaked with water during wet seasons, the soil swells and the cracks are closed. The opening and closing of desiccation cracks generates fissures in the soil (Blight and Williams, 1971). It has been recognized that the strength of stiff fissured clays is

governed mainly by the orientation and spacing of fissures (Terzaghi and Peck, 1967). If the origin and the extent of the fissures are known, its effect on the performance of fissured soils can be assessed with more confidence.

Soils containing a significant amount of clay will experience high volume changes during dry and wet seasons. This type of soil is commonly known as "expansive soil". The main engineering problem associated with expansive soil is the distress caused to light structures as a result of volume changes. A rational engineering design approach is to place the foundation units of a light structure in stable ground conditions below the active zone of expansive soil (Can. Geotech. Soc., 1978). However, this approach is not always economical, especially in the case of highway construction. Recently, vertical moisture barriers have been used in highway construction to prevent the expansive foundation soil from detrimental seasonal volume changes (see Fig. 1.03, Picornell, 1985). The function of the barrier is to reduce the infiltration of rainfall into the desiccation cracks within the foundation soils in wet seasons and to prevent the foundation soils from excessive drying in dry seasons. A knowledge of the maximum crack depth is required to design this type of moisture barriers.

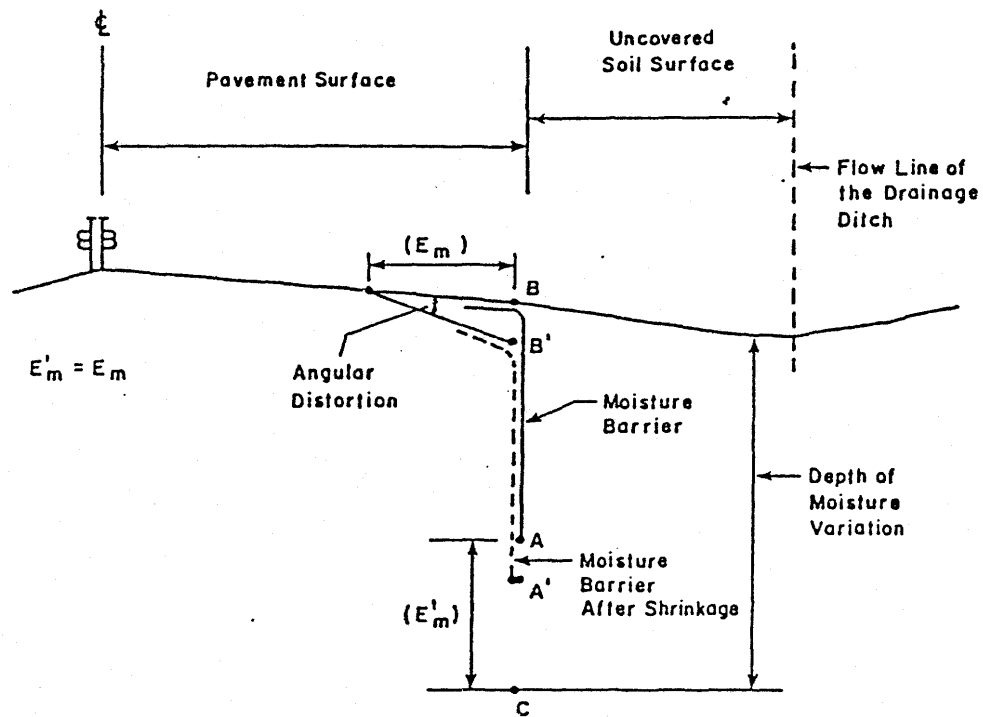


Fig. 1.03: Installation of a vertical moisture barrier along the edge of a highway pavement (after Picornell, 1985).

1.3 THE NEEDS

When the depths of cracks are known, it is usually not difficult to incorporate their effect into an engineering analysis as discussed in Section 1.2. However, the depth of cracking remains a difficult variable to obtain in the analysis (Baker, 1981). Taylor reviewed this problem in 1948 and stated:

"The questionable action and the questionable depth of the tension zone have considerable bearing on the limited dependability of many stability analyses, and the action within the tension zone is a subject that is worthy of much study."

Unfortunately, the study of tension cracking in soils has been neglected in the engineering disciplines (Lee et al, 1982). In Codes of Practices (1951) as well as in many textbooks (Terzaghi and Peck 1967, Lambe and Whitman 1969, Chowdhury 1978 and Craig 1978), the depth of tension crack is customarily estimated using the Rankine theory of earth pressure.

$$Z_C = \frac{2 c'}{\gamma} \tan (45 + \phi' / 2) \quad [1.01]$$

where:

Z_C = depth of tension crack.
 c' = effective cohesion intercept.
 ϕ' = effective friction angle.
 γ = the unit weight of soils.

Spencer (1968) suggested a procedure in his method of slope stability computation to determine the line of thrust of the interslice forces. If the position of the line of thrust is not reasonable, a tension crack is introduced and a different line of thrust is determined. The depth of tension crack can be estimated, when a reasonable line of thrust is obtained. The depth of tension crack can also be determined using variational approach to slope stability analysis (Baker, 1981).

All the above analyses deal with the shear strength behavior of the soils. However, there are other factors, such as expansion/contraction caused by frost action and the shrinkage of the clay due to drying, which have important effects on the depth to which cracks extend (Taylor, 1948). Other than the above methods, there exist no other rational means for the estimation of the depth of desiccation cracks.

1.4 THE SCOPE OF THIS DISSERTATION

The purposes of this thesis are to study the mechanism of desiccation cracking in soils and to propose a mathematical model for the prediction of depth of cracking.

The investigation consists of conducting a literature review, a laboratory experimental program and an analytical program. The principal objectives of the investigation are,

- a) to study the cracking patterns of desiccating soil,
- b) to identify the parameters that influence the cracking pattern and the depth of cracking,
- c) to study the effect of soil suction on the desiccation cracking in soils,
- d) to propose a mathematical model for the prediction of crack depth, and
- e) to evaluate the effects of different soil parameters on the prediction of crack depth.

This dissertation is divided into eight (8) chapters. A general introduction to the desiccation cracking in soils is provided in Chapter 1. Chapter 2 contains a summary of the existing knowledge on the desiccation cracking of soils. Mathematical expressions for the prediction of crack depth are given as part of the theory in Chapter 3. Descriptions of the analytical and experimental programs are provided in

Chapter 4. The results of the analytical and experimental programs and a discussion of results are presented in Chapters 5, 6 and 7, respectively. Conclusions derived from this study and recommendations on future research are given in Chapter 8.

CHAPTER 2

LITERATURE REVIEW

2.1 INTRODUCTION

Research literature was reviewed from the geology, soil science and engineering disciplines that pertained to the problem of shrinkage and desiccation cracking in soils. Most of the information provided by geologists deal with the physical observation on the aerial patterns of desiccation cracks. The information provided by the soil scientists is concerned with the physical behavior of soil shrinkage. There is a limited amount of information provided from the engineering field which considers the strength characteristics of soils. It appears that not one researcher has completely assessed or defined an approach to the problem of shrinkage and desiccation cracking of soils. However, the literature review given in this chapter provides some insight into the behavior of desiccation cracking in soils.

2.2 SHRINKAGE OF SOILS

Soils shrink in response to a change in the stress state. The stress state depends on various environmental

factors such as, land use and annual climatic conditions. Haines (1923) studied blocks of soil moulded from a paste and distinguished three main phases of soil shrinkage that accompanied water withdrawal: normal, residual and no shrinkage as shown in Fig. 2.01. Normal shrinkage occurs when the change in soil volume equals to the water lost. Residual shrinkage occurs when air enters the soil and the reduction in soil volume is less than volume of water lost. At the no shrinkage phase, soil does not shrink upon further drying.

Stirk (1954) defined a fourth phase of shrinkage termed structural shrinkage (Fig. 2.02). It has similar characteristics to residual shrinkage (i.e., water loss greater than volume change) but occurs at the wet end of the moisture range and is associated with the removal of water from coarse pores.

Large volume changes due to shrinkage (i.e., up to 34.0% of original soil volume) on compacted clayey soils have been reported by various researchers (Stirk (1954) and Chang and Warkentin (1968)). The actual amount of shrinkage due to drying depends on factors such as type and amount of clay minerals, soil fabric arrangements, initial water content and confining pressure (Mitchell, 1976).

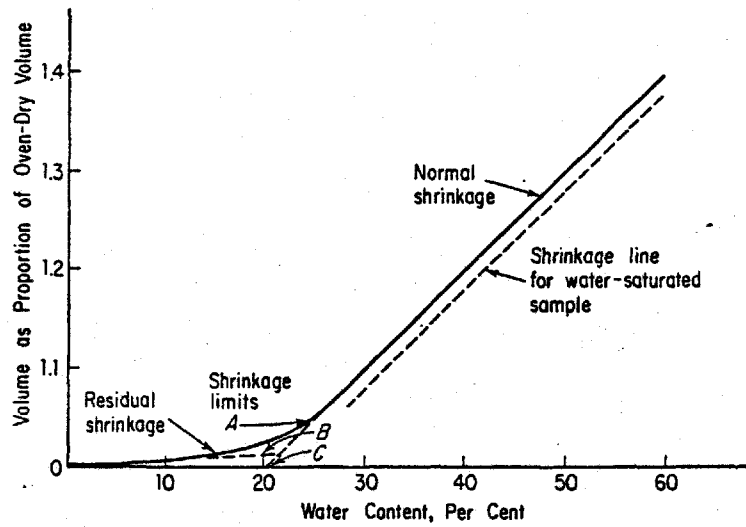


Fig. 2.01: Shrinkage curve for typical clay soils.

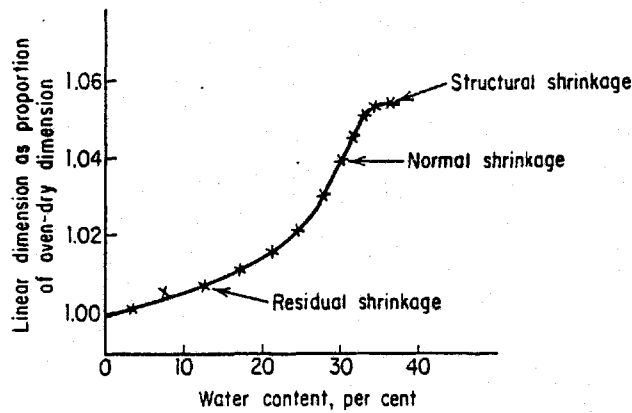


Fig. 2.02: Shrinkage curve for soils with crumb structure (after Yong and Warkentin, 1966).

The amount of shrinkage in soil increases with the plasticity of the soils (i.e., the more plastic the soils, the more the potential shrinkage). It would be expected that, for an equal amount of clay minerals in a soil, montmorillonites undergo a greater volume change on drying and wetting than do kaolinites. If two samples of a given clay are at the same initial water content, but have different soil fabrics, the one with the dispersed structure shrinks most. Lambe (1958) reported that "clay with oriented particles shrinks the most in a direction perpendicular to the plates and least parallel to the plates and a clay with randomly oriented particles shrinks equally in all directions."

Several investigators were concerned with other parameters which affect shrinkage of clay. Gokhale and Anandakrishnan (1970) mixed clay (i.e., either kaolinite or montmorillonite) with sand and noted that the addition of sand generally reduces the shrinkage. Kleppe and Olson (1985) conducted shrinkage tests on compacted clay-sand mixtures and concluded that the addition of sand to clayey soil reduces the amount of drying shrinkage. They further concluded that shrinkage strains were essentially linear functions of compaction water content and did not depend on dry density for the range of compaction effort and water content used in their investigation. Sridharan and Rao (1971) found that the void ratio of a kaolinite mixed with

organic fluid (i.e., carbon tetrachloride) was higher than that of the soil mixed with clear water. It was suggested that shrinkage was dependent on the dielectric constant of the pore fluid.

2.2.1 Other Soil Shrinkage and Cracking Phenomena

There are other phenomena that may produce soil shrinkage and cracking. Skempton and Northey (1952) have suggested that, in London Clay, "fissures developed as a result of syneresis, a colloidal process whereby the particles draw themselves together under the action of attractive forces and expel some of the pore water". White (1961) also noted that cracks can be formed in a sedimenting clay through "syneresis".

Lachenbruch (1962) studied the crack patterns in permafrost regions and contended that tensile stresses set up due to thermal contraction of the surficial frozen soils during winter causes fracture. Water then fills these cracks during summer thawing, becomes frozen, and builds up vertical ice-wedges of a considerable thickness after many seasonal cycles.

Burst (1965) noticed in laboratory tests that swelling clays under water can crack because of shrinkage in response to increases in salinity. Barbour (1986) suggested

osmotically induced and/or osmotic consolidation as the cause of the volume change of clay soils that were exposed to brine solutions. This kind of volume reduction may ultimately cause cracking in soils.

Hamilton (1966) noticed that freezing of compacted clay samples composed of mostly montmorillonite and illite, caused a reduction in soil volume for degrees of saturation less than 90%. Samples with degrees of saturation over 90% expanded. Reduction in volume ranged from 2.0% to 10.0%. Presumably, this type of shrinkage could lead to cracking as well.

The orientation of fissures and discontinuities in over-consolidated clays described by Fookes (1965) and Fookes and Wilson (1966) appear to be strongly related to past tectonic movements, such as folds, faults or shear zones in the bedrock. Skempton et al (1969) suggested that stress release and weathering are important factors in the genesis of fissures.

Kulhawy and Gurtowski (1976) reported that hydraulic fracturing, or the formation of hydraulically induced cracking can occur at the core of a dam when the water pressure at a given depth exceeds the total stress at the same depth.

2.3 DESICCATION CRACKING OF SOILS

As a result of volume reduction due to sub-aerial drying or desiccation, cracks would be induced in cohesive sediments such as alluvial and lacustrine deposits, flood plain clay or dried-out lake (i.e., playa) deposits. The joints in flood plain clays can be accounted for by seasonal variations in water content which cause alternating expansion and contraction (Terzaghi, 1955). Vertical joints in tills have been attributed to shrinkage during drying out by Boulton and Paul (1976).

Desiccation cracks have been observed in playa (see Figs. 2.03 and 2.04, Longwell, 1928, and Fig. 2.05, Willden and Mabey, 1961), in clayey till deposits after heavy rain (see Figs. 2.06 and 2.07), in varved sequence of lacustrine clays and silts (see Fig. 2.08, Babcock, 1977) and in dried-out hydraulic fill of intermixed and interlayered silty fine sand and moderately to highly plastic clayey silt (see Figs. 2.09 and 2.10). Desiccation cracks are characterized by their aerial patterns, spacings and depths of the cracks.



Fig. 2.03: Hexagonal mud crack pattern on a playa surface composed of very uniform sediments, Nevada. (after Longwell, 1928, notes: the hammer and handle measured 330 mm (13.0 in.)).



Fig. 2.04: Playa cracks with large polygons of irregular shape in Nevada. The edges are noticeably rounded probably due to slaking and to wind action (after Longwell, 1928).

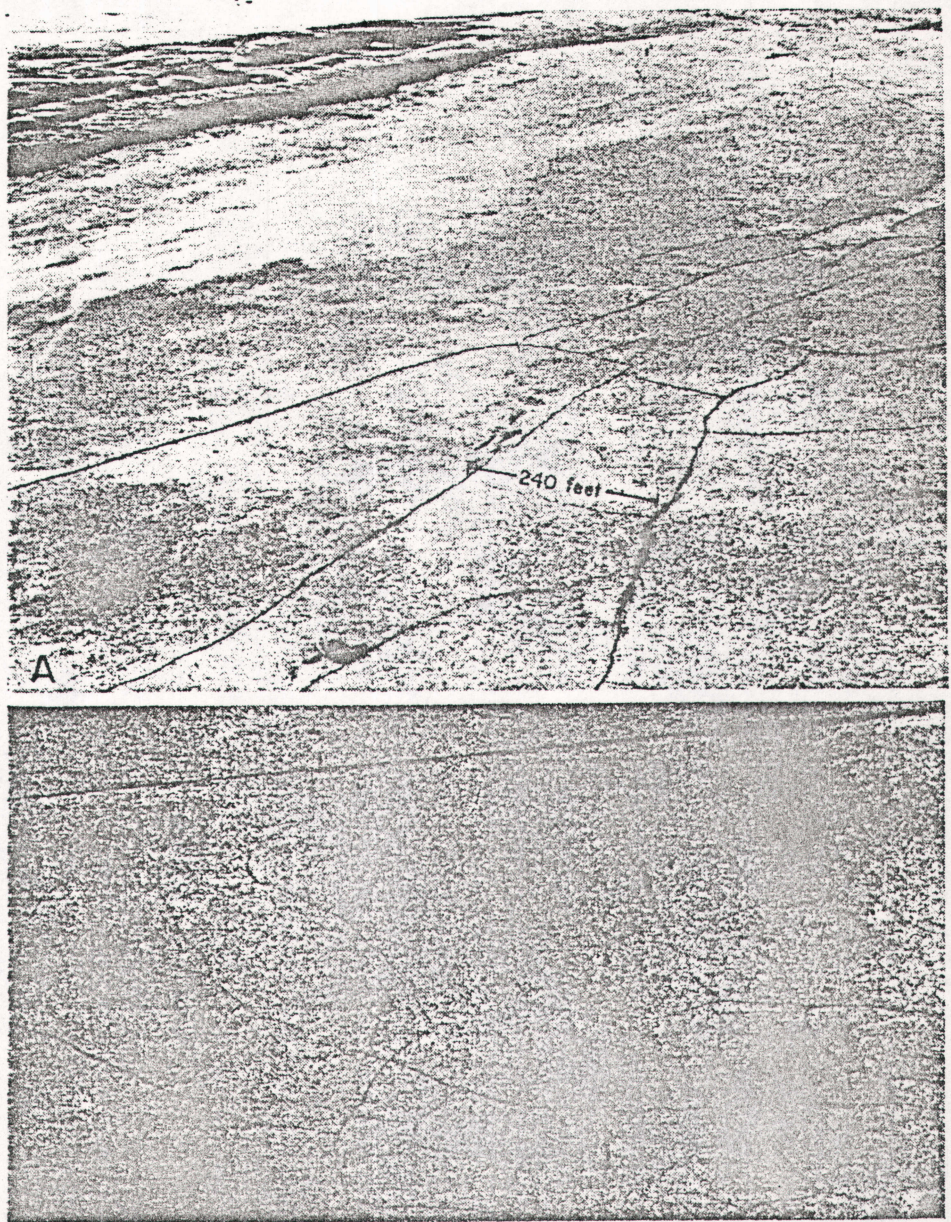


Fig. 2.05: Giant desiccation cracks on the Black Rock and Smoke Creek Deserts, Nevada. (Note that the fissures are about 61.0 m to 73.1 m (200 ft. to 240 ft.) apart, the highway and the car tracks are visible in the photo) (after Willden and Mabey, 1961).



Fig. 2.06: Orthogonal cracks pattern in till after rain, University of Saskatchewan campus, Saskatoon, Saskatchewan, Canada.



Fig. 2.07: Crack pattern in till deposits, located in a highway ditch, near Davidson, Saskatchewan, Canada.

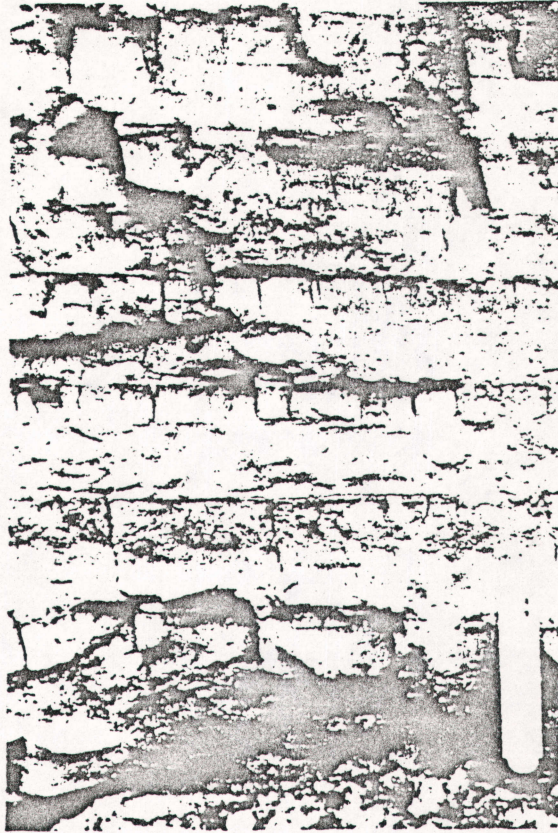


Fig. 2.08: Desiccation fractures in varved sequence of clays and silts. Open fractures are confined to fine-grained clay rich layers, in Drumheller areas, Alberta (Note: compass as shown is 75 mm long, after Babcock, 1977).



Fig. 2.09: Desiccation cracking in a dried-out hydraulic fill site in Los Angeles (after Mitchell, 1986).



Fig. 2.10: A close-up view of the desiccation crack at the hydraulic fill site in Los Angeles (after Mitchell, 1986).



Fig. 2.11: Orthogonal crack patterns on frozen ground in permafrost (after Lachenbruch, 1962).

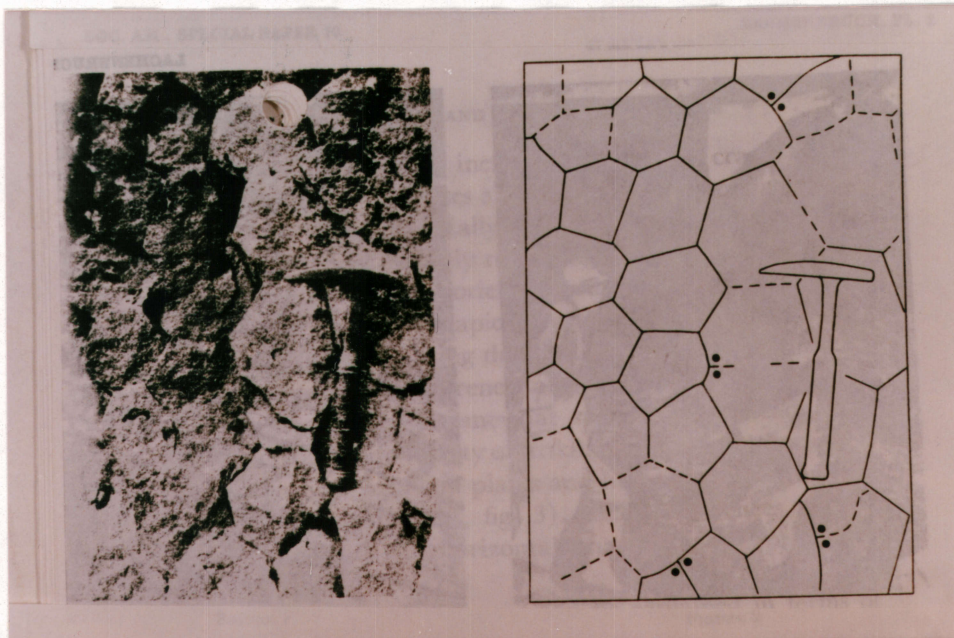


Fig. 2.12: Hexagonal cracks patterns on cooling joints in andesite, Mt. Rainer National Park, Washington (after Lachenbruch, 1962).

2.3.1 Aerial Pattern

Desiccation cracks are rarely straight. The cracks bound polygons which may have as few as three and as many as eight sides. Polygons with three to five sides are most abundant (Twenhofel, 1950). The often-repeated statement that mud-cracked polygons have six sides has little basis in observation. Desiccation cracks usually form a pattern of orthogonal polygons and hexagonal polygons are an exception (Brenner et al, 1981).

Corte and Higashi (1960) carried out a laboratory study of desiccation cracks formed from different soil thickness placed in container with different bottom materials and found that the predominant number of sides of polygons was four or five.

Lachenbruch (1962) identified two polygonal crack systems in his study on ice-wedge polygons, namely orthogonal and non-orthogonal systems, depending on the intersection angle of the cracks. Orthogonal patterns, in which cracks are formed perpendicular to one another, suggests that one of the cracks predated the other. Non-orthogonal intersections are normally composed of three fracture elements which would radiate to form angles of 120 degree.

Lachenbruch (1962) contended that the orthogonal systems of polygons are characteristics of a somewhat non-homogeneous or plastic media in which the stress builds up gradually with cracks forming first at loci of low strength or high stress concentration. Non-orthogonal systems of polygons, on the other hand, are the results of a very homogeneous and relatively non-plastic media subjected to uniform stress conditions. These are believed to be much less common in nature than are orthogonal systems. Figures 2.07 and 2.11 show some of the orthogonal systems of polygons resulting from normal desiccation cracking in temperate or arid areas and, thermal contraction cracking in permafrost, respectively.

Perfect hexagonal systems are rarely observed. Some occurrences of hexagonal polygons have been observed from thermal contraction cracking in lava (see Fig. 2.12) and from desiccation cracking in a playa in Nevada (see Fig. 2.03). The soils in the playa consisted of a very uniform fine-grained soil without any lamination or other structure to a depth of several feet. These rarely observed hexagonal patterns have persistent 3-element intersections at obtuse angles close to 120 degree.

Laboratory experiments conducted by Corte and Higashi (1960) showed that, in general, mud cracks tend to form orthogonal intersections (i.e., forming right angles).

Babcock (1977) studied the fractures in glacio-lacustrine sediment outcrops in Central Alberta (i.e., Drumheller area) and found that orthogonal or random patterns of desiccation cracks were observed in most outcrops.

2.3.2 Crack Spacing and Crack Depth

The positions of desiccation cracks in sediments are in general determined by objects or conditions in the soils that decrease cohesion. Inhomogeneities such as holes, different soil thickness, and other foreign matters often determine the location of cracking (Twenhofel, 1950). Cracks extend along the points of least cohesion. Desiccation cracks tend to be vertical to varying depths. Twenhofel (1950) suggested that the first crack formed tended to be the longest, deepest and widest.

Longwell (1928) described the desiccation cracks in playa sediments (see Figs. 2.03 and 2.04) in the desert of Southern Nevada. These crack have spacings varying from about 75 mm to 150 mm (3 to 6 inches) and the cracks appeared to be shallow.

In Western Texas, Simpson (1934) reported that the desiccation of clays in the dry season proceeded to a depth

as deep as 6.1 m (20.0 feet). Within this depth the clay was broken up by shrinkage cracks.

In Poland, a regular polygonal (penta- and hexagonal) network of crackings, 1.5 m to 3.0 m (meters) in diameters was reported (Jahn, 1950) as having resulted from rapid drying of a silt layer that was laid down under water.

According to Horberg (1951), residents of North Dakota reported "desiccation cracks up to 150 mm (6.0 inches) in crack spacing and over 3.0 meters (10.0 feet) in depth" in the clays of Lake Agassiz.

Large polygons, averaging 24.5 m to 27.5 m (meters) in diameter and occurring on Playa de los Pinos, New Mexico, have occurred as a result of the desiccation phenomena (Knechtel, 1952). Seasonal frost was also given as a possible alternative explanation.

Willden and Mabey (1961) described giant desiccation fissures on Black Rock and Smoke Creek Deserts of Nevada (Fig. 2.05). The fissures intersect to form an orthogonal network dividing the playa into blocks with edges from 30.5 to 76.3 meters (100 to 250 feet) long. The fissure appeared to be vertical, and some are open to depths in excess of 1.22 m (4.0 feet), although the widest and oldest fissures

were generally shallow because material had slumped into the openings.

Zein El Abedine and Robinson (1971) conducted detailed measurements on the desiccation cracks of some swelling clay soils (i.e., vertisols, clay content of 30% or more) in Sudan. The average drying period was about three to six months during their studies. They found that the average crack spacing (see Table 2.01) varied from 0.28 m for soils under natural (non-irrigated) conditions to about 0.50 m for soils located in delta areas, that were subject to flooding conditions (or irrigated soils). They also found that the soils in grassy areas cracked at a wider spacing (0.51 m) than soils under treed areas (i.e., cracked at an average spacing of 0.39 m). Using a 3 mm in diameter and 1.50 m long probe, Zein El Abedine and Robinson measured crack depths. They found that the crack depths (see Table 2.02) ranged between 0.65 m in depth in irrigated soils to 1.35 m in the non-irrigated soils. They observed that areas covered with grass developed shallow cracking, whereas areas under trees developed deep cracks. They then concluded that the crack spacing and crack depth are related to the amount of precipitation or irrigation, the kind and density of vegetation and the history of soil development.

Blight and Williams (1971) measured open shrinkage cracks in South Africa to a depth of 0.65 m with closed

Spaces (cm)	Gezira					Link Canal		Gash delta	
	GTO3	GTO4	GTO5	GTO6	GRF	O4H	O4MH	GHATO5	GHB
<21	20	14	22	5	39	19	31	17	6
21-40	40	41	29	30	53	26	33	49	19
41-60	32	19	20	35	7	21	18	22	41
61-80	4	8	20	19	1	31	8	8	19
81-100	4	6	7	11	-	3	6	4	9
>100	-	12	2	-	-	-	2	-	6
Average spacing of profile (cm)	39	52	45	54	28	51	39	39	62

Table 2.01: Average crack spacing and frequency of occurrence for some vertisols in Sudan (after Zein El Abedine and Robinson, 1971).

Range (cm)	Gezira					Link Cannal		Gash delta	
	irrigated					natural condition		flooded every 3 years	
	GTO3	GTO4	GTO5	GTO6	GRF	O4H	O4MH	GHAT5	GHB7
<16	12	5	4	2	1	10	3	11	4
16-25	46	17	9	8	24	30	14	16	8
26-35	27	38	23	41	21	18	24	11	8
36-45	15	29	31	44	11	14	17	8	16
46-55	-	10	27	5	8	13	25	5	28
56-65	-	1	6	-	6	10	9	4	6
66-75	-	-	-	-	9	5	5	15	3
76-85	-	-	-	-	6	-	3	15	9
86-95	-	-	-	-	7	-	-	7	8
96-105	-	-	-	-	1	-	-	3	4
106-115	-	-	-	-	4	-	-	4	3
>115	-	-	-	-	2	-	-	1	3
Profile aver. cm	26	34	39	35	51	42	36	60	60

Table 2.02: Frequencies of occurrence percent, and average depths of cracks in Sudan (after Zein El Abedine and Robinson, 1971).

Date of Observation	Width		Depth		Average Crack Spacing	Crack Volume m ³ ha ⁻¹
	Mean	S.D.	Mean	S.D.		
			cm			
CANADA AG. FARM SITE, SASKATOON (REGINA SOIL)						
July 26, 1984 [†]	1.7	0.9	38.1	20.8	210	38
Aug. 9, 1984 [†]	1.9	0.8	44.9	30.6	190	54
Sept. 6, 1984 [†]	2.2	1.0	52.1	38.2	154	91
Sept. 6, 1984	1.5	1.1	34.8	25.6	91	82
Oct. 12, 1984 [†]	1.8	0.9	52.1	31.1	250	nd
Oct. 12, 1984	1.4	1.0	59.5	31.3	345	nd
MATADOR SITE (SCEPTRE SOIL)						
Aug. 16, 1984 [†]	0.9	0.6	28.2	15.9	70	43
July 19, 1985	0.9	0.6	29.1	10.0	210	nd
LEADER SITE (SCEPTRE SOIL)						
July 20, 1985	2.0	1.3	40.1	18.4	111	89
Aug. 27, 1985	2.2	0.7	41.7	18.5	120	83
TISDALE SITE (TISDALE SOIL)						
Aug. 29, 1985	1.6	0.7	36.5	20.0	154	39

nd - not determined.

† Cracks measured along a 2 x 20 m fixed distance. Others measured at random.

Table 2.03: Crack widths and crack depths in selected clay soil sites in Saskatchewan (after Dasog, 1986).

cracks extending to 1.45 m. Ritchie and Adam (1974) described cracks in Houston Black clay to depths of 0.9 m.

Spectacular scenes of desiccation cracks were observed (Fig. 2.09 and 2.10, Mitchell, 1986) at a dried-out surface of a hydraulic fill site in Los Angeles. The hydraulic fill was about 13.0 m (40.0 feet) thick at placement, and consisted of intermixed and interlayered silty fine sand and moderately to highly plastic clayey silt. Orthogonal crack patterns were noted, with crack spacings of about 0.6 m to 1.0 m, and an average open crack depth exceeding 1.5 m. The site settled about 0.9 m to 1.5 m (3.0 feet to 5.0 feet) between the spring of 1983 and April 1986.

Dasog (1986) measured desiccation cracks on selected highly plastic clay soil sites in Saskatchewan (Table 2.03). He found that the measured crack spacing ranged between 0.70 m and 3.45 m with an average of 1.70 m and the crack depths ranged between 0.28 m and 0.60 m. He observed that the desiccation cracks in Saskatchewan are less than one-half as intense as those in Israel or in Sudan. It was concluded that the diversity in cracking among different swelling clay soils was due to the different climatic conditions.

2.4 FRACTURE MECHANICS AND DESICCATION CRACKING OF SOILS

Although fracture mechanics developed mainly in the 60's and 70's, the basic concept of crack propagation was established by Griffith in 1921. Griffith (1921, 1924) stated that crack propagation will occur if the energy released upon crack growth is sufficient to provide all the energy that is required for crack growth. Let us consider a crack, as shown in Fig. 2.13, in a uniform tensile stress field. If we consider the work done by external forces (or change of strain energy per unit thickness) when the crack extend by a distance δa , then for propagation, we have,

$$\frac{\delta U}{\delta a} = \frac{\delta W}{\delta a} \quad [2.01]$$

$$\frac{\delta U}{\delta a} = G \quad [2.02]$$

$$\frac{\delta W}{\delta a} = R \quad [2.03]$$

where:

U = elastic energy release.

W = energy required for crack growth.

R = crack resistance.

G = elastic energy release rate per crack tip
or also called "crack driving force".

G is a function of Poisson's ratio μ , elastic modulus E, and stress intensity factor K.

Let us examine the details of an elastic stress distribution in the vicinity of the crack tip. The predominant terms giving the stress and displacement

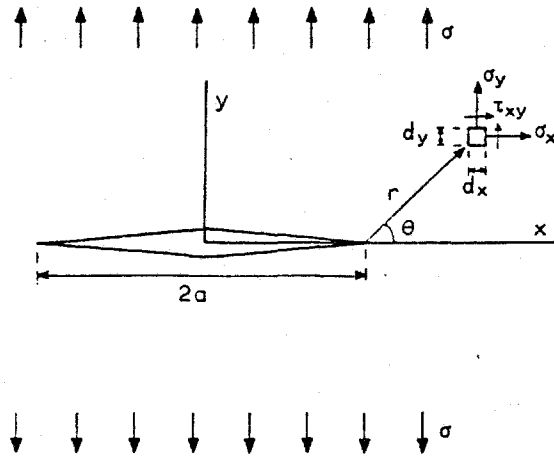


Fig. 2.13: Crack in a finite plate.

$$\sigma_x = \frac{K_I}{\sqrt{2\pi r}} \cos \frac{\theta}{2} \left(1 - \sin \frac{\theta}{2} \sin \frac{3\theta}{2} \right)$$

$$\sigma_y = \frac{K_I}{\sqrt{2\pi r}} \cos \frac{\theta}{2} \left(1 + \sin \frac{\theta}{2} \sin \frac{3\theta}{2} \right)$$

$$\tau_{xy} = \frac{K_I}{\sqrt{2\pi r}} \sin \frac{\theta}{2} \cos \frac{\theta}{2} \cos \frac{3\theta}{2}$$

$$u = \frac{K_I}{4G} \sqrt{\frac{r}{2\pi}} \left[(2\kappa - 1) \cos \frac{\theta}{2} - \cos \frac{3\theta}{2} \right]$$

$$v = \frac{K_I}{4G} \sqrt{\frac{r}{2\pi}} \left[(2\kappa + 1) \sin \frac{\theta}{2} - \sin \frac{3\theta}{2} \right]$$

Equation [2.04]

where

$$\kappa = (3 - 4\nu) \text{ for plane strain}$$

$$= (3 - \nu)/(1 + \nu) \text{ for plane stress}$$

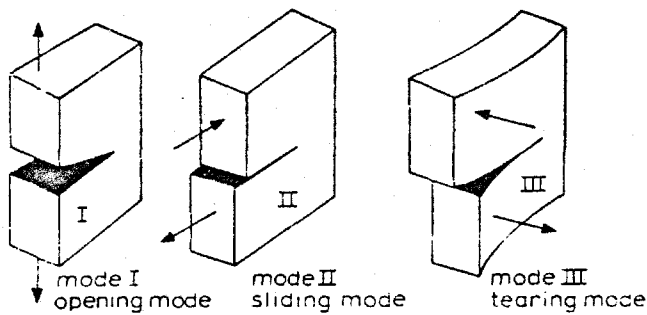


Fig. 2.14: The three modes of cracking.

distribution are given in equations 2.04 (Zienkiewicz, 1977). K_1 is called the stress intensity factor, which depends on the mode of cracking, orientation of cracks and the size of cracks. In three-dimensional problems, three possible modes of crack extension are illustrated in Fig. 2.14. In each case the local stress distribution is similar in form to those given in equation 2.04.

The energy condition of equation 2.01 states that G must be at least equal to R before crack propagation can occur. If R is a constant, this means that G must exceed a certain critical value, G_{1C} . Accordingly, K , the stress intensity factor, would approach a critical value K_{1C} , which is called the "fracture toughness".

For brittle materials, R consists of surface energy only, while for ductile materials, plastic deformation occurs at the crack tip. Hence, much work is required in producing a new plastic zone at the tip of the advancing crack in ductile materials.

Broek (1984) stated that "high strength materials usually have low fracture toughness (K_{1C}), plane strain fracture problems in these materials can be successfully applied by means of fracture mechanics Low strength materials usually have a high fracture toughness (K_{1C}) and the size of the plastic zone may be so large, at present

(1984) a versatile method to treat crack problems in high toughness materials is not yet available".

Based upon Muskhelishvili's (1953) stress perturbation analysis of a crack in an elastic medium and the Modified Griffith's Theory of macroscopic fracture (Irwin, 1948 and Orowan, 1950), Lachenbruch (1961) derived a set of graphs for the estimation of depth and spacing of tension cracks in brittle media, such as permafrost. Reasonable numerical values of crack depth and spacing for ice-wedge polygons in permafrost were obtained by Lachenbruch (1962). In spite of the apparent success in using the theory of macroscopic fracture to the ice-wedge polygons in permafrost, Lachenbruch (1961) admitted that the theory of brittle fracture cannot be applied to the desiccation cracking of soils, owing to its plasticity.

Several studies (Blight and Williams, 1971, Briones and Uehara, 1977, and Raats, 1984) using the Griffith's brittle fracture theory have been applied to the desiccation cracking of soils, however, with little success. Briones and Uehara (1977) performed beam flexure tests on soil samples at several stages of drying to obtain strain release parameters and elastic constants. They concluded that the fracture theory was not sufficient to predict cracking even with a knowledge of soil parameters.

Within the field of fracture mechanics, the cracking problem is essentially treated as a mechanical process, and the failure (cracking) criterion is based on the critical stress field. However, Corte and Higashi (1960) stressed that "cracking by desiccation is entirely different from mechanical cracking in the sense that the material loses mass during the process". Furthermore, fracture mechanics deals only with the propagation of cracking, the initiation or on-set of cracking has not been addressed.

Based on the foregoing discussions, it appears that fracture mechanics is not adequate when dealing with the problem of desiccation cracking in soils.

2.5 FACTORS AFFECTING THE SHRINKAGE AND CRACKING OF SOILS

Most of the earlier works on the shrinkage and cracking of soils were performed by geologists and soil scientists. Their research was mainly focused on the aerial patterns and on the spacing of desiccation cracks. Kindle (1917) conducted small scale laboratory experiments using a 150 mm diameter porcelain vessel. The experiments were performed using a slurried Ontario lake clay. He concluded that temperature and tenacity of material are two primary factors in controlling the spacing of mud cracks. Rapid desiccation was found to produce widely spaced cracks and the addition

of marly material or sand gave polygons which were much smaller than those formed in clay mud. In the case of a sandy mud, an sufficient amount of sand entirely prevents the formation of mud cracks.

Longwell (1928) studied the mud cracks in Nevada and questioned whether Kindle's conclusion on the effect of desiccation rate was valid in the field. He suggested that there were other factors governing crack spacing. In 1950, Twenhofel pointed out that crack spacing depended on the character of the mud, the rate of drying, the thickness of the mud, the character of the water in which the mud was deposited, the nature of the underlying material, and the presence of foreign matters. He did not present any quantitative relationships between crack spacing and these physical factors.

Washburn (1956) studied the origin of different patterned ground and suggested that non-sorted polygonal patterns in temperate regions are due to the contraction resulting from desiccation or drying. He pointed out that once a fissure pattern is formed it tends to persist or reform in the same places after later wet/dry cycles. The fissures keep pace with the reduction of the land surface and lowering of the water table.

Further experimental works were performed on desiccation cracks in soils by Corte and Higashi (1960). They concluded that crack patterns depend largely on the thickness of soil layer and the bottom material of the container. Widely spaced cracks and large polygons were formed in "thick" layers of mud, and closely spaced cracks and mud curls in thin-bedded muds. The maximum thickness of soils used was about 46 mm. Corte and Higashi (1960) criticized Kindle's conclusions saying that the results were incorrect due to the small vessel used in his experiments.

Lachenbruch (1962) studied the ice-wedge polygons in permafrost and theorized that crack spacing of any polygonal patterned ground is a function of the frequency of flaws (or inhomogeneities) in the ground. The inhomogeneities include non-uniform strength within the soil mass and the non-uniform drying conditions or thermal conditions in case of frozen patterned ground caused by local variation in relief and shrinkage properties. He further suggested that flaws with an average separation of several polygon diameters have little effect on either uniformity or magnitude of crack spacing. Those flaws with an average separation on the order of a polygon diameter primarily affect the uniformity of spacing, and those whose separation is an order of magnitude less affect the size of crack spacing.

Lachenbruch (1961) also pointed out that shallow, closely spaced cracks relieve surficial tension developed by rapid desiccation after a rain. Deeper cracks, more widely spaced, might present seasonal desiccation. Profound cracks with spacing of the order of 3.0 m to 30.0 m (meter) could correspond to the draining of a marsh or perhaps to a regional climatic trend toward aridity (Willden and Mabey, 1961).

Discussions in the geological papers consist mostly of physical observations and the authors do not investigate any measureable parameters which control soil cracking. A model of soil cracking for use in engineering application requires measureable parameters and therefore, papers from the geological literature will not be discussed in further details.

Croney and Coleman (1953) and Aitchison and Woodburn (1969) showed that within limits, most soils decrease in volume and water content as soil suction increases. Conversely, the soil volume and water content increases as soil suction is reduced.

Means and Parcher (1963) suggested that the shrinkage of clays is caused by tension in the pore-water, through the action of meniscii, reacting against the soil grains (Fig. 2.15).

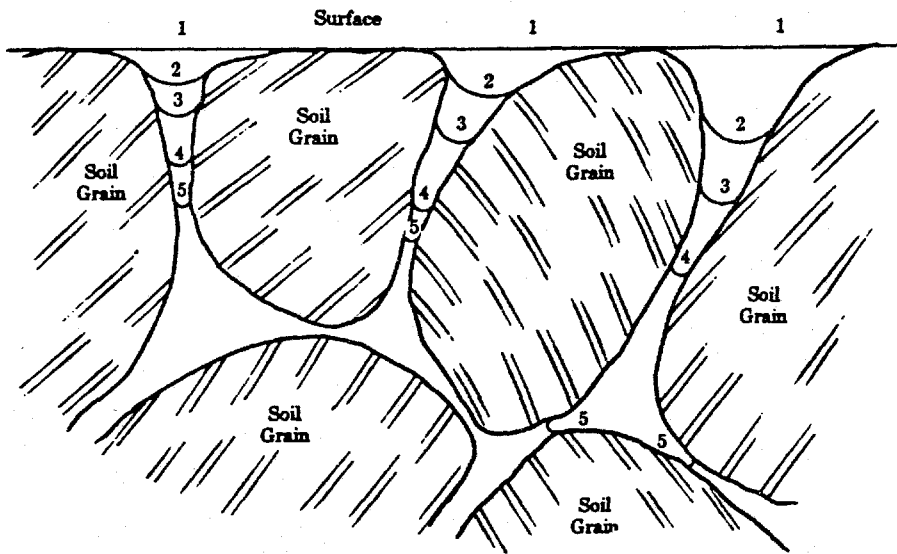


Fig. 2.15: Idealized section through soil (after Means and Parcher, 1963).

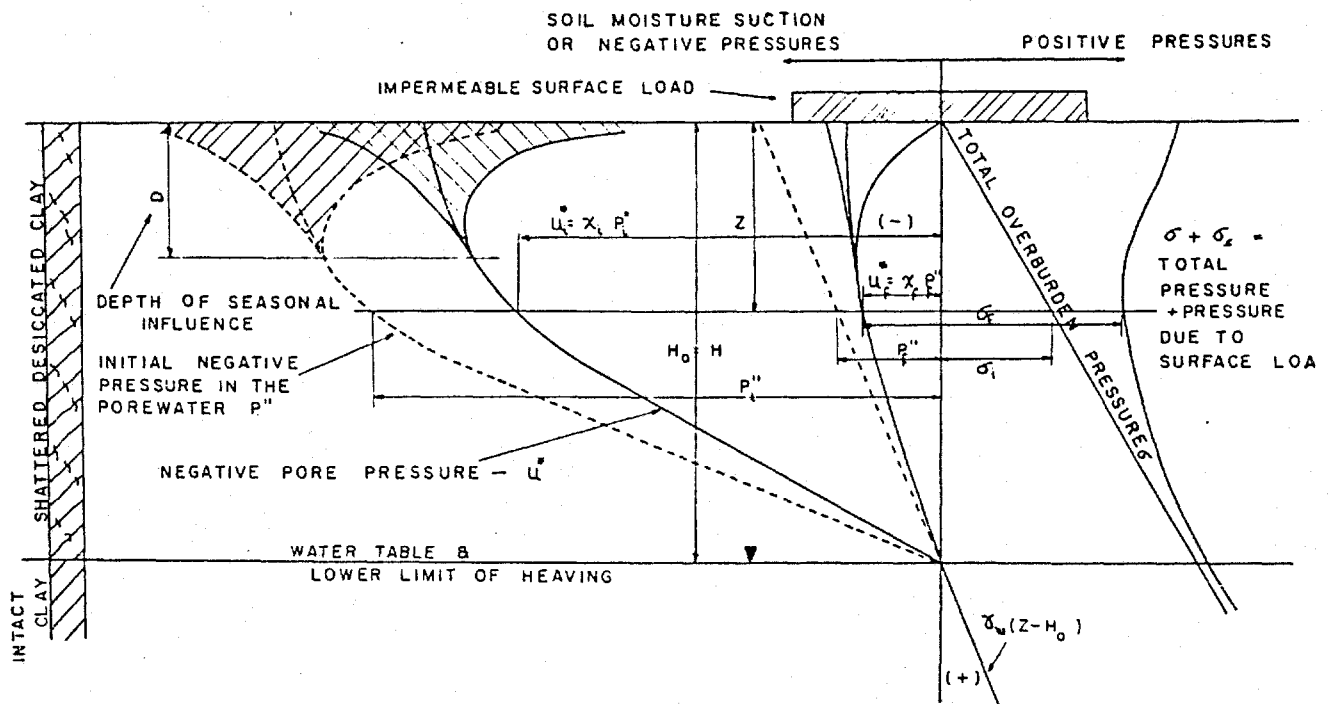


Fig. 2.16: Water pressure and stresses in subsoil under a building on an expansive clay subsoils (after Jennings, 1961).

Blight and Williams (1971) applied the theories of shear strength and Griffith's failure criterion to explain the formation of fissures in South Africa soils. Pore-water tension was incorporated in the estimation of the shrinkage stress. However, they considered cracking in terms of a stress criterion.

Papers presented to the symposium on "The Influence of Vegetation on Clay" (Driscoll, 1984, Ravina, 1984 and Wakeling, 1984) suggested that soil suction should be used as a control variable to describe the tendency of a clay soil to shrink or swell.

Picornell (1985) and Picornell and Lytton (1987) used the soil suction as the parameter to estimate the shrinkage and crack depth for the design of vertical moisture barriers in Texas.

2.5.1 Observations from Soil-Cement Pavement Studies

Shrinkage cracking is a major problem in the use of soil-cement. The conclusions of numerous soil-cement studies

that may be applicable to soils are summarized by Cauley and Kennedy (1972) as follows:

a) Crack intensity (area of cracks divided by total area) increases with percentage of clay particles and depends on the type of clay.

b) Large aggregates (i.e., greater than 25 mm) increase crack intensity.

c) Crack spacing and width are dependent upon tensile strength, tensile modulus of elasticity and coefficient of friction between base and subgrade of pavement. Higher cement contents will result in greater shrinkage and greater tensile strength but wider crack spacing. Higher coefficients of friction can decrease crack intensity but this parameter is not as important as cement content.

d) Rate of evaporation is very important with high rate yielding large shrinkage stresses and substantial cracking.

e) Total amount of shrinkage was appreciably higher at compaction water contents greater than optimum.

2.5.2 Significance of Soil Suction in Desiccation of Soil

It has long been recognized that any combination of the possible factors involved, such as soil volume properties, proximity of tree root systems (Perpich et al 1953, Holtz, 1984), lowering of the groundwater table, and climatic variations (Jennings, 1953, Willden and Mabey, 1961) could be the cause of soil desiccation. Desiccation can be serious in any local situation where moisture is lost from a cohesive soil over an extended period of time, such as the 1975 - 1976 drought in northern Europe (Driscoll, 1984).

It has been discussed in Section 2.5 that soil suction has been used as a parameter to relate the shrinkage or volume change of soils. The factors affecting the soil suction are in response to environmental changes (Peter, 1979). The environmental factors include, climate, topography, drainage pattern, proximity of building, the garden composition, the application of chemicals (e.g. salts), confinement within the soil due to surcharge and the position of groundwater table.

The effect of the groundwater table and the location of surface structures on the suction profile was demonstrated by Jennings (1961) (see Fig. 2.16). Where fluctuations occur

in the water table throughout the year, suction changes will occur in the suction profile, but not necessarily in phase with the water table (Fredlund, 1981).

2.5.2.1 Effect of Evaporation and Vegetation on Soil Suction

When the soil in the field is wet, it will lose water by evaporation. The loss of water at the surface and the resulting upward flow of water in the profile will cause the soil to dry, unless a shallow groundwater is present which provides continual flow of water to the evaporative soil surface without materially changing the soil moisture. However, once the top soil surface is dry, further drying is reduced considerably due to low hydraulic conductivity of the drying soil (Ravina, 1984). From field measurement, Ritchie and Adams (1974) concluded that evaporation from a dried soil surface is nearly zero. The influence of soil evaporation is believed to be restricted to less than the uppermost 0.3 m (1.0 foot) in the soil profile (Williams and Pidgeon, 1983, and Picornell, 1985). The water content and the soil suction below the dry top layer remains practically unchanged (Ravina, 1984).

When the soil surface is covered with vegetation, soil water is transferred to the atmosphere by transpiration, which takes place from the stomata of the plant. Soil water

is extracted by the roots which permeate the soils and is transmitted through the stems to the continuously transpiring leaves. In the presence of vegetation the soil may dry more rapidly and to greater depths than a bare soil. It has been observed by Zein El Abedine and Robinson (1971) (see Section 2.3.2) that the presence of vegetations can increase shrinkage and cracking of soils . It was reported that the maximum suction that can be imposed by the roots of vegetation is the wilting point (Williams & Pidgeon 1984) at about 1555 kPa to 3100 kPa (i.e., pF 4.2 - 4.5 where pF is the logarithm to the base of 10 of the suction head of water in cm). The presence of vegetation, and its rooting depth are therefore important factors on the soil suction profile.

2.5.2.2 Effect of Soil Cracking on Soil Suction

When there are shrinkage cracks in a desiccated soil, evaporation from the crack surface may take place due to wind or radiative drying. The removal of water vapor from cracks by wind was found to be more effective than that by radiation (Selim and Kirkham, 1970).

Adams et al (1969) showed that evaporation of the crack surface increases with increasing crack width and wind speed. However, these effects decrease with depth inside the crack. Based upon the findings from a number of field studies by other researchers, Picornell (1985) contended

that the removal of water from the crack surface deeper than 0.6 m is quite unlikely. The effect of evaporation from the crack surface on the soil suction is hence believed to be restricted to the top 0.6 m (2.0 feet) of soils.

2.5.3 Tensile Strength of Soils

Soils, in general are weak in tension. In the analysis and design of earth structures, it is usually reasonable to neglect the tensile strength of soils. However, a knowledge of the stress-strain relationships of the soils in tension is of importance for an understanding of cracking in soils. A limited amount of research has been conducted on the tensile properties of soils. The findings obtained from these studies are summarized by Krishnayya et al (1974) as follow:-

- a) Soils have a low tensile strength ranging from zero to a few pounds per square inch (1.0 lb/sq. in. = 6.89 kPa)
- b) Soils of high plasticity are , in general, more flexible (i.e., they can undergo a higher tensile strain) than the soils of low plasticity.
- c) In case of compacted soils, an increase of molding water content from 2% to 3% dry of Proctor

optimum to nearly optimum substantially increases the flexibility of soil.

d) The rate of straining has a considerable influence on the tensile characteristics of soils.

It seems reasonable to assume that soil cracking is a result of the application of tensile stresses. Leonards and Narain (1963) presented data from beam flexure tests and found the tensile strains-at-failure (at rupture or cracking) for compacted clay samples ranged from 0.05% to 0.33%. Krishnayya et al (1974) defined failure as the maximum tensile stress in the indirect (Brazilian) test. It was found that the maximum tensile stress for a compacted low plastic till was about 3.5 kPa (0.5 lb/sq. in.) with tensile strain-at-failure of 0.2% to 3.0%. Ajaz and Perry (1975) performed both beam flexure and direct tension tests on two clays and found that tensile strain at failure (defined at maximum tensile stresses.) were 2.0% to 15.0% for flexure tests and 1.0 to 5.0% for direct tension tests. In general, all the above tests suggested that tensile strains-at-failure increase with increases in water content. Other conclusions on tensile strain-at-failure are impossible as values of strain appear to vary with test type, loading rates and definition of failure.

Krishnayya et al (1974) also pointed out that the ratio of unconfined compressive strength to the tensile strength increases with the water content. As the water content increases, for a low plastic soil, the tensile strength decreases rapidly.

Fang and Chen (1972) showed that tensile strength increases but unconfined compressive strength to tensile strength ratio decreases as plasticity index increases (see Figs. 2.17 and 2.18). It was found that the range of unconfined compressive strength to tensile strength ratio for compacted silty clay varied from 6.0 to 13.0.

Bishop & Garga (1969) conducted drained tension tests on London clay and found that the tensile stress at failure lies in the range 26.2 kPa to 33.1 kPa (3.8 to 4.8 lb/sq. in) for intact samples and unconfined compressive strength to tensile strength ratio ranged from 5.6 to 6.9. They also found that the tensile strength for remolded London clay was small (close to zero). They concluded that remoulding would almost completely destroy cementation or other bonds that were capable of withstanding tensile stress.

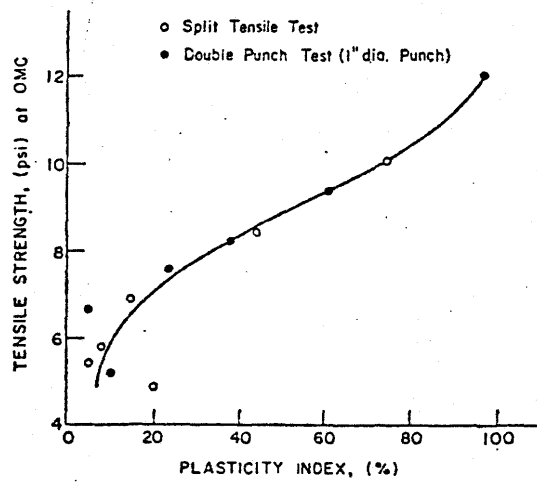


Fig. 2.17: Relationship between tensile strength and plasticity index (after Fang and Chen, 1972).

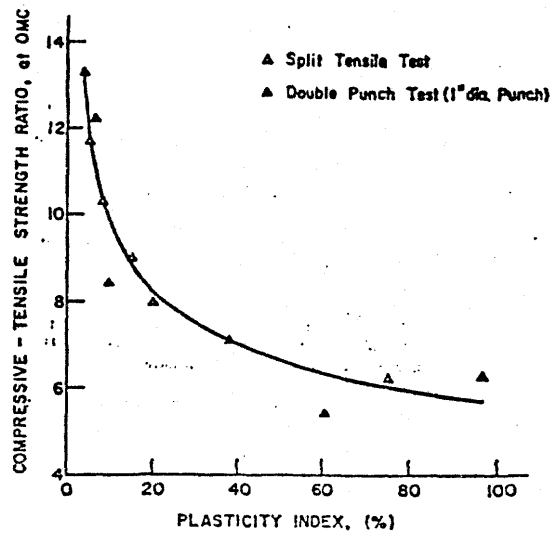


Fig. 2.18: Relationship between unconfined compressive strength - tensile strength ratio to plasticity index (after Fang and Chen, 1972).

2.5.4 Failure Criterion of Soils Under Tension

If the stresses or strains in the field could be estimated, then prediction of cracking would then depend on a choice of a failure criterion. In soils mechanics, the definition of failure has not been given in general terms. In cohesive soils, the failure situation can be defined either at the beginning of loss of shearing resistance or at a relatively advanced state in the loss of shearing resistance (Newmark, 1960). The best known and most widely used failure criterion is the Mohr-Coulomb theory as illustrated in Fig. 2.19. The shear strength of a soil at a point on a particular plane in term of effective stresses can be expressed as a linear function.

$$\tau_f = c' + \sigma_n' \tan \phi' \quad [2.05]$$

where:

$$\begin{aligned} \tau_f &= \text{shear strength.} \\ c' &= \text{effective cohesion intercept.} \\ \sigma_n' &= \text{normal stress.} \\ \phi' &= \text{effective friction angle.} \end{aligned}$$

From Fig. 2.19 the relationship between the effective principal stresses at failure and the shear strength parameters can also be obtained.

$$\sin \phi' = \frac{(\sigma_1' - \sigma_3')/2}{c' \cot \phi' + (\sigma_1' + \sigma_3')/2} \quad [2.06]$$

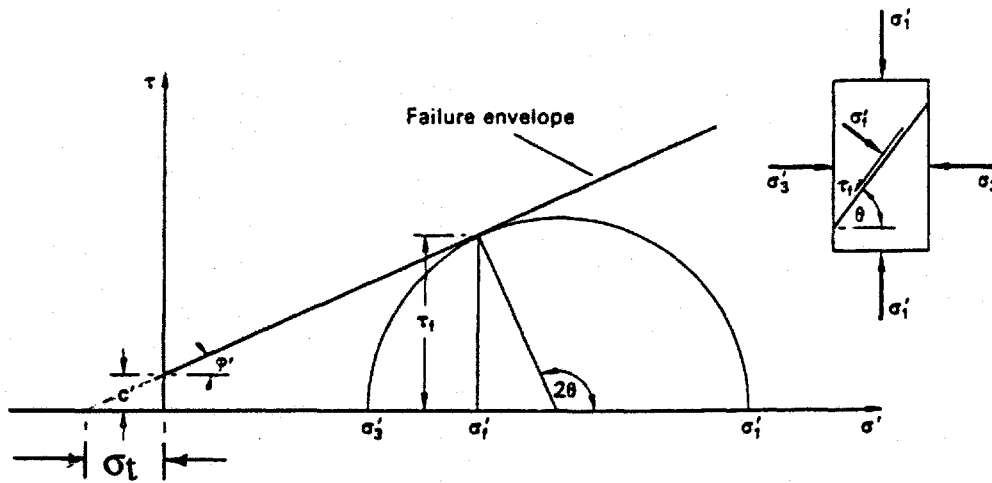


Fig. 2.19: Mohr-Coulomb failure criterion.

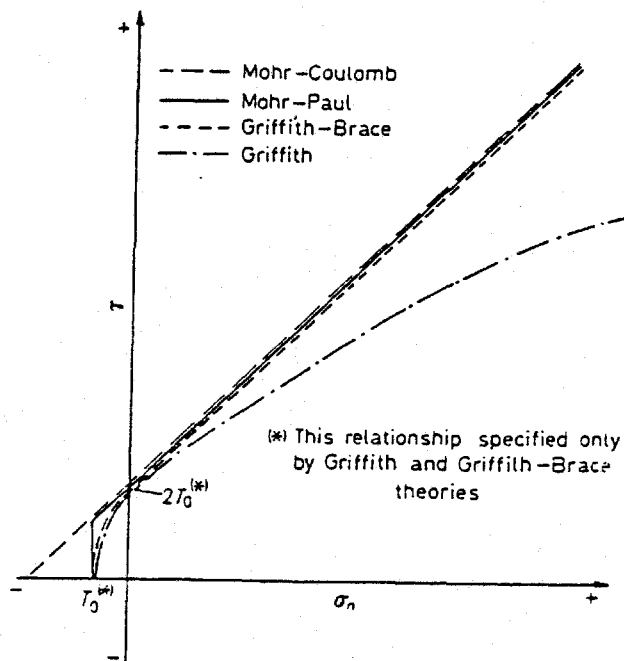


Fig. 2.20: Failure envelopes according to different criteria (after Lee and Ingles, 1968).

$$\text{and, } (\sigma_1' - \sigma_3') = 2 c' \cos \phi' + (\sigma_1' + \sigma_3') \sin \phi' \quad [2.07]$$

where: σ_1', σ_3' = effective principal stresses.

Equation [2.07] is referred to as the Mohr-Coulomb failure criterion. It is seen that the Mohr-Coulomb theory predicts a ratio of unconfined compressive strength Q_u to tensile strength σ_t , which varies according to the frictional properties of the material:

$$\frac{Q_u}{\sigma_t} = \frac{2 \sin \phi'}{(1 - \sin \phi')} \quad [2.08]$$

Although the Mohr-Coulomb failure criterion is widely used with success in engineering practice to describe the soil behavior under compressive forces, the criterion is a poor representation of the behavior of soils in tension, since the yield conditions in the zone of negative (tensile) stress is highly non-linear (Brace, 1960, Frydman, 1967).

There are other failure criteria, such as Mohr-Paul, Griffith, Griffith-Brace and Modified Mohr-Coulomb theories (Figs. 2.20 and 2.21, Lee and Ingles, 1968 and Fang and Chen, 1971, 1972) which have been proposed to describe the soil behavior under tensile forces.

The Mohr-Paul theory is less satisfactory than the Mohr-Coulomb theory as there is no relationship whatsoever

between the unconfined compressive strength and tensile strength, though any observed ratio will be not less than that given by the Mohr-Coulomb theory.

The derived Mohr envelope for the Griffith's theory is,

$$\tau_f^2 - 4 \sigma_t \sigma_n - 4 \sigma_t^2 = 0 \quad [2.09]$$

From Fig. 2.20, the predicted tensile strength is equal to one half the apparent cohesion. Also, Griffith's theory requires that the ratio of unconfined compressive strength to tensile strength be a constant equal to 8.0.

The Griffith-Brace Theory, better known as the Modified Griffith's Theory (Brace, 1960), is a combination of Mohr and Griffith theories. The compressive portion of Griffith-Brace theory is essentially equal to the Mohr-Coulomb criterion, whereas the tensile portion is equal to the Griffith's criterion. Again, the tensile strength must be equal to half of the "Apparent Cohesion". However, the Modified Griffith theory requires that the unconfined compressive strength to tensile ratio is a function of the frictional properties of the soils (Lee and Ingles, 1968).

The Modified Mohr-Coulomb Criterion (Fig. 2.21), proposed by Fang and Chen (1971, 1972), does not require any condition with respect to the ratio of apparent cohesion to

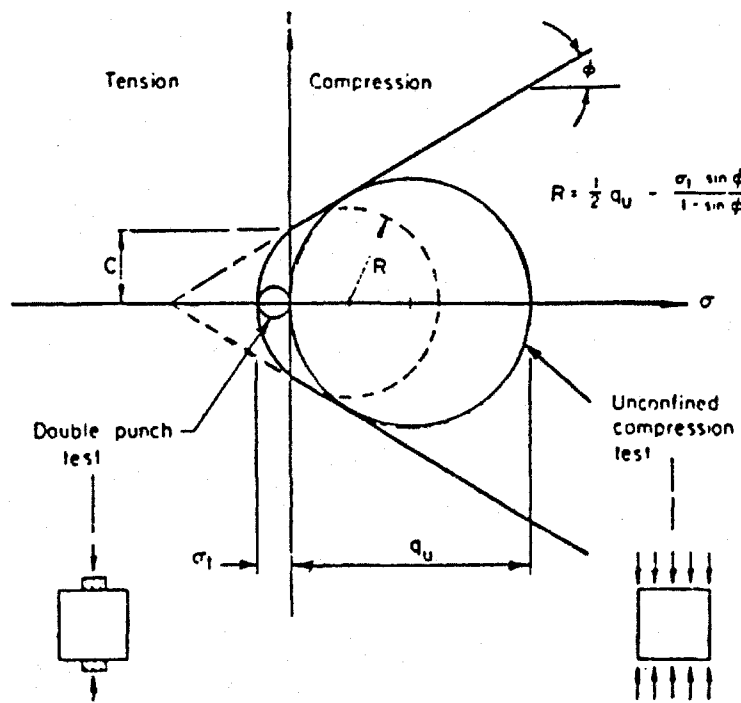


Fig. 2.21: Modified Mohr-Coulomb criterion (after Fang and Chen, 1972).

tensile strength and the ratio of unconfined compressive strength to tensile strength.

As there is not enough experimental information to allow a definition of the non-linear part of the failure criterion (Baker, 1981), the Modified Mohr-Coulomb failure criterion seems to be superior to other criteria as it does not specify any "apparent cohesion" to tensile strength ratio. Furthermore, a different ratio of unconfined compressive strength to tensile strength is allowed in the criterion.

2.6 SUMMARY

This chapter has contained an outline of existing literature concerning shrinkage and desiccation of soils, the physical behavior between fracture mechanics theory and the soil cracking, and the factors affecting soil shrinkage and cracking. Although the solution to the problem of desiccation cracking is not obvious, the following main points are apparent:

- a) Soils shrink in response to a change in the state of stress. The state of stress depends on different environmental factors, such as land use and climate.

b) The amount of soil shrinkage depends on the type and amount of clay minerals, soil fabric , initial water content and confining pressure.

c) Desiccation cracking is the result of volume reduction in soils due to shrinkage (or contraction) during the drying process.

d) In nature, orthogonal patterns are usually observed in desiccation cracking. Orthogonal intersections suggest that one of the cracks predates the other crack.

e) Wide ranges in crack spacing, varying from about 75 mm (milli-meters) to 76.0 m (meters) have been observed in playa (dried-out lake) sediments, alluvial and lacustrine deposits, and glacial till deposits. In general, rapid rates of desiccation produce a smaller crack spacing.

f) Crack spacing is highly dependent upon local disturbance (i.e., non-homogeneities), such as non-uniform strength within the soils and the non-uniform drying conditions.

g) The depth of crack within a desiccated soil mass has received little attention in the past.

h) Fracture mechanics, at its present stage, appears not to be suitable for solving the problem of desiccation cracking in soils.

i) Recent studies conducted by soil scientists and geotechnical engineers have used soil suction as the stress state variable to relate the shrinkage behavior of soils.

j) The soil suction is affected by different environmental changes, such as climate, proximity of structures, and the position of groundwater table.

k) The presence of vegetation, and its rooting depth are important factors on soil suction.

l) Soils have a low tensile strength ranging from zero to a few pounds per square inch (1.0 lb/sq. in equal to 6.89 kPa). The tensile strains-at-failure for compacted soils increase with increases in water content.

m) Tensile strength increases but the ratio of unconfined compressive strength to tensile strength decreases as plasticity index increases.

o) The Modified Mohr-Coulomb failure criterion appears to be more flexible for describing the shear strength behavior of soils under tension.

CHAPTER 3

THEORY OF CRACKING IN SOILS

3.1 INTRODUCTION

Little attention has been paid in the past to the problem of cracking in a desiccated soil. Although the depth of cracking is often required in some boundary value and limit equilibrium analyses, little information on the prediction of crack depth can be found in the literature.

The objective of this chapter is to derive mathematical expressions for the prediction of theoretical crack depth. Unsaturated soils mechanics principles are employed throughout the derivation. Two mathematical expressions are derived. The first expression is obtained using the volume change behavior (i.e., elastic equilibrium analysis) of unsaturated soils. The second expression is derived using the shear strength (i.e., plastic equilibrium analysis) behavior of unsaturated soils. The predicted crack depths are expressed in term of stress state variables and various soil parameters.

3.2 STRESS STATE VARIABLES FOR UNSATURATED SOIL MECHANICS

Fredlund and Morgenstern (1977) showed from a stress field analysis that any two of the three possible stress state variables can be used to define the stress state in an unsaturated soil. Possible combinations are (a) $(\sigma - u_a)$ and $(u_a - u_w)$, (b) $(\sigma - u_w)$ and $(u_a - u_w)$, and (c) $(\sigma - u_a)$ and $(\sigma - u_w)$, where σ = total normal stress, u_a = pore air pressure, and u_w = pore water pressure. Experiments have been performed to verify the proposed stress state variables (Fredlund, 1973).

The two stress state variables that appear to be most satisfactory for most soil mechanics problems are $(\sigma - u_a)$ and $(u_a - u_w)$ (Fredlund, 1979). The $(\sigma - u_a)$ term is called the net total stress and the $(u_a - u_w)$ term is called the matric suction. It should be noted that the pore air pressure is usually equal to zero relative to the atmosphere. Its inclusion in the equations is somewhat academic since it will usually disappear during an analysis.

3.3 MATRIC SUCTION PROFILES

The matric suction of an unsaturated soil depends on many different environmental factors, such as the presence of vegetation, proximity of any structure and the position of water table. Let us consider a saturated soil with a

water table at the ground surface. As a result of evaporation, the water table is drawn below the ground surface. The total stress on the sediments remains essentially constant while the pore-water pressure is reduced (see Fig. 3.01). The pore-water pressure becomes negative (i.e., soil suction) with respect to atmospheric pressure above the water table.

Where the water table exists close to the surface, that is 6 m in clay, 3 m in sandy clay and silts, and 1 m in sand, Peter (1979) suggested that the equilibrium suction profile should be that given by the extension of hydrostatic water table, regardless of the climate.

When the soil is subjected to excessive evaporation due to dry weather, the matric suction profile is pulled away to the left from the hydrostatic profile as shown in Fig. 3.01. In localities where the water table is deep, the matric suction profile near the ground surface remains constant with depths (Peter, 1979). Fig. 3.02 shows the effect of the position of water table and various environmental factors on the matric suction profile.

In order to quantify the matric suction at a given depth in any mathematical analysis, two idealized matric suction profiles are proposed in Figs. 3.03 and 3.04. Although the actual matric suction profile in nature may not

EVAPORATION

EVAPO - TRANSPIRATION

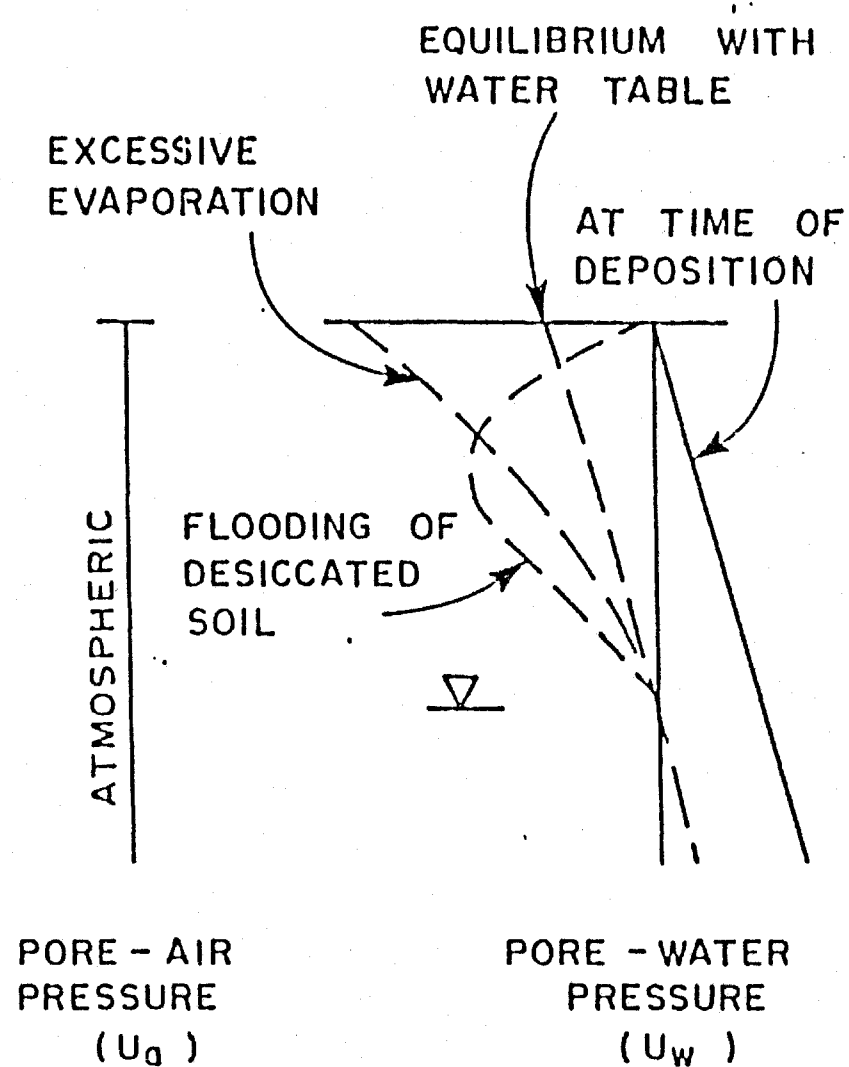
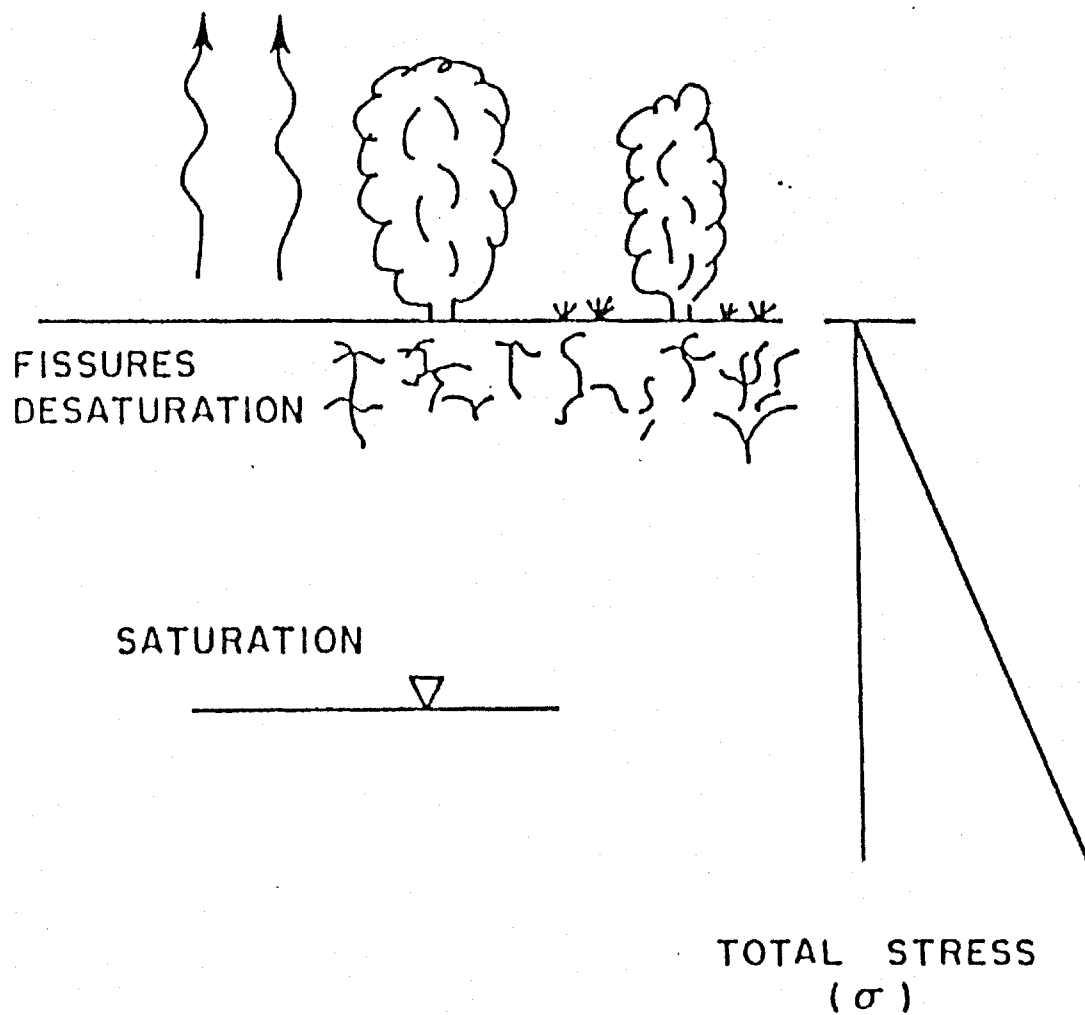


Fig. 3.01: Stress distribution during desiccation of a soil (after Fredlund, 1981).

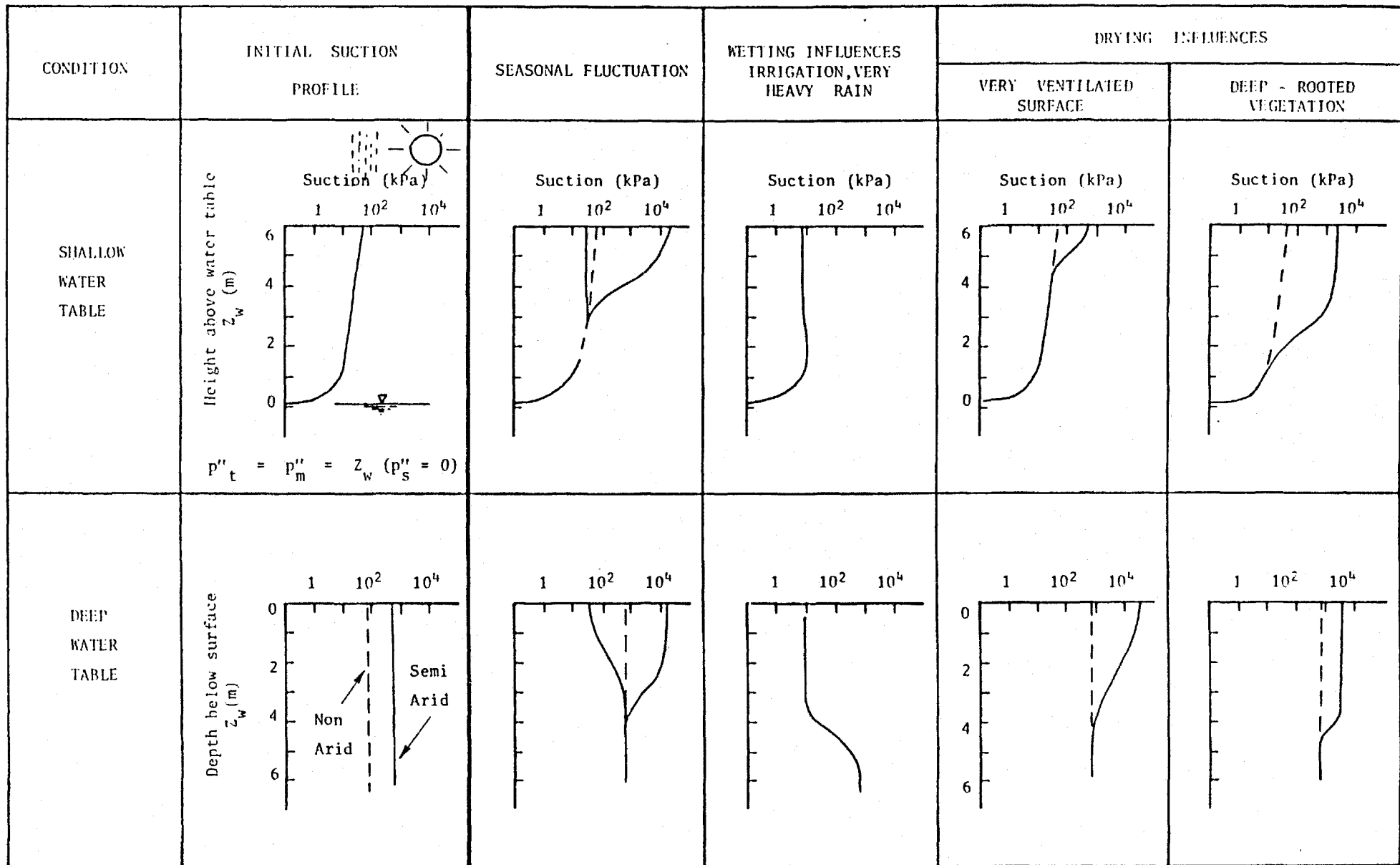
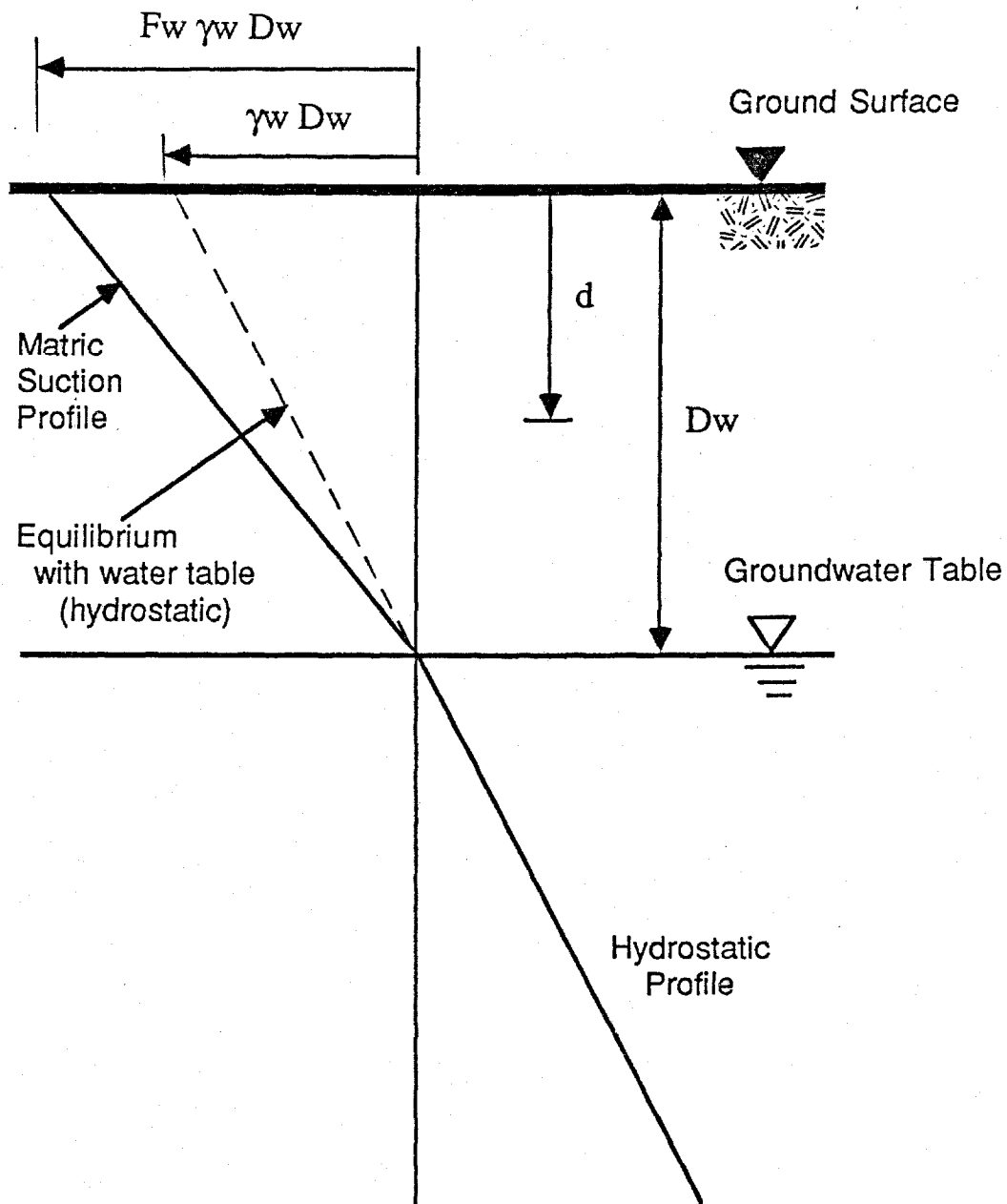


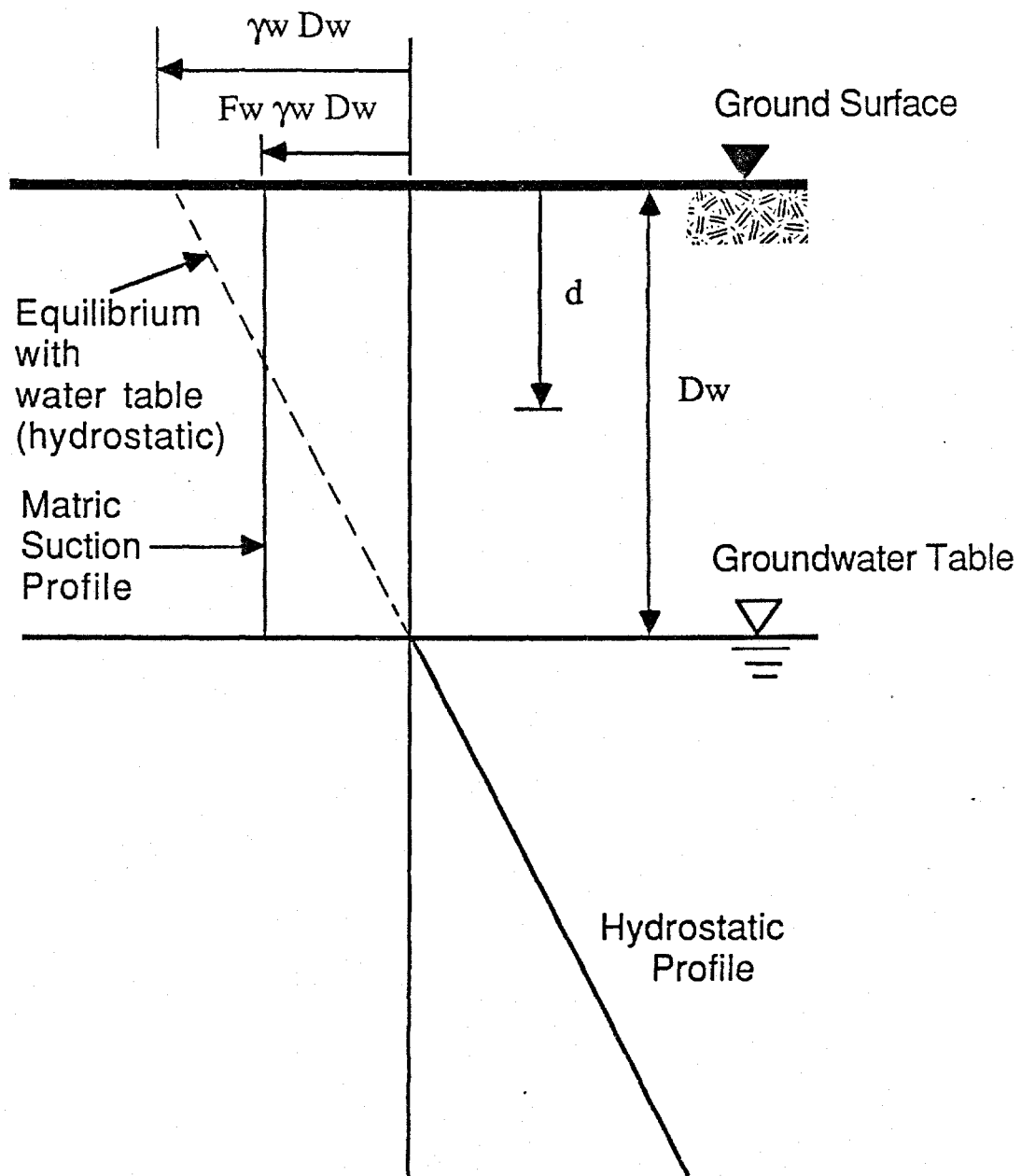
Fig. 3.02: Effect of various environmental conditions on the matric suction profile (after Peter, 1979).



Matric suction at depth d above the water table is,

$$(u_a - u_w)_d = F_w \gamma_w (D_w - d)$$

Fig. 3.03: Idealized matric suction profile "A" (i.e., matric suction varies with depth).



Matric suction at depth d above the water table is,

$$(u_a - u_w)d = F_w \gamma_w D_w$$

Fig. 3.04: Idealized matric suction profile "B" (i.e., matric suction is constant with depth).

considered to be adequate for the present analysis. Matric suction profile "A" represents a linear matric suction relationship with depth and profile "B" represents constant matric suction with depth.

If the matric suction at ground surface is in static equilibrium with the groundwater table, the matric suction at ground surface is equal to the product of unit weight of water γ_w and the depth to water table D_w (i.e., $\gamma_w D_w$). Both the matric suction profiles "A" and "B" are related by a matric suction profile factor, F_w , to the one which is in static equilibrium with the water table. Hence, the matric suction at any depth, for different matric suction profiles can be evaluated (see Figs. 3.03 and 3.04).

For matric suction profile "A", matric suction at depth d is,

$$(u_a - u_w)_d = F_w \gamma_w (D_w - d) \quad [3.01]$$

For matric suction profile "B", matric suction at depth d is,

$$(u_a - u_w)_d = F_w \gamma_w D_w \quad [3.02]$$

3.4 ELASTIC EQUILIBRIUM ANALYSIS

The volume change behavior of any soils can be expressed as a function of independent stress state variables and its material properties. Two constitutive relationships, one for the soil structure and the other for the water phase, have been proposed (Fredlund, 1979) to describe the volume change characteristics of unsaturated soils.

The soil is first assumed to behave as an isotropic, linear elastic material. The constitutive relations for the soil structure were developed in a semi-empirical manner as an extension of the elasticity formulation used for saturated soils as follow:

$$\epsilon_x = \frac{(\sigma_x - u_a)}{E} - \mu \frac{(\sigma_y + \sigma_z - 2u_a)}{E} + \frac{(u_a - u_w)}{H} \quad [3.03]$$

$$\epsilon_y = \frac{(\sigma_y - u_a)}{E} - \mu \frac{(\sigma_z + \sigma_x - 2u_a)}{E} + \frac{(u_a - u_w)}{H} \quad [3.04]$$

$$\epsilon_z = \frac{(\sigma_z - u_a)}{E} - \mu \frac{(\sigma_x + \sigma_y - 2u_a)}{E} + \frac{(u_a - u_w)}{H} \quad [3.05]$$

where:

$\epsilon_x, \epsilon_y, \epsilon_z$ = strain in the x, y, and z directions.

$\sigma_x, \sigma_y, \sigma_z$ = stress in the x, y, and z directions.

E = elastic modulus with respect to $(\sigma - u_a)$.

H = elastic modulus with respect to $(u_a - u_w)$.

μ = Poisson's ratio.

Similarly, the constitutive relation for the water phase was proposed as,

$$\Delta\theta_w = \frac{(\sigma_x + \sigma_y + \sigma_z - 3u_a)}{3H_1} + \frac{(u_a - u_w)}{R_1} \quad [3.06]$$

Where :

$\Delta\theta_w$ = change in the amount of water by volume in a given soil element.

H_1 = water phase modulus with respect to $(\sigma - u_a)$.

R_1 = water phase modulus with respect to $(u_a - u_w)$.

Let the soil has a tensile strain equal to ϵ_h . At elastic limiting equilibrium conditions, the stresses in the horizontal directions are equal to σ_h , and the stresses in the vertical direction are equal to σ_v . That is,

$$\sigma_x = \sigma_y = \sigma_h \quad [3.07]$$

$$\sigma_z = \sigma_v \quad [3.08]$$

$$\text{and, } \epsilon_x = \epsilon_y = \epsilon_h \quad [3.09]$$

Substituting equations [3.07], [3.08] and [3.09] into equations [3.03] and [3.04], gives an identical expression,

$$\epsilon_h = \frac{(1 - \mu)(\sigma_h - u_a)}{E} - \frac{\mu(\sigma_v - u_a)}{E} + \frac{(u_a - u_w)}{H} \quad [3.10]$$

$$\Rightarrow \frac{(\sigma_h - u_a)}{(\sigma_v - u_a)} = \frac{\mu}{(1 - \mu)} + \frac{\{E \epsilon_h - (u_a - u_w)E/H\}}{(1 - \mu)(\sigma_v - u_a)} \quad [3.11]$$

Let us consider a desiccated soil with vertical cracks extending to a depth of d_c as shown in Fig. 3.05. At the bottom of the desiccation crack, that is at depth d_c , the

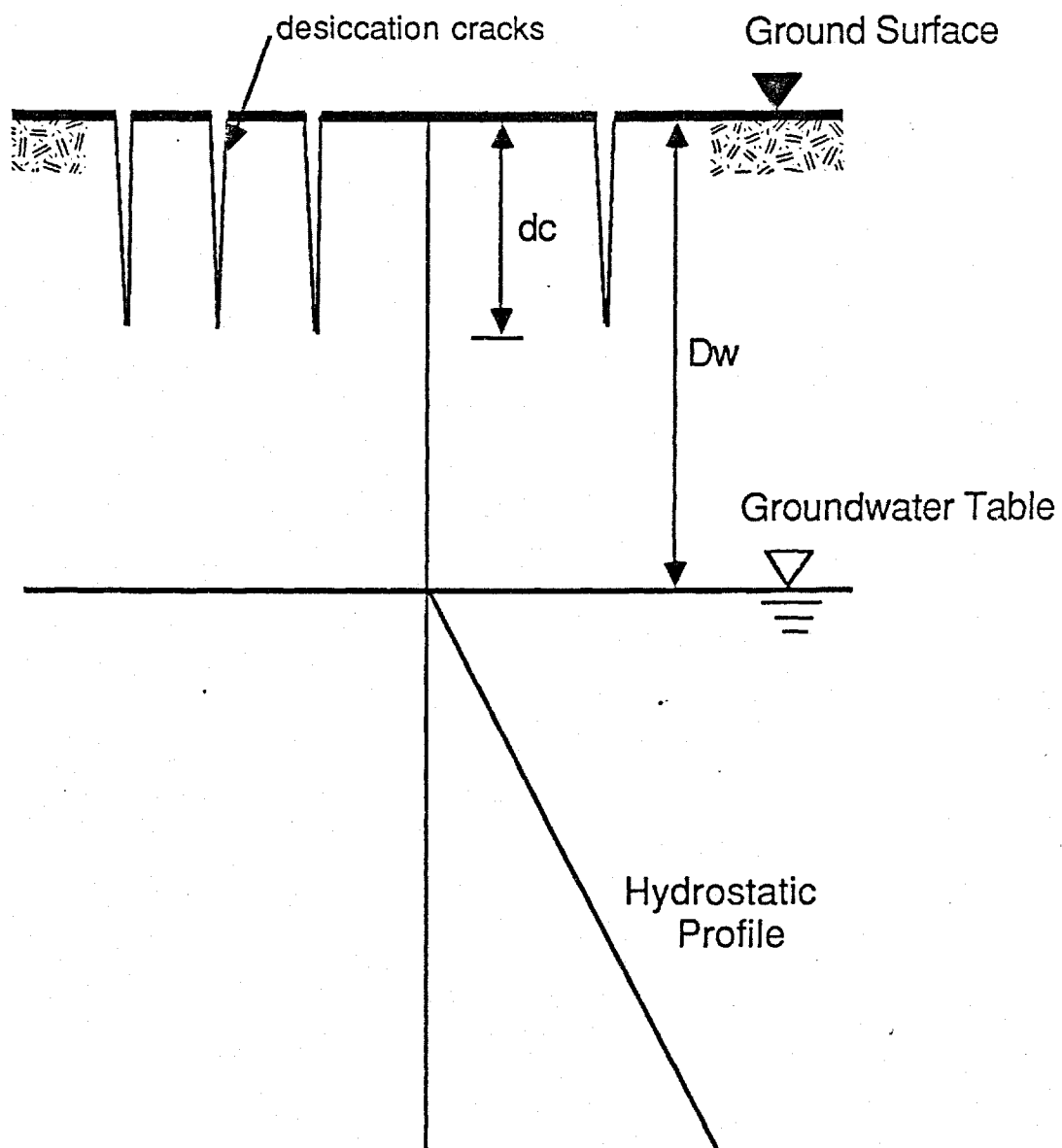


Fig. 3.05: A typical desiccated soil.

total horizontal stress, $(\sigma_h - u_a)$ will be equal to zero. Hence, equation [3.11] becomes

$$0 = \frac{\mu}{(1 - \mu)} + \frac{\{E \epsilon_h - (u_a - u_w)_{dc} E/H\}}{(1 - \mu) (\sigma_v - u_a)_{dc}} \quad [3.12]$$

The total stress at depth dc , $(\sigma_v - u_a)_{dc}$ is equal to the product of total soil unit weight γ and the crack depth dc . The matric suction at depth dc is dependent upon the in-situ matric suction profiles prior to cracking. Let us consider two type of matric suction profiles as discussed in section 3.3.

For matric suction profile "A", the matric suction at depth dc is,

$$(u_a - u_w)_{dc} = F_w \gamma_w (D_w - dc) \quad [3.13]$$

For matric suction profile "B", the matric suction at depth dc is,

$$(u_a - u_w)_{dc} = F_w \gamma_w D_w \quad [3.14]$$

The total stress at depth dc is,

$$(\sigma_v - u_a)_{dc} = \gamma dc \quad [3.15]$$

Where :

- γ = total unit weight of soil.
- γ_w = total unit weight of water.
- D_w = depth to groundwater table.
- dc = depth of crack.
- F_w = matric suction profile factor.

Substituting equations [3.13], [3.14], and [3.15] into equation [3.12], gives two expressions for the crack depth for the two matric suction profiles.

For matric suction profile "A", the depth of crack is given as,

$$dc = \frac{Dw - \frac{H \epsilon_h}{Fw \gamma_w}}{1 + \frac{\mu \gamma}{Fw \gamma_w} \frac{1}{(E/H)}} \quad [3.16]$$

For matric suction profile "B", the depth of crack is given as,

$$dc = \frac{Dw - \frac{H \epsilon_h}{Fw \gamma_w}}{\frac{\mu \gamma}{Fw \gamma_w} \frac{1}{(E/H)}} \quad [3.17]$$

where:

- dc = depth of crack.
- γ = total unit weight of soil.
- γ_w = total unit weight of water.
- Dw = depth to groundwater table.
- Fw = matric suction profile factor.
- μ = Poisson's ratio.
- ϵ_h = tensile strain of soil.
- E = elastic modulus with respect to total stress.
- H = elastic modulus with respect to matric suction.

3.5 PLASTIC EQUILIBRIUM ANALYSIS

For a given failure criterion, the shear strength of any soils can be expressed as a function of independent stress state variables and the soil shear strength parameters. Let us consider the shear strength of unsaturated soils in terms of the $(\sigma - u_a)$ and $(u_a - u_w)$ stress state variables. Fredlund et al (1978) proposed a shear strength equation,

$$\tau = c' + (\sigma - u_a) \tan \phi' + (u_a - u_w) \tan \phi^b \quad [3.18]$$

where:

- τ = shear strength.
- c' = cohesion intercept where the two stress variables are zero.
- ϕ' = friction angle with respect to changes in $(\sigma - u_a)$.
- ϕ^b = friction angle with respect to changes in $(u_a - u_w)$.

The Mohr circles corresponding to the failure conditions can be plotted on a three-dimensional diagram as shown in Fig. 3.06. The axes in the horizontal plane are the stress state variables and the ordinate is the shear strength.

It is possible to consider the matric suction term as part of the cohesion of soil. In other words, matric suction increases the cohesion of the soil (Fredlund, 1979).

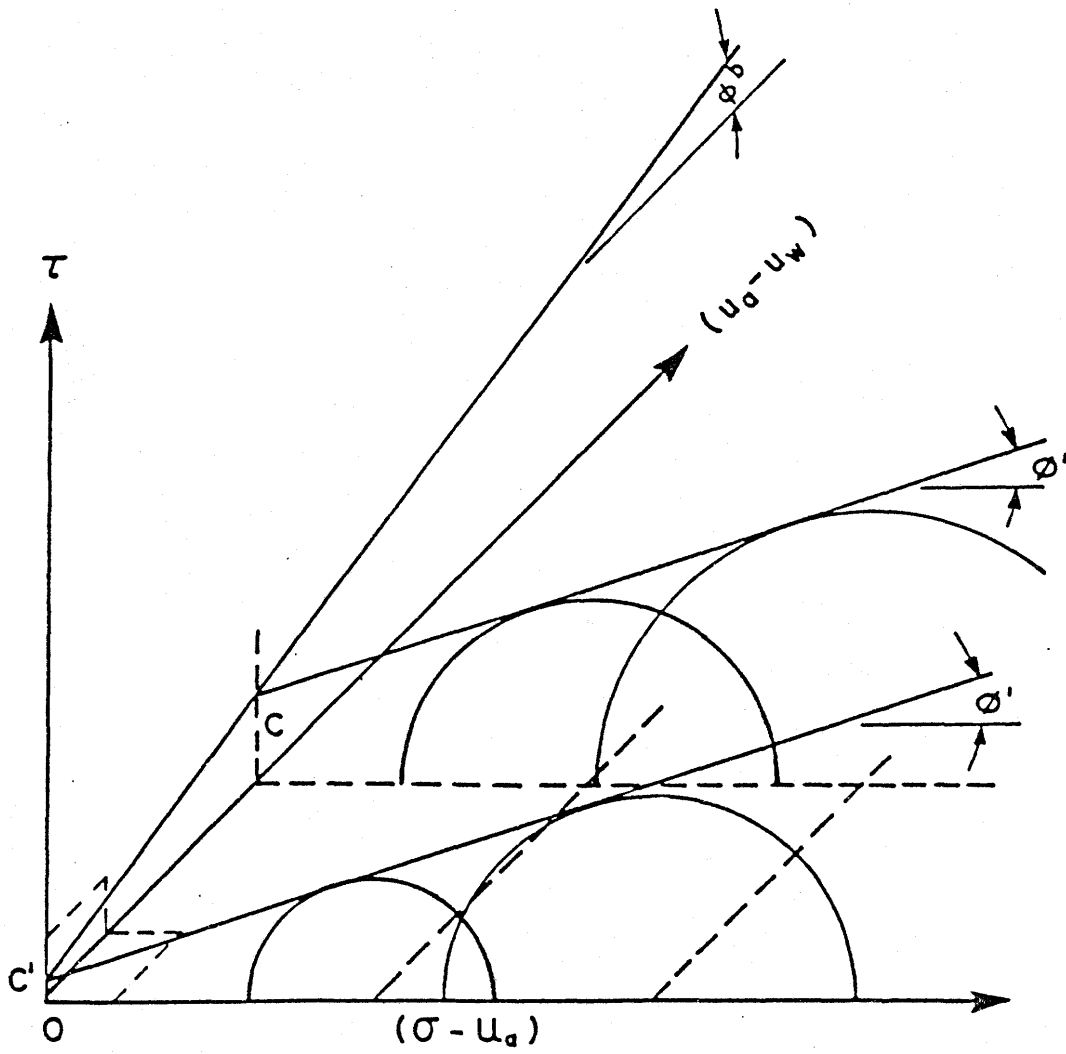


Fig. 3.06: Three dimensional failure surface using stress variable $(\sigma - u_a)$ and $(u_a - u_w)$ (after Fredlund, 1981).

Therefore, the cohesion of the soil, c , has two components.

$$c = c' + (u_a - u_w) \tan \phi^b \quad [3.19]$$

Substituting equation [3.19] into [3.18], gives

$$\tau = c + (\sigma - u_a) \tan \phi' \quad [3.20]$$

The three-dimensional failure surface in Fig. 3.06 is applicable to unsaturated soils under compression. In order to describe the behavior of soil under tension, a failure criterion extended to the tension zone is required. It has been discussed in section 2.5.4 that the Modified Mohr-Coulomb Failure Criterion (Fang and Chen, 1971, 1972) appears to be appropriate for describing the behavior of soils under tension. Accordingly, this criterion is used to study the soil cracking under plastic equilibrium conditions.

Let us consider a soil element locating at the tip of a vertical soil crack as shown in Fig. 3.07. If both the horizontal and vertical stresses are assumed to be principal stresses, the stress condition of this soil element is given by the Mohr circle "A" as shown in Fig. 3.08. The minor and major principal stresses of this soil element would be equal to the allowable tensile strength σ_t and the total overburden pressure σ_v , respectively.

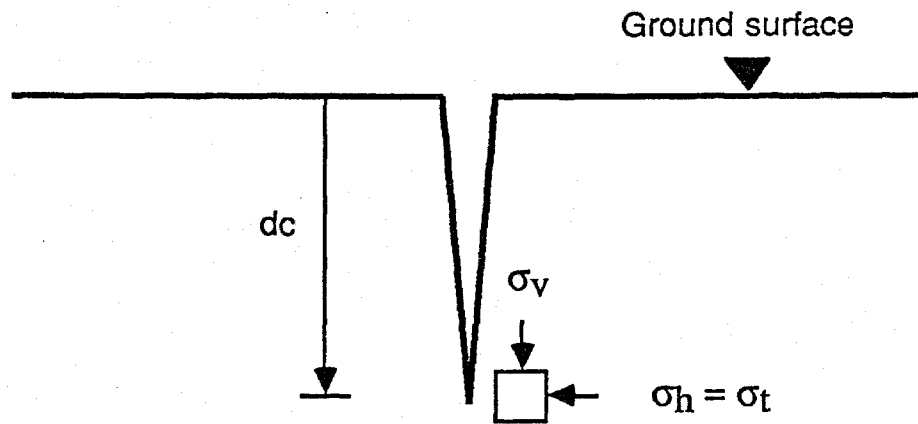
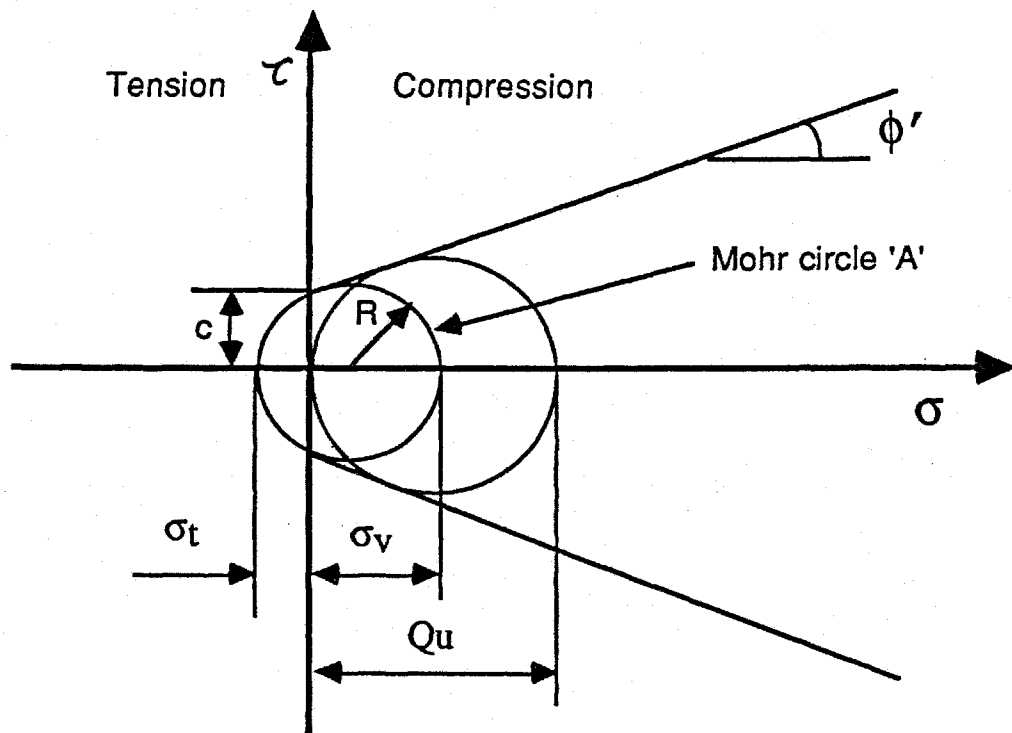


Fig. 3.07: A typical soil element at the tip of a desiccation crack.



$$R = \left[\frac{Q_u}{2} - \frac{\sigma_t \sin \phi'}{(1 - \sin \phi')} \right]$$

Fig. 3.08: Modified Mohr-Coulomb Failure Criterion (after Fang and Chen, 1971, 1972).

By definition of the Modified Mohr-Coulomb Failure Criterion, the radius, R of the Mohr Circle "A" is

$$R = \frac{Q_u}{2} - \frac{\sigma_t \sin \phi'}{(1 - \sin \phi')} \quad [3.21]$$

where :

R = radius of the Mohr circle as shown in Fig. 3.19.
 Q_u = unconfined compressive strength
 σ_t = allowable tensile strength
 ϕ' = effective friction angle.

The allowable tensile strength can be related to the unconfined compressive strength by a factor Ft, such that

$$\frac{Q_u}{\sigma_t} = \frac{1}{Ft} \quad [3.22]$$

From Fig. 3.08, the major principal stress (i.e., the vertical total stress) is given by,

$$\sigma_v = 2R - \sigma_t \quad [3.23]$$

Substituting equations [3.21] and [3.22] into [3.23], gives,

$$\sigma_v = \frac{2c \cos \phi'}{(1 - \sin \phi')} \left[1 - Ft - \frac{2 Ft \sin \phi'}{(1 - \sin \phi')} \right] \quad [3.24]$$

As matric suction increases the cohesion of an unsaturated soil (equation [3.20], Fredlund, 1979), the cohesion at the bottom of the crack can be expressed as

$$c = c' + (u_a - u_w)_{dc} \tan \phi^b \quad [3.25]$$

Also, stress in the vertical direction is,

$$\sigma_v = dc \gamma \quad [3.26]$$

where: dc = depth of crack
 c' = cohesion intercept where $(\sigma - u_a)$ and $(u_a - u_w)$ are zero.
 ϕ^b = friction angle with respect to $(u_a - u_w)$.
 γ = total unit weight of soil.
 σ_v = overburden pressure.
 $(u_a - u_w)_{dc}$ = matric suction at the crack depth level.

Substituting equations [3.25] and [3.26] into [3.24], gives,

$$dc \gamma = \frac{2 \cos \phi' \{c' + (u_a - u_w)_{dc} \tan \phi^b\}}{(1 - \sin \phi')} \left[1 - Ft - \frac{2Ft \sin \phi'}{(1 - \sin \phi')} \right] \quad [3.27]$$

Let us consider two matric suction profiles as discussed in section 3.3. Substituting equations [3.13] and [3.14] into [3.27], gives two expressions for the crack depths for two matric suction profiles.

For matric suction profile "A", the depth of crack is given as,

$$dc = \frac{\frac{c'}{\gamma_w} + F_w D_w \tan \phi^b}{X + F_w \tan \phi^b} \quad [3.28]$$

$$\text{where: } X = \frac{\frac{\gamma}{\gamma_w} (1 - \sin \phi')^2}{2 \cos \phi' \{ (1-F_t) - (1+F_t) \sin \phi' \}} \quad [3.29]$$

For matric suction profile "B", the depth of crack is given as,

$$dc = \frac{2 (c' + F_w D_w \gamma_w \tan \phi^b) Y}{\gamma} \quad [3.30]$$

$$\text{where: } Y = \frac{\cos \phi'}{(1 - \sin \phi')} \left[1 - F_t - \frac{2 F_t \sin \phi'}{(1 - \sin \phi')} \right] \quad [3.31]$$

where:

- dc = depth of crack.
- γ = total unit weight of soil.
- γ_w = total unit weight of water.
- D_w = depth to groundwater table.
- F_w = matric suction profile factor.
- F_t = ratio of tensile strength to unconfined compressive strength.
- c' = cohesion intercept where the two stress variables are zero.
- ϕ' = friction angle with respect to changes in $(\sigma - u_a)$.
- ϕ^b = friction angle with respect to changes in $(u_a - u_w)$.

CHAPTER 4

ANALYTICAL AND EXPERIMENTAL PROGRAM

4.1 INTRODUCTION

This chapter describes the analytical and experimental programs that were undertaken in this study. The objectives and the methodology of each program are presented.

4.2 ANALYTICAL PROGRAM

The objective of the analytical program was to relate pertinent soil properties to the prediction of crack depth. The program consisted of deriving mathematical expressions for the prediction of theoretical crack depth. The mathematical expressions were expressed in terms of stress state variables and material properties. The relative effect of various soil parameters on the theoretical depth of desiccation cracks was investigated.

The volume change and the shear strength behavior of a desiccated soil can be described using unsaturated soil mechanics principles. Two expressions for the theoretical crack depth can be obtained using the elastic equilibrium

(i.e., volume change) and the plastic equilibrium (i.e., shear strength) analyses. The derivation of these expressions were presented in Chapter 3.

In order to evaluate the relative effect of various soil parameters on the crack depth, a parametric study was conducted using the theoretical expressions. The parametric study consists of generating graphs for the theoretical crack depth using normal ranges of soil parameters.

Since the ratio between the E and H moduli is required to describe elastic equilibrium conditions in a soil, the relationship between these moduli must be evaluated. The empirical relationship between the E and H moduli was investigated in Chapter 5. Experimental data on suction tests and one-dimensional consolidation tests performed by others were analysed to estimate the normal range of the E to H ratio for slurried Regina Clay and compacted silt.

4.3 EXPERIMENTAL PROGRAM

The objective of the experimental program was to study the characteristics of cracking and shrinkage of soils. The program consisted of conducting shrinkage tests and cracking tests on slurried soils. A total of three shrinkage tests and six cracking tests were performed. The factors that

control crack spacing were considered by observing the behavior of soils cracking during the experimental program. The matric suction, water content and the amount of soil shrinkage were measured during the desiccation process.

4.3.1 Soils

Two types of soils were used for the experiments. The materials were glacial till and clay with common local names as Indian Head Till and Regina Clay, respectively. All soils were obtained with the co-operation of the Saskatchewan Department of Highways and Transportation, Regina Branch.

In the laboratory, the soils were spread on a table and allowed to dry in air. Large soil lumps were crushed by means of a rubber hammer. The soils were then sieved through a #10 (2.0mm) screen and stored in the laboratory.

The Indian Head Till is a well-graded material with clay to gravel sized particles as illustrated by the gradation curve shown in Fig. 4.01. It is moderately plastic, having a liquid limit of 34.3% and a plastic limit of 14.2%.

The Regina Clay is a material with clay to silt sized particles as illustrated by the gradation curve shown in

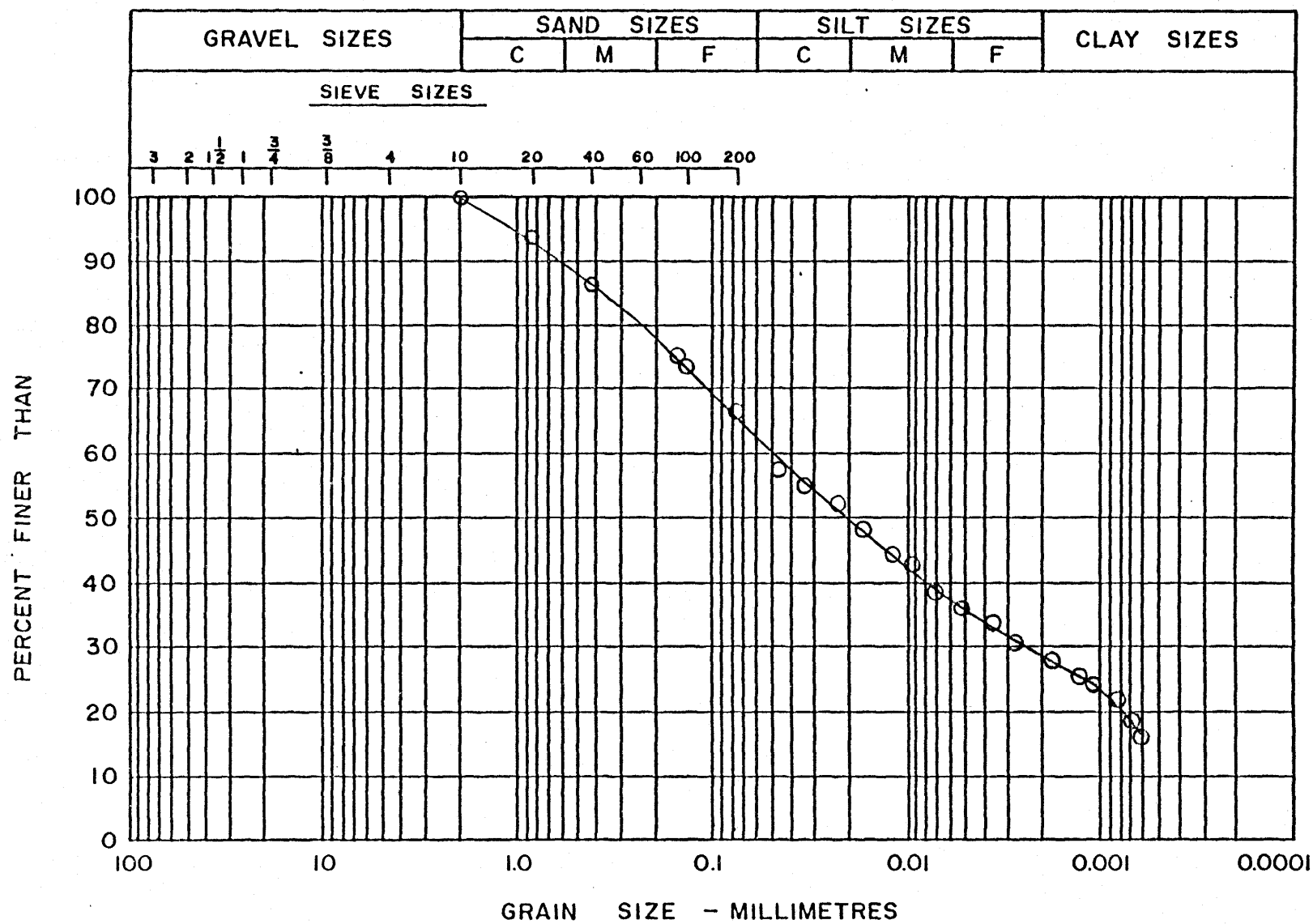


Fig. 4.01: Grain size gradation curve for Indian Head Till.

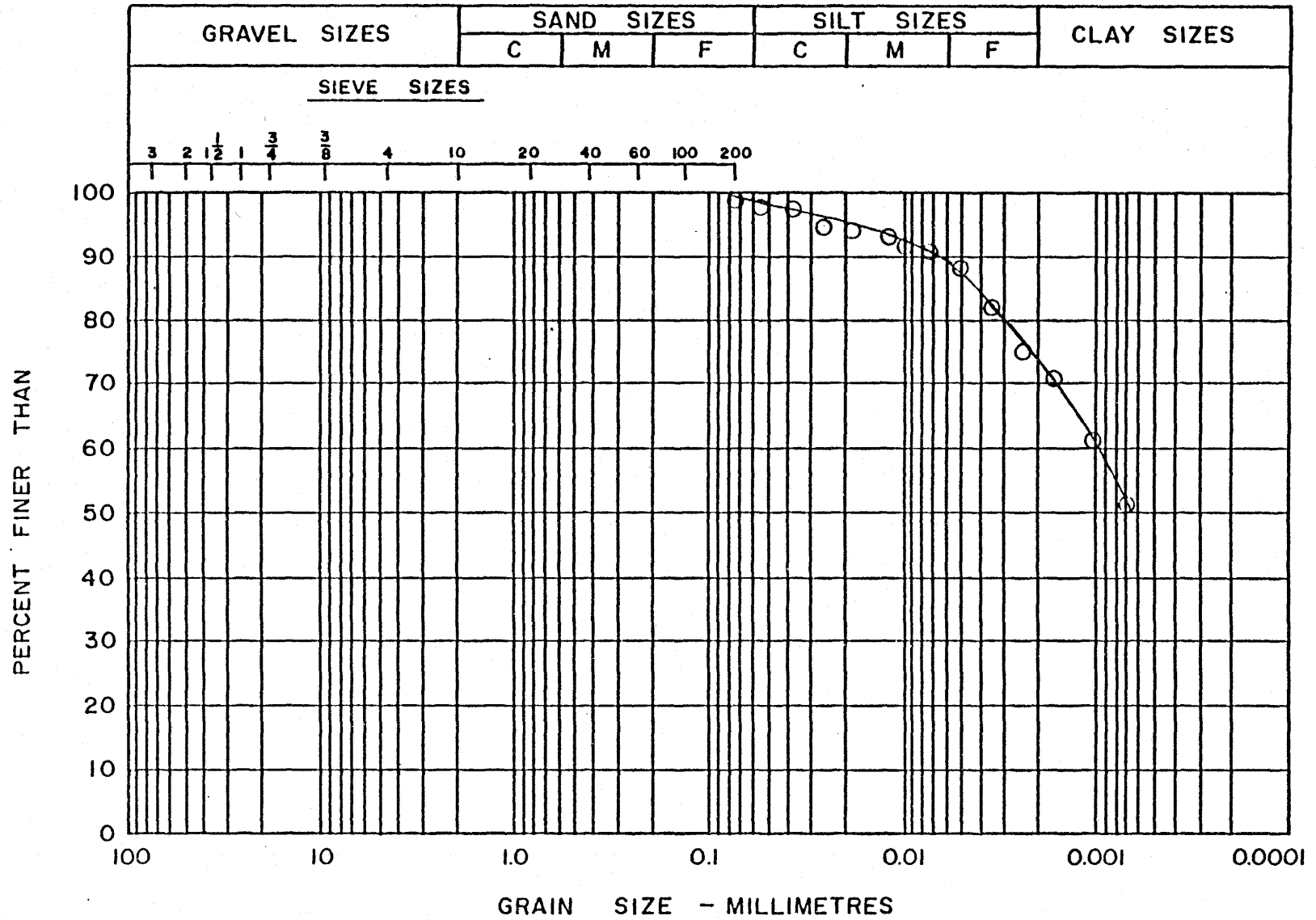


Fig. 4.02: Grain size gradation curve for Regina Clay.

Table 4.01: Summary of the properties of the soils used in the laboratory testing program.

	Indian Head till	Regina Clay
% Sand	37.5%	NIL
% Silt	34.0%	27.0%
% Clay	28.5%	73.0%
Liquid Limit	34.3%	80.5%
Plastic Limit	14.2%	26.2%
Plasticity Index	20.1%	54.3%
Shrinkage Limit	14.0%	22.0%

Fig. 4.02. It is highly plastic, having a liquid limit of 80.5% and a plastic limit of 26.2%. The physical properties of the till and clay are summarized in Table 4.01.

4.3.2 Containers

The shrinkage tests were conducted using a cylindrical brass container of 61.50 mm internal diameter and 22.85 mm deep. A set of three brass containers were used for each shrinkage test as shown in Fig. 4.03. The interior walls of all the brass containers were sprayed with a layer of dry lubricant (polytetra-fluro-ethylene) in order to reduce the adhesion and friction between the soil paste and the containers.

The experiments on the cracking of soils were carried out in a flat wooden container of 0.61 x 0.61 m² plan area and 76 mm deep as shown in Fig. 4.04. The interior walls of the container were lined with a layer of formica panel to refrain any soil water from migrating into the wood. Clear silicon was also applied to the interior edges and corners of the container to seal the gaps in between the walls. Holes (8 mm in diameter) were drilled on the bottom and side walls of the container to provide access for the installation of ceramic cup sensors (from the tensiometer) into the soil. Four dial guages were installed at four

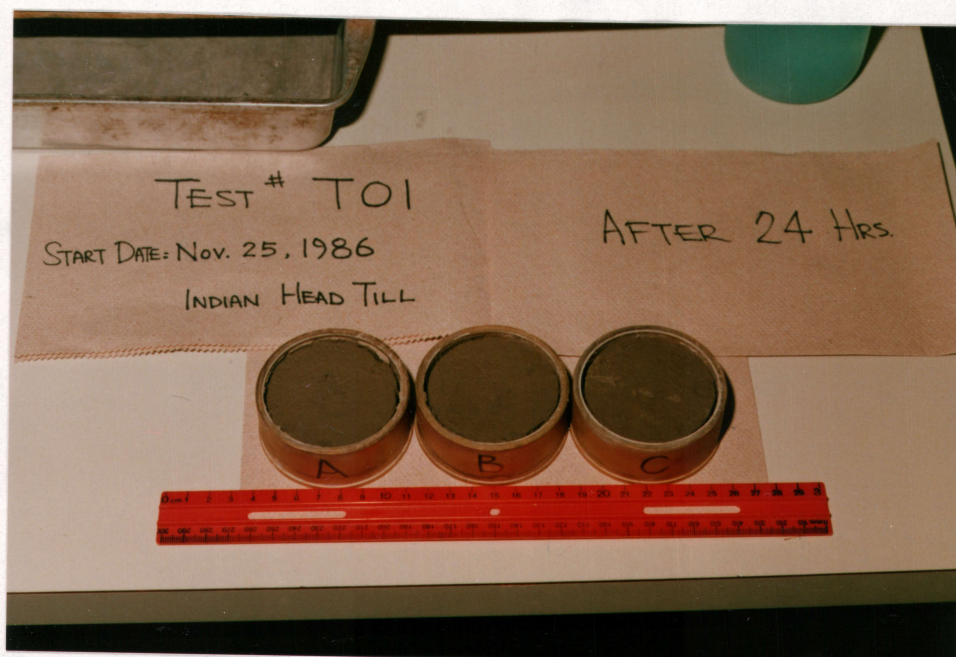
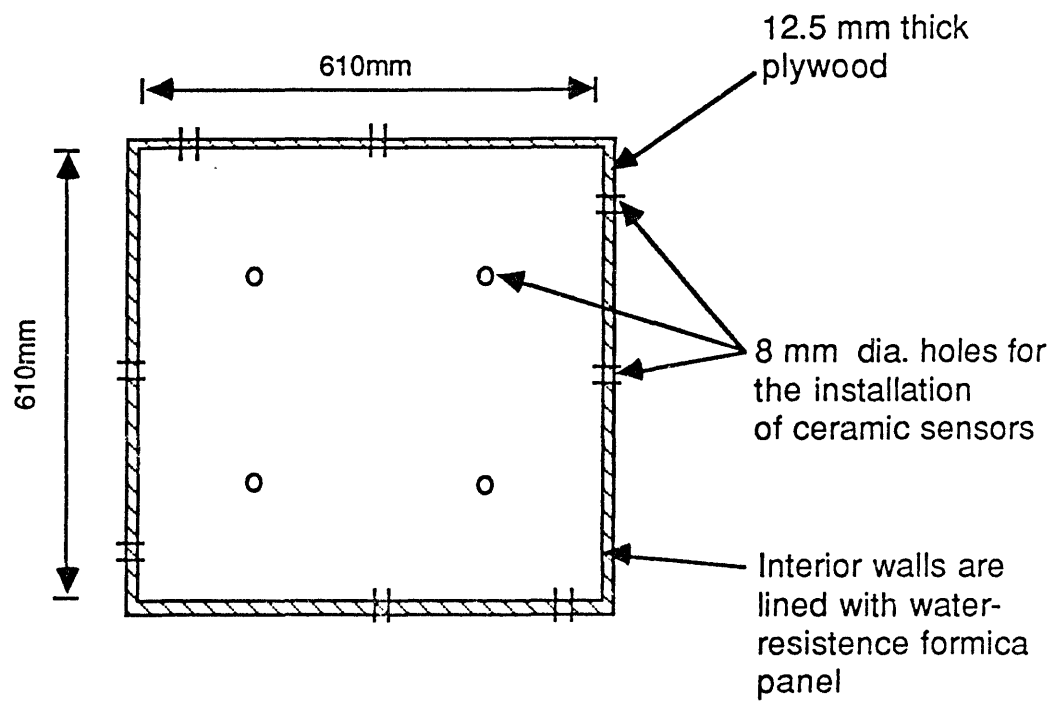
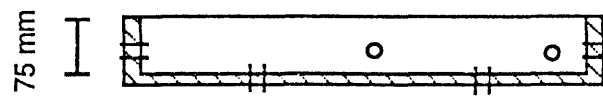


Fig. 4.03: Brass containers of 61.50 mm I.D. and 22.85 mm deep were used for the shrinkage test.



PLAN VIEW



SIDE VIEW

Fig. 4.04: Dimensions of the wooden container used for the cracking test.

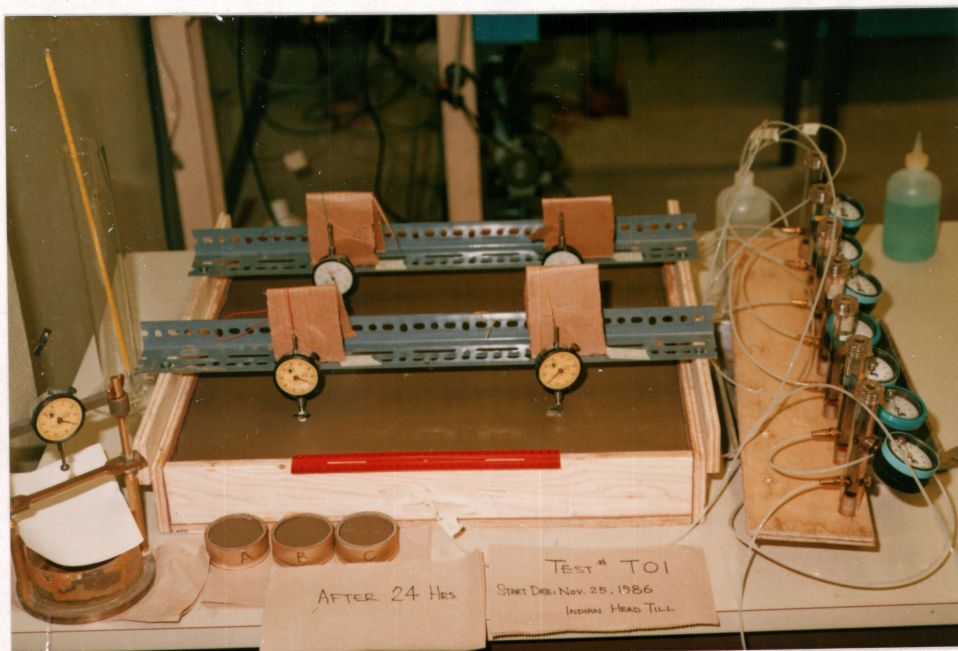


Fig. 4.05: The layout of equipment for the cracking test.

quadrants of the container to measure the vertical soil shrinkage during desiccation. The set up of the equipment for the cracking test is shown in Fig. 4.05.

4.3.3 Tensiometer

Four flexible tube tensiometers (Soilmoisture Equipment Corp. Model No. 2100F) were used to measure the matric suction of the soils during the cracking tests. The upper part of the flexible plastic tube tensiometer (Fig. 4.06) is about 150 mm long and serves as a water reservoir and the housing for a vacuum dial gauge. Attached to the base of the reservoir is a 1 m (metre) long flexible tube with an outside diameter of 3 mm. A 25 mm long and 6 mm in diameter porous ceramic cup sensor is attached to the end of the flexible tube.

Before the tensiometers were assembled, all vacuum dial gauges were calibrated with an known vacuum source. De-aired distilled water was used to fill the reservoir of the tensiometer. All tensiometers used in the experiments were installed in accordance with the manufacturer's recommended procedures as provided in Appendix B. After initial installation, the tensiometer is in balance with the soil suction in the soil. The suction value on the vacuum dial gauge indicates the suction at the porous ceramic cup. The

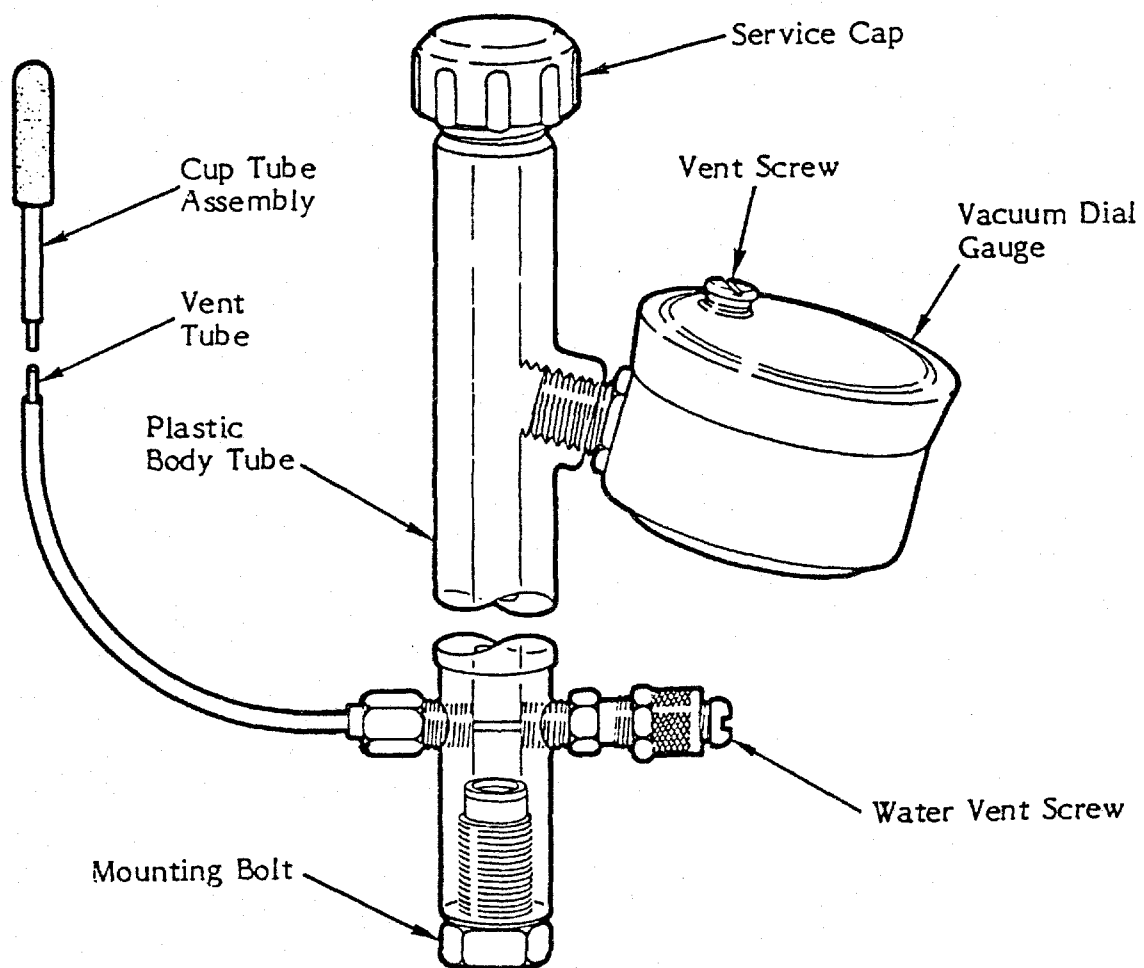


Fig. 4.06: Flexible tube tensiometer (after Soilmoisture Equipment Corp. Model No. 2100F).

range of soil suction over which the tensiometer can be used reliably is 0 to 85 kPa.

4.3.4 Temperature and Humidity

All experiments were carried out in the Soil Mechanics graduate students' laboratory at the University of Saskatchewan. Precautions were taken to prevent sunlight or air current (ventilation) from striking directly the soil surface. The room temperature was kept at a range between 23 and 25 degrees Celsius. Although the laboratory had no humidity control, the humidity was maintained fairly constant at about 25% to 30% throughout the experiments.

4.3.5 Experimental Procedures

A total of three shrinkage tests (i.e., Test Nos. S01 to S03) and six cracking tests (i.e., Test Nos. T01 to T06) were conducted. Detailed conditions of all the tests are summarized in Table 4.02.

The shrinkage test consists of continuously measuring the changes in soil volume and water content when a given amount of slurried soil was allowed to dry in the

Table 4.02: Detailed conditions of the shrinkage tests and cracking tests.

Shrinkage Test No.	Soil type	Mixing water content (w%)
S01	Till	37.7%
S02	Till	31.0%
S03	Clay	80.0%

Cracking Test No.	Soil type	Mixing w%	Average Soil thickness
T01	Till	37.7%	58.8 mm
T02	Till	38.2%	54.1 mm
T03	Till	31.1%	60.4 mm
T04	Till	38.1%	33.7 mm
*T05	Clay	82.5%	59.7 mm
*T06	Till	37.5%	60.8 mm

* Remarks: Container side walls were lined with wax papers and aluminum foils for Test Nos. T05 and T06

laboratory. A total of three soil samples were used in each shrinkage test. Two shrinkage tests (i.e., Test No. S01 and S02) were carried out on Indian Head Till with water contents of 37.7% and 31.0%. One shrinkage test (i.e., Test No. S03) was performed on Regina Clay which was mixed at a water content of 80.0%.

About 45 kg (i.e., 100 lb) dry soils was used in each cracking test. All soils were hand-mixed to the desired water content in a large container as shown in Fig. 4.07. After the soil had been thoroughly mixed to a smooth paste, it was placed in the wooden container. The soil paste was vibrated slightly for a duration of about two minutes using a handheld electric vibrating probe (Fig. 4.08) to drive out the occluded air bubbles. The soil surface was spread smoothly and levelled using a trowel.

Upon completion of the soil mixing process, four ceramic cup sensors were installed within the soil at the desired locations. The soil was then allowed to cure for a period of about 24.0 hours in room temperature. In order to prevent any loss of water during the curing period, a layer of 50 mm thick styrofoam and a layer of plastic sheet were placed on top of the wooden container.

At the beginning of the cracking test, the plastic sheet and the styrofoam were removed. Four dial gauges were



Fig. 4.07: The soils for the cracking test was hand-mixed to the desired water content.



Fig. 4.08: After mixing, the soils was placed in the wooden container and was vibrated slightly to reduce occluded air bubbles.



Fig. 4.09: Small amount of soil was sampled to determine the water content during the cracking test. After sampling, the cavity was filled with soils of suitable water content.

installed at four quadrants of the container. During the test, the matric suction and any vertical soil shrinkage were monitored from the tensiometers and the dial gauges, respectively. After the cracking started, soil water contents were measured periodically at selected soil depths. The measurements were made by taking a small amount of soil at different soil depth each time. Cavities made by the sampling process were filled with soil of suitable water content immediately after sampling (Fig. 4.09). Photographs were also taken periodically to record the development of the soil cracking pattern.

Five cracking tests were performed on Indian Head Till: Test Nos. T01, T02, T04 and T06 were performed at water contents of about 38% (i.e., about 4% above its liquid limit), and Test No. T03 was at a water content of 31.1%. One cracking test (i.e., Test No. T05) was conducted on Regina Clay, which was mixed at a water content of 82.5% (i.e., about 2% above its liquid limit).

The soil thickness for all the tests ranged between 54.1 mm and 60.8 mm, with the exception of Test No. T04, which was 33 mm thick. Wax paper and aluminum foil were placed on the interior side walls of the container in Test Nos. T05 and T06 in order to study the effect of side wall adhesion on soil cracking.

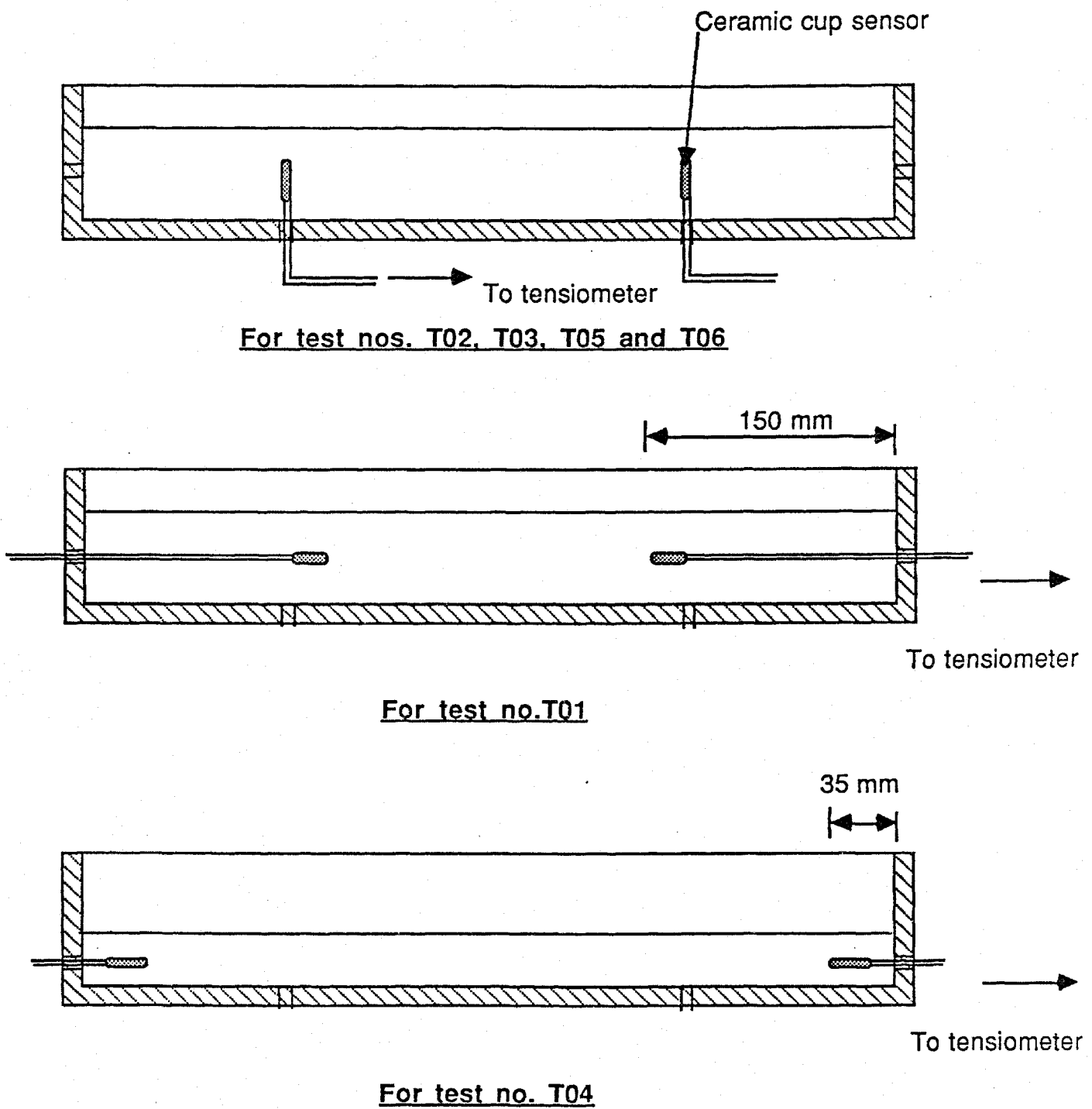


Fig. 4.10: Various positions for the installation of the ceramic cup sensors in different cracking tests.

The ceramic cup sensors of the tensiometer were originally installed horizontally 150 mm into the soil paste from the side wall of the container. After Test No. T01, it was found that the positions of the sensors seemed to produce a strong influence on the cracking pattern. In Test Nos. T02, T03, T05 and T06, all the ceramic cup sensors were installed vertically from the bottom of the container (Fig. 4.10) to minimize soil disturbance. Since the soil was too thin in Test No. T04, the sensors had to be installed horizontally 35 mm into the soil from the container side wall.

CHAPTER 5

RELATIONSHIP BETWEEN THE ELASTIC MODULI E AND H

5.1 INTRODUCTION

Using the elastic equilibrium analysis, a mathematical expression for the prediction of theoretical crack depth was derived in Section 3.4. The expression was expressed as a function of the ratio between the elastic modulus E and the elastic modulus H . In order to use the expression for the prediction of crack depth, the E/H ratio is required. The relationship between these moduli must either be experimentally evaluated or estimated. At present, there is little experimental data on the direct measurement of these moduli. The purpose of this chapter is to study the empirical relationship between the E and H moduli. The possible range of the E/H ratio is estimated using the experimental data from the suction tests and one-dimensional consolidation tests performed by other researchers.

5.2 EMPIRICAL RELATIONSHIP BETWEEN THE E AND H MODULI

There is little information in the literature on the relationship between the elastic modulus E , with respect to

net total stress and the elastic modulus H , with respect to matric suction. Let us consider the relationship between these moduli from a semi-empirical approach. The constitutive relationships for the volume change behavior of an elastic material can be expressed as,

$$\epsilon_x = \frac{\sigma_x}{E} - \frac{\mu (\sigma_y + \sigma_z)}{E} \quad [5.01]$$

$$\epsilon_y = \frac{\sigma_y}{E} - \frac{\mu (\sigma_z + \sigma_x)}{E} \quad [5.02]$$

$$\epsilon_z = \frac{\sigma_z}{E} - \frac{\mu (\sigma_x + \sigma_y)}{E} \quad [5.03]$$

The volumetric strain due to a change of stress is

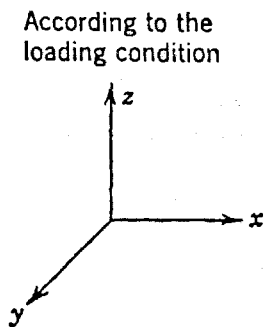
$$-\frac{\delta V}{V} = \epsilon_{vol} = \epsilon_x + \epsilon_y + \epsilon_z \quad [5.04]$$

where:

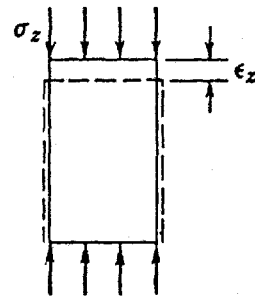
- $\epsilon_x, \epsilon_y, \epsilon_z$ = strains in the x, y and z directions.
- $\sigma_x, \sigma_y, \sigma_z$ = stresses in the x, y, and z directions.
- μ = Poisson's ratio.
- E = elastic modulus.
- δV = a change in volume.
- V = original volume.
- ϵ_{vol} = volumetric strain.

If we consider the K_0 or one-dimensional compression loading condition as shown in Fig. 5.01, the strains in the horizontal directions are zero, that is,

$$\epsilon_x = \epsilon_y = 0 \quad [5.05]$$



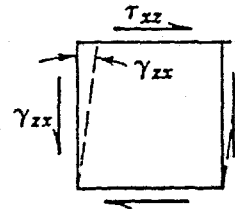
Uniaxial loading



Young's modulus

$$E = \frac{\sigma_z}{\epsilon_z}$$

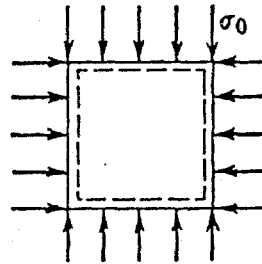
Simple shear



Shear modulus

$$G = \frac{\tau_{xz}}{\gamma_{xz}}$$

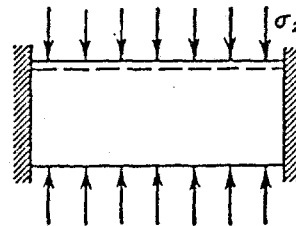
Isotropic compression



Bulk modulus

$$B = \frac{\sigma_0}{3\epsilon_z}$$

Confined compression



Constrained modulus

$$D = \frac{\sigma_z}{\epsilon_z}$$

Fig. 5.01: Various types of loading conditions and moduli (after Lambe and Whitman, 1969).

Substituting equation [5.05] into [5.01], [5.02] and [5.03] gives,

$$\sigma_x = \sigma_y = \frac{\mu}{(1 - \mu)} \sigma_z \quad [5.06]$$

$$\text{and,} \quad \varepsilon_z = \frac{\sigma_z}{E} \frac{(1 + \mu)(1 - 2\mu)}{(1 - \mu)} \quad [5.07]$$

For K_0 loading conditions, the constrained modulus D is defined as,

$$D = \frac{\sigma_z}{-(\delta V/V)} \quad [5.08]$$

Substituting equations [5.04], [5.05] and [5.07] into [5.08], the constrained modulus D becomes,

$$D = \frac{E (1 - \mu)}{(1 + \mu)(1 - 2\mu)} \quad [5.09]$$

Since the matric suction is a three-dimensional, isotropic loading condition, the bulk modulus B_m and the elastic modulus H with respect to the matric suction are defined as,

$$B_m = \frac{\delta(u_a - u_w)}{\varepsilon_{vol}} \quad [5.10]$$

$$\text{and,} \quad H = \frac{\delta(u_a - u_w)}{\varepsilon_x} \quad [5.11]$$

For an isotropic soil, the strains in the x, y, and z directions will be the same, that is,

$$\epsilon_x = \epsilon_y = \epsilon_z = \epsilon \quad [5.12]$$

Substituting equations [5.12] into [5.04], the volumetric strain for an isotropic soil subjected to isotropic loading conditions is,

$$\epsilon_{vol} = 3 \epsilon \quad [5.13]$$

The bulk modulus B_m can be related to the elastic modulus H using equations [5.10], [5.11] and [5.13] as,

$$B_m = \frac{H}{3} \quad [5.14]$$

Combining equations [5.09] and [5.14], a theoretical relationship between the elastic moduli E and H is given by,

$$\frac{E}{H} = \frac{1}{3} \frac{D}{B_m} \frac{(1 + \mu)(1 - 2\mu)}{(1 - \mu)} \quad [5.15]$$

The constitutive relationships for the soil structure of an unsaturated soil are given in equations [3.03], [3.04] and [3.05]. For one-dimensional loading conditions, Fredlund (1979, 1981) proposed a three dimensional plot of the stress state variables versus void ratio (Fig. 5.02). The constitutive surface can be linearized over a wider range of stress change using the logarithm of stress state

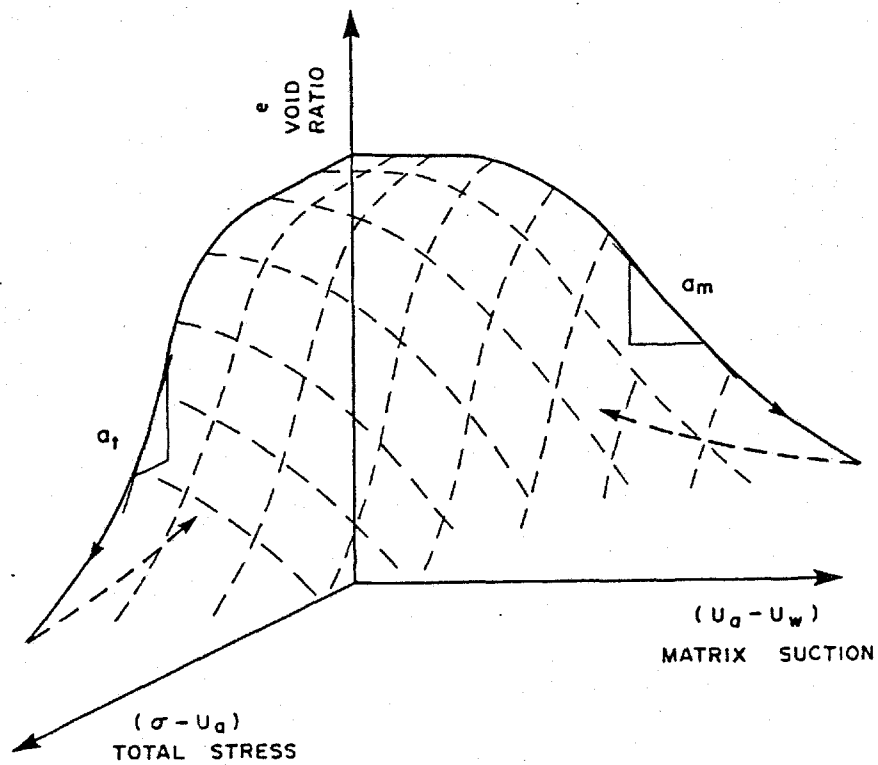


Fig. 5.02: Arithmetic representation of stress state variables versus void ratio (after Fredlund, 1979).

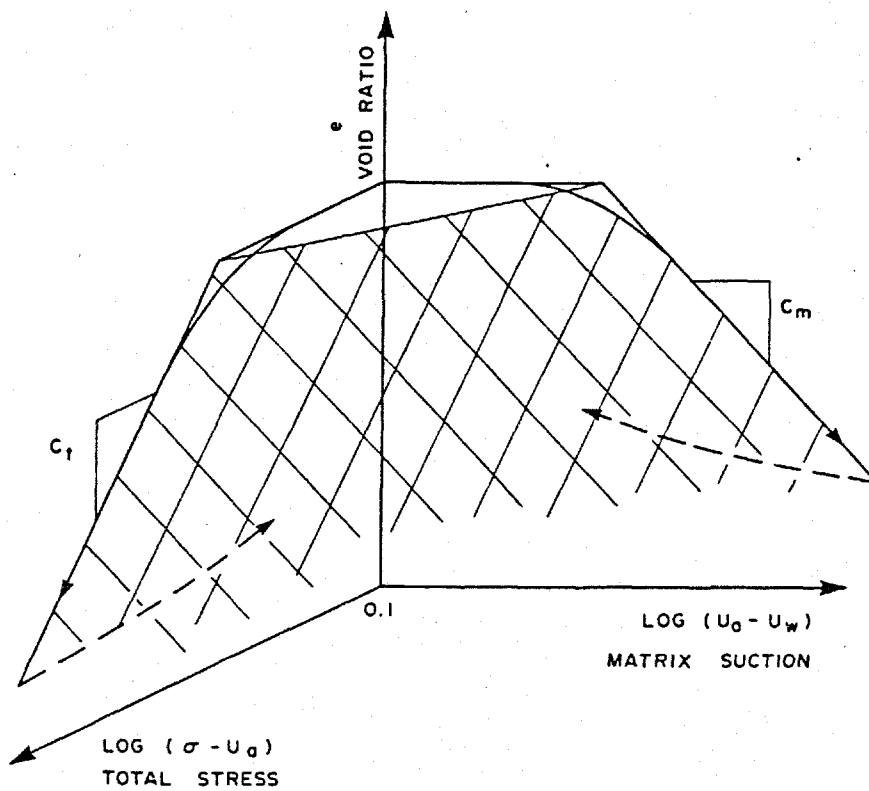


Fig. 5.03: Logarithm of stress state variables versus void ratio (after Fredlund, 1979).

variables (Fig. 5.03). According to Fig. 5.03, the void ratio under any set of stress conditions can be written as,

$$e_f = e_o - C_t \log \delta(\sigma - u_a) - C_m \log \delta(u_a - u_w) \quad [5.16]$$

where:

C_t = compressive index with respect to a change of total stress $(\sigma - u_a)$.

C_m = compressive index with respect to a change of matric suction $(u_a - u_w)$.

e_o = initial void ratio.

e_f = final void ratio.

The constrained modulus D with respect to the net total stress $(\sigma - u_a)$ can be related to the compressive index obtained from a one-dimensional consolidation test (Lambe and Whitman, 1969) as,

$$D = \frac{(1 + e_o) \delta(\sigma_v - u_a)}{(e_f - e_o)} \quad [5.17]$$

$$\text{and,} \quad D = \frac{(1 + e_o) (\sigma_v - u_a)_a}{0.435 C_t} \quad [5.18]$$

where:

$(\sigma_v - u_a)_a$ = average of initial and final net total stresses.

e_o = initial void ratio.

e_f = final void ratio.

Let us consider the plot of logarithm of matric suction versus void ratio in Fig. 5.03. Since the matric suction is

an isotropic loading process, equations [5.17] and [5.18] can also be used to calculate the bulk modulus B_m , that is,

$$B_m = \frac{(1 + e_o) \delta(u_a - u_w)}{(e_f - e_o)} \quad [5.19]$$

$$\text{and,} \quad B_m = \frac{(1 + e_o) (u_a - u_w)_a}{0.435 C_m} \quad [5.20]$$

where:

$(u_a - u_w)_a$ = average of initial and final net matric suction.

For the same stress range of net total stress and net matric suction (i.e., $(\sigma_v - u_a)_a$ is equal to $(u_a - u_w)_a$), the relationship between D , B_m , C_t and C_m is given by combining equations [5.18] and [5.20], that is,

$$\frac{D}{B_m} = \frac{C_m}{C_t} \quad [5.21]$$

Substituting equation [5.21] into [5.15] gives a theoretical relationship between the E and H ratio and the compressive indices C_m and C_t as,

$$\frac{E}{H} = \frac{1}{3} \frac{C_m}{C_t} \frac{(1 + \mu)(1 - 2\mu)}{(1 - \mu)} \quad [5.22]$$

When the degree of saturation approaches 100%, C_t is approximately equal to C_m (Fredlund, 1981), and C_t becomes equal to the conventional compressive index, C_c . At low degrees of saturation, C_t will be greater than C_m . The C_m/C_t

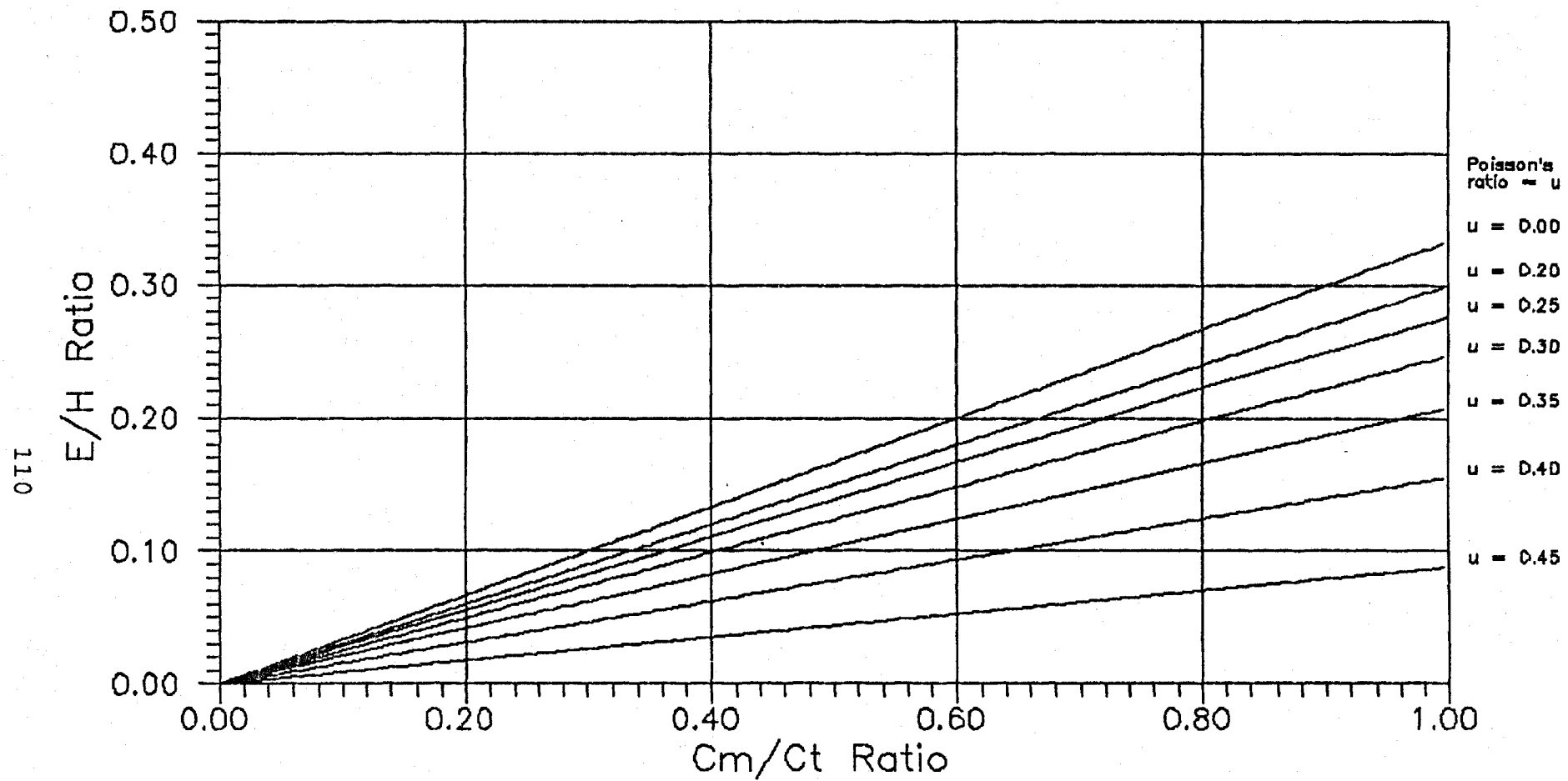


Fig. 5.04: Theoretical C_m/C_t ratio versus E/H ratio.

ratio will therefore have a possible value between zero and one. At present, the literature contains little data on the quantitative relationship between the compressive indices for soils with low degrees of saturation (Fredlund, 1981). The theoretical relationship between the E/H ratio and the C_m/C_t ratio according to equation [5.22] is shown in Fig. 5.04. It can be noted that the maximum theoretical E/H ratio is $1/3$, when C_m/C_t is equal to unity and the Poisson's ratio is zero. When C_m/C_t is zero, the minimum theoretical E/H ratio is equal to zero.

5.3 EXPERIMENTAL DATA ON E/H RATIO

Fredlund (1964) conducted suction tests and one-dimensional consolidation tests on slurried Regina Clay. Plots of logarithm of matric suction versus void ratio and logarithm of effective stress versus void ratio obtained from the experiments are shown in Figs. 5.05 and 5.06, respectively. The elastic moduli E , with respect to total stress at different stress levels were calculated using equations [5.09] and [5.17] as shown in Table 5.01. Similarly, the elastic moduli H , with respect to matric suction were estimated using equations [5.14] and [5.19] as shown in Table 5.02. The estimated ratios between E and H , at different stress levels are shown in Table 5.02 or in Fig. 5.07. From Fig. 5.08 the slurried Regina Clay is shown

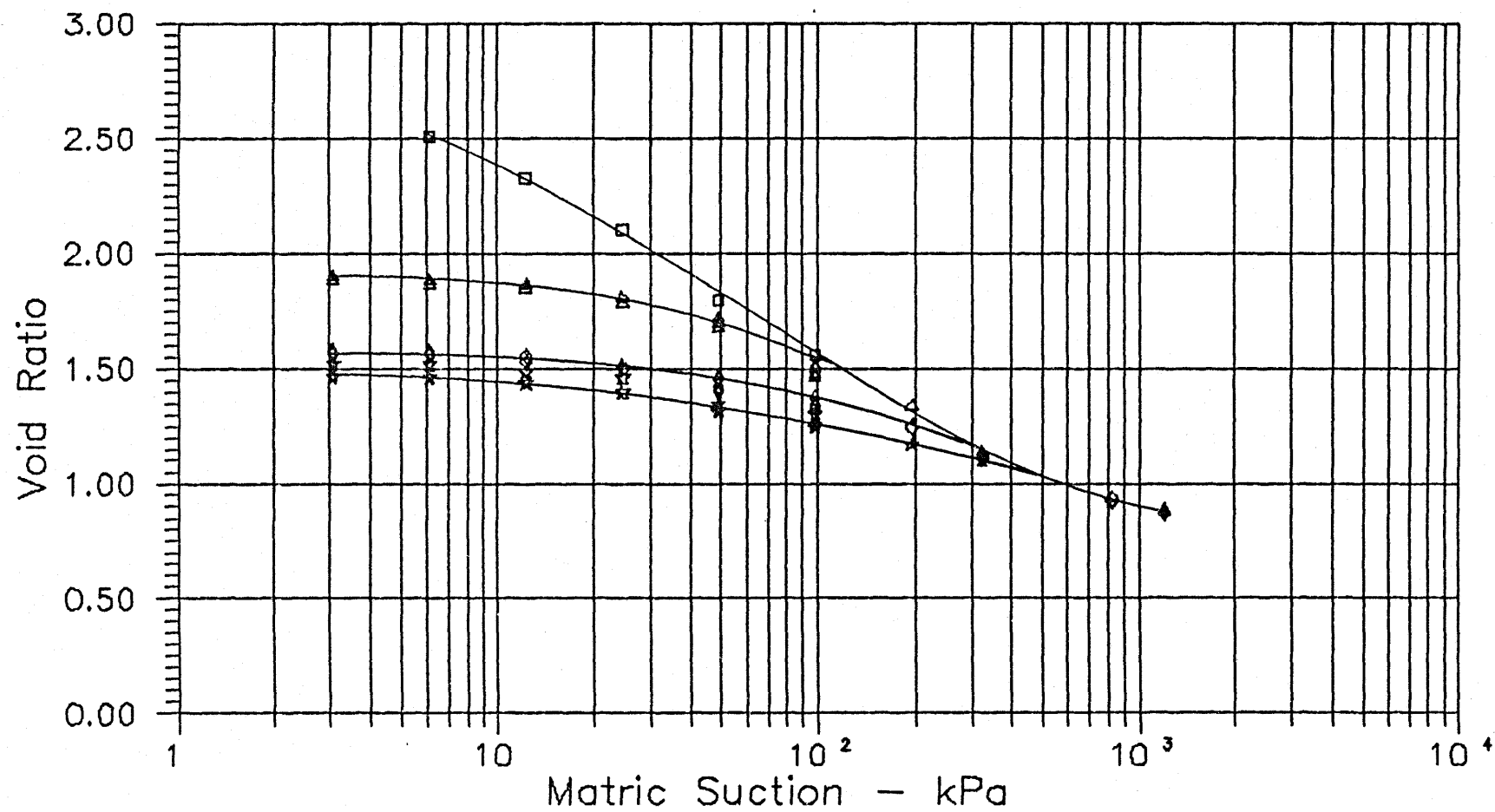


Fig. 5.05: Logarithm of matric suction versus void ratio, suction tests on slurried Regina Clay, (data obtained from Fredlund, 1964).

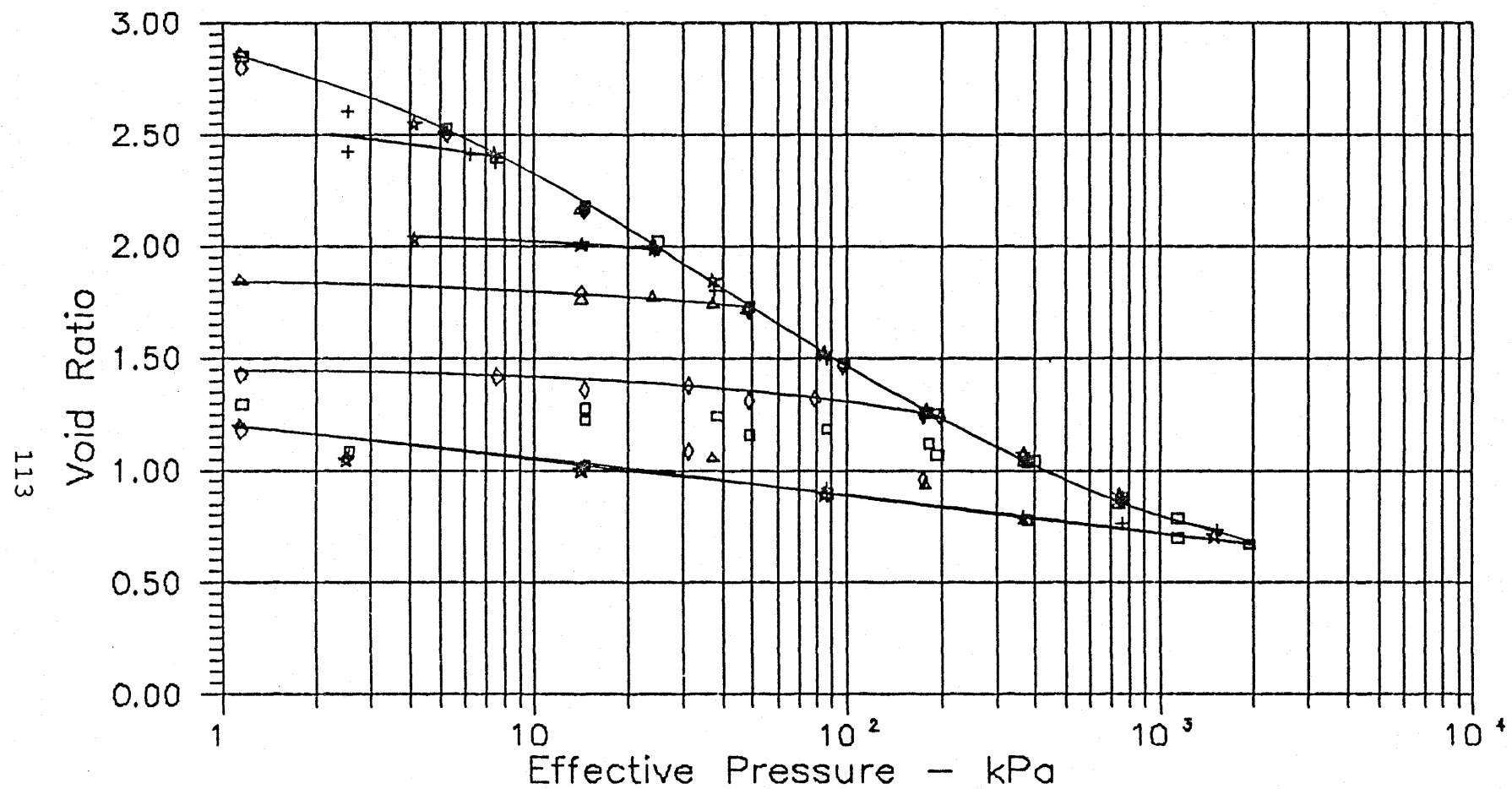


Fig. 5.06: Logarithm of effective stress versus void ratio, one-dimensional consolidation tests on Regina Clay, (data obtained from Fredlund, 1964).

Table 5.01: Determination of the elastic modulus E, for the slurried Regina Clay from one-dimensional consolidation test results (data obtained from Fredlund, 1964).

Initial Stress kPa	Final Stress kPa	Initial void ratio	Final void ratio	Average Stress kPa	D kPa	Poisson ratio			
						0.30	0.35	0.40	0.45
						E Modulus kPa			
5.49	9.81	2.500	2.289	7.65	72	53	45	33	19
9.81	19.62	2.289	1.989	14.72	81	60	50	38	21
19.62	49.05	1.889	1.702	34.34	455	338	283	212	120
49.05	68.67	1.702	1.580	58.86	435	323	271	203	115
68.67	88.29	1.580	1.488	78.48	550	409	343	257	145
88.29	98.10	1.488	1.450	93.20	642	477	400	300	169
98.10	196.20	1.450	1.247	147.15	1184	880	738	553	312
196.20	294.30	1.247	1.128	245.25	1852	1376	1154	864	488
294.30	392.40	1.128	1.044	343.35	2485	1846	1548	1160	655
392.40	490.50	1.044	0.978	441.45	3038	2257	1893	1418	801
490.50	588.60	0.978	0.925	539.55	3661	2720	2281	1709	965
588.60	686.70	0.925	0.880	637.65	4196	3117	2615	1958	1106
686.70	760.28	0.880	0.850	723.49	4611	3425	2873	2152	1216

Table 5.02: Determination of the elastic modulus H, for the slurried Regina Clay from suction test results (data obtained from Fredlund, 1964).

Initial Stress kPa	Final Stress kPa	Initial void ratio	Final void ratio	Average Stress kPa	B _m kPa	H Modulus kPa	Poisson ratio			
							0.30	0.35	0.40	0.45
							E/H ratio			
5.18	9.81	2.510	2.400	8.00	116	347	0.153	0.128	0.096	0.054
9.81	19.62	2.400	2.020	14.72	88	263	0.228	0.191	0.143	0.081
19.62	49.05	2.020	1.794	34.34	393	1180	0.286	0.240	0.180	0.102
49.05	68.67	1.794	1.650	58.86	391	1142	0.283	0.237	0.178	0.100
68.67	88.29	1.650	1.560	78.48	578	1733	0.336	0.198	0.148	0.084
88.29	98.10	1.560	1.530	93.20	837	2511	0.190	0.159	0.119	0.067
98.10	196.20	1.530	1.285	147.15	1013	3039	0.289	0.243	0.182	0.103
196.20	294.30	1.285	1.170	245.25	1949	5848	0.235	0.197	0.148	0.084
294.30	392.40	1.170	1.106	343.35	3242	10025	0.184	0.154	0.115	0.065
392.40	490.50	1.106	1.057	441.45	4183	12548	0.180	0.151	0.113	0.064
490.50	588.60	1.057	1.017	539.55	4995	14984	0.182	0.152	0.114	0.064
588.60	686.70	1.017	0.982	637.65	5801	17403	0.179	0.150	0.113	0.064
686.70	784.80	0.982	0.953	735.75	6570	19710	0.174	0.146	0.109	0.062

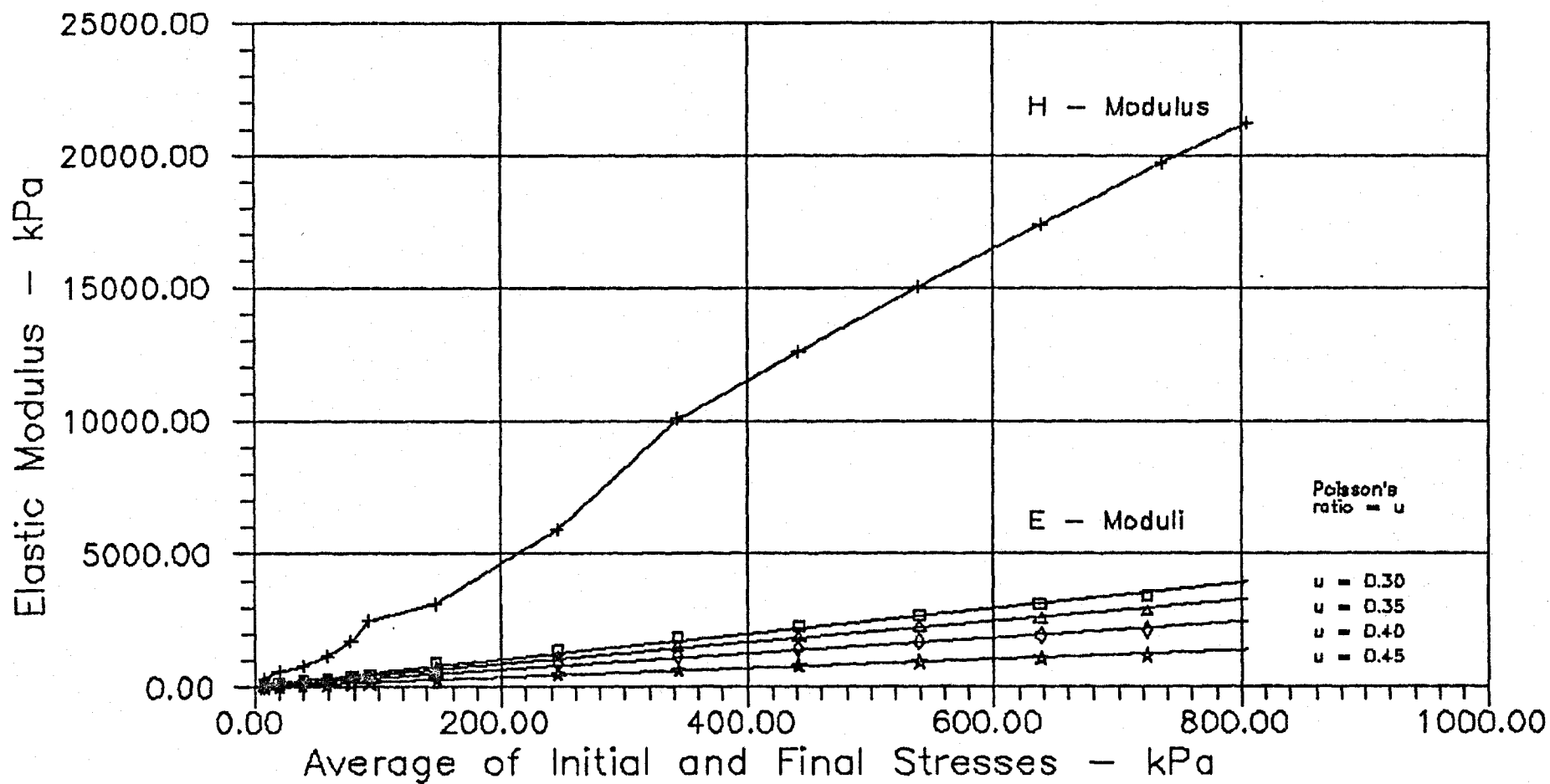


Fig. 5.07: Average initial and final stresses versus elastic modulus
(data obtained from Fredlund, 1964).

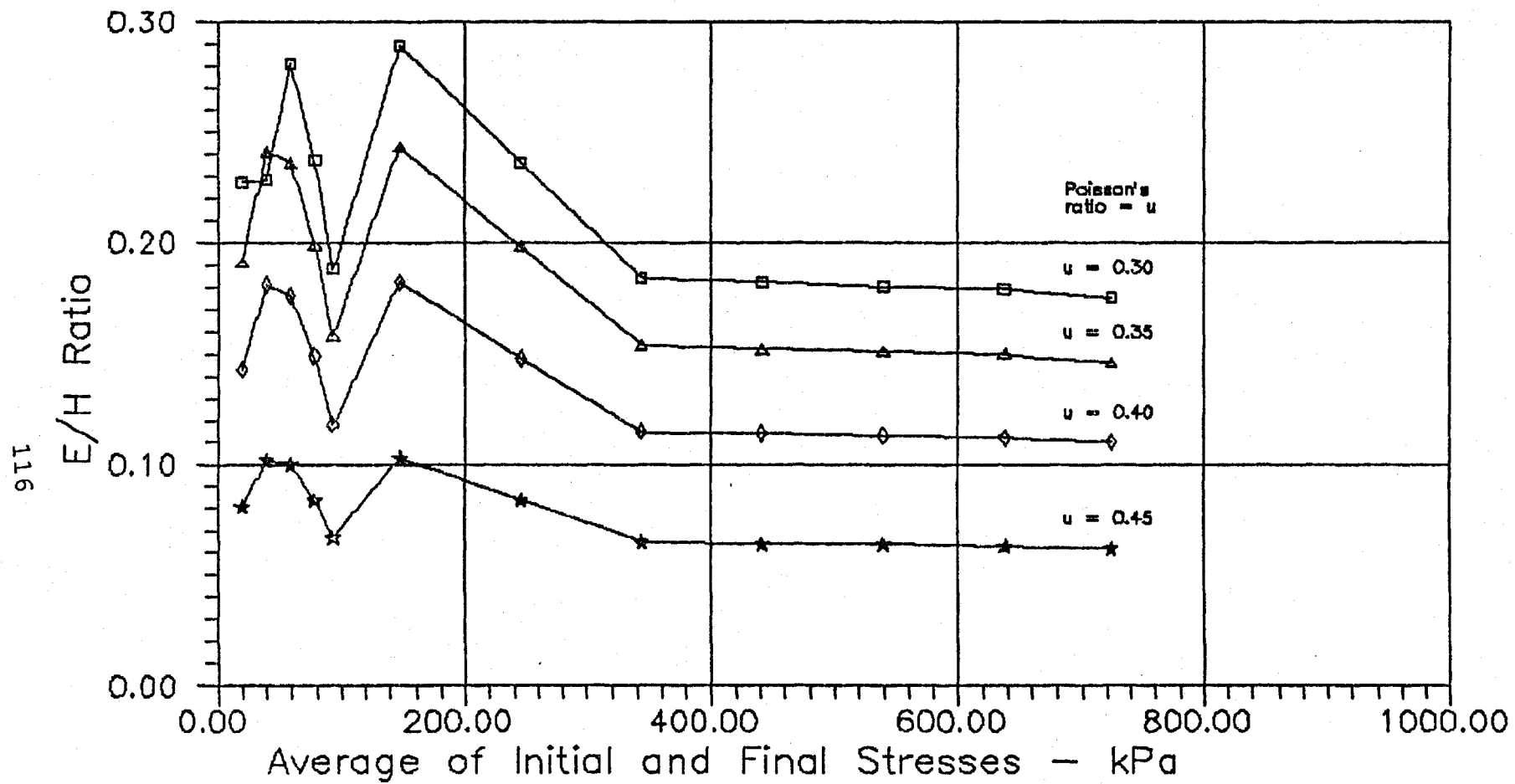


Fig. 5.08: Average initial and final stresses versus E/H ratio
(data obtained from Fredlund, 1964).

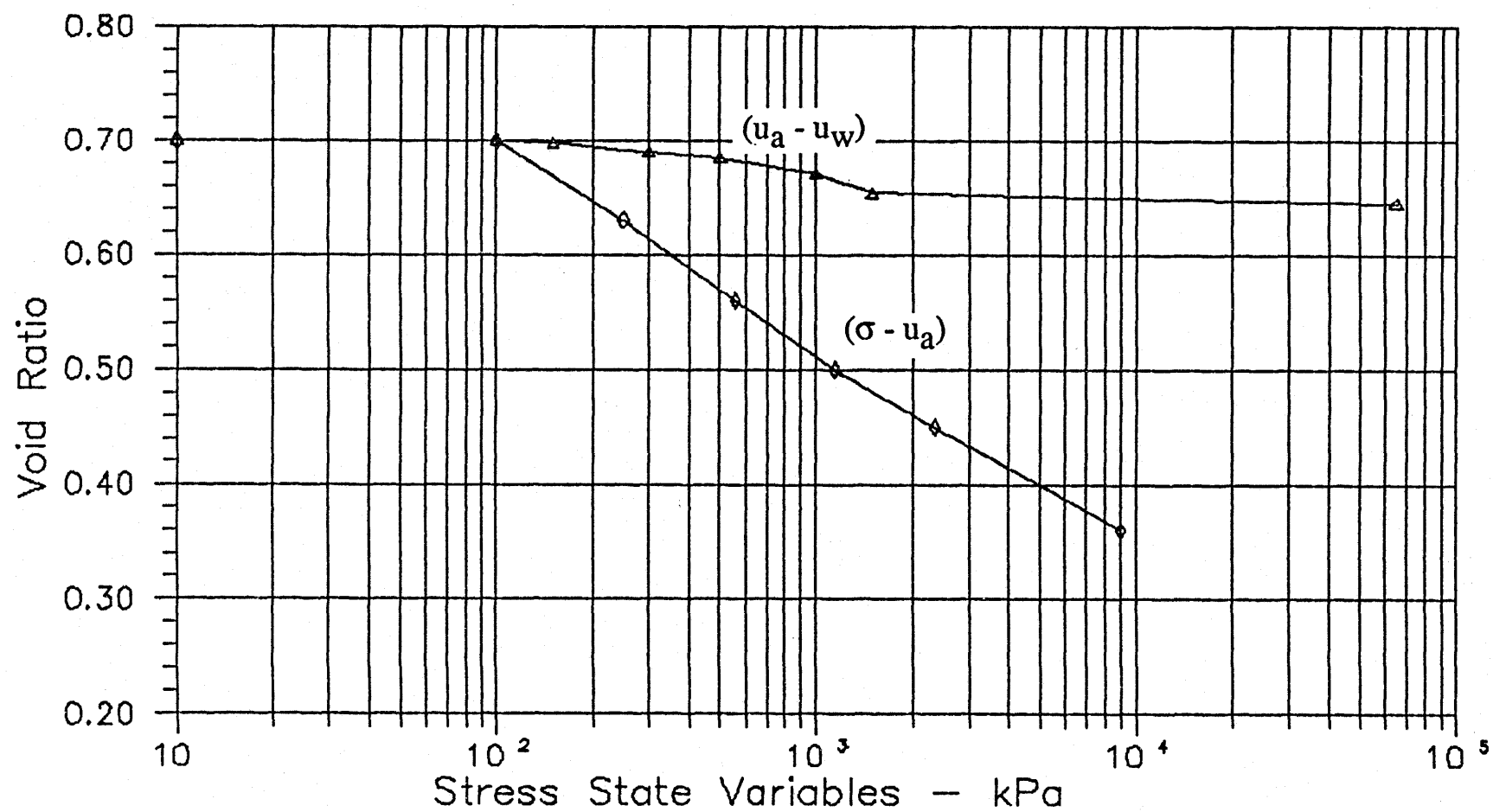


Fig. 5.09: Logarithm of stress state variables versus void ratio for silt compacted dry of optimum water content (after Ho, 1987).

to have a E/H ratio ranging between 0.06 and 0.18, for a Poisson's ratio between 0.45 and 0.30, respectively.

Ho (1987) performed suction tests and one-dimensional consolidation tests on silt compacted dry of optimum water content (i.e., initial water content is equal to 16.0%). For a stress range between 100 kPa and 1500 kPa, the compressive indices, C_t and C_m obtained from the plot of stress state variables versus void ratio (see Fig. 5.09) were estimated to be 0.178 and 0.039, respectively. With a C_m/C_t ratio of about 0.22, the theoretical E/H ratio would vary (i.e., using equation [5.15] or Fig. 5.04) between 0.02 and 0.05, for a Poisson's ratio between 0.45 and 0.30, respectively.

Based on the foregoing experimental data, it can be concluded that the E/H ratio for clay soil is higher than that for silty soil. Silty soils have larger soil grains, and have a less compressible (i.e., stronger) soil structure than clayey soils. The difference in the E/H ratio appears to be due to the matric suction stress ($u_a - u_w$) being more effective in deforming the soil structure for clayey soils than for silty soils. Although the maximum theoretical E/H ratio is equal to one third (when Poisson's ratio is equal to 0), the normal range of the E/H ratio for clayey soils is believed to vary between zero and 0.2.

CHAPTER 6

PRESENTATION OF RESULTS

6.1 INTRODUCTION

The data derived from the analytical and experimental programs are presented in this chapter. Because of the large amount of data, only a graphical presentation of results is given. Complete summaries of the analytical and experimental results are provided in Appendix C and Appendix D, respectively.

6.2 PREDICTION OF CRACK DEPTH

In Chapter 3, two sets of mathematical expressions for the prediction of crack depth were derived using the elastic and plastic equilibrium analyses. The crack depth was expressed in terms of stress state variables and various soil parameters. In order to study the relative effects of the various soil parameters on the value of the crack depth, a parametric study is presented in the following sections.

6.2.1 Elastic Equilibrium Analysis

Using the elastic equilibrium analysis, the predicted crack depth for a given matric suction profile was expressed in Section 3.4 as follows:

For matric suction profile "A" (i.e., matric suction varies linearly with depth), the depth of crack was written as,

$$d_c = \frac{D_w - \frac{H \epsilon_h}{F_w \gamma_w}}{1 + \frac{\mu \gamma}{F_w \gamma_w} \frac{1}{(E/H)}} \quad [6.01]$$

For matric suction profile "B" (i.e., matric suction is constant with depth), the depth of crack was written as,

$$d_c = \frac{D_w - \frac{H \epsilon_h}{F_w \gamma_w}}{\frac{\mu \gamma}{F_w \gamma_w} \frac{1}{(E/H)}} \quad [6.02]$$

where: d_c = theoretical crack depth.
 D_w = depth to water table.
 F_w = matric suction profile factor.
 γ = total unit weight of soils.
 γ_w = total unit weight of water.
 μ = Poisson's ratio.
 E = elastic modulus with respect to total stress ($\sigma - u_a$).
 H = elastic modulus with respect to matric suction ($u_a - u_w$).
 ϵ_h = tensile strain of soils.

Soils, in general are quite weak in tension. Leonards and Narain (1963) conducted beam flexure tests on compacted clay and found that the tensile strain-at-failure was a

small fraction of the compression strain-at-failure. The ratio of tensile strain to compressive strain varies from 0.01 to 0.1 with no consistent pattern. The tensile strain-at-failure under three dimensional loading conditions has not been presented in the literature to the author's knowledge. However, it appears that the tensile strain-at-failure would be quite small for most soils under three-dimensional loading conditions.

Let us consider a clayey soil (e.g., Regina Clay) having a tensile strain equal to 0.1%. As matric suction generally decreases with depth, the matric suction at the vicinity of the crack tip is expected to be low. At low matric suction (e.g., less than 50 kPa), the elastic modulus H , as suggested in Table 5.02, would equal to 1000 kPa. With F_w and γ_w equal to 1.0 and 9.8 kN/m³, respectively, the term containing the allowable tensile strain, ϵ_h in equations [6.01] and [6.02] will equal to 0.1 m. The denominators in equations [6.01] and [6.02] are greater than unity. It is seen that the decrease in crack depth d_c , due to ϵ_h will not be significant. Furthermore, neglecting the effect of tensile strain in equations [6.01] and [6.02] produces a more conservative (i.e., slightly deeper) estimate of the crack depth. It is therefore reasonable to assume the allowable tensile strain be equal to zero. Equations [6.01] and [6.02]

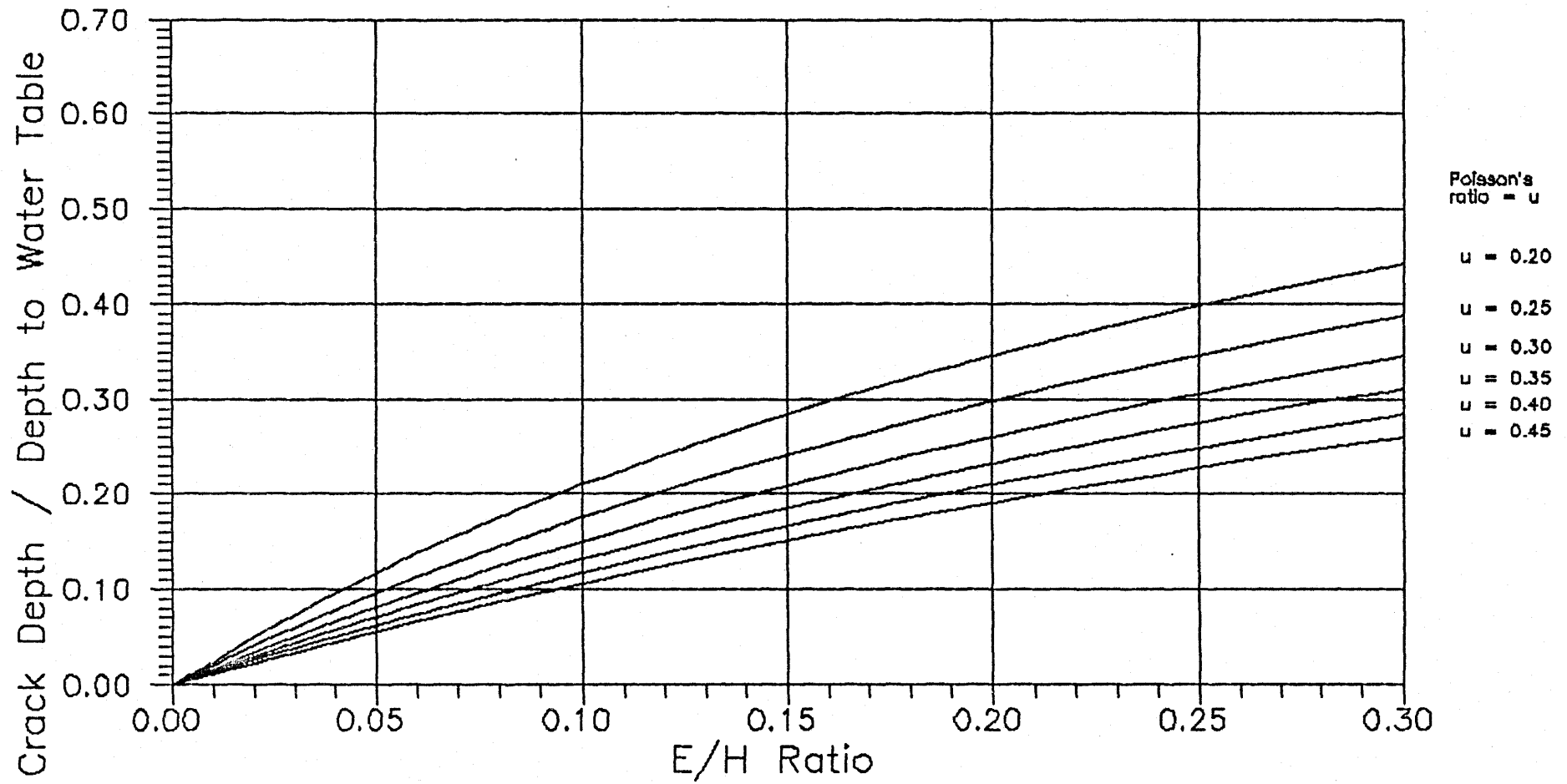


Fig. 6.01: E/H ratio versus crack depth to the depth to water table ratio (d_c/D_w), using elastic equilibrium analysis, suction profile "A" (i.e., matric suction varies linearly with depth), $F_w = 1.0$, $\gamma = 18.5 \text{ kN/m}^3$.

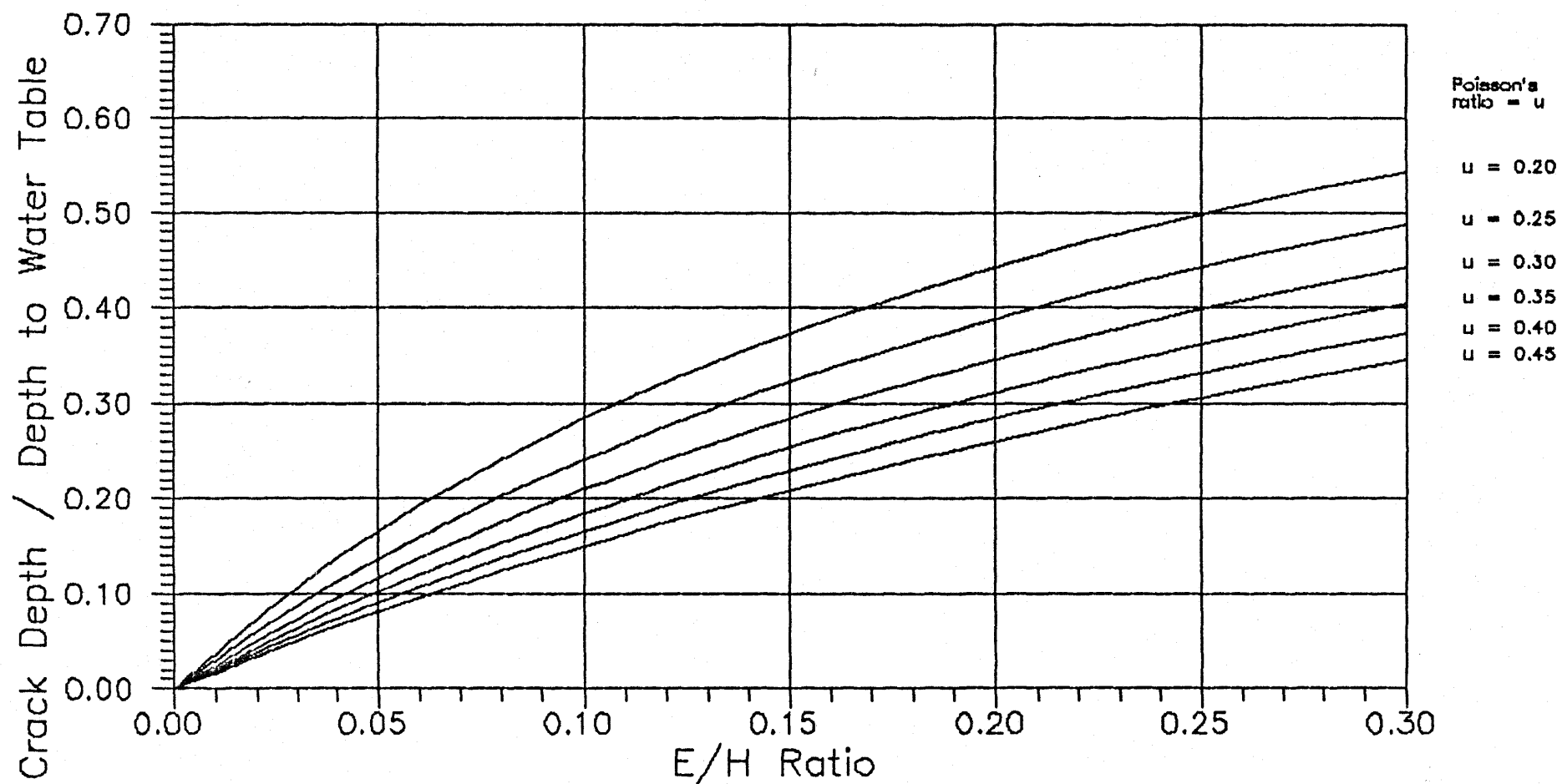


Fig. 6.02: E/H ratio versus crack depth to the depth to water table ratio (d_c/D_w), using elastic equilibrium analysis, suction profile "A" (i.e., matric suction varies linearly with depth), $F_w = 1.5$, $\gamma = 18.5 \text{ kN/m}^3$.

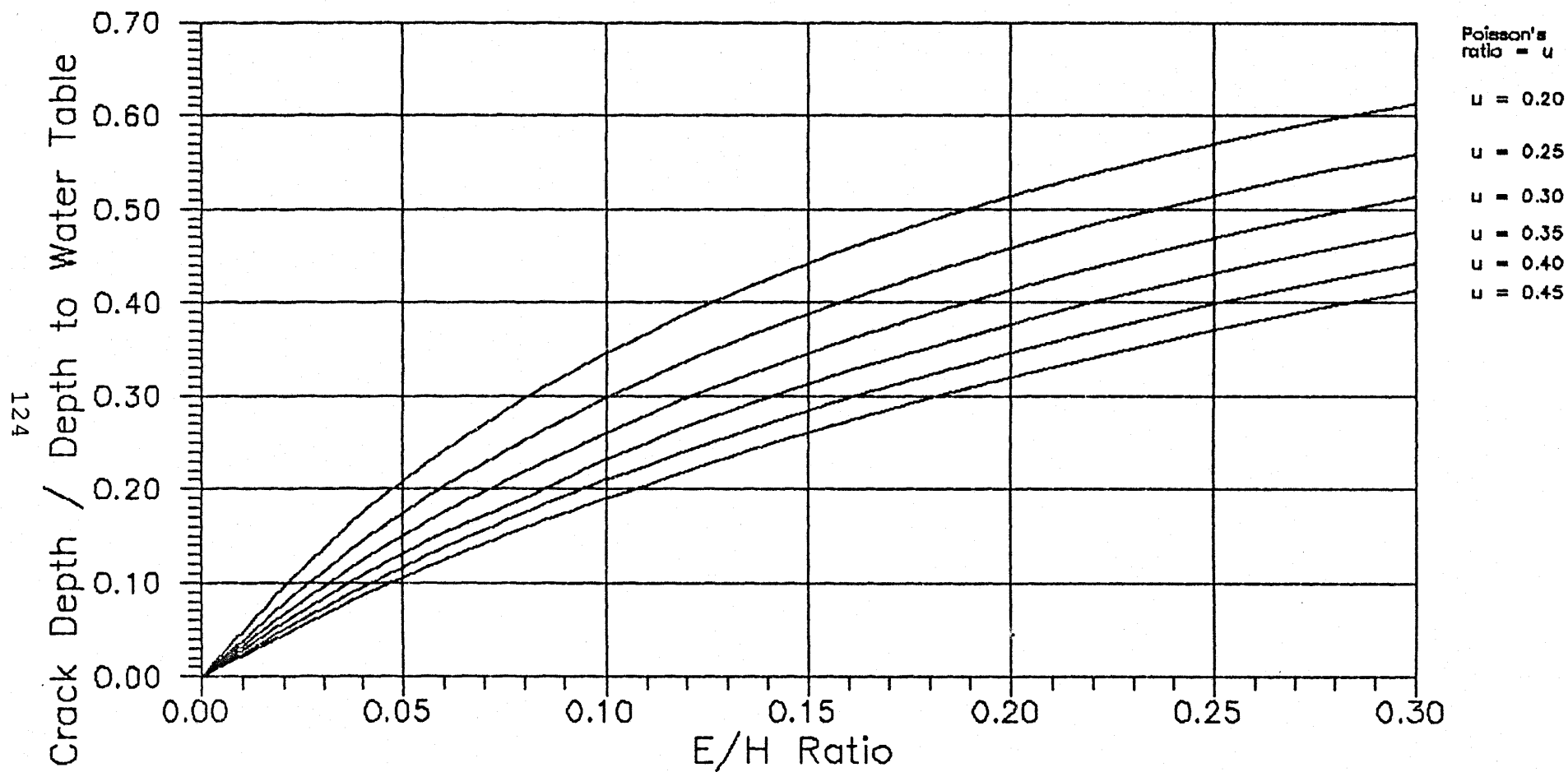


Fig. 6.03: E/H ratio versus crack depth to the depth to water table ratio (d_c/D_w), using elastic equilibrium analysis, suction profile "A" (i.e., matric suction varies linearly with depth), $F_w = 2.0$, $\gamma = 18.5 \text{ kN/m}^3$.

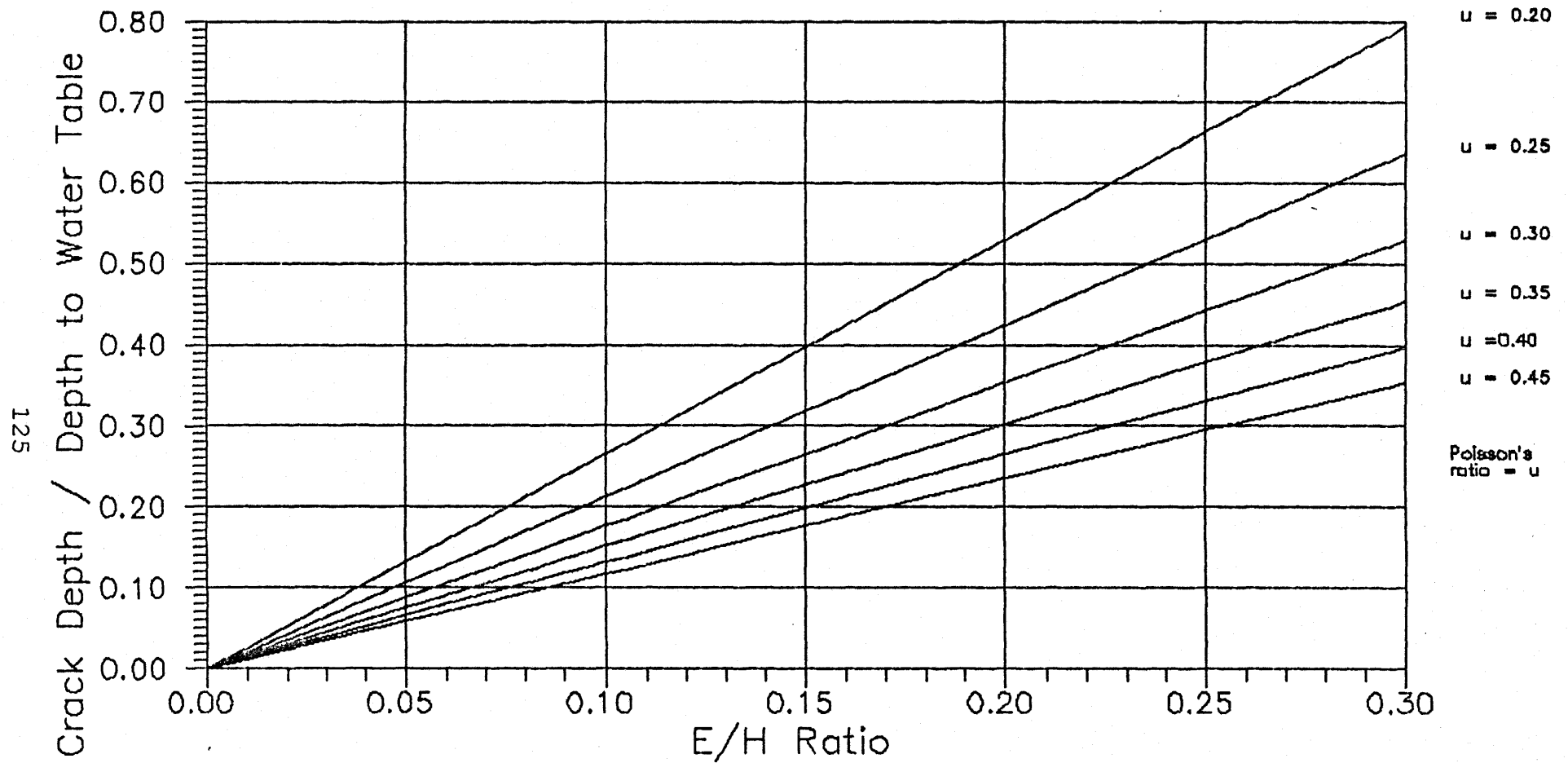


Fig. 6.04: E/H ratio versus crack depth to the depth to water table ratio (d_c/D_w), using elastic equilibrium analysis, suction profile "B" (i.e., matric suction is constant with depth), $F_w = 1.0$, $\gamma = 18.5 \text{ kN/m}^3$.

can be simplified as follows:

For matric suction profile "A" (i.e., matric suction varies linearly with depth), the depth of cracking is simplified as,

$$dc = \frac{Dw}{1 + \frac{\mu \gamma}{Fw \gamma_w} \frac{1}{(E/H)}} \quad [6.03]$$

For matric suction profile "B" (i.e., matric suction is constant with depth), the depth of cracking is simplified as,

$$dc = \frac{Dw}{\frac{\mu \gamma}{Fw \gamma_w} \frac{1}{(E/H)}} \quad [6.04]$$

In Section 5.2, the theoretical E/H ratio was shown to have a possible range of values between zero and one third. The normal range of Poisson's ratio μ , for most soils varies between 0.20 and 0.50 (Winterkorn and Fang, 1975). Let us consider a soil with a total unit weight equal to 18.5 kN/m³. For a given matric suction profile and normal ranges of soil parameters, the relationship between the ratio of crack depth to the depth to water table (dc/Dw), and the E/H ratio using the elastic equilibrium analysis are shown in Figs. 6.01 to 6.04, inclusively.

6.2.2 Plastic Equilibrium Analysis

Using the plastic equilibrium analysis, the predicted crack depth for a given matric suction profile was expressed in Section 3.5 as follows:

For matric suction profile "A" (i.e., matric suction varies linearly with depth), the depth of cracking was written as,

$$dc = \frac{\frac{c'}{\gamma_w} + F_w D_w \tan \phi^b}{X + F_w \tan \phi^b} \quad [6.05]$$

$$\text{where } X = \frac{\frac{\gamma}{\gamma_w} (1 - \sin \phi')^2}{2 \cos \phi' \{ (1-F_t) - (1+F_t) \sin \phi' \}} \quad [6.06]$$

For matric suction profile "B" (i.e., matric suction is constant with depth), the depth of crack was written as,

$$dc = \frac{2 (c' + F_w D_w \gamma_w \tan \phi^b) Y}{\gamma} \quad [6.07]$$

$$\text{where } Y = \frac{\cos \phi'}{(1 - \sin \phi')} \left[1 - F_t - \frac{2 F_t \sin \phi'}{(1 - \sin \phi')} \right] \quad [6.08]$$

where:

dc = depth of crack.

c' = cohesion intercept when total stress and matric suction are equal to zero.

ϕ' = friction angle with respect to $(\sigma - u_a)$.

ϕ^b = friction angle with respect to $(u_a - u_w)$.

Ft = ratio of tensile strength and unconfined compressive strength.

Fw = matric suction profile factor.

γ = total unit weight of soil.

γ_w = total unit weight of water.

Table 6.01: Relationship between X and Y terms and ϕ' angles.

$$\gamma = 18.5 \text{ kN/m}^3, \quad \gamma_w = 9.8 \text{ kN/m}^3.$$

ϕ'	1/Ft=6		1/Ft=8		1/Ft=10		1/Ft=12		1/Ft=14	
	X	Y	X	Y	X	Y	X	Y	X	Y
5°	1.08	0.87	1.02	0.93	0.98	0.96	0.96	0.98	0.95	1.00
10°	1.04	0.91	0.96	0.98	0.92	1.02	0.90	1.05	0.88	1.07
15°	1.01	0.93	0.92	1.03	0.87	1.08	0.84	1.12	0.82	1.15
20°	1.00	0.94	0.89	1.06	0.83	1.14	0.80	1.19	0.77	1.22
25°	1.02	0.93	0.87	1.09	0.80	1.18	0.76	1.25	0.73	1.29
30°	1.09	0.87	0.87	1.08	0.78	1.21	0.73	1.30	0.69	1.36
35°	1.28	0.74	0.91	1.03	0.78	1.21	0.71	1.33	0.67	1.41
40°	1.88	0.50	1.04	0.91	0.81	1.16	0.71	1.32	0.66	1.44

where:

γ = total unit weight of soils.

γ_w = total unit weight of water.

ϕ' = friction angle with respect to total stress.

Ft = ratio of tensile strength and unconfined compressive strength.

Table 6.02: Minimum X and maximum Y terms and their corresponding ϕ' angles.

$$\gamma = 18.5 \text{ kN/m}^3, \quad \gamma_w = 9.8 \text{ kN/m}^3.$$

	1/Ft=6	1/Ft=8	1/Ft=10	1/Ft=12	1/Ft=14
minimum					
X	1.000	0.866	0.774	0.707	0.655
ϕ'	19.5°	27.0°	32.6°	37.0°	40.3°
maximum					
Y	0.943	1.088	1.217	1.334	1.440
ϕ'	19.5°	27.0°	32.6°	37.0°	40.3°

where:

γ = total unit weight of soils.

γ_w = total unit weight of water.

ϕ' = friction angle with respect to total stress.

Ft = ratio of tensile strength and unconfined compressive strength.

The terms X and Y are a function of the friction angle ϕ' , and the ratio of tensile strength and unconfined compressive strength F_t . The values of X and Y calculated from equation [6.06] and [6.08] are not particularly sensitive to the normal range of ϕ' angles (i.e., 10 to 30 degrees, see Table 6.01). If minimum X and maximum Y values are used in equations [6.05] and [6.07], the maximum theoretical crack depths under different matric suction profiles can be obtained. The minimum X and the maximum Y values, and their corresponding ϕ' angles are given in Table 6.02.

Although there is no fixed relationship between the unconfined compressive strength and the tensile strength in the literature, the normal range of unconfined compressive strength and tensile strength ratio (i.e., $1/F_t$) may vary between 6.0 and 13.0 (Fang and Chen, 1972). Based on limited experimental data (Ho, 1981 and Gan, 1986), the possible range of ϕ^b angle for most types of soils ranges between zero and 30 degrees. Let us consider a soil with a zero effective cohesion intercept and with a total unit weight equal to 18.5 kN/m^3 . The relationship between the predicted crack depth to the depth to water table ratio (d_c/D_w) and the ϕ^b angle using the plastic equilibrium analysis are shown in Figure 6.05 to 6.09, inclusively. If the soil has an effective cohesion intercept c' , of 10 kPa and the matric suction profile factor F_w , is equal to 1.0, the increase in

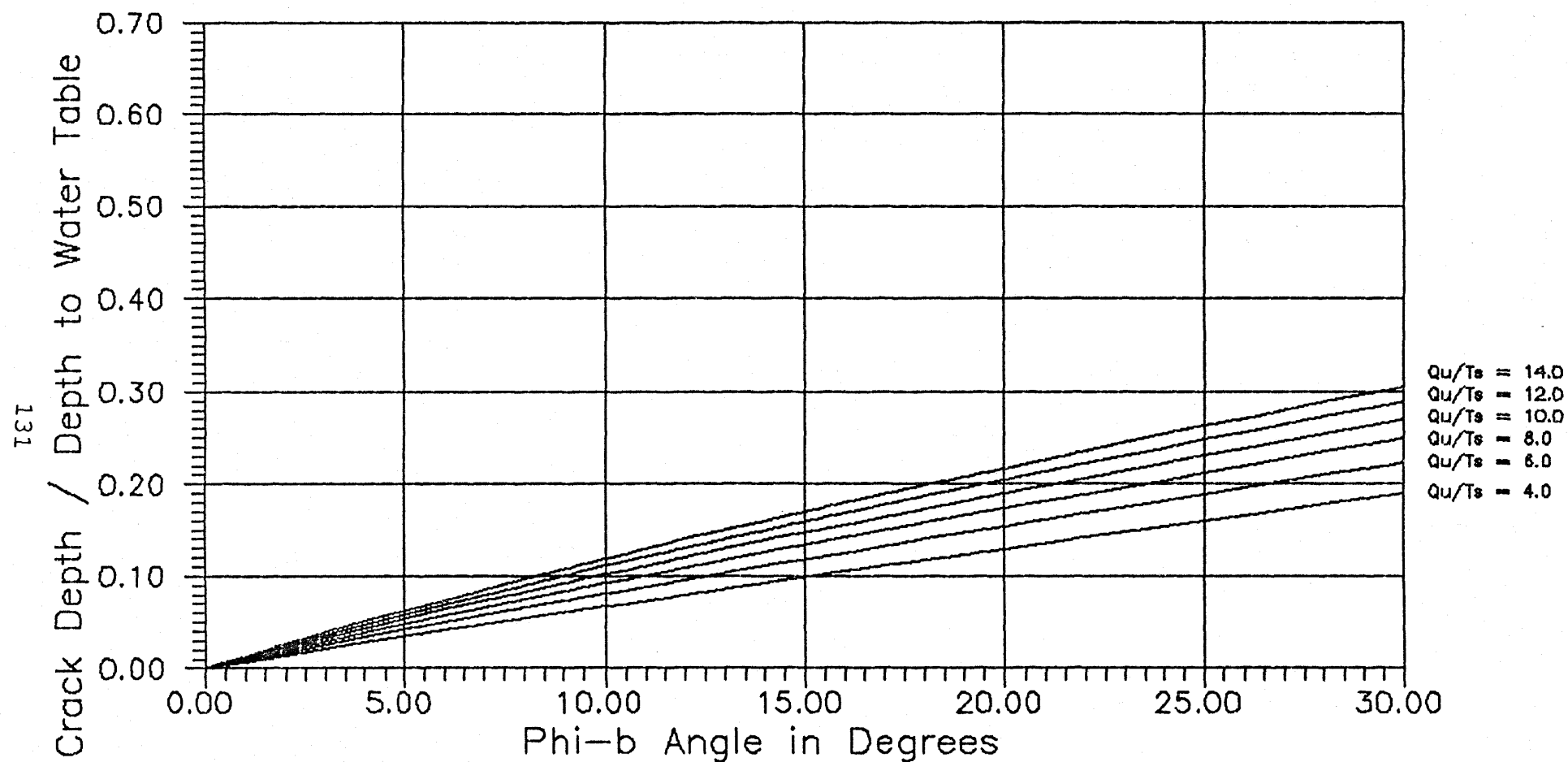


Fig. 6.05: ϕ^b angles versus crack depth to the depth to water table ratio (d_c/D_w), using plastic equilibrium analysis, suction profile "A" (i.e., matric suction varies linearly with depth), $F_w = 0.5$, $c' = 0$, $\gamma = 18.5 \text{ kN/m}^3$ (note: Q_u = unconfined compressive strength and T_s = tensile strength).

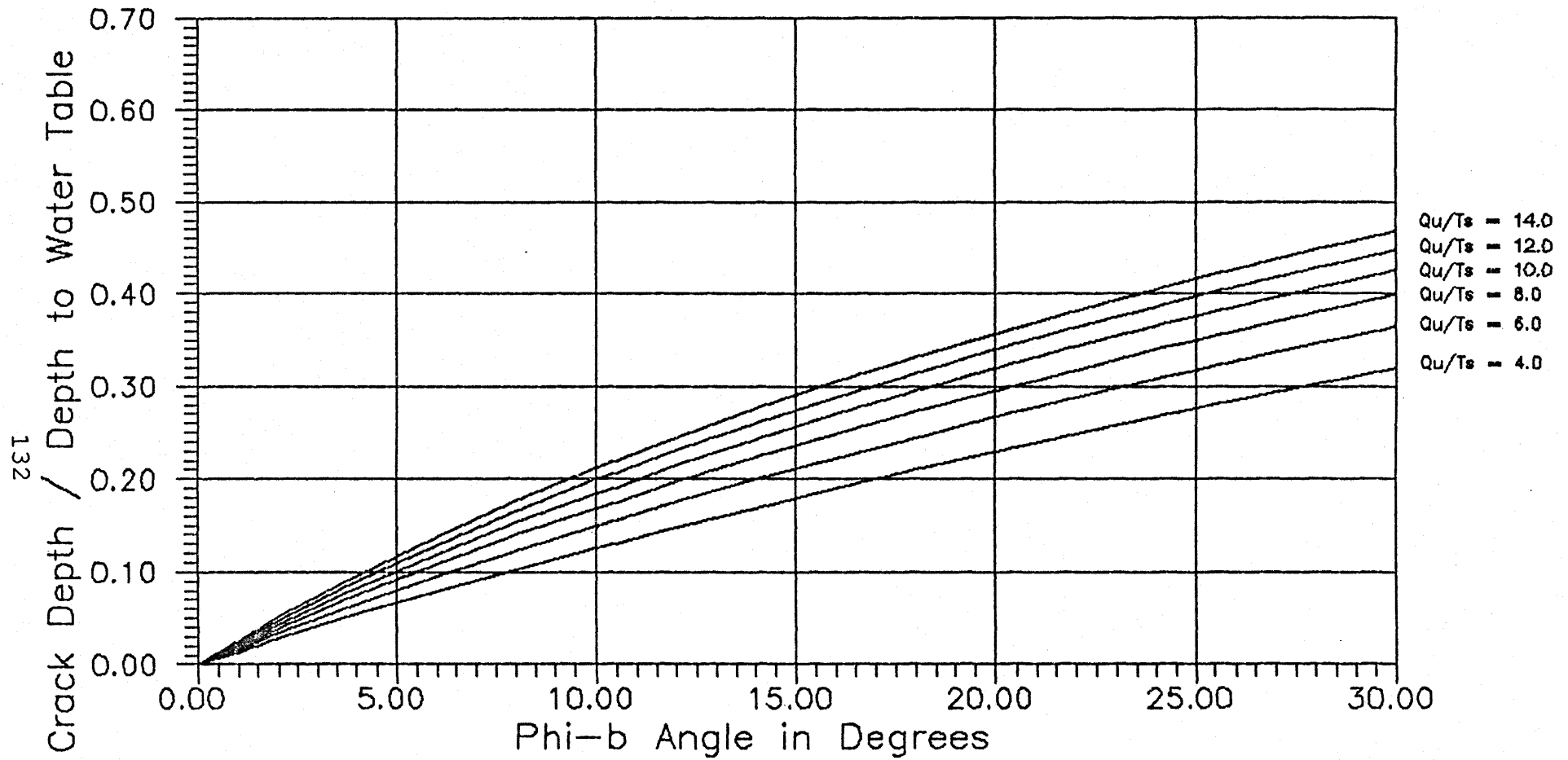


Fig. 6.06: ϕ^b angles versus crack depth to the depth to water table ratio (d_c/D_w), using plastic equilibrium analysis, suction profile "A" (i.e., matric suction varies linearly with depth), $F_w = 1.0$, $c' = 0$, $\gamma = 18.5 \text{ kN/m}^3$. (note: Q_u = unconfined compressive strength and T_s = tensile strength).

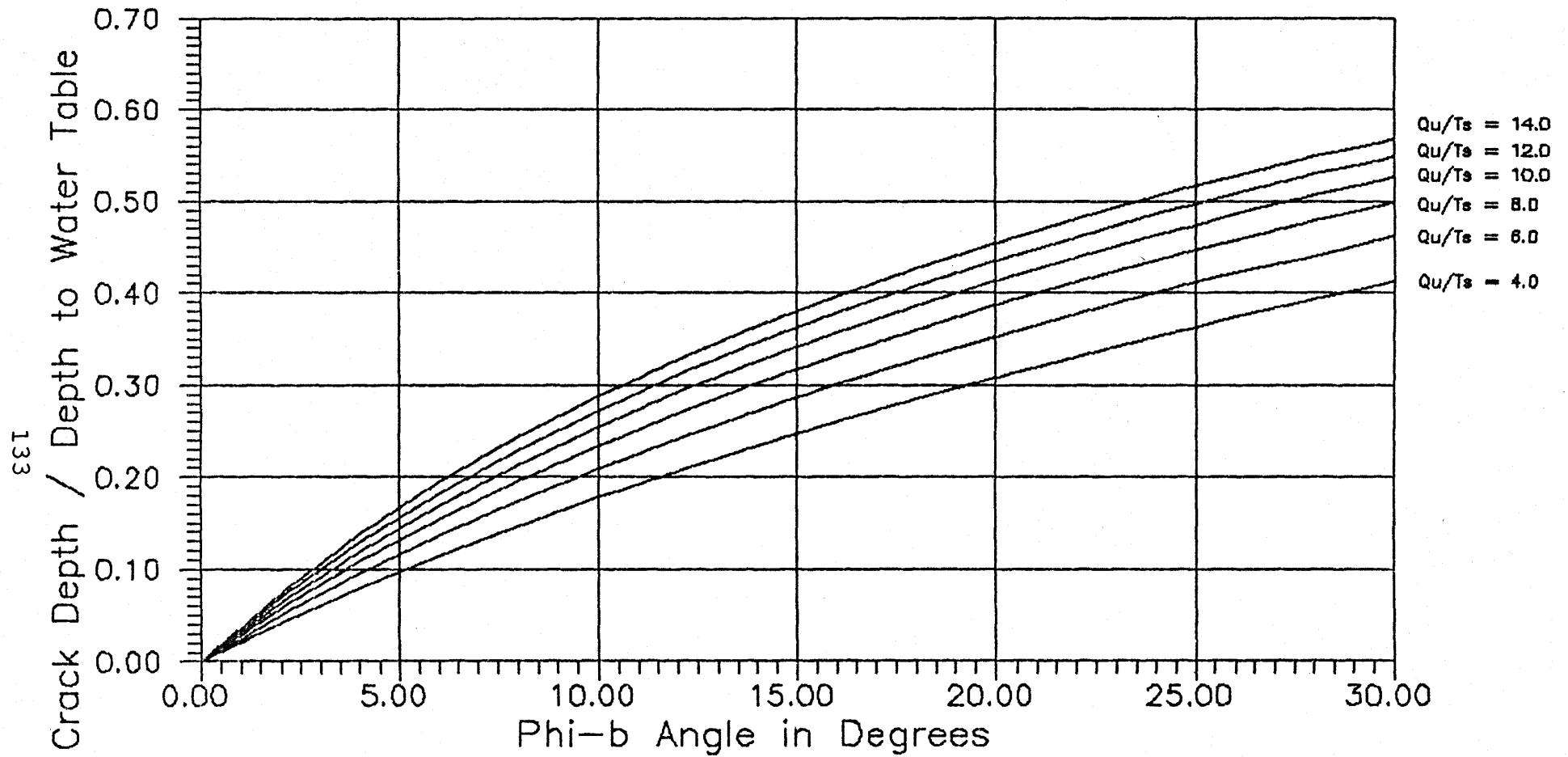


Fig. 6.07: ϕ^b angles versus crack depth to the depth to water table ratio (d_c/D_w), using plastic equilibrium analysis, suction profile "A" (i.e., matric suction varies linearly with depth), $F_w = 1.5$, $c' = 0$, $\gamma = 18.5 \text{ kN/m}^3$. (note: Q_u = unconfined compressive strength and T_s = tensile strength).

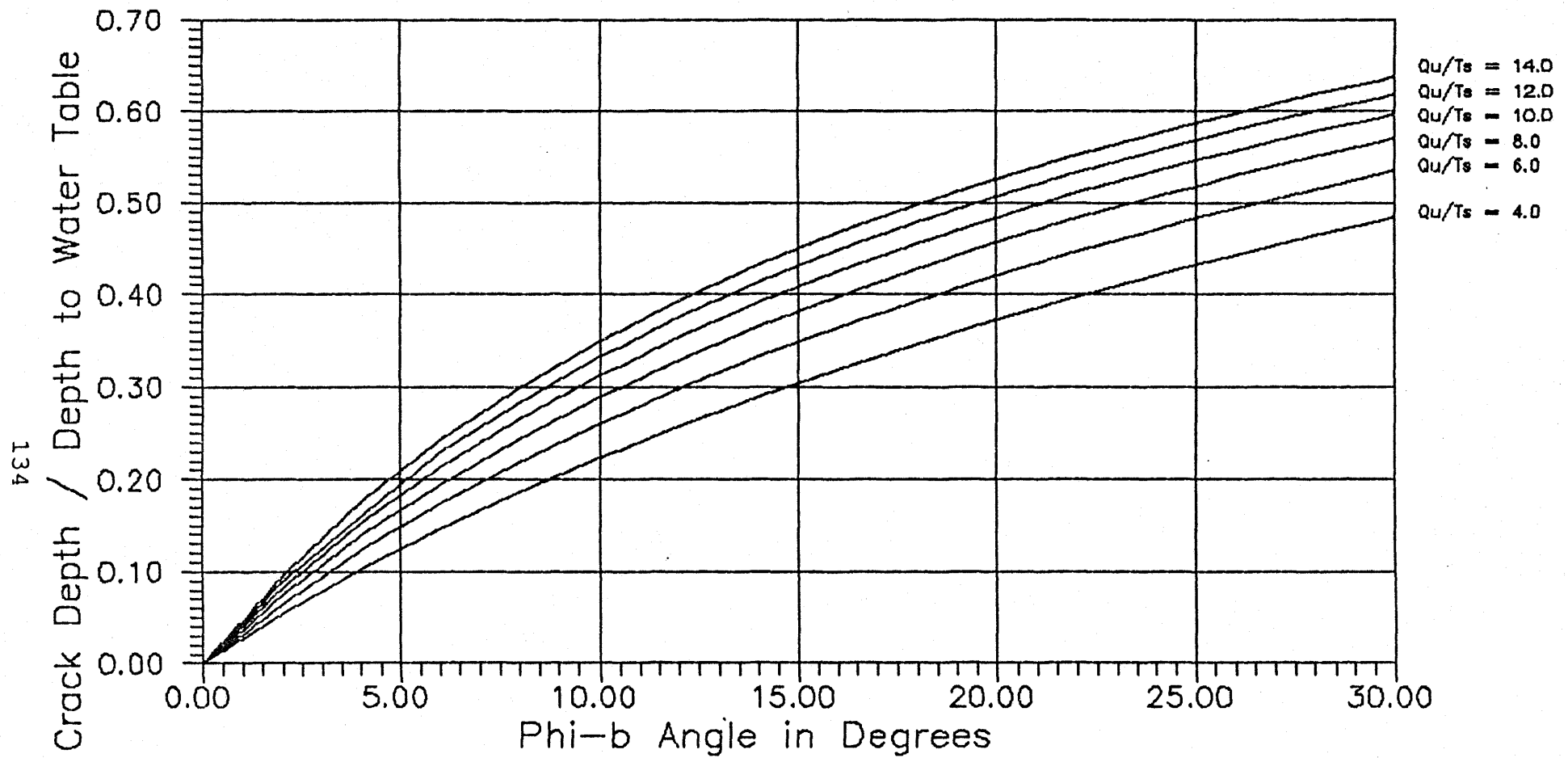


Fig. 6.08: ϕ^b angles versus crack depth to the depth to water table ratio (d_c/D_w), using plastic equilibrium analysis, suction profile "A" (i.e., matric suction varies linearly with depth), $F_w = 2.0$, $c' = 0$, $\gamma = 18.5 \text{ kN/m}^3$. (note: Q_u = unconfined compressive strength and T_s = tensile strength).

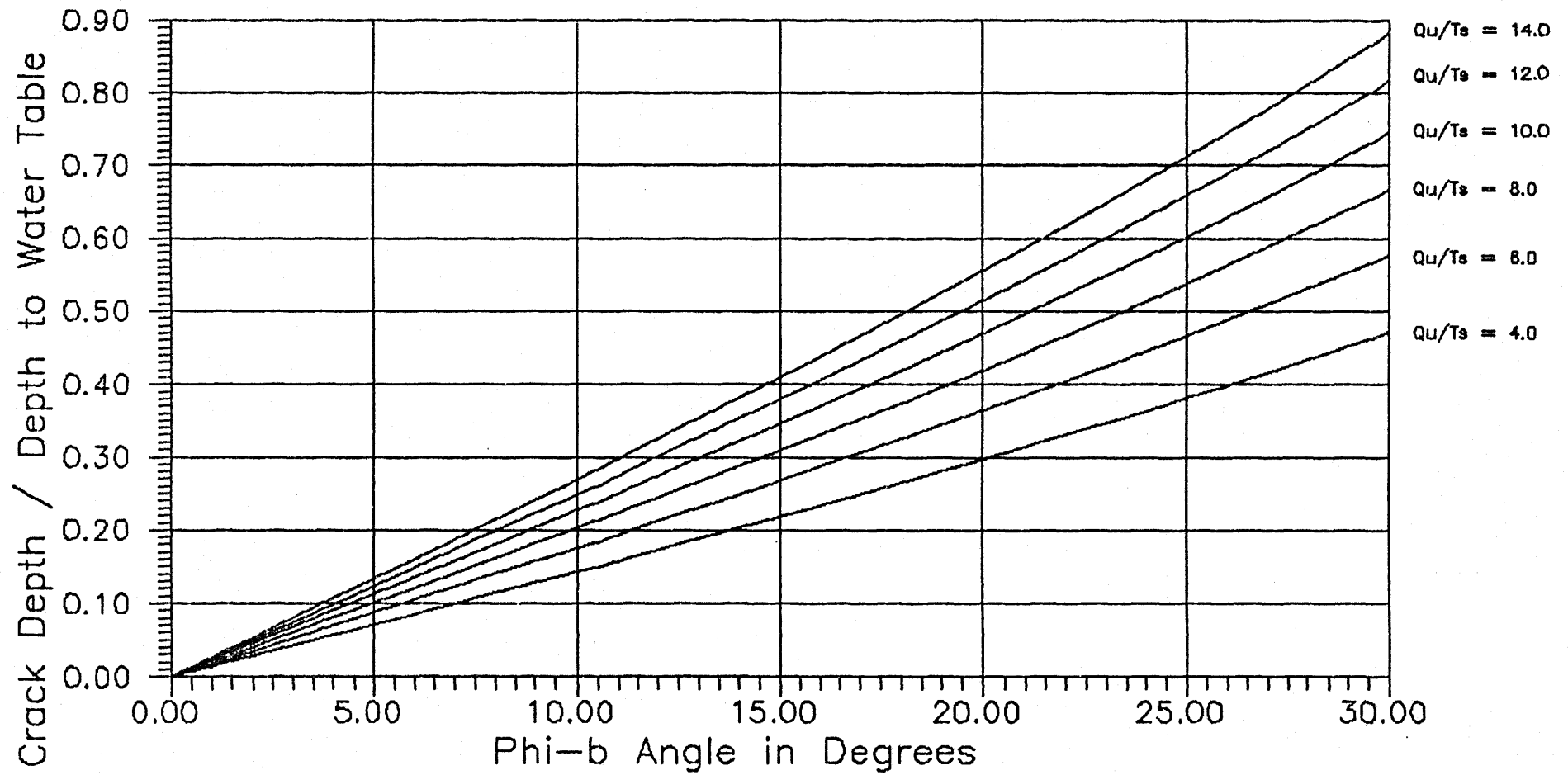


Fig. 6.09: ϕ^b angles versus crack depth to the depth to water table ratio (d_c/D_w), using plastic equilibrium analysis, suction profile "B" (i.e., matric suction is constant with depth), $F_w = 1.0$, $c' = 0$, $\gamma = 18.5 \text{ kN/m}^3$.
(note: Q_u = unconfined compressive strength and T_s = tensile strength).

Table 6.03: The increase in predicted crack depth due to cohesion intercept c' .

For matric suction profile "A" (i.e., matric suction varies with depth)

$$c' = 10.0 \text{ kPa}, \quad F_w = 1.0$$

$$\gamma = 18.5 \text{ kN/m}^3, \quad \gamma_w = 9.8 \text{ kN/m}^3$$

ϕ^b	1/Ft=6	1/Ft=8	1/Ft=10	1/Ft=12	1/Ft=14
	Increase in crack depth (in m) due to c'				
0°	1.02m	1.18m	1.32m	1.44m	1.61m
5°	0.94m	1.07m	1.18m	1.28m	1.42m
10°	0.87m	0.98m	1.07m	1.15m	1.26m
15°	0.80m	0.90m	0.98m	1.05m	1.13m
20°	0.75m	0.83m	0.90m	0.95m	1.02m
25°	0.70m	0.77m	0.82m	0.87m	0.93m
30°	0.65m	0.71m	0.75m	0.79m	0.84m

For matric suction profile "B" (i.e., matric suction is constant with depth)

$$c' = 10.0 \text{ kPa}, \quad F_w = 1.0$$

$$\gamma = 18.5 \text{ kN/m}^3, \quad \gamma_w = 9.8 \text{ kN/m}^3$$

The increases in crack depth due to cohesion c' do not vary with ϕ^b angles, and are given as follows:

	1/Ft=6	1/Ft=8	1/Ft=10	1/Ft=12	1/Ft=14
	Increase in crack depth (in m) due to c'				
all ϕ^b	1.02m	1.18m	1.32m	1.44m	1.61m

where:

c' = cohesion intercept when total stress and matric suction are equal to zero.

γ = total unit weight of soils.

γ_w = total unit weight of water.

ϕ^b = friction angle with respect to matric suction.

Ft = ratio of tensile strength and unconfined compressive strength.

F_w = matric suction profile factor.

the theoretical crack depth is given in Table 6.03. It should be noticed that the minimum X and maximum Y values were used in all the calculation of crack depth.

6.3 EXPERIMENTAL RESULTS

A total of three shrinkage tests (Test Nos. S01 to S03) and six cracking tests (Test Nos. T01 to T06) were conducted in the experimental program. Indian Head Till and Regina Clay mixed at water contents close to their liquid limits were used in the experiments.

6.3.1 Shrinkage Tests

Two shrinkage tests (i.e., Test Nos. S01 and S02) were carried out on Indian Head Till with water contents of 37.7% and 31.0%. One shrinkage test (i.e., Test No. S03) was performed on Regina Clay mixed at a water content of 80.0%.

The relationships between the water content and the specific volume (i.e., the reciprocal of dry density) of the drying soils for all the shrinkage tests are shown in Figs. 6.10 and 6.11. The shrinkage limits of the Indian Head Till and the Regina Clay, as estimated from Figs. 6.10 and 6.11, were 14.0% and 22.0%, respectively.

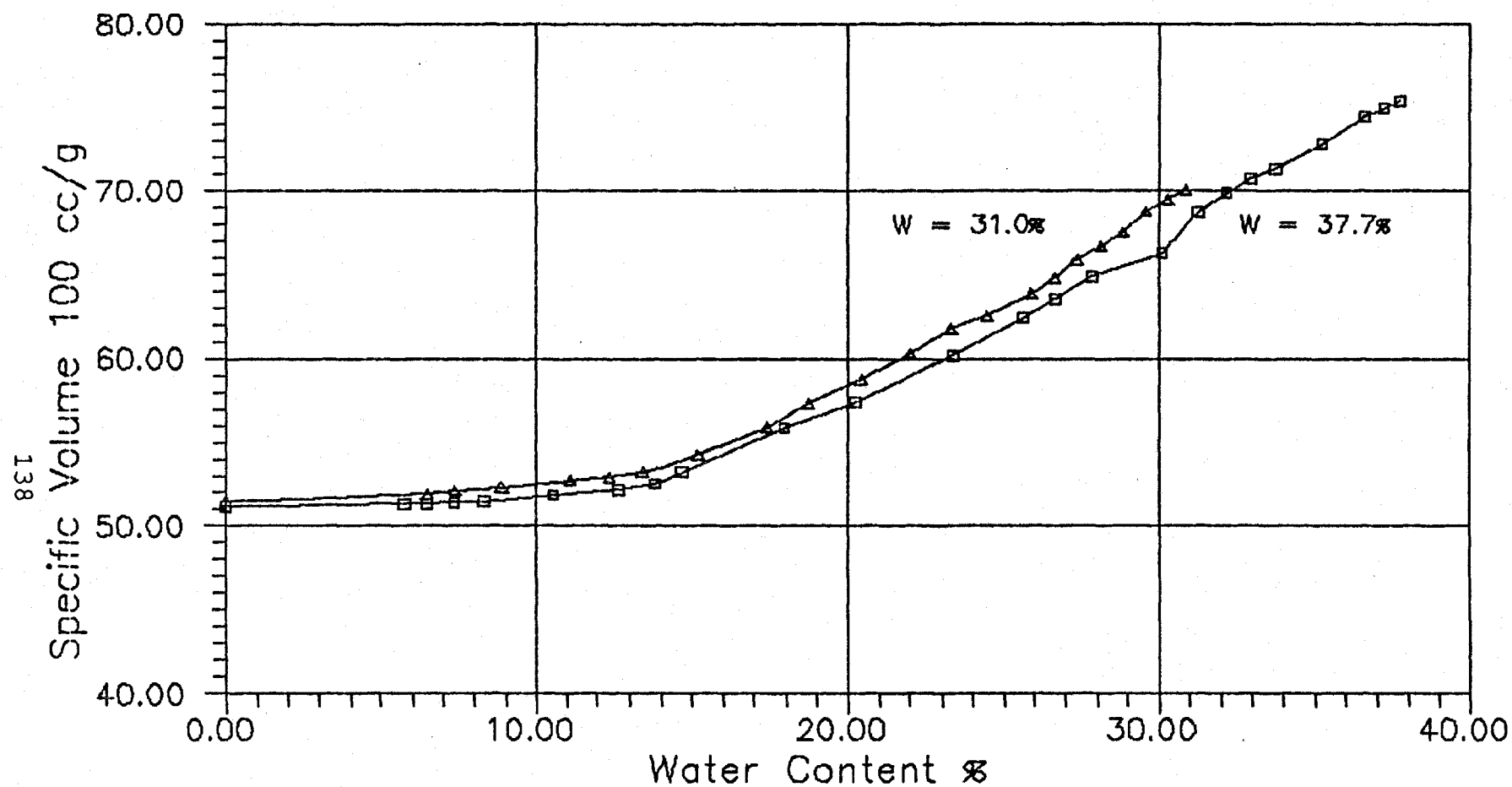


Fig. 6.10: Water content versus specific volume for Indian Head Till mixed at water contents of 31.0% and 37.7% and allowed to dry in a brass container (Test Nos. S01 and S02).

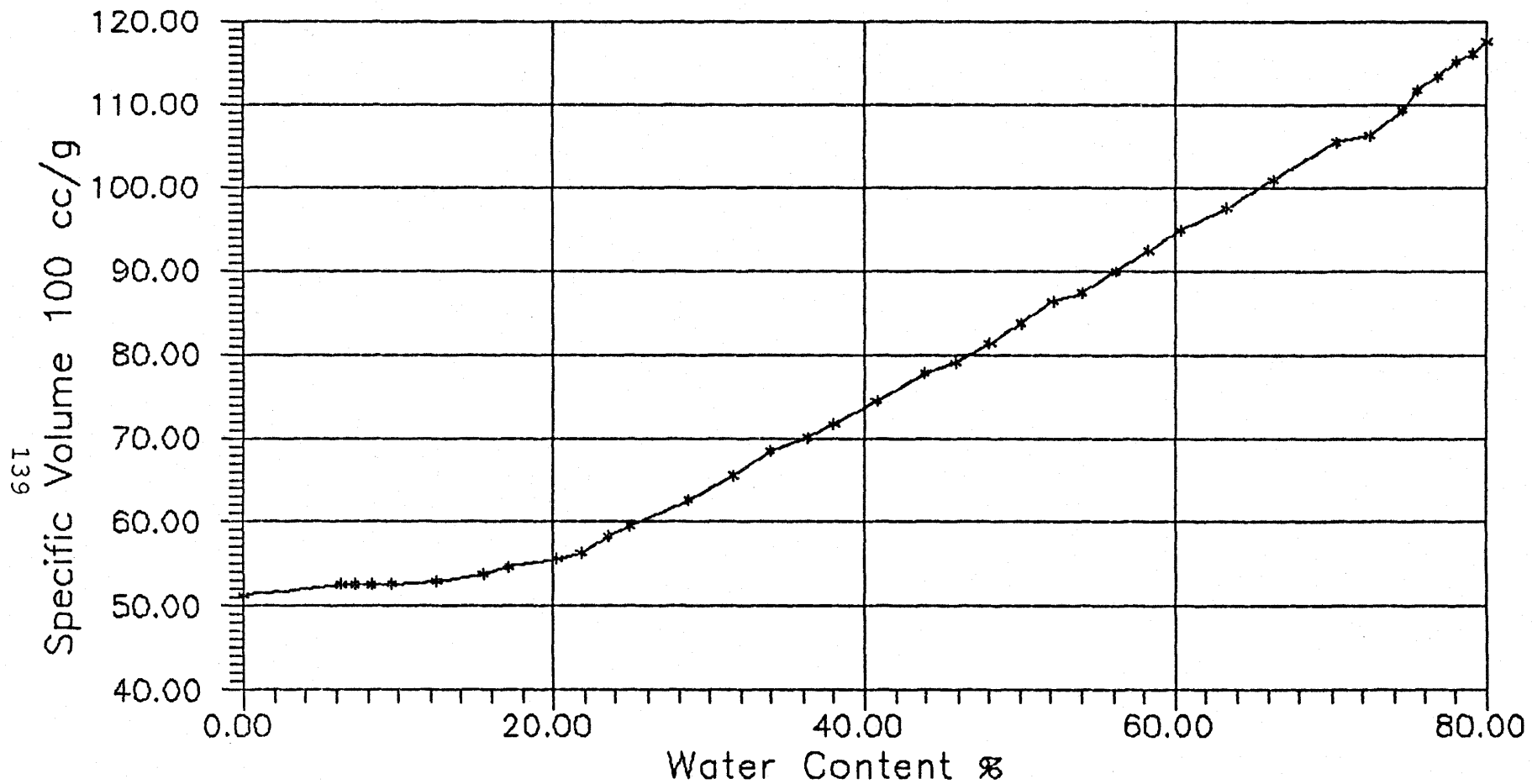


Fig. 6.11: Water content versus specific volume for Regina Clay mixed at water content of 80.0% and allowed to dry in a brass container (Test No. S03).

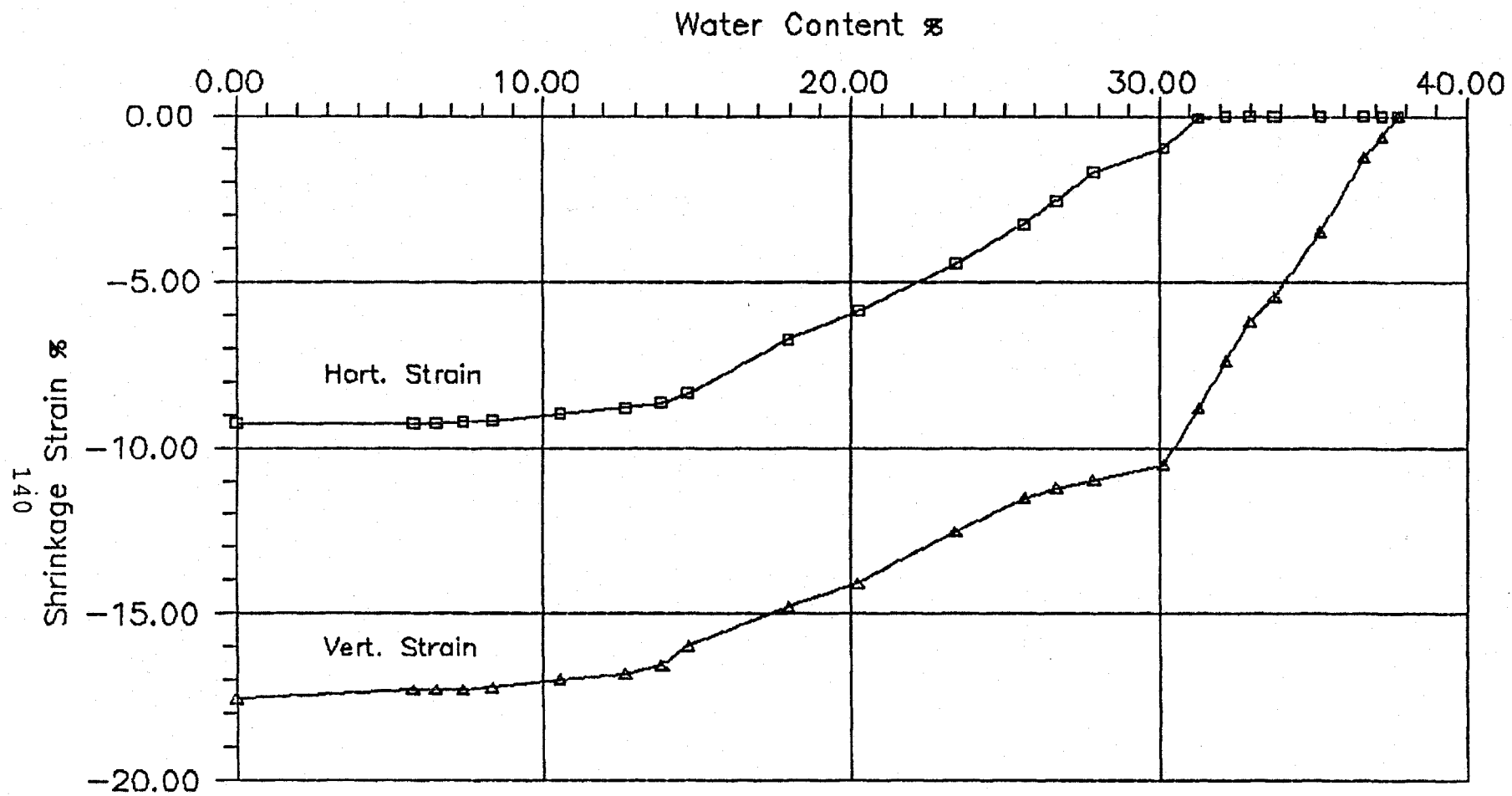


Fig. 6.12: Water content versus shrinkage strain for Indian Head Till mixed at water content of 37.7% and allowed to dry in a brass container (Test No. S01).

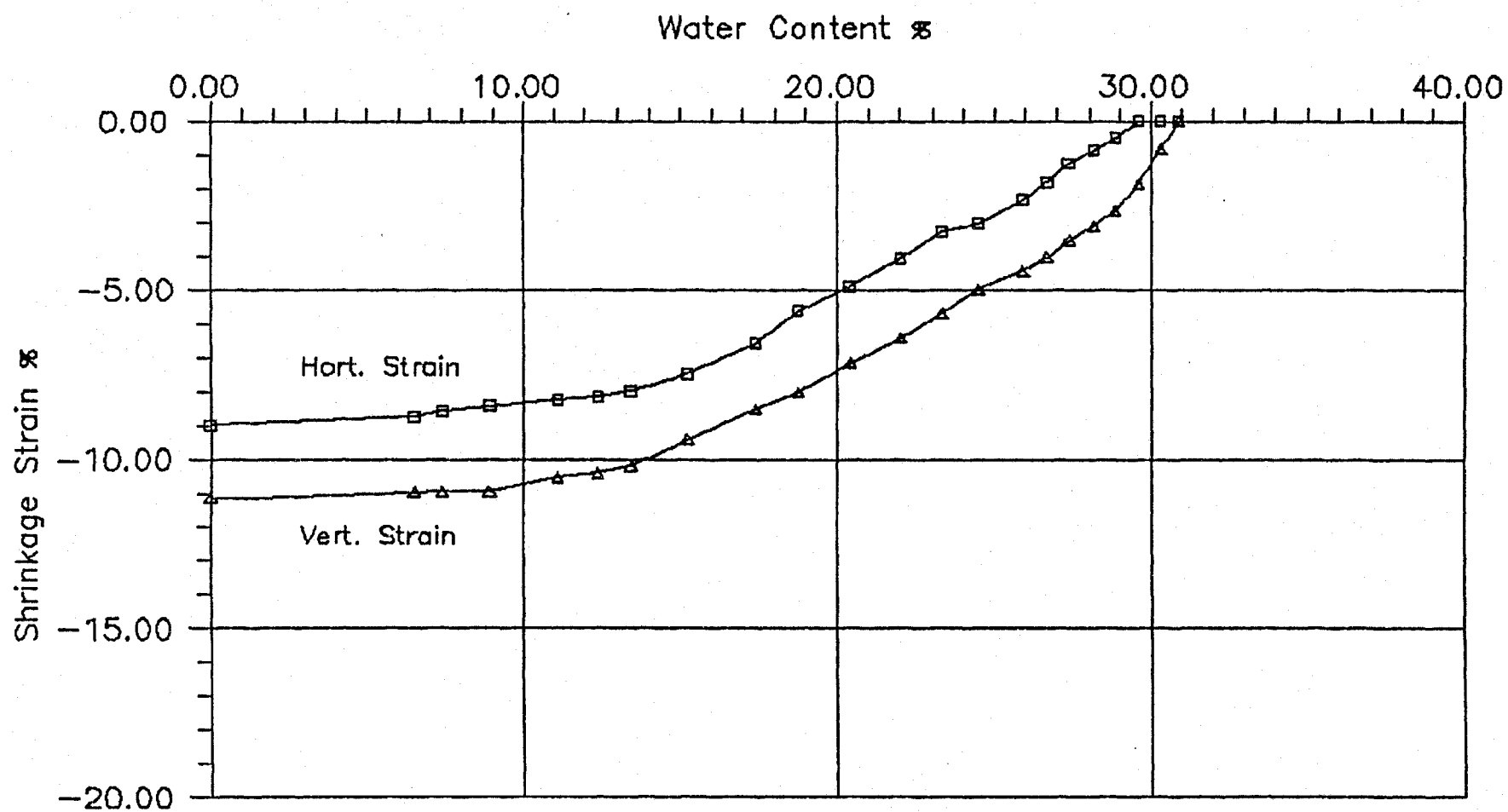


Fig. 6.13: Water content versus shrinkage strain for Indian Head Till mixed at water content of 31.0% and allowed to dry in a brass container (Test No. S02).

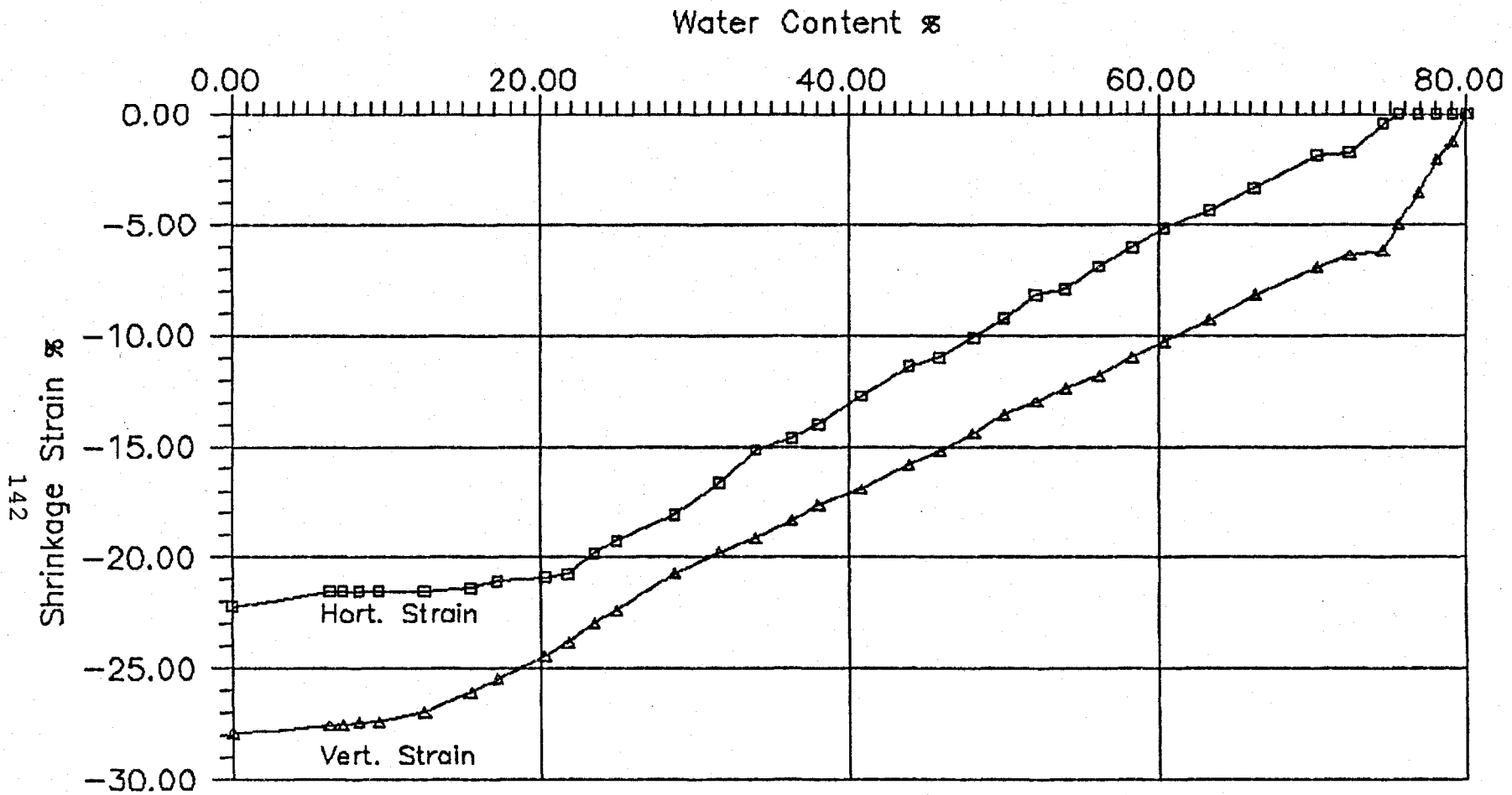


Fig. 6.14: Water content versus shrinkage strain for Regina Clay mixed at water content of 80.0% and allowed to dry in a brass container (Test No. S03).

Table 6.04: A summary of the shrinkage test results during various conditions.

Initial Conditions

Shrinkage Test No.	Soil type	Water content
S01	Till	37.7%
S02	Till	31.0%
S03	Clay	80.0%

Conditions when the horizontal strain was noticed

Shrinkage Test No.	Time elapsed	Vertical strain	Water content
S01	11.6 hrs	8.8%	31.3%
S02	3.0 hrs	2.7%	28.9%
S03	5.0 hrs	6.2%	74.6%

Conditions when the increase rate of vertical and horizontal strains were small

Shrinkage Test No.	Time elapsed	Horizontal strain	Vertical strain	Water content
S01	65.3 hrs	9.2%	17.2%	8.3%
S02	40.5 hrs	8.4%	10.9%	8.9%
S03	105.3 hrs	21.5%	27.4%	9.5%

Conditions when the soil samples were completely dried

Shrinkage Test No.	Horizontal strain	Vertical strain
S01	9.3%	17.5%
S02	9.0%	11.1%
S03	22.2%	27.9%

The relationships between the water content and the shrinkage strains for all the shrinkage tests are shown in Figs. 6.12 to 6.14. Detailed shrinkage test results at different stages of drying are summarized in Table 6.04.

6.3.2 Cracking Tests

Five cracking tests (i.e., Test Nos. T01 to T05) were performed on Indian Head Till and one test (i.e., Test No. T06) was conducted on Regina Clay. The purpose of conducting these six cracking tests was to study the effects of soil type, initial water content, soil thickness and the container side wall condition on the behavior of the soil cracking. During the tests, the matric suction, water content and the vertical shrinkage strain were measured.

Detailed cracking test results at various stages of desiccation are summarized in Table 6.05. The relationships between the time (i.e., stages of desiccation) and the vertical shrinkage strain for all the tests are shown in Figs. 6.15 to 6.20. Different stages of cracking in all six tests were recorded using photographs as shown in Figs. 6.21 to 6.44, inclusively. Interfacial markings were observed on most of the cracking surfaces, the close-up views of these markings are shown in Figs. 6.45 and 6.46.

Table 6.05: A summary of the cracking test results.

Initial conditions

Cracking Test No.	Soil type	Mixing water content	Average soil thickness
T01	till	37.7%	58.8 mm
T02	till	38.2%	54.1 mm
T03	till	31.1%	60.4 mm
T04	till	38.1%	33.7 mm
*T05	clay	82.5%	59.7 mm
*T06	till	37.5%	60.8 mm

Conditions when the first crack was noticed

Cracking Test No.	Time elapsed	Average matric suction	w%	Average vert. strain
T01	43.0 hrs	3.6 kPa	32.3%	6.3%
T02	34.5 hrs	3.6 kPa	32.6%	6.3%
T03	4.0 hrs	1.8 kPa	28.8%	1.0%
T04	22.5 hrs	4.5 kPa	33.0%	6.9%
T05	56.5 hrs	5.9 kPa	71.6%	4.7%
T06	81.5 hrs	11.9 kPa	27.6%	9.3%

Note:

* Container side walls were lined with wax paper and aluminum foils.

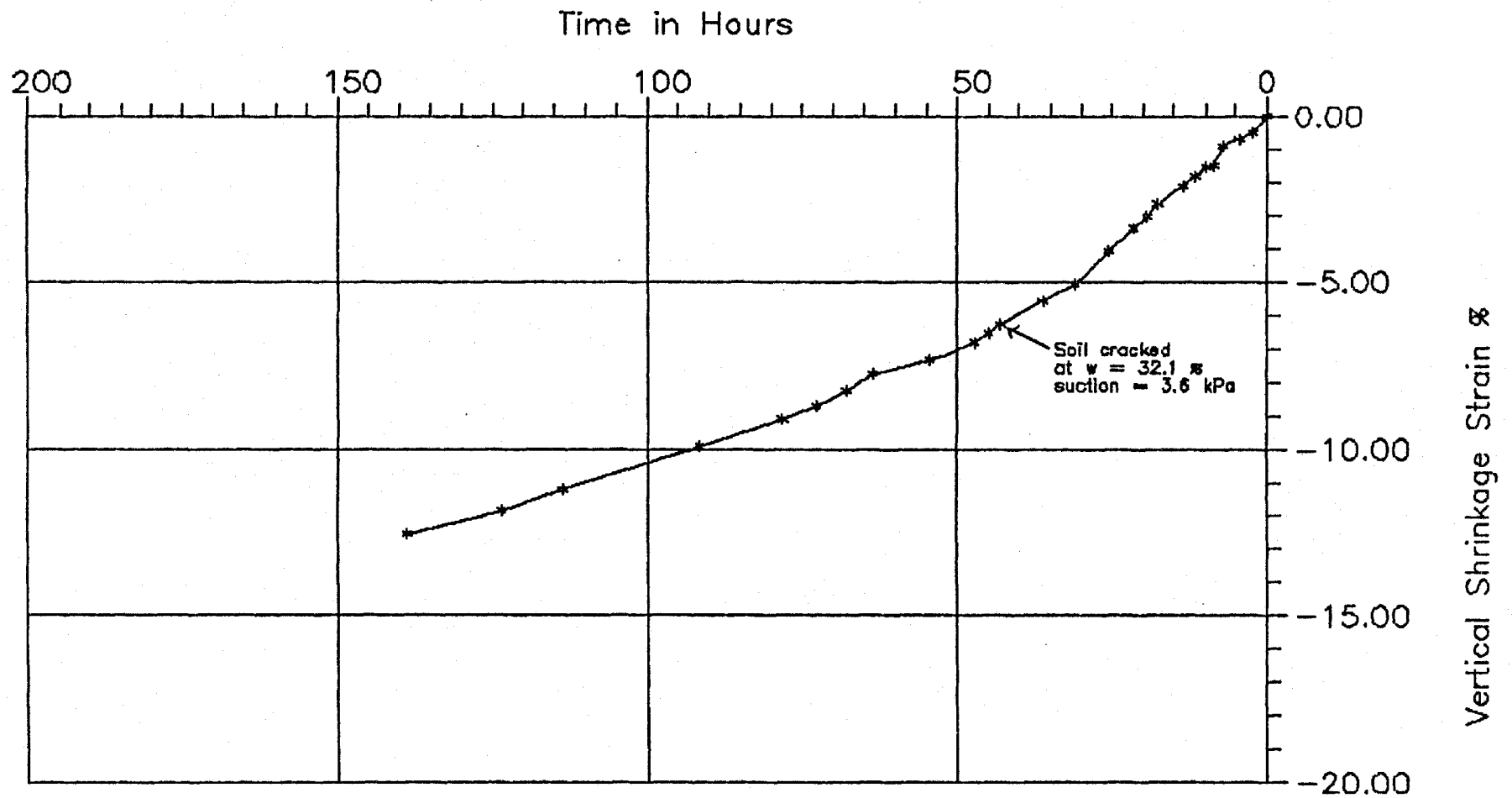


Fig. 6.15: Time versus vertical shrinkage strain for Indian Head Till mixed at initial water content of 37.7% and the soil sample was 58.8 mm thick (Test No. T01).

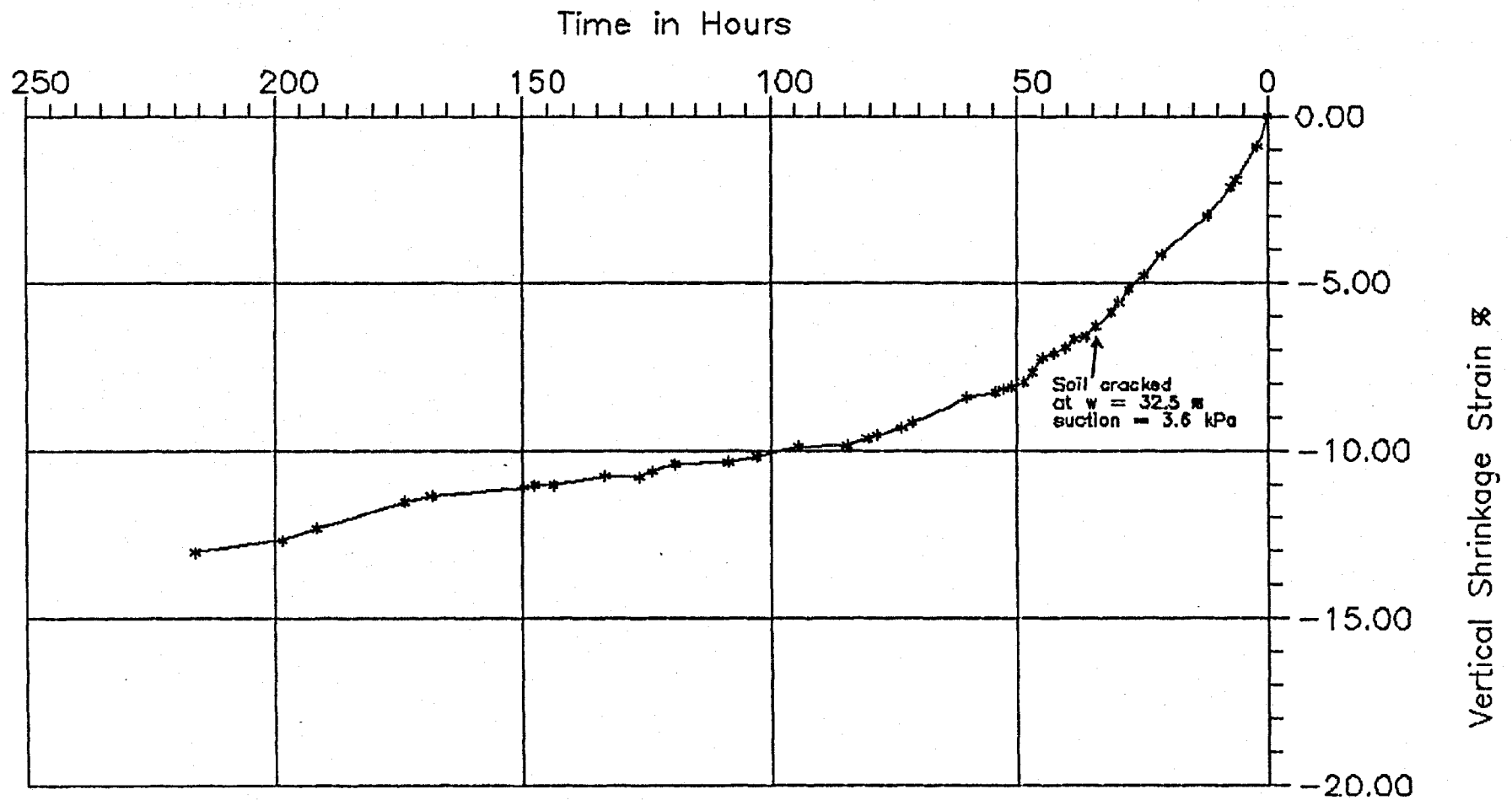


Fig. 6.16: Time versus vertical shrinkage strain for Indian Head Till mixed at initial water content of 38.2% and the soil sample was 54.1 mm thick (Test No. T02).

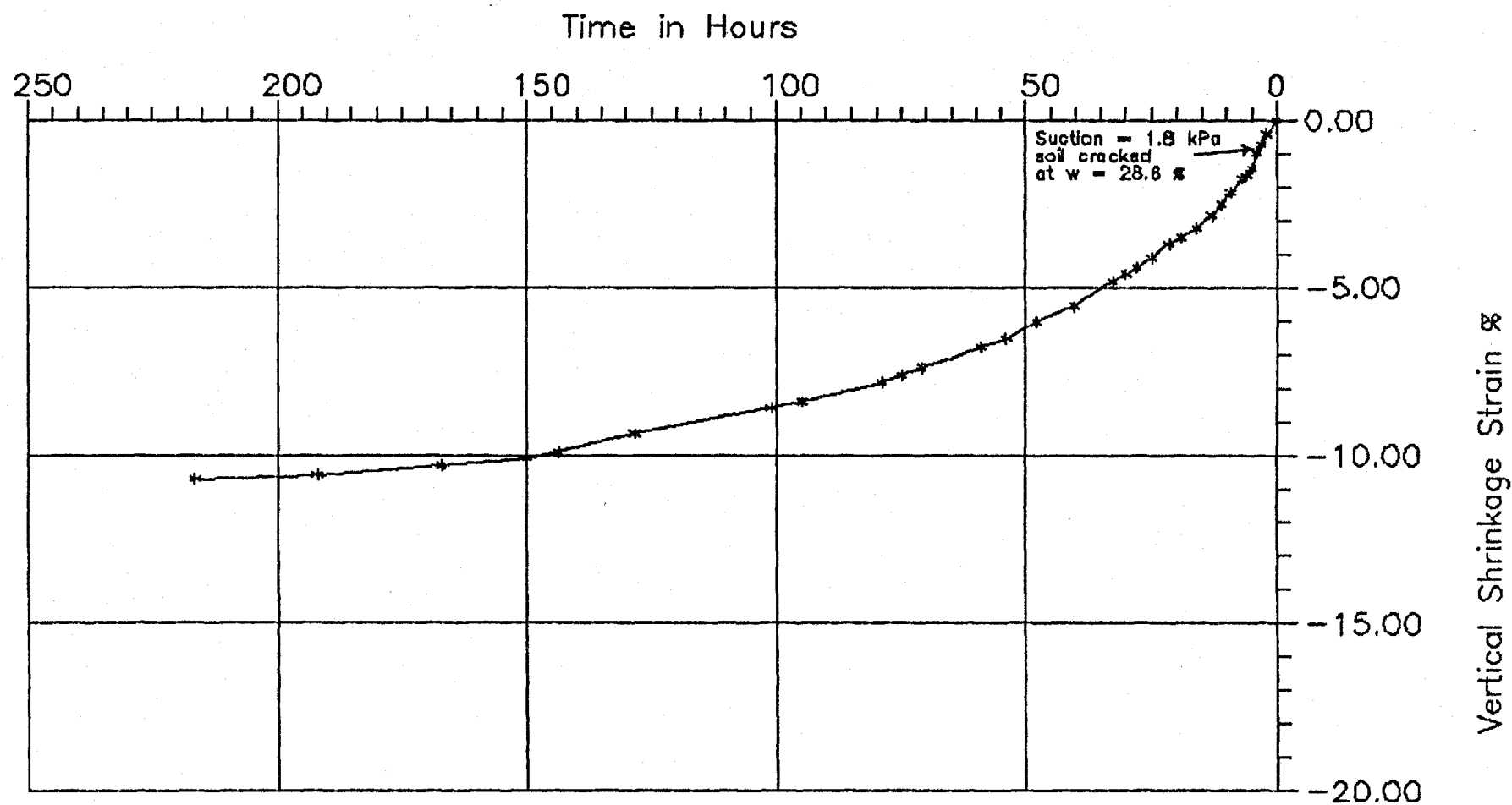


Fig. 6.17: Time versus vertical shrinkage strain for Indian Head Till mixed at initial water content of 31.1% and the soil sample was 60.4 mm thick (Test No. T03).

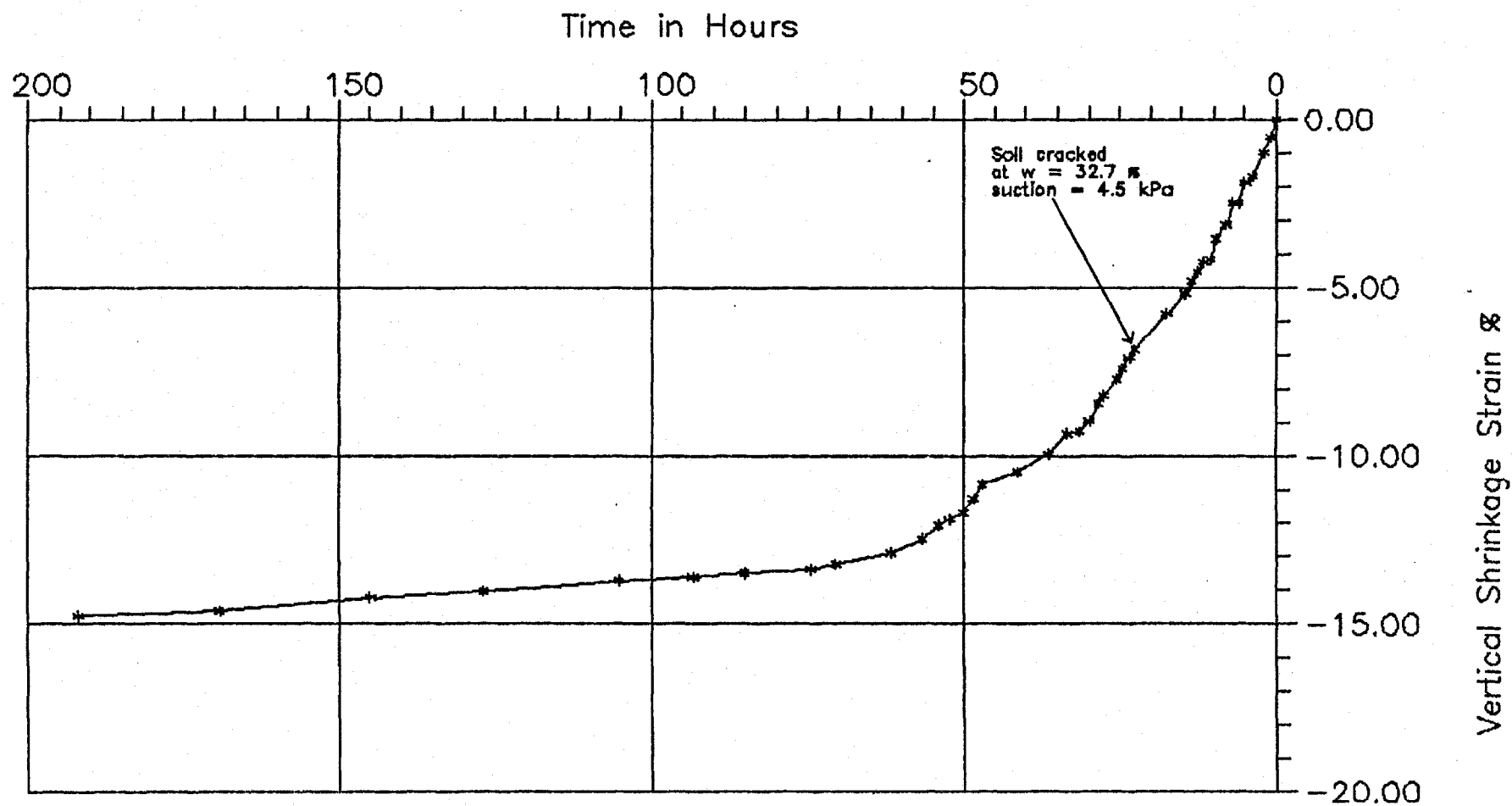


Fig. 6.18: Time versus vertical shrinkage strain for Indian Head Till mixed at initial water content of 38.1% and the soil sample was 33.7 mm thick (Test No. T04).

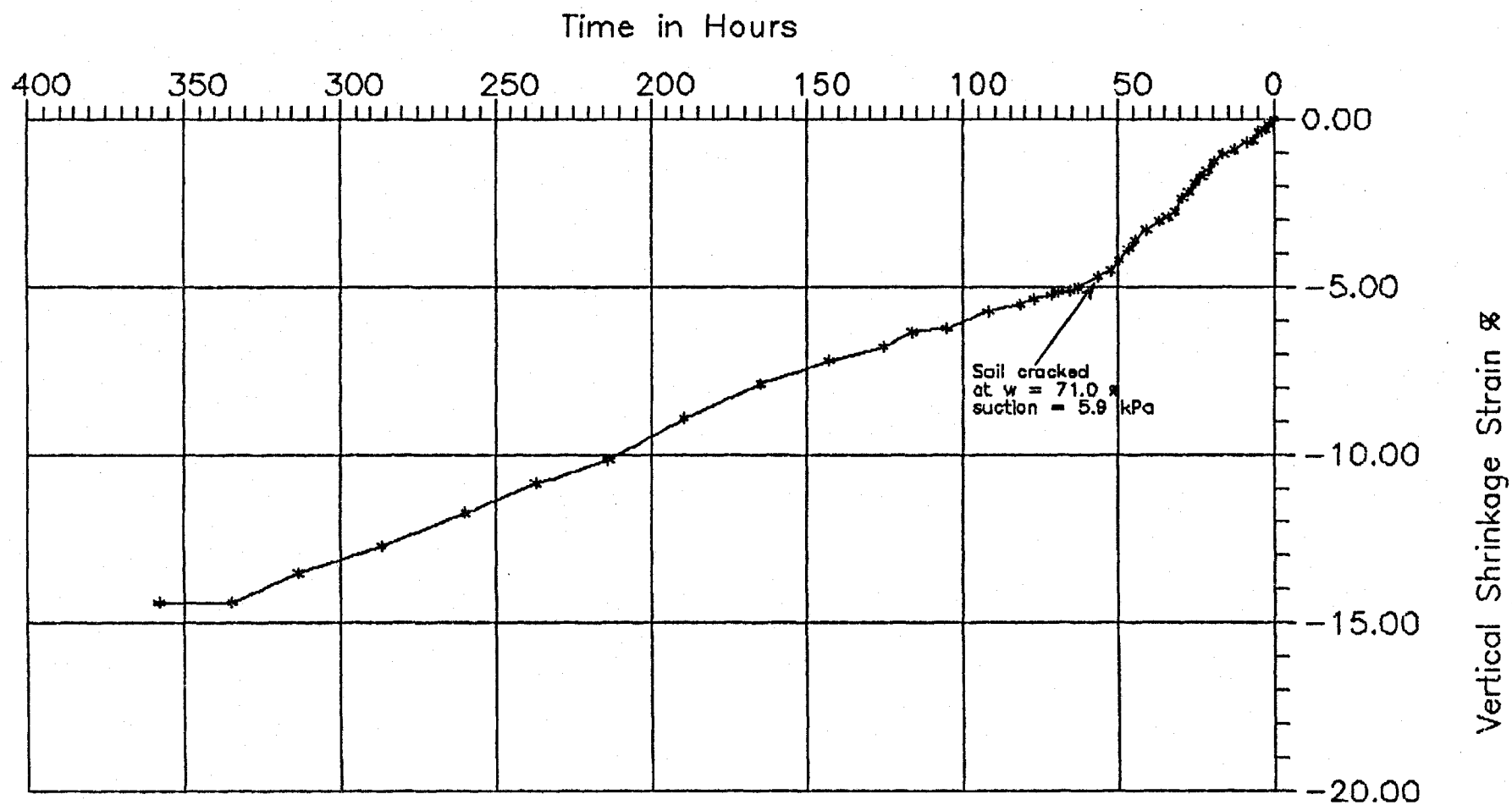


Fig. 6.19: Time versus vertical shrinkage strain for Regina Clay mixed at initial water content of 82.5% and the soil sample was 59.7 mm thick (Test No. T05).

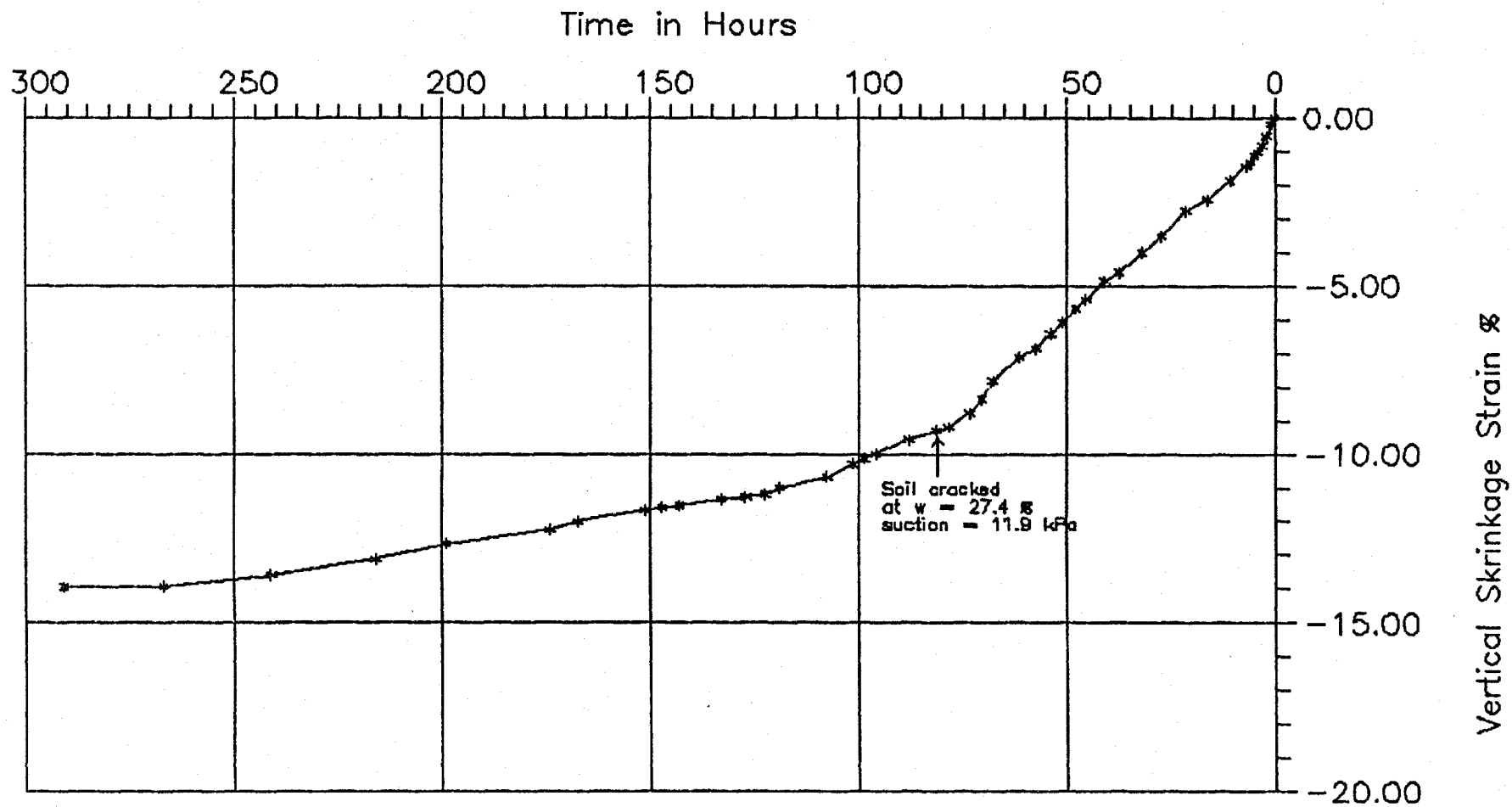


Fig. 6.20: Time versus vertical shrinkage strain for Indian Head Till mixed at initial water content of 37.5% and the soil sample was 60.8 mm thick (Test No. T06).

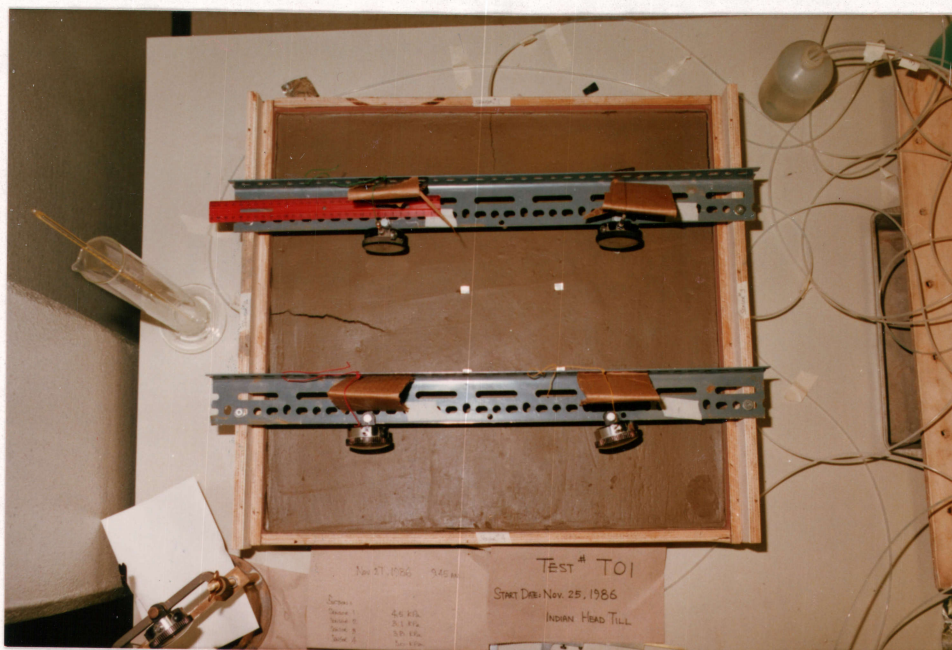


Fig. 6.21: Cracking test T01 on till after 43.0 hours. The water content of the sample was about 33.0%. All ceramic cup sensors were installed horizontally from the container sidewalls, 150 mm into the soil.

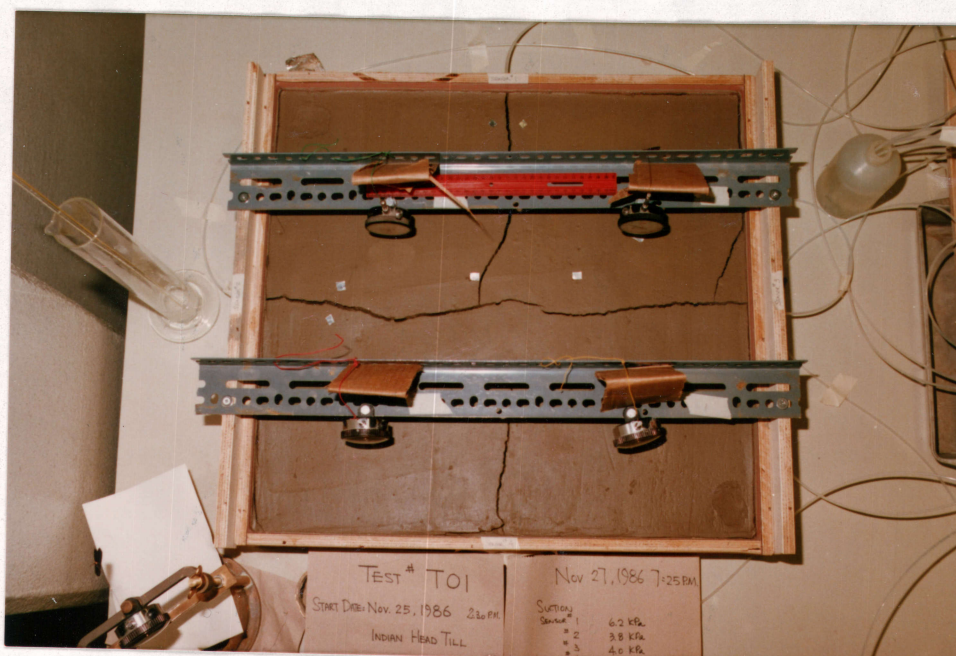


Fig. 6.22: Cracking test T01 on till after 54.6 hours. The water content of the sample was about 29.0%.

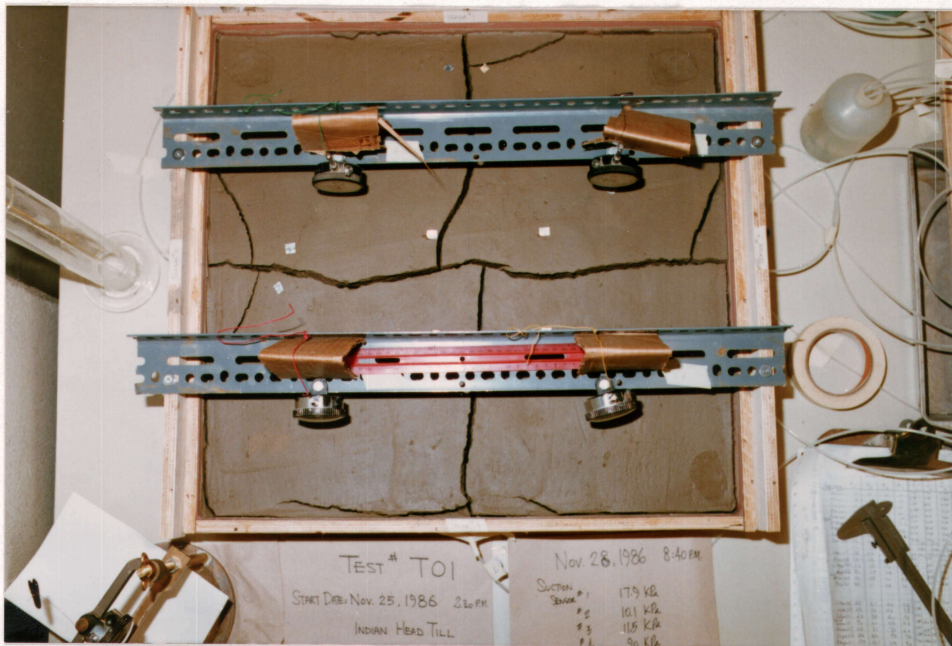


Fig. 6.23: Cracking test T01 on till after 78.2 hours. The water content of the sample was about 27.0%.

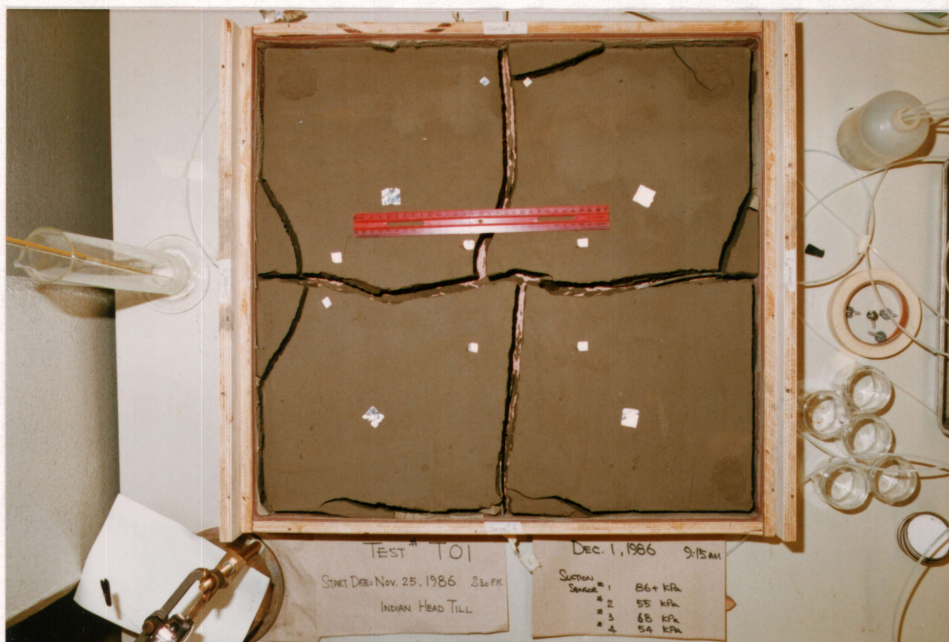


Fig. 6.24: Cracking test T01 on till after 138.9 hours. The water content of the sample was about 23.4%.

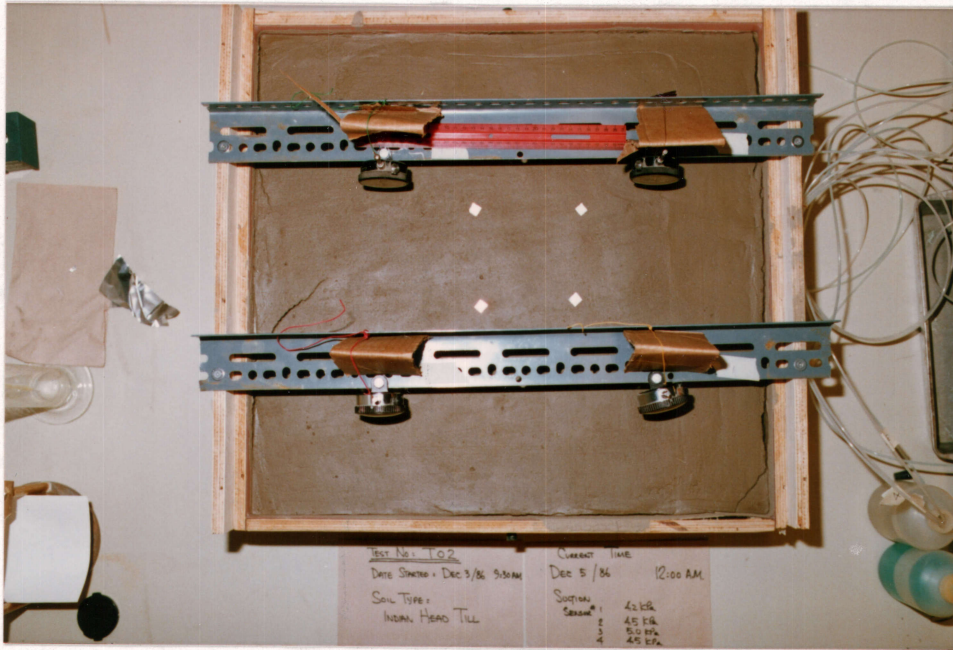


Fig. 6.25: Cracking test T02 on till after 38.5 hours. The water content of the sample was about 32.0%. All ceramic cup sensors were installed vertically from the bottom of the container, 35 mm into the soil.

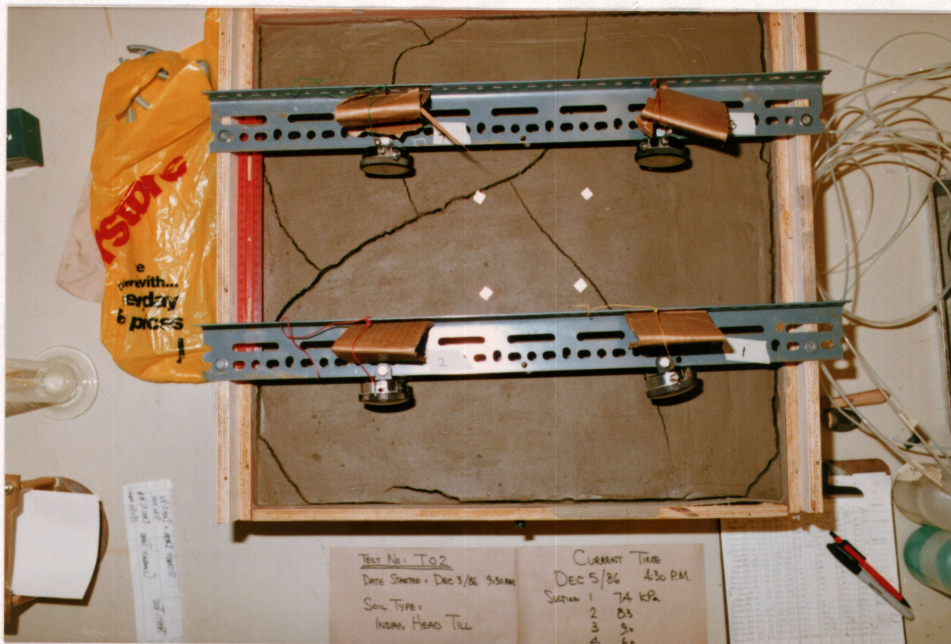


Fig. 6.26: Cracking test T02 on till after 54.5 hours. The water content of the sample was about 30.0%.

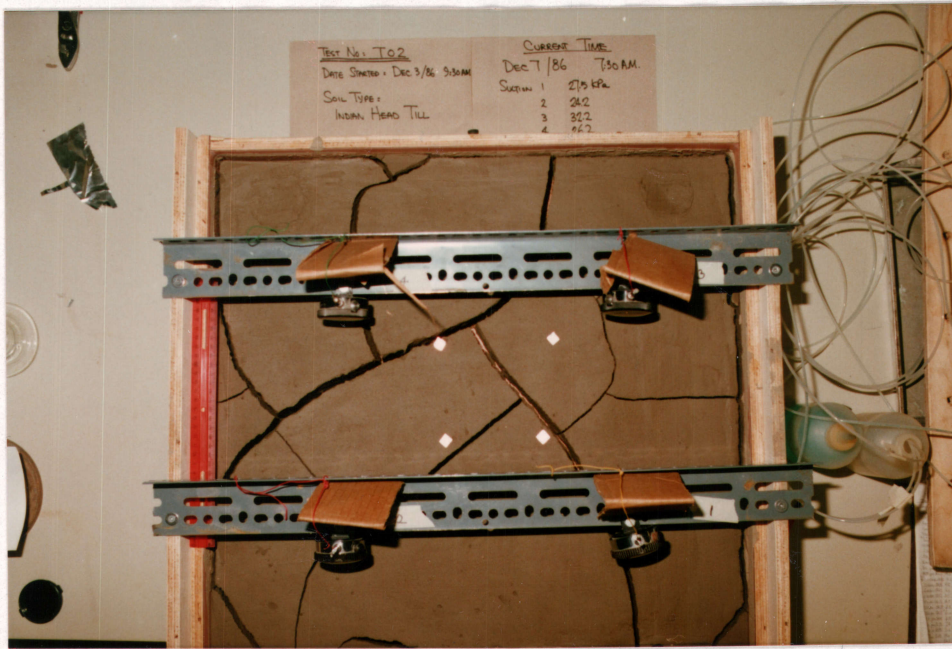


Fig. 6.27: Cracking test T02 on till after 94.3 hours. The water content of the sample was about 25.8%.

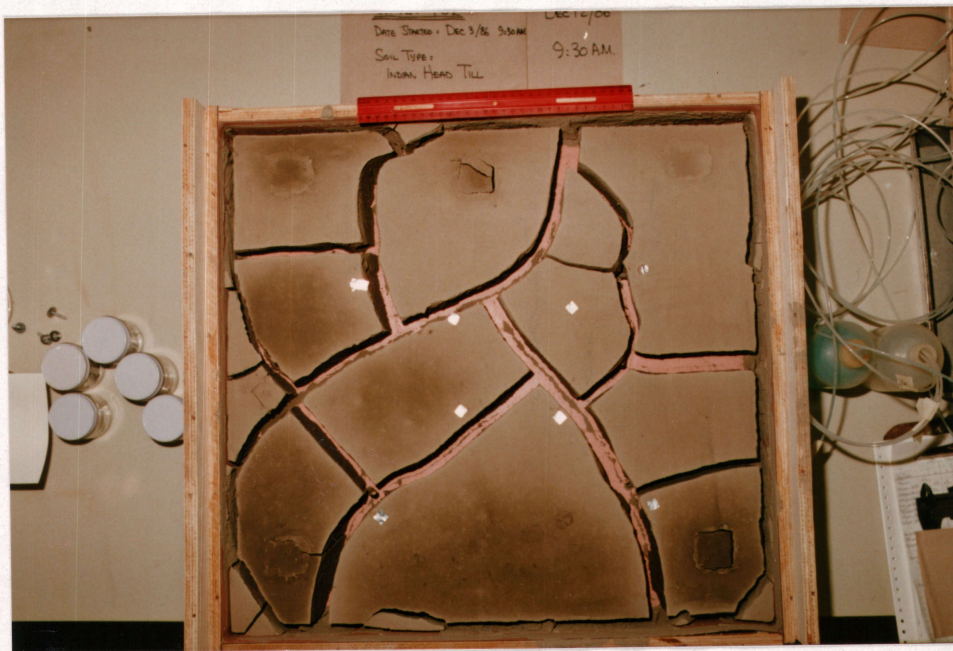


Fig. 6.28: Cracking test T02 on till after 216.0 hours. The water content of the sample was about 9.5%.

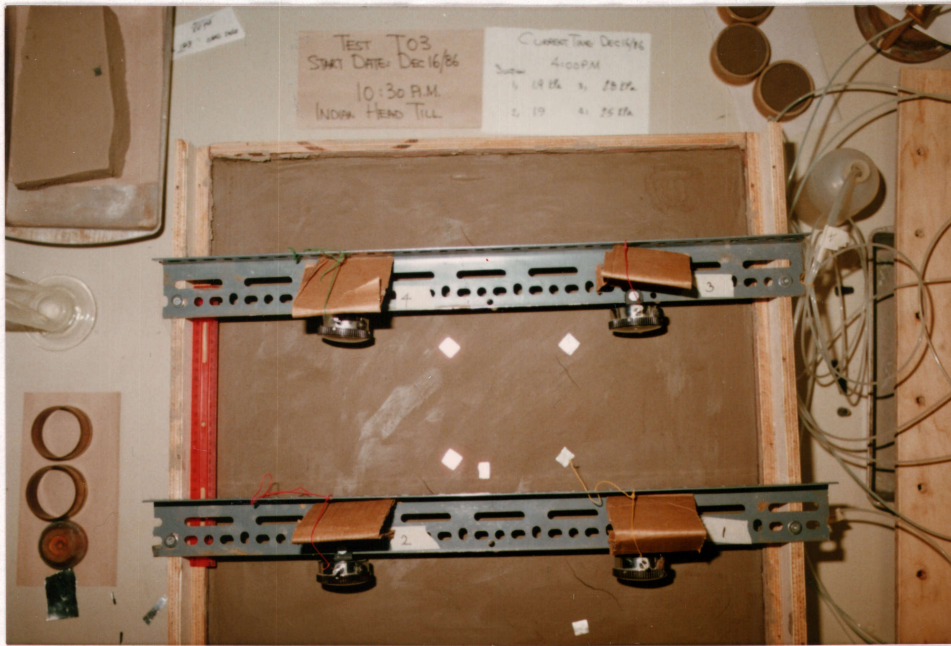


Fig. 6.29: Cracking test T03 on till after 6.0 hours. The water content of the sample was about 28.5%. All ceramic cup sensors were installed vertically from the bottom of the container, 35 mm into the soil.



Fig. 6.30: Cracking test T03 on till after 11.0 hours. The water content of the sample was about 28.0%.

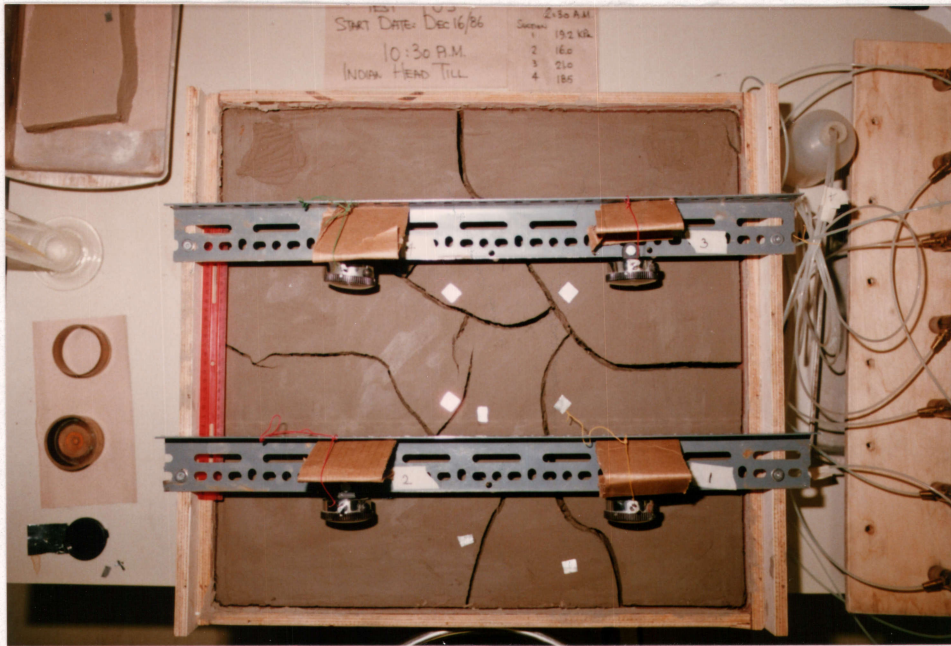


Fig. 6.31: Cracking test T03 on till after 40.5 hours. The water content of the sample was about 25.5%.

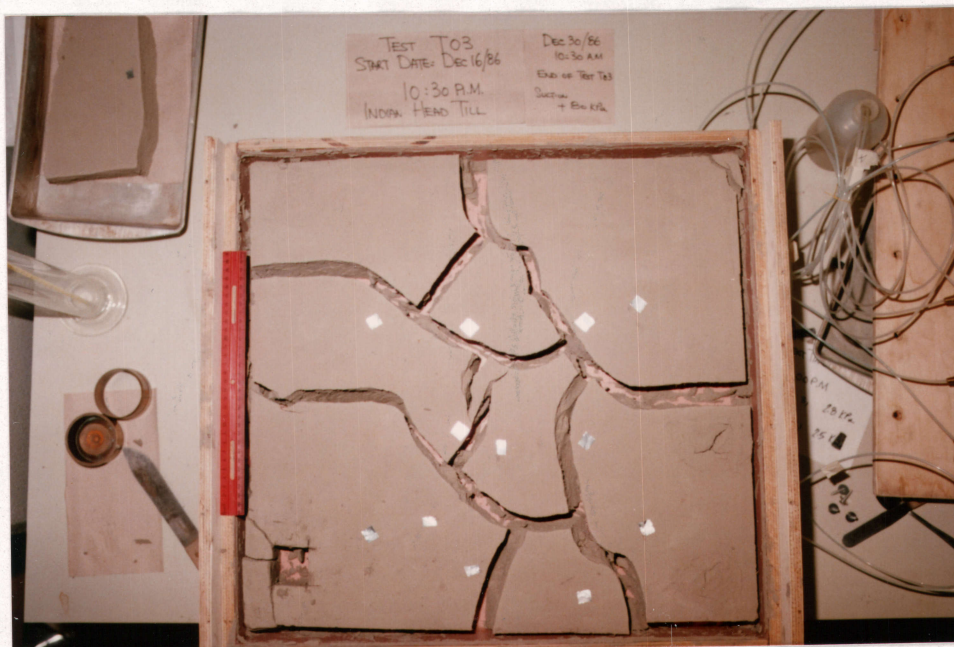


Fig. 6.32: Cracking test T03 on till after 337.0 hours. The water content of the sample was about 3.3%.

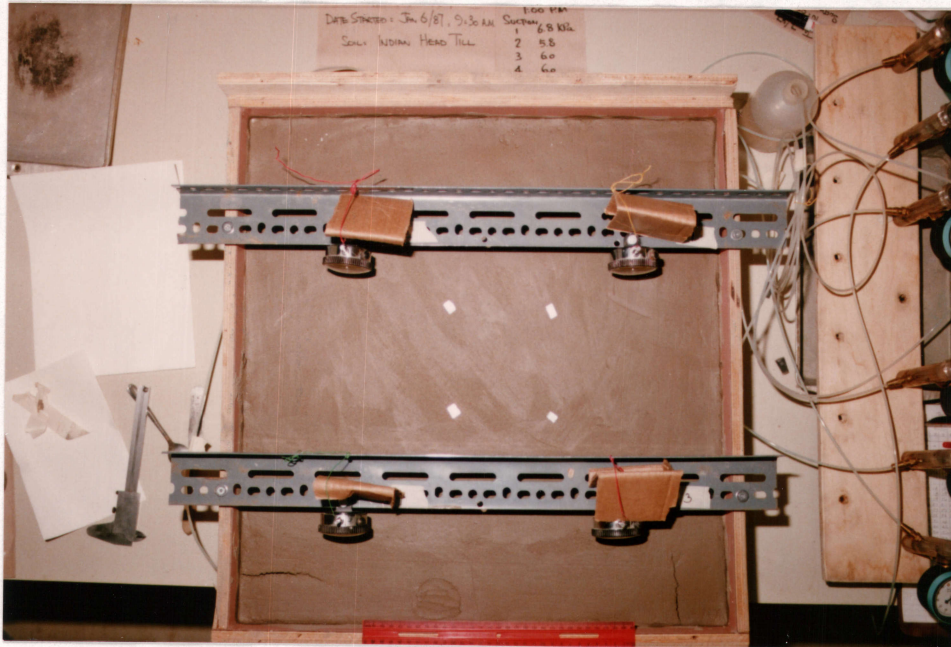


Fig. 6.33: Cracking test T04 on till after 27.5 hours. The water content of the sample was about 32.5%. All ceramic cup sensors were installed horizontally from the container sidewalls, 35 mm into the soil.

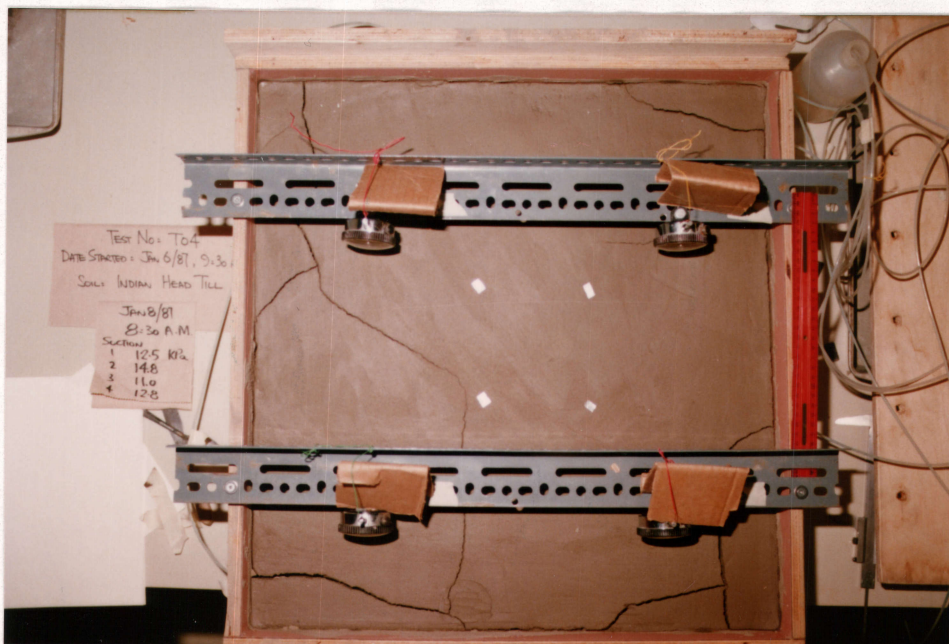


Fig. 6.34: Cracking test T04 on till after 47.0 hours. The water content of the sample was about 28.5%.

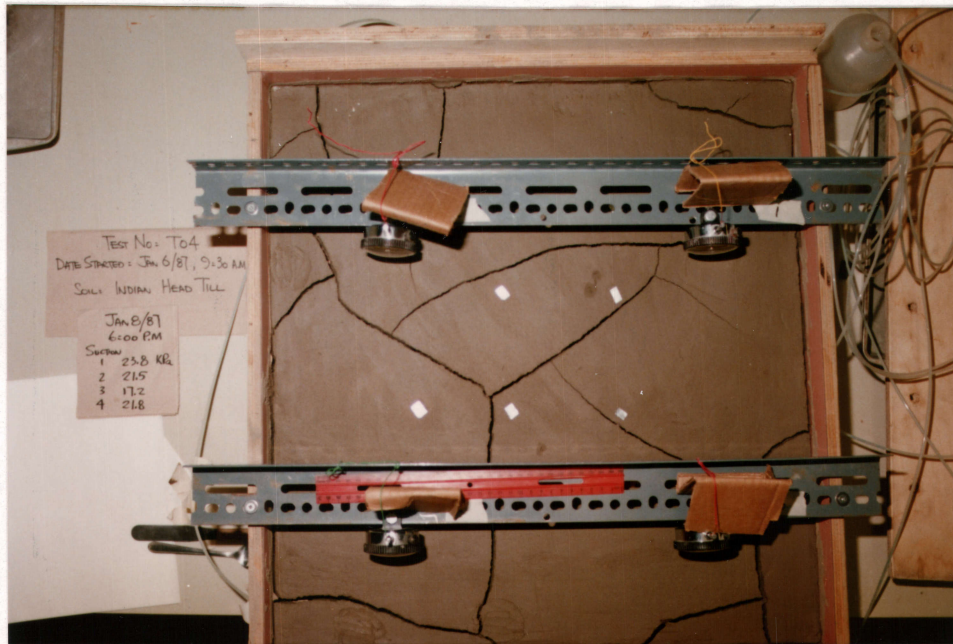


Fig. 6.35: Cracking test T04 on till after 56.5 hours. The water content of the sample was about 26.6%.

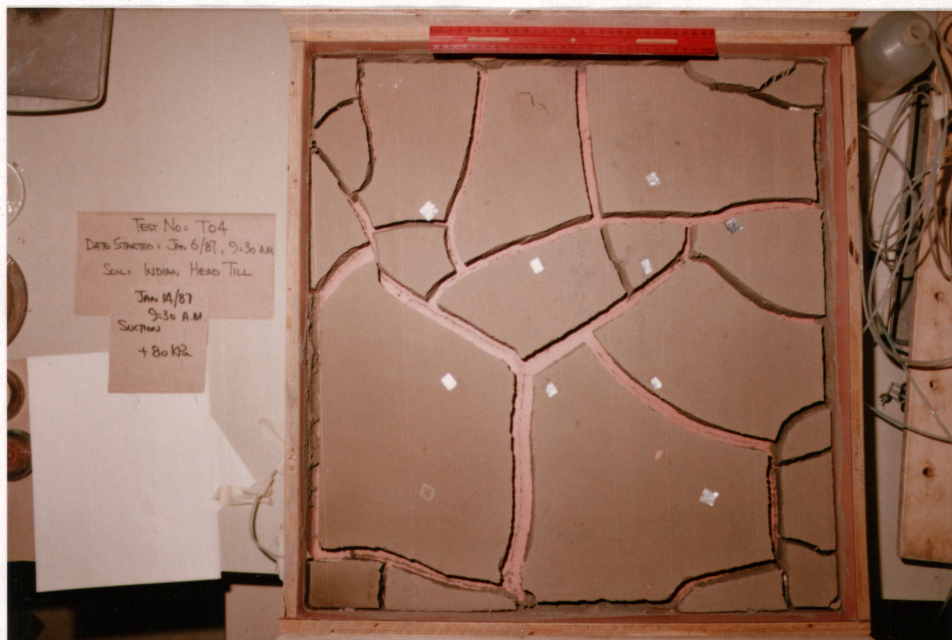


Fig. 6.36: Cracking test T04 on till after 192.0 hours. The water content of the sample was about 5.7%.

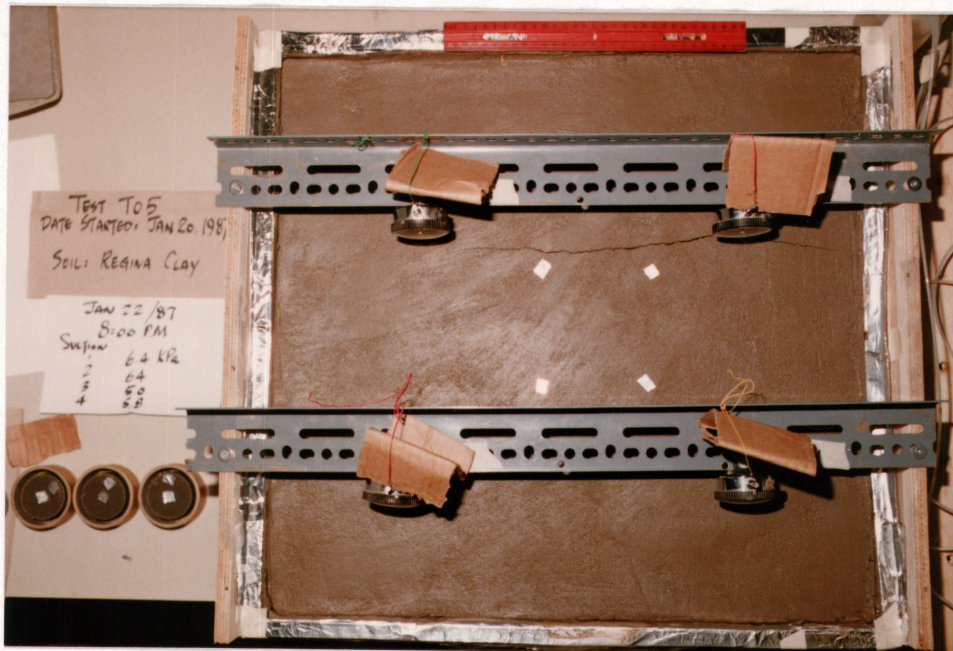


Fig. 6.37: Cracking test T05 on clay after 56.5 hours. The water content of the sample was about 71.0%. All ceramic cup sensors were installed vertically from the bottom of the container, 35 mm into the soil. Container side walls were lined with wax paper and aluminum foils.



Fig. 6.38: Cracking test T05 on clay after 92.0 hours. The water content of the sample was about 66.7%.

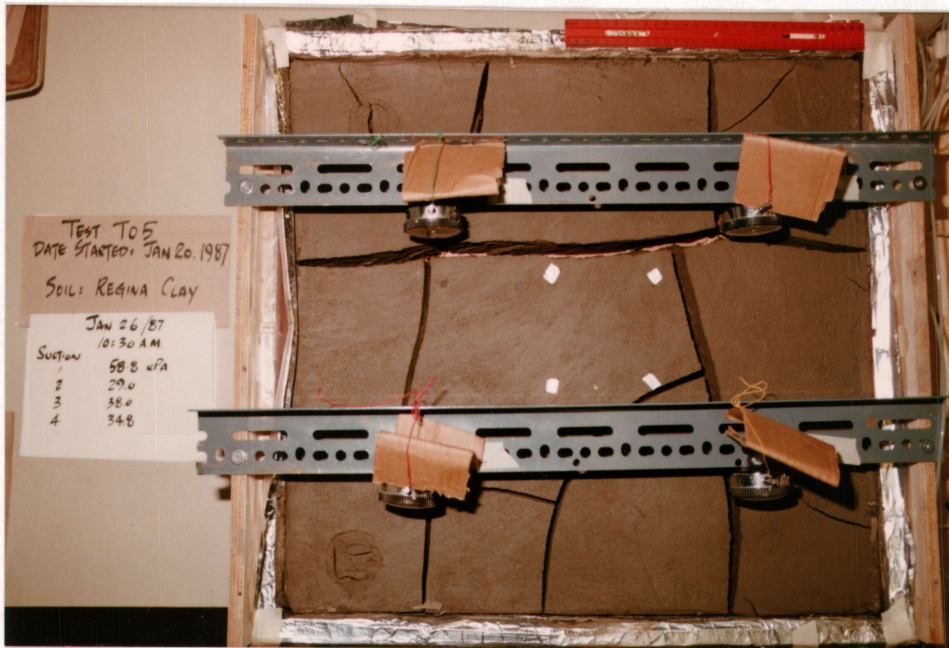


Fig. 6.39: Cracking test T05 on clay after 143.0 hours. The water content of the sample was about 57.0%.



Fig. 6.40: Cracking test T05 on clay after 358.0 hours. The water content of the sample was about 23.5%.

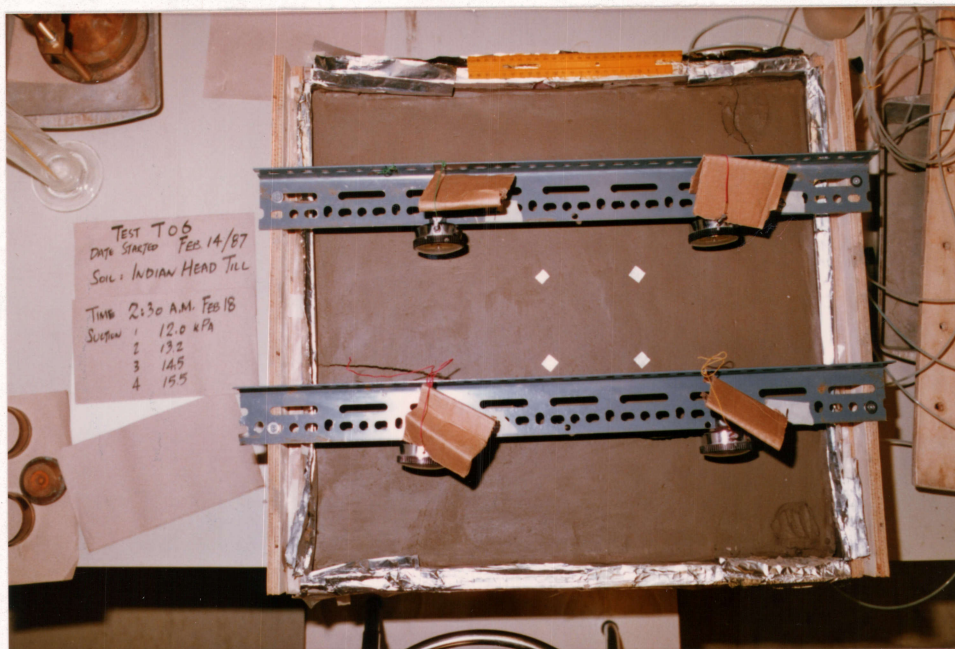


Fig. 6.41: Cracking test T06 on till after 81.5 hours. The water content of the sample was about 27.5%. ceramic cup sensors were installed vertically from the bottom of the container, 35 mm into the soil. Container side walls were lined with wax paper and aluminum foils.

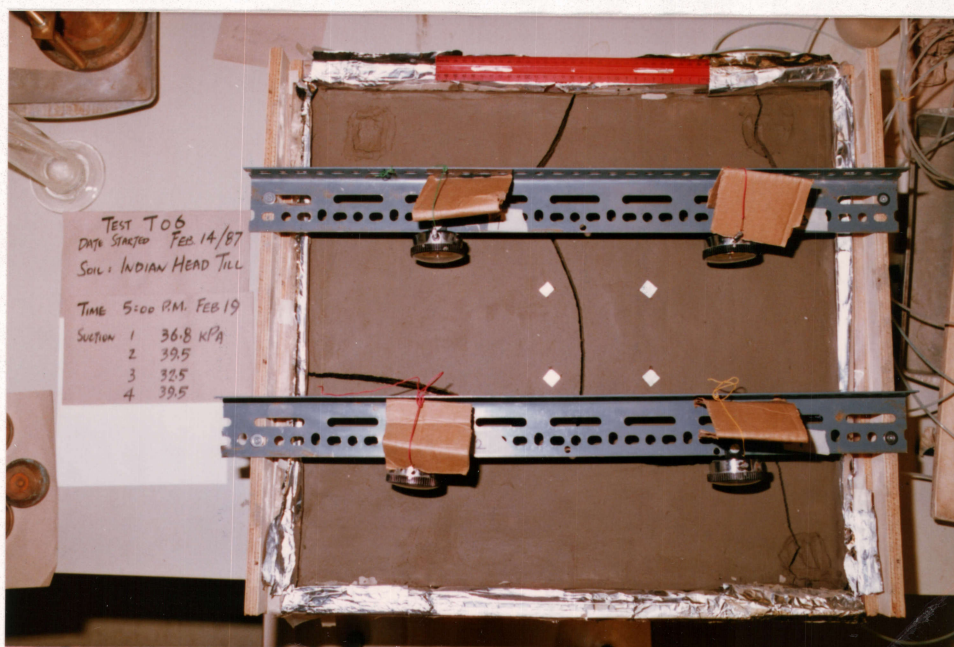


Fig. 6.42: Cracking test T06 on till after 127.0 hours. The water content of the sample was about 25.0%.

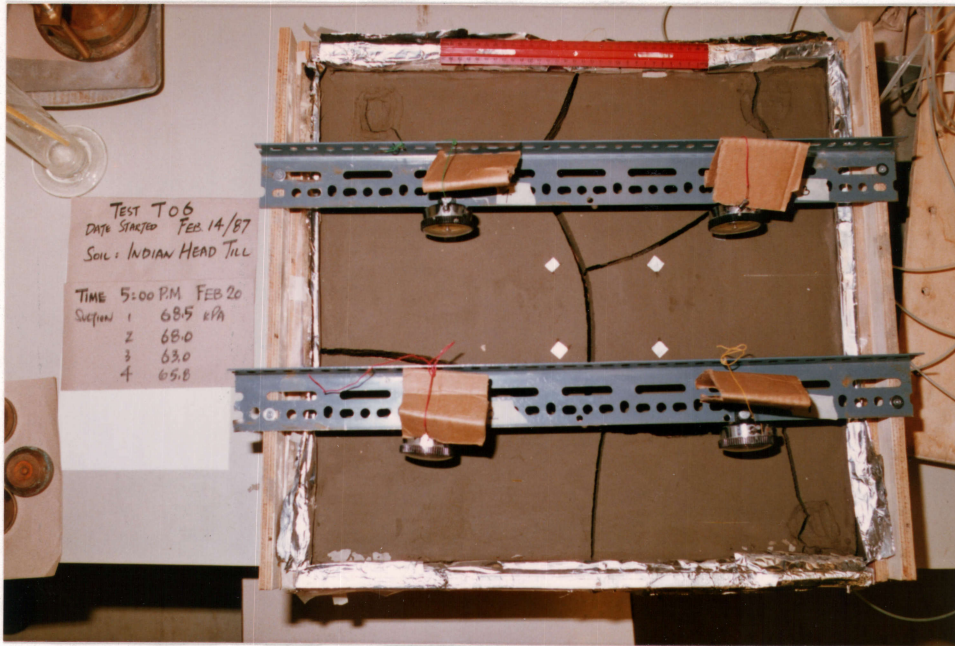


Fig. 6.43: Cracking test T06 on till after 151.0 hours. The water content of the sample was about 23.0%.

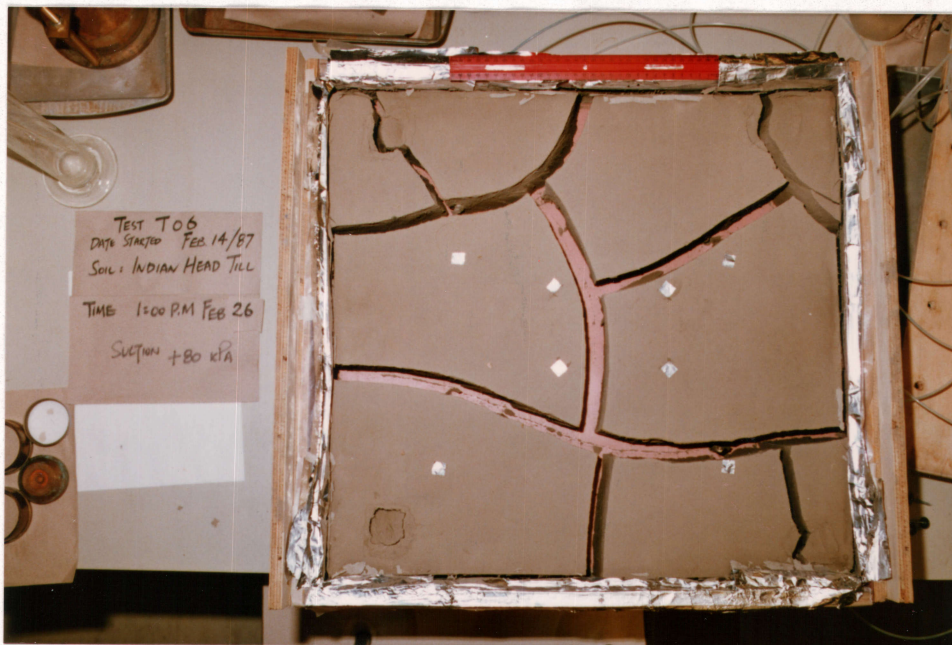


Fig. 6.44: Cracking test T06 on till after 291.0 hours. The water content of the sample was about 7.2%.



Fig. 6.45: Interfacial markings on the cracked soil surface (Test No. T04).

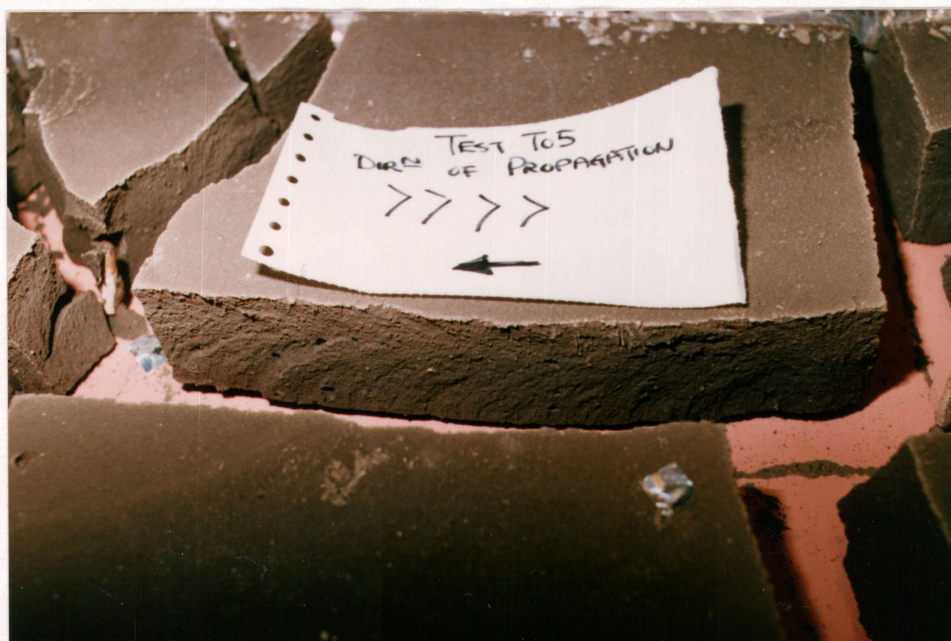


Fig. 6.46: Interfacial markings on the cracked soil surface (Test No. T05).

CHAPTER 7

DISCUSSION OF RESULTS

7.1 INTRODUCTION

The data obtained from the analytical and experimental programs are discussed in this chapter. The discussions are be divided into two sections. The first section deals with the laboratory test results and the characteristics of desiccation cracking in soils. The relative effects of different soil parameters on the predicted crack depth are discussed in the second section.

7.2 CHARACTERISTICS OF DESICCATION CRACKING IN SOILS

Laboratory test results observed in this study generally indicate that desiccation cracks were formed slowly in a sequential manner. Desiccation cracks did not bifurcate (i.e., did not branch out). Orthogonal intersections (i.e., forming right angle intersections) were observed in most of the tests. The predominant number of sides of desiccation polygons was found to be four or five.

Cracking in soils can be assumed to be the result of the application of excessive tensile stresses. Tension cracks tend to propagate in the direction perpendicular to the applied maximum tension. After the first desiccation crack was formed, any further crack advancing in an oblique direction will tend to be normal to the first crack after entering its zone of stress relief. Therefore, orthogonal intersections are the result. A typical orthogonal cracking pattern due to desiccation is shown in Fig. 7.01.

Some oblique intersections were observed at the interface between the soil and the container side wall in Test Nos. T01, T02, T03 and T04. In these tests, soils adhered to the container side wall as a result of adhesion between the soil and the container side wall. As soil shrinks during desiccation, cracks initiated at the adhered interface, forming oblique intersection. However, when the container side walls were lined with wax paper and aluminum foil in Test Nos. T05 and T06, orthogonal intersections were formed at the interface.

Interfacial fracture marking with a characteristic herringbone appearance were observed on most of the cracking surfaces. The orientation of the herringbone fracture markings was always in the same direction as the propagation of cracking (see Figs. 6.45 and 6.46). These markings

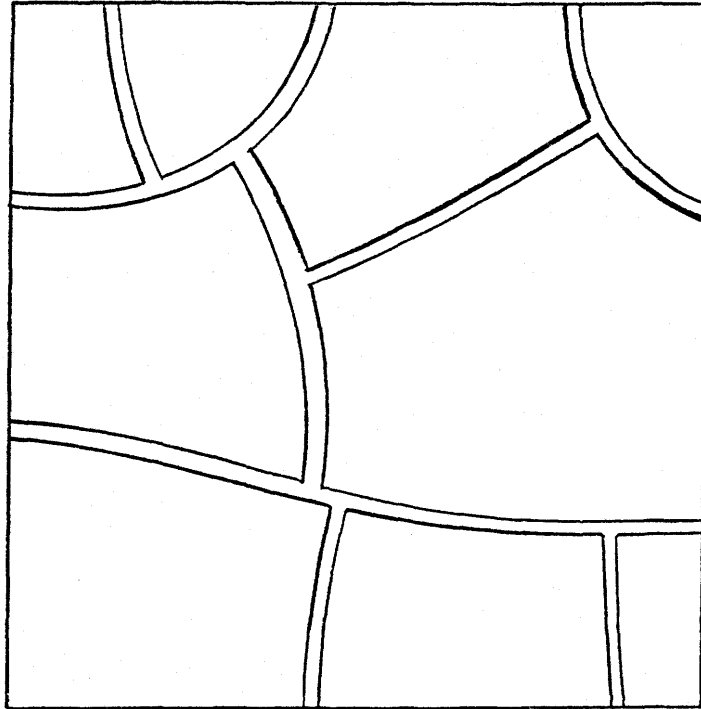


Fig. 7.01: A typical orthogonal cracking pattern (after Test No. T06).

were formed due to the interaction between the adhesion at the container bottom and the propagation of the tension cracks at the soil surface.

7.2.1 Crack Spacing

In Test Nos. T01, T04, T05 and T06, the first desiccation cracks were initiated at the position of the ceramic cup sensors. In Test No. T02, the first crack was located at the interface between the container side wall and the soil. The soils used in Test No. T03 was mixed at a lower water content (i.e., about 3.5% below the liquid limit), an appreciable amount of air bubbles was occluded in the soil paste. Desiccation cracks were initiated from these occluded air bubbles in Test No. T03.

Based upon the foregoing observations, it can be concluded that the locations of the desiccation crack (or the crack spacing) are highly dependent upon the positions of local inhomogeneities. The inhomogeneities include the presence of foreign matters (e.g., ceramic cup sensors), boundary conditions and material properties.

Figs. 7.02 and 7.03 show two different cracking patterns when different thicknesses of slurried Indian Head Till were allowed to dry in a small container. Well-

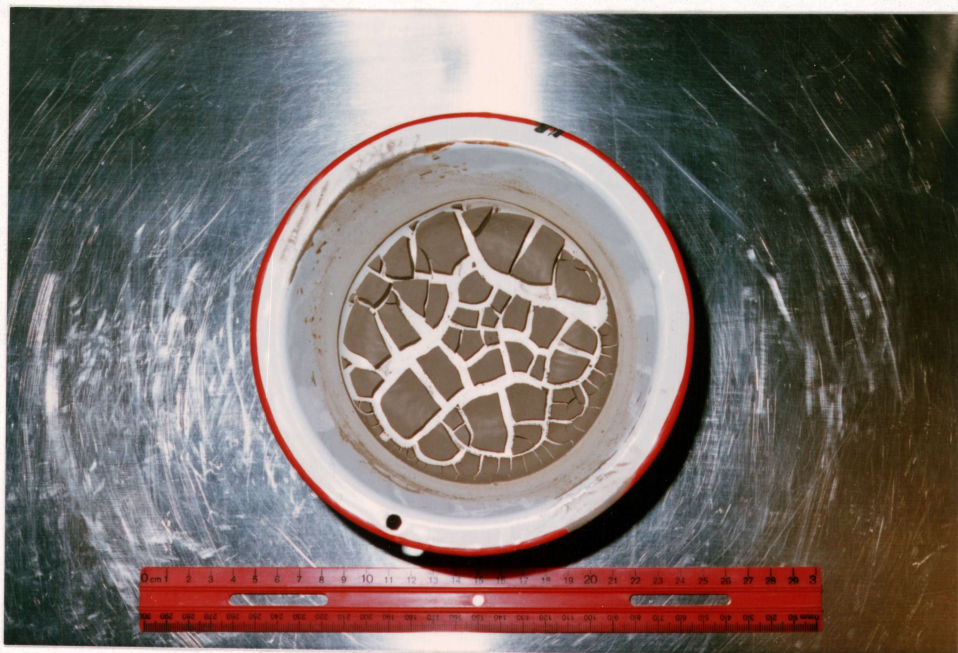


Fig. 7.02: Crack pattern in 10mm thick slurried Indian Head Till after desiccation.

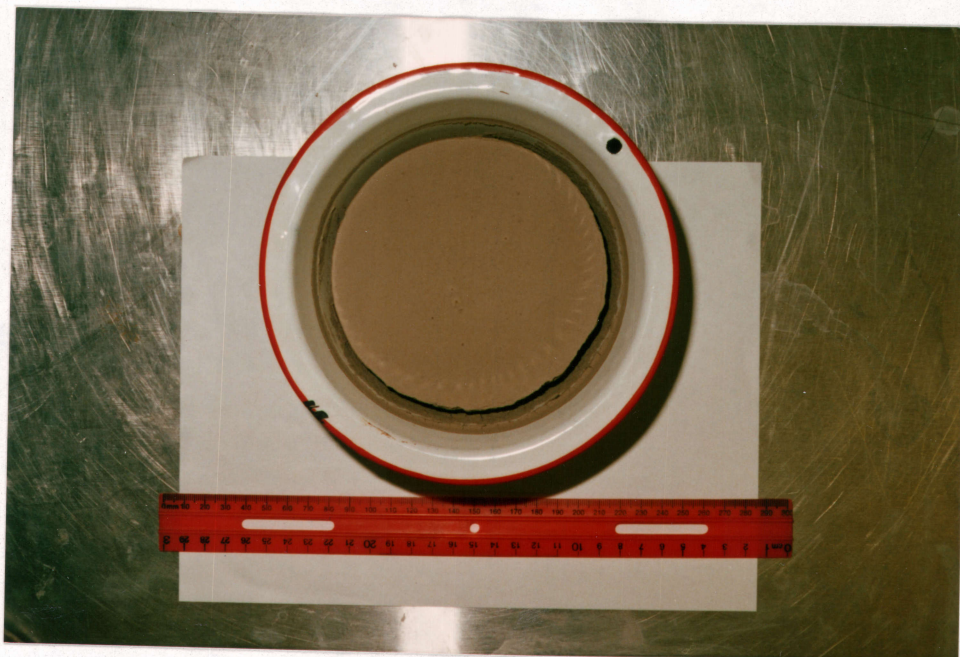


Fig. 7.03: No crack was observed in 40mm thick slurried Indian Head Till after desiccation.

developed orthogonal cracking patterns were observed in the thin soil slurry, whereas no cracks were observed in the thick soil slurry. Based on these observations, it can be concluded that the cracking patterns of a desiccated soil depend on the thickness of the soil deposits.

Test Nos. T05 and T06 were tested under the same conditions. The observations noted from these two tests tend to indicate that clayey soils (i.e., Regina clay) would have a higher cracking frequency (or a smaller crack spacing) than silty soils (i.e., Indian Head Till).

7.2.2 Soil Suction

Most of the cracking patterns observed in the cracking tests were initiated within the 0 to 85 kPa range of soil suction. At higher soil suction (i.e., greater than 85 kPa), no new desiccation crack was formed, and the cracks were widened as a result of further soil shrinkage.

Let us consider the results of all the cracking tests conducted on Indian Head Till as shown in Table 6.05. Test No. T03, which had a larger amount of occluded air bubbles due to low mixing water content, required less time to crack. The average matric suction at cracking was relatively low, and was equal to 1.8 kPa. On the other hand, Test No.

T06, which was free from any container side wall effect, required a longer time to crack. The average matric suction at cracking for Test No. T06 was comparatively higher than those obtained from Test Nos. T01 and T02, and was equal to 11.9 kPa. Based upon the above observations, it can be seen that a soil containing frequent flaws (e.g., Test No. T03) would require a shorter period of time and a lower matric suction to produce cracking.

The matric suction at cracking for Test No. T04, which had a thinner layer of soil, was higher than those obtained in Test Nos. T01 and T02. It appears that the increase in matric suction at cracking for Test No. T04 was due to the effect of adhesion at the container bottom. The adhesion between the soil and the container bottom is believed to have a greater influence on the stress conditions of a thinner layer of soil.

In Test Nos. T05 and T06, no constraint was provided between the soil and the container side wall during desiccation. The matric suction at cracking for Regina Clay (i.e., Test No. T05) was 5.9 kPa, which was lower than that for Indian Head Till (i.e., at 11.9 kPa for Test No. T06). In the field, where lateral constraints are present, the matric suction at cracking for the same soils under similar desiccation environments is expected to be less than those obtained from Test Nos. T05 and T06.

Based on the above discussions and the experimental results, it can be concluded that desiccation cracks are expected to form at a low soil suction (i.e., below 10 kPa). The matric suction at cracking for silty soils is expected to be higher than that for clayey soils. Silty soils have a less compressible soil structure than clayey soils, and therefore requires a higher matric suction at cracking than clayey soils.

7.2.3 Shrinkage Strain

Vertical shrinkage strains were measured during the shrinkage tests and the cracking tests (see Tables 6.04 and 6.05). Based on the water contents measured during the cracking tests and the shrinkage test results (i.e., Fig. 6.10 and 6.11), the volumetric shrinkage strain at cracking can be estimated. Let us consider the volumetric shrinkage strains for all the cracking tests as given in Table 7.01.

The volumetric shrinkage at cracking for Indian Head Till mixed at water contents of about 38% (i.e., Test Nos. T01, T02, and T04) varied between 6.9% in T01 and 7.7% in T04. The effect of the strong influence of container bottom adhesion is believed to be the cause for the higher volumetric shrinkage strain at cracking measured in Test No.

Table 7.01: A summary of the volumetric shrinkage strains for the cracking test results.

Initial conditions

Cracking Test No.	Soil type	Mixing water content	Average soil thickness	#Specific volume 100cc/g
T01	till	37.7%	58.8 mm	75.39
T02	till	38.2%	54.1 mm	75.87
T03	till	31.1%	60.4 mm	70.02
T04	till	38.1%	33.7 mm	75.77
*T05	clay	82.5%	59.7 mm	120.52
*T06	till	37.5%	60.8 mm	75.15

Conditions when the first crack was noticed

Cracking Test No.	w%	Average vertical strain	#Specific volume 100cc/g	Volumetric shrinkage strain
T01	32.30%	6.3%	69.75	7.5%
T02	32.60%	6.3%	70.06	7.7%
T03	28.80%	1.0%	67.19	4.0%
T04	33.04%	6.9%	70.52	6.9%
T05	71.63%	4.7%	107.18	11.1%
T06	27.63%	9.3%	64.91	13.6%

Notes:

* Container side walls were lined with wax paper and aluminum foils.

The specific volume of the soil were deduced from the shrinkage test results as shown in Figs. 6.10 and 6.11.

T04. The relatively low volumetric shrinkage strain at cracking in Test No. T03 can be explained as being due to the premature cracking as a result of the presence of inhomogeneities (i.e., occluded air bubbles) in the soils.

Little horizontal shrinkage was observed in Test Nos. T01, T02 and T04 prior to the formation of desiccation cracks. The vertical strains measured prior to cracking in these tests would, therefore, be approximately equal to the volumetric strain. It can be seen that the vertical strain at cracking for Test Nos. T01, T02 and T04 closely agreed to the volumetric strains estimated from the water content results and the shrinkage test results.

With the installation of wax paper and aluminum foil at the container side wall, the soils in Test Nos. T05 and T06 were allowed to shrink in the horizontal directions prior to the formation of the cracks. The volumetric shrinkage strain at cracking in Test No. T06 (i.e., Till) was, therefore, higher than those obtained in Test nos. T01 and T02. Under the same desiccation conditions, the volumetric strain at cracking for Indian Head Till was higher than that for Regina Clay (i.e., 13.6% versus 11.1% in Test Nos. T06 and T05, respectively).

In the field, where soils are constrained in the horizontal directions, the horizontal boundary conditions

are similar to those in Test No. T01 and T02. The volumetric strain at cracking for slurried Indian Head Till with horizontal constraints was about 7%. Based on the results of Test Nos. T05 and T06, the slurried Regina Clay is expected to require a lower volumetric strain (i.e., lower than 7%) before the formation of desiccation cracks in the field (i.e., with horizontal constraints).

Kleppe and Olson (1985) studied the desiccation cracking in compacted clay liners and concluded that 5% volumetric shrinkage strain would lead to minor cracking in the field. In spite of the fact that the soils used in the cracking tests were of higher water contents and had not been compacted, the volumetric shrinkage strains at cracking closely agreed to that suggested by Kleppe and Olson (1985). It is apparent that the effect of compaction (i.e., density) would not have a significant influence on the volumetric strain at cracking.

7.3 PREDICTION OF CRACK DEPTH

Two sets of mathematical expressions for the prediction of crack depth were presented in Chapters 3 and 6 using the plastic and elastic equilibrium analyses. Unsaturated soil mechanics principles were employed throughout the derivation of the expressions. The predicted theoretical crack depth

was expressed in terms of stress state variables ($\sigma - u_a$) and ($u_a - u_w$), different matric suction profiles and various soil parameters.

7.3.1 Matric Suction Profiles

Two types of matric suction profiles and a profile factor F_w , were proposed in section 3.2 to quantify the matric suction profile in nature. Suction profile "A" (as shown in Fig. 3.01) represents a shallow groundwater table condition, whereas suction profile "B" (as shown in Fig. 3.02) represents a deep groundwater table condition. The matric suction profile factor F_w is a measure of the environment effect on the soil suction. The environmental effects include the position of the groundwater table and the climatic conditions. A high F_w value means that the soil is subjected to a drier condition.

When a water table is close to the ground surface, (i.e., 6 m in clay, 3 m in sandy clay and silts, and 1 m in sand), Peter (1979) suggested that the equilibrium suction profile is equal to the extension of the hydrostatic water table, regardless of the climate. Under this condition, the matric suction profile is equal to suction profile "A" with F_w equals to 1.0. When the soil is subjected to excessive evaporation due to dry weather, the matric suction profile

is simulated by suction profile "A" with a Fw factor greater than unity. In localities where the water table is deep, the matric suction profile is given by soil suction profile "B".

At a given Fw value, the matric suction given by matric suction profile "B" (i.e., constant matric suction throughout the soil depth) is greater than the one given by matric suction profile "A" (i.e., matric suction varies linearly with the soil depth). In both elastic and plastic analyses, the predicted crack depths obtained from matric suction profile "B" were deeper than those obtained from matric suction "A".

7.3.2 Elastic Equilibrium Analysis

The elastic equilibrium analysis simulates the volume change behavior of an unsaturated soil. The soil was assumed to behave as an elastic isotropic linear elastic material. The theoretical crack depth predicted by the elastic equilibrium analysis in Section 3.4 was found to be a function of,

- a) matric suction profile between the ground surface and the groundwater table,

b) the ratio between the elastic modulus E , with respect to total stress and the elastic modulus H , with respect to matric suction,

c) the Poisson's ratio of the soils,

d) the tensile strain-at-failure of the soils, and

e) the unit weight of the soils.

The variation in the unit weight of natural inorganic fine-grained soils is usually small. Its effect on the predicted crack depth is therefore expected to be minimal. It has been mentioned in Section 6.2.1 that the effect of tensile strain-at-failure is relatively insignificant. Neglecting the tensile strain-at-failure in the analysis results a slightly deeper (more conservative for most engineering application) prediction of crack depth.

The crack depth predicted by the elastic equilibrium analysis are given in Figs. 6.01 to 6.04, inclusively. It can be noted that the predicted crack depth increases with,

a) an increase in the matric suction profile factor F_w ,

Table 7.02 Range of Poisson's ratio for different soils
(after Winterkorn and Fang, 1975).

Soil type	Poisson's ratio
clay, saturated	0.50
clay with sand and silt	0.30 - 0.42
clay, unsaturated	0.35 - 0.40
loess (silt)	0.44
sandy soils	0.15 - 0.25
sand	0.30 - 0.35

b) an increase in the ratio of elastic moduli E to H , and

c) an decrease in the Poisson's ratio.

Table 7.02 shows the range of Poisson's ratio for different soil types. The normal range of Poisson's ratio for unsaturated clayey and silty soils is expected to vary between 0.30 to 0.40. It can be seen from Figs. 6.01 to 6.04 that the predicted crack depth is quite sensitive to the E/H ratio. In Chapter 5, the E/H ratio for clayey silty soils was shown to be higher than that for silty soils. The predicted crack depth for clayey soils is therefore expected to be deeper than that for silty soils.

7.3.3 Plastic Equilibrium Analysis

The plastic equilibrium analysis simulates the shear strength behavior of an unsaturated soil. When a soil is said to be in a state of plastic equilibrium, every part of the mass is assumed on the verge of failure (Terzaghi and Peck, 1967). The theoretical crack depth predicted by the

plastic equilibrium analysis in Section 3.5 was found to be a function of,

- a) matric suction profile between the ground surface and the groundwater table,
- b) the tensile strength of the soil,
- c) the effective cohesion intercept c' ,
- d) the effective friction angle ϕ' ,
- e) the friction angle ϕ^b , and
- f) the unit weight of the soils.

The effects of the unit weight of soils and the matric suction profile on the predicted crack depth for the elastic analysis are the same for plastic analysis. It was discussed in Section 6.2.2 that the predicted crack depth is not sensitive to the normal range of effective friction angle ϕ' (i.e., between 10 and 30 degrees). However, the value of friction angle ϕ^b is affected by friction angle ϕ' at low matric suction (which will be discussed later). The ϕ' angles which yield the maximum crack depth (see Table 6.02)

were used to calculate the crack depths as given in Figs. 6.05 to 6.09. It can be noted from Figs. 6.05 to 6.09 that the crack depth predicted by the plastic equilibrium analysis increases with,

a) an increase in the matric suction profile factor F_w ,

b) an increase in friction angle ϕ^b , with respect to matric suction,

c) an increase in effective cohesion intercept c' , and

d) an increase in unconfined compression strength to tensile strength ratio (or an decrease in tensile strength).

For a normally-consolidated clay, the effective cohesion intercept c' approaches zero. Whereas for an over-consolidated clay, c' has a value typically between 4.8 kPa and 24.0 kPa depending on its stress history (Lambe and Whitman, 1969). For the usual range of angle ϕ^b , (i.e., between 12 and 23 degrees, Fredlund, 1985), the increase in predicted crack depth due to effective cohesion intercept c' is about 1.0 m (meter) for every 10 kPa increase in c' as shown in Table 6.03.

Fang and Chen (1972) conducted tensile tests on compacted clay and found that the ratio between unconfined compressive strength and tensile strength decreases with an increase in plasticity index. The range of unconfined compressive strength to tensile strength ratio varied from 6 to 13 for soils with different plasticity indices as given in Fig. 7.04.

The friction angle ϕ^b , has been assumed to be constant with matric suction (Ho, 1981). However, Gan (1986) showed by experiments that the friction angle ϕ^b varies with matric suction as shown in Figs. 7.05 and 7.06. When the soil is saturated, ϕ^b is equal to ϕ' regardless of the pore pressure range. Once the soil begins to desaturate, ϕ^b becomes increasingly smaller than ϕ^b . Beyond a certain matric suction values, ϕ^b attains a relatively constant value. Table 7.03 summarizes the experimental results of the average value of angle ϕ^b (i.e., by assuming a constant ϕ^b value at any matric suction) on soils from various parts of the world. At moderate matric suction level, the average value of angle ϕ^b is commonly in the range of 17 degrees (Fredlund, 1985). From Figs. 6.05 to 6.09, it can be noted that the predicted crack depth is quite sensitive to the values of the angle ϕ^b .

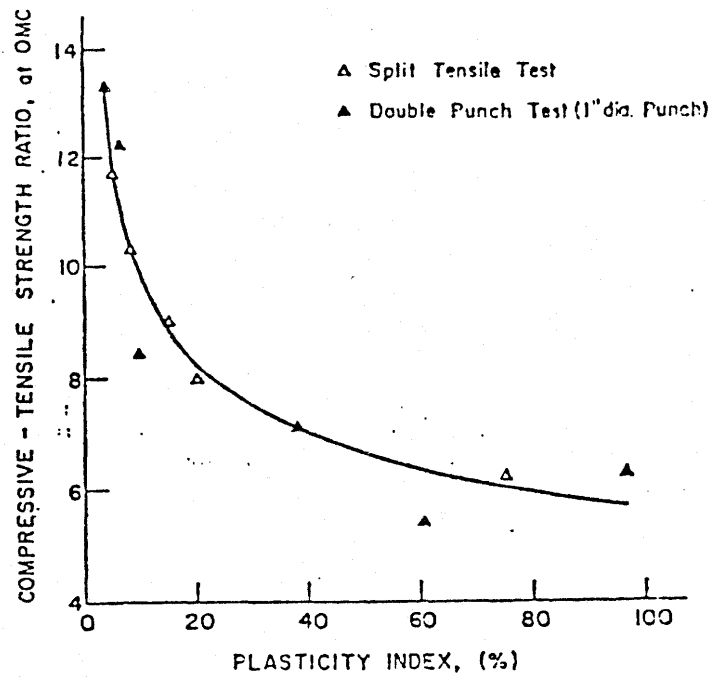


Fig. 7.04: Plasticity Index versus ratio of unconfined compressive strength to tensile strength (after Fang and Chen, 1972).

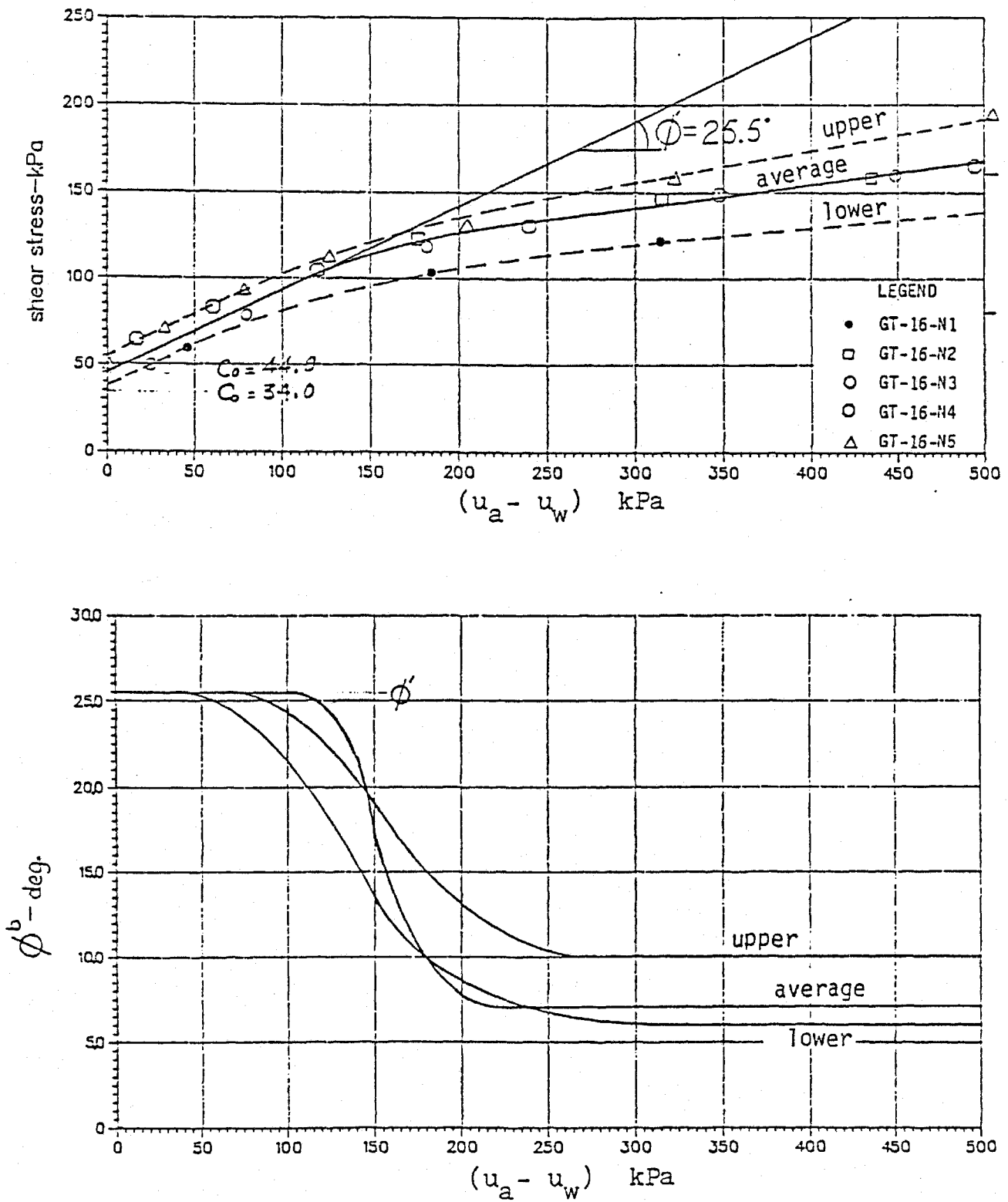


Fig. 7.05: Matric suction versus ϕ^b and shear stresses for compacted Indian Head Till (after Gan, 1986).

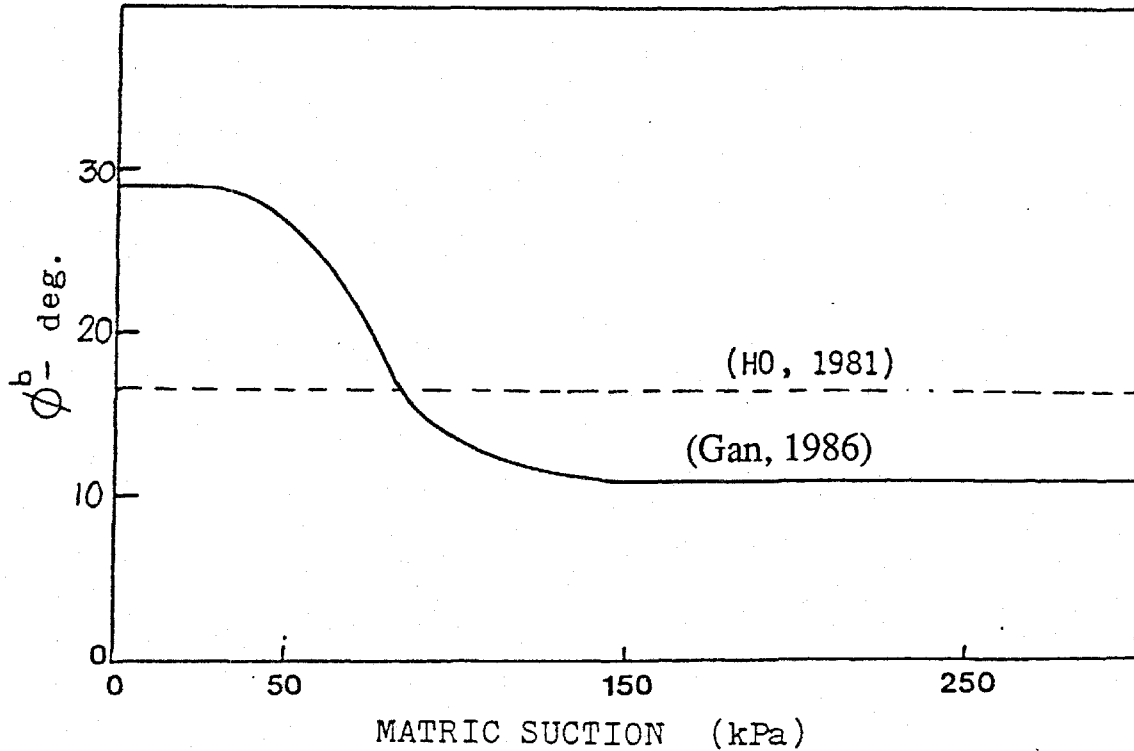
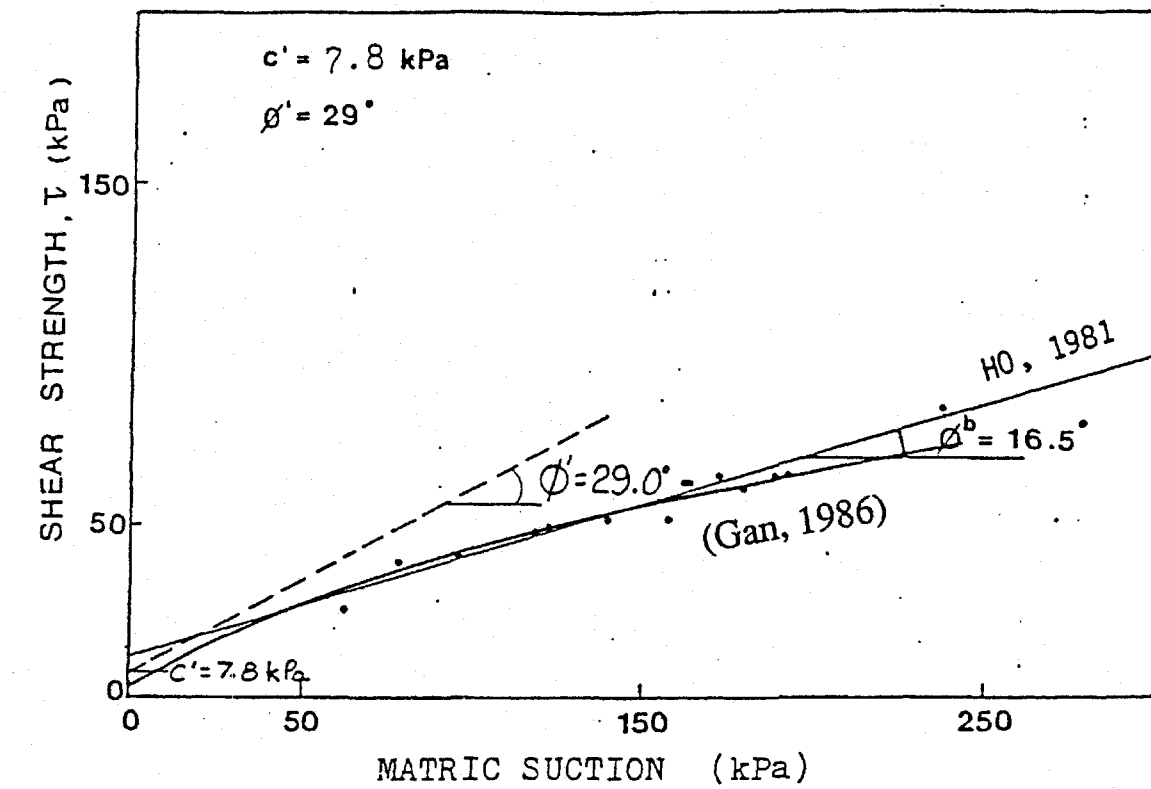


Fig. 7.06: Matric suction versus ϕ^b and shear stresses for low density samples of Dhanauri Clay (after Gan, 1986).

Soil Type	ϕ^b [Degrees]	Test Procedure	Reference
Compacted Shale; $w = 18.6\%$	18.1	Constant Water Content Triaxial	Bishop, Alpan, Donald and Blight, 1960
Boulder Clay; $w = 11.6\%$	21.7	Constant Water Content Triaxial	Bishop, Alpan, Donald and Blight, 1960
Dhanauri Clay; $w = 22.2\%$, $\gamma_d = 15.5 \text{ kN/m}^3$	16.2	Consolidated Drained Triaxial	Satija, 1978
Dhanauri Clay; $w = 22.2\%$, $\gamma_d = 14.5 \text{ kN/m}^3$	12.6	Consolidated Drained Triaxial	Satija, 1978
Dhanauri Clay; $w = 22.2\%$, $\gamma_d = 15.5 \text{ kN/m}^3$	22.6	Constant Water Content Triaxial	Satija, 1978
Dhanauri Clay; $w = 22.2\%$, $\gamma_d = 14.5 \text{ kN/m}^3$	16.5	Constant Water Content Triaxial	Satija, 1978
Madrid Gray Clay; $w = 29\%$, $\gamma_d = 13.1 \text{ kN/m}^3$	16.1	Consolidated Drained, Direct Shear	Escario, 1980
Undisturbed Decomposed Granite; Hong Kong	15.3	Consolidated Drained, Multi-Stage Triaxial	Ho and Fredlund, 1982
Undisturbed Decomposed Rhyolite; Hong Kong	13.8	Consolidated Drained, Multi-Stage Triaxial	Ho and Fredlund, 1982
Cranbrook Silt	16.5	Consolidated Drained, Multi-Stage Triaxial	Fredlund (unpublished)

Table 7.03: Some experimental values for ϕ^b (by assuming a constant ϕ^b value with matric suction, Fredlund, 1985).

7.3.4 Comparison of Elastic and Plastic Equilibrium Analyses

In the absence of complete data on the soil parameters, matric suction profile and the actual depth of cracks in the field, the validity of the elastic and plastic equilibrium analyses cannot be verified. Nevertheless, it is interesting to compare the crack depth predicted by the elastic and plastic analyses using average properties of a given soil.

Let us consider a saturated soil that has never been subjected to desiccation. The properties of the soil are assumed to be the same as those of Indian Head Till. The unit weight of the soil is assumed to be 18.5 kN/m^3 . As the soil is allowed to desiccate, the resulting matric suction profile is assumed to vary linearly with the hydrostatic water table (i.e., similar to matric suction profile "A" with F_w equals to 1.0).

According to Table. 7.02 (Winterkorn and Fang, 1975), the normal range of Poisson's ratio for unsaturated silty to clayey soil varies between 0.30 and 0.40. Having considered the experimental data on the possible ranges of E/H ratio for slurried Regina Clay and compacted silt in Section 5.3, the possible range of E/H ratio for a silty to clayey soil is expected to vary between 0.05 to 0.15. The range of predicted crack depth for the assumed conditions is shown in

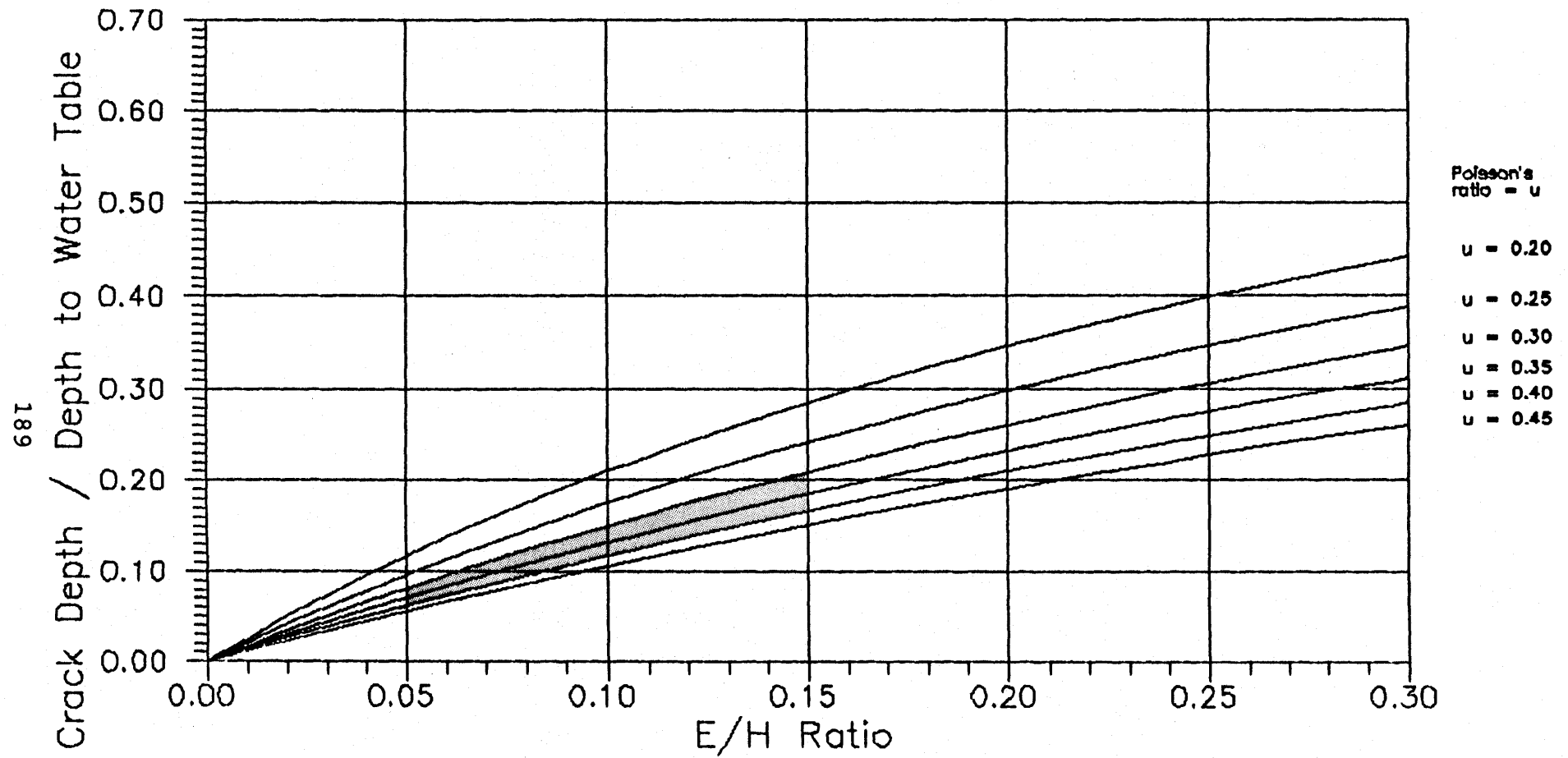


Fig. 7.07: The range of predicted crack depth for Indian Head Till, using elastic equilibrium analysis, suction profile "A" (i.e., matric suction varies linearly with depth), $F_w = 1.0$, $\gamma = 18.5 \text{ kN/m}^3$.

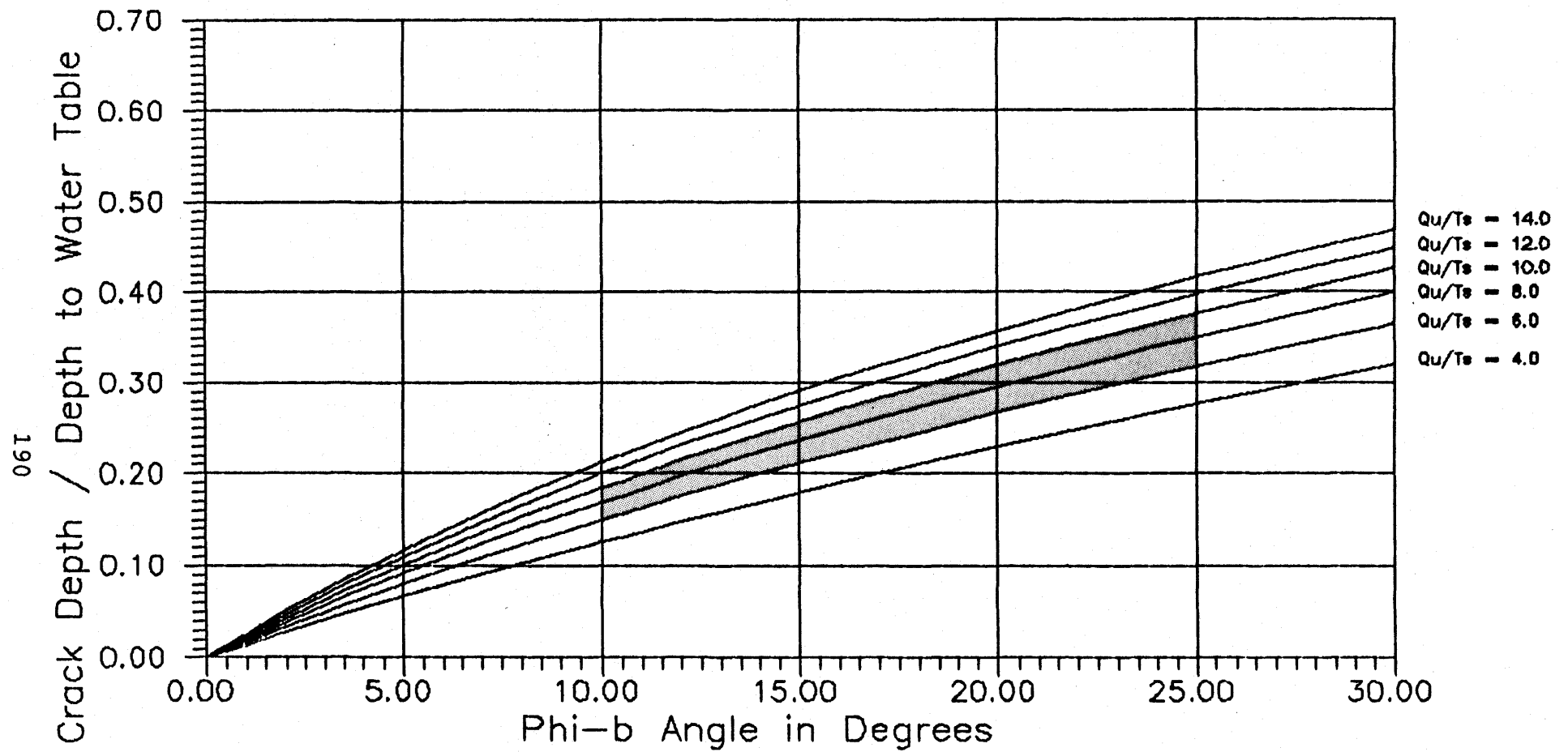


Fig. 7.08: The range of predicted crack depth for Indian Head Till, using plastic equilibrium analysis, suction profile "A" (i.e., matric suction varies linearly with depth) $F_w = 1.0$, $\gamma = 18.5 \text{ kN/m}^3$.

the shaded area in Fig. 7.07. It can be seen that the predicted crack depth using the elastic analysis varies from 0.06 to 0.21 of the depth to water table from the ground surface.

Let us consider the same soil subjected to the same set of desiccation conditions. As the soil is allowed to desaturate due to drying, the angle ϕ^b would initially have a value of about 25 degrees (i.e., ϕ' angle) and decreases to about 10 degrees according to Fig. 7.05 (Gan, 1986). Based upon Fig. 7.04 (Fang and Chen, 1972), the ratio of unconfined compressive strength to tensile strength of a moderately plastic soil is expected to vary between 6 to 10. The effective cohesion intercept c' is assumed to be zero. The range of the predicted crack depth is shown in the shaded area in Fig. 7.08. The crack depth predicted by the plastic equilibrium analysis varies from 0.15 to 0.37 of the depth to water table from the ground surface.

It can be noted from Figs. 7.07 and 7.08 that the crack depth predicted by the plastic equilibrium analysis is almost two times as deep as that predicted by the elastic equilibrium analysis. If a drier matric suction profile (i.e., F_w is greater than 1.0 or matric suction profile "B") is used in the foregoing discussions, the plastic equilibrium analysis will predict an even deeper crack depth.

The results of the experimental program in this thesis tend to confirm that desiccation cracking is the result of volume reduction in soils due to shrinkage. The shrinkage of a soil is caused by the tension in the pore-water through the action of menisci (Means and Parcher, 1963). As matric suction is an internal (i.e., isotropic) stress, it does not produce shearing stresses at the particle contacts (Gan, 1986). During the formation of a desiccation crack, the soil particles are simply pulled apart as a result of the suction stresses. The mode of failure of a desiccated soils is therefore different from that described by the plastic equilibrium analysis. Since desiccation cracking is the result of soil volume reduction, the elastic equilibrium analysis is believed to be conforming to the physical behavior of desiccation cracking in soils. Based upon the foregoing discussions, it is concluded that elastic equilibrium analysis appears to be more appropriate for the prediction of crack depth.

CHAPTER 8

CONCLUSIONS AND RECOMMENDATIONS

8.1 CONCLUSIONS

Based upon the literature review conducted in this thesis, the following conclusions are derived as follows:

A1) Desiccation cracking in soils is the result of volume reduction due to a change in stress state. Matric suction can be used as a stress state variable to describe the shrinkage behavior of soils.

A2) Wide ranges in crack spacing, varying from about 75 mm (milli-meters) to 76.0 m (meters) have been observed in nature.

A3) Fracture mechanics, at its present stage, appears to not be adequate for the prediction of desiccation cracking in soils.

A4) The Modified Mohr-Coulomb failure criterion appears to be appropriate for describing the shear strength behavior of unsaturated soils under tension.

Based upon the results of the experimental program conducted in this thesis, the following conclusions are provided as follows:

B1) Desiccation cracks were formed slowly in a sequential manner and did not bifurcate (i.e., did not branch out).

B2) Four or five-sided orthogonal polygons were usually observed in desiccation cracking.

B3) The observations noted in the experimental program suggest that the locations of the desiccation crack and the crack spacing are highly dependent upon the position of local inhomogeneities. The inhomogeneities include the presence of foreign matter, boundary conditions, stress conditions and material properties.

B4) The laboratory test results indicated that cracking pattern is dependent on the thickness of a soil layer.

B5) Based upon the observations obtained from two tests (i.e., Test Nos. T05 and T06), it appears that clayey soils would have a smaller crack spacing than silty soils.

B6) Based upon the experimental results, it is concluded that desiccation cracks are initiated at a matric suction of

less than 10 kPa for most soil types. The matric suction at cracking for silty soils appears to be higher than that for clayey soils.

B7) The volumetric shrinkage strain at the first sign of cracking for Indian Head Till mixed at water contents close to its liquid limit was about 7%. The volumetric shrinkage strain at cracking for slurried Regina Clay is believed to be lower (i.e., less than 7%) than that for Indian Head Till.

Based upon the results of the analytical program conducted in this thesis, the following conclusions are provided as follows:

C1) Using unsaturated soil mechanics principles, two sets of mathematical expressions for the prediction of crack depth have been derived. The first expression simulates the volume change behavior (i.e., elastic equilibrium analysis) of the unsaturated soils. The second expression simulates the shear strength behavior (i.e., plastic equilibrium analysis) of the unsaturated soils.

C2) The theoretical crack depth predicted by the elastic equilibrium analysis was found to be a function of a) the matric suction profile, b) the ratio of the elastic moduli E to H , c) the Poisson's ratio, d) the tensile strain-at-

failure, and e) the unit weight of the soils. The crack depth predicted by elastic equilibrium analysis was found to be quite sensitive to the value of the E/H ratio.

C3) Using the one-dimensional consolidation and suction test results, typical, empiricial E/H ratios were established. The theoretical range of the E/H ratio varies between zero and one third.

C4) Based upon limited experimental results by others, the normal E/H ratio for clayey soils is expected to range between zero and 0.2, and the E/H ratio for clayey soil is believed to be higher than that for silty soils.

C5) The theoretical crack depth predicted by the plastic equilibrium analysis was found to be a function of a) the matric suction profile, b) the tensile strength of soils, c) the effective cohesion intercept c' , d) the effective friction angle ϕ' , e) the friction angle ϕ^b with respect to matric suction, and f) the unit weight of soils. The crack depth predicted by plastic equilibrium analysis was found to be quite sensitive to the friction angle ϕ^b .

C6) The crack depth predicted by the plastic equilibrium analysis is almost twice as deep as that predicted by the elastic equilibrium analysis.

C7) Since the formation of desiccation cracks is the result of soil volume reduction, the elastic equilibrium analysis appears to be more appropriate for the prediction of crack depth.

8.2 RECOMMENDATIONS FOR FUTURE RESEARCH

Recommendations for future research are as follows:

1) Since there is no complete data set on the depth of cracks, soil parameters, and matric suction profile in the field, the validity of the predicted crack depth from different analyses cannot be confirmed. It is recommended that laboratory testing be conducted to simulate the cracking of soils in the vertical direction. The container for the testing should be large enough to reduce the container side wall effect and deep enough to obtain a meaning experimental crack depth. Silty materials should be used for the test as they require less time to desaturate.

2) As the E/H ratio is required in the prediction of crack depth in elastic equilibrium analysis, its relationship with different soil types, stress history and stress conditions should be investigated.

3) It is recommended that field studies on desiccation crackings be conducted so that the theoretical expressions on the prediction of crack depth can be verified. Sites with relatively homogeneous soil and groundwater conditions are ideal for the field study. The field study should include the observation of the cracking pattern, measuring the crack depth and crack spacing, measuring the groundwater table level, and obtaining the necessary soil parameters for the prediction of crack depth.

REFERENCES

Adams, J. E., J. T. Ritchie, E. Burnett, and D. W. Fryrear, 1969. "Evaporation From a Simulated Soil Shrinkage Crack," Soil Sci. Soc. of Amer., Proc., Vol. 33, pp. 609-613.

Aitchison, G. D., and J. A. Woodburn, 1969. "Soil Suction in Foundation Design," Proc. 7th Int. Conf. Soil Mech. Found. Eng. (Mexico), Vol. 2, pp. 1-8.

Ajaz, A., and R. H. G. Parry, 1975. "Stress-Strain Behaviour of Two Compacted Clays in Tension and Compression," Geotechnique, Vol. 25, No. 3, pp. 495 - 512.

Babcock, E. A., 1977. "A Comparison of Joints in Bedrock and Fractures in Overlying Pleistocene Lacustrine Deposits, Central Alberta, Canada," Can. Geotech. J., Vol. 14, No. 3, pp. 357-366.

Baker, R., 1981. "Tensile Strength, Tension Cracks, and Stability of Slopes," Soils and Foundations, Vol. 21, pp. 1-17.

Barbour, S. L., 1986. "Osmotic Flow and Volume Change in Clay Soils," Ph.D. Thesis, Dep. of Civil Eng., Univ. of Saskatchewan, Saskatoon, Saskatchewan, Canada.

Barden, L., A. O. Madedor, and G. R. Sides, 1969. "Volume Change Characteristics of Unsaturated Clay," Proc. ASCE, J. Soil Mech. Found. Div., Vol. 95, SM1, pp. 33-51.

Bishop, A. W., and V. K. Garga, 1969. "Drained Tension Tests on London Clay," Geotechnique, Vol. 11, pp. 309-313.

Blight, G. E., and A. A. B. Williams, 1971. "Cracks and Fissures by Shrinkage and Swelling," Proc. 5th Reg. Conf. for Africa on Soil Mech. Found. Eng. (Angola), pp. 1.16-1.21.

Boulton, G. S., and M. A. Paul, 1976. "The Influence of Genetic Process on Some Geotechnical Properties of Glacial Tills," Quarterly J. Eng. Geology, Vol. 9, pp. 159-194.

- Brace, W. F., 1960. "An Extension of the Griffith Theory of Fracture to Rocks," J. Geophysical Res., Vol. 65, No. 10, pp. 3477-3480.
- Brenner, R. P., P. Nutalaya, G. V. Chilingarian, and J. O. Robertson, Jr., 1981. "Engineering Geology of Soft Clay," Chapter 2 of Soft Clay Engineering, ed. by E. W. Brand and R. P. Brenner, Elsevier Scientific Publishing Co., pp. 159-231.
- Briones, A. A., and G. Uehara, 1977. "Soil Elastic Constant:II Application to Analysis of Soil Cracking," Soil Sci. Soc. Amer. J., Vol. 41, No. 1, pp. 26-29.
- Broek, D., 1984. Elementary Fracture Mechanics, Martinus Nijhoff Publishers, Boston.
- Burst, J. F., 1965. "Subaqueously Formed Shrinkage Cracks in Clay," J. of Sedimentary Petrology, Vol. 35, No. 2, pp. 348-353.
- Canadian Geotechnical Society, 1978. Canadian Foundation Engineering Manual, Canadian Geotechnical Society, The Foundation Committee, pp. 56.
- Cauley, R. F., and T. W. Kennendy, 1972. "Improved Tensile Strength for Cement-Treated Bases and Sub-Bases," Research Report No. 98-11, Center of Highway Res., The Univ. of Texas at Austin, Texas.
- Chang, R. K., and B. P. Warkentin, 1968. "Volume Change of Compacted Clay Soil Aggregate," Soil Science, Vol. 105, No. 2, pp. 106-111.
- Chowdhury, R. N., 1978. Slope Analysis, Elsevier Scientific Publishing Company.
- Codes of Practices, 1951. "Earth Retaining Structure," CECP 2, Civil Eng. Codes of Practices Joint Committee, Inst. of Civil Eng., London.

- Corte, A., and A. Higashi, 1960. "Experimental Research on Desiccation Cracks in Soil," U. S. Army Snow Ice and Permafrost Research Establishment Research Report No. 66, Corps of Engineers, Wilmette, Illinois, U. S. A..
- Craig, R. F., 1978. Soil Mechanics, 2nd Ed., Van Nostrand Reinhold Company, New York.
- Croney, D., and J. D. Coleman, 1953. "Soil Moisture Suction Properties and Their Bearing on the Moisture Distribution in Soils," Proc. 3rd Int. Conf. Soil Mech. Found. Eng. (Switzerland), Vol. 1, pp. 13-18.
- Dasog, G. S., 1986. "Properties, Genesis and Classification of Clay Soils in Saskatchewan," Ph.D. Thesis, Dep. of Soil Science, Univ. of Saskatchewan, Saskatoon, Canada.
- Driscoll, R., 1984. "The Influence of Vegetation on the Swelling and Shrinkage of Clay soils in Britain," Symp. on The Influence of Vegetation on Clays, Inst. of Civil Eng., Thomas Telford Ltd., London, pp. 6-18.
- Fang, H. Y., and W. F. Chen, 1971. "New Method for Determination of Tensile Strength of Soils," Highway Res. Record, No. 345, pp. 62-68.
- Fang, H. Y., and W. F. Chen, 1972. "Further Study of Double-Punch Test for Tensile Strength of Soils," Proc. 3rd Southeast Asian Conf. on Soil Mech. Found. Eng. (Hong Kong), pp. 211-215.
- Fookes, P. G., 1965. "Orientation of Fissures in Stiff Over-Consolidated Clay of the Siwalik System," Geotechnique, Vol. 15, No. 2, pp. 195-206.
- Fookes, P. G., and D. D. Wilsons, 1966. "The geometry of Discontinuities and Slope Failures in Siwalik Clay," Geotechnique, Vol. 16, No. 4, pp. 305-320.
- Fredlund, D. G., 1964. "Comparison of Soil Suction and One Dimensional Consolidation Characteristics of a Highly Plastic Clay," M.Sc. Thesis, Univ. of Alberta, Edmonton, Alberta, Canada.

- Fredlund, D. G., 1979. "Second Canadian Geotechnical Colloquium: Appropriate Concepts and Technology for Unsaturated Soils," Can. Geotech. J., Vol. 16, pp. 121- 139.
- Fredlund, D. G., 1981. "The Behavior of Unsaturated Soils," Class Notes, Dep. of Civil Eng., Univ. of Saskatchewan, Saskatoon, Saskatchewan, Canada.
- Fredlund, D. G., 1985. "Soil Mechanics Principles That Embrace Unsaturated Soils," Proc. 11th Int. Conf. Soil Mech. Found. Eng. (San Francisco), Vol. 2, pp. 465-472.
- Fredlund, D. G., and N. R. Morgenstern, 1977. "Stress State Variables for Unsaturated Soils," ASCE J. Geotech. Eng., Vol. 103, GT5, pp. 447-466.
- Fredlund, D. G., N. R. Morgenstern, and R. A. Widger, 1978. "The Shear Strength of Unsaturated Soils," Can. Geotech. J., Vol. 15, pp. 313-321.
- Frydman, S., 1967. "Triaxial and Tensile Strength Tests on Stabilized Soil," Proc. 3rd Asian Reg. Conf. Soil Mech. Found. Eng. (Haifa), Vol. 1, pp. 269-271.
- Gan, K. M., 1986. "Direct Shear Strength Testing of Unsaturated Soils," M.Sc. Thesis, Dep. of Civil Eng., Univ. of Saskatchewan, Saskatoon, Canada.
- Gokhale, K. V. G. K., and M. Anandakrishnan, 1970. "Role of Active Clay in the Shrinkage Behavior in Multi-component Clay Sand Systems," Soil and Foundation, Japanese Soc. of Soil Mech. Found. Eng., Vol. 10, No. 3, pp. 92-94.
- Griffith, A. A., 1921. "The Phenomena of Rupture and Flow in Solids," Trans. Royal Soc. of London, Ser. A, Vol. 221, pp. 163-198.
- Griffith, A. A., 1924. "The Theory of Rupture," Proc. Int. Congr. Applied Mech., 1st Delft, pp. 55-63.

- Haines, W. B., 1923. "The volume Change Associated With Variations of Water Content in Soils," J. Agri. Sci., Vol. 13, part 3, pp. 296-310.
- Hamilton, A. B., 1966. "Freezing Shrinkage in Compacted Clays," Can. Geotech. J., Vol. 3, No. 1, pp. 1-17.
- Ho, D. F., 1981. "The Shear Strength of Unsaturated Hong Kong Soils," M.Sc. Thesis, Dep. of Civil Eng., Univ. of Saskatchewan, Saskatoon, Canada.
- Ho, D. F., 1987. "The Relationship Between the Volumetric Deformation Moduli of Unsaturated Soils," Ph.D. Thesis in preparation, Dep. of Civil Eng., Univ. of Saskatchewan, Saskatoon, Canada.
- Hoek, E., 1964. "Fracture of Anisotropic Rock," J. South African Institute of Mining and Metallurgy, May, pp. 501-518.
- Holtz, W. G., 1984. "The Influence of Vegetation on the Swelling and Shrinkage of clays in the United States of America," in The Influence of Vegetation on Clays, Inst. of Civil Eng., Thomas Telford ltd., London.
- Horberg, L., 1951. "Intersecting Minor Ridges and Pre-glacial Features in the Lake Agassiz Basin, North Dakota," J. Geol., Vol. 59, pp. 1-18.
- Irwin, G. R., 1948. "Fracture Dynamics," in Fracturing of Metals, Amer. Soc. of Metals, Cleveland, Ohio.
- Irwin, G. R., 1957. "Analysis of Stresses and Strains Near the End of a Crack Traversing a Plate," J. Applied Mechanics, Vol. 24, No. 3, pp. 361-364.
- Jahn, A., 1950. "Osoblúve Formy Poligonálne Natakachw Dolonie Wieprza," Acta Geologica Polonica, Vol. 1, No. 2, pp. 150-157.
- Jennings, M. J. E., 1953. "The Heaving of Building on Desiccated Clay," Proc. 3rd Int. Conf. Soil Mech. Found. Eng. (Switzerland), Vol. 1, pp. 390-396.

- Jennings, M. J. E., 1961. Discussion on "Expansion and Shrinkage of Non-Saturated Soils," Proc. 5th Int. Conf. Soil Mech. Found. Eng. (Paris), Vol. 3, p. 201.
- Kindle, E. M., 1917. "Some Factors Affecting the Development of Mud Cracks," J. Geol., Vol. 25, pp. 135-144.
- Kleppe, J. H., and R. E. Olson, 1985. "Desiccation Cracking of Soil Barriers," ASTM Spec. Techn. Publ. No. 874.
- Knechtel, M. M., 1952. "Pimpled Plains of Eastern Oklahoma," Bull. Geol. Soc. of Amer., Vol. 63, pp. 689-700.
- Krishnayya, A. V., Z. Eisenstein, and N. R. Morgenstern, 1974. "Behavior of Compacted Soil in Tension," Proc. ASCE, J. Geotech. Eng. Div., Vol. 100, Sept., GT9, pp. 1051-1061.
- Kulhawy, F. H., and T. M. Gurtowski, 1976. "Load Transfer and Hydraulic Fracturing in Zoned Dam," J. Soil Mech. Found. Div., ASCE Proc., Vol. , GT9, pp. 963-1028.
- Lachenbruch, A. H., 1961. "Depth and Spacing of Tension Cracks," J. Geophysical Res., Vol. 66, pp. 4273-4292.
- Lachenbruch, A. H., 1962. "Mechanics of Thermal Contraction Cracks and Ice-Wedge Polygons in Permafrost," Geological Survey of America Special Paper No. 70, New York.
- Lambe, T. W., 1958. "The Structure of Compacted Clay," ASCE, J. Soil Mech. Found. Div., Vol. 84, SM2, p. 1654-1 to 1654-34.
- Lambe, T. W., and R. V. Whitman, 1969. Soil Mechanics, John Wiley & Sons, Inc., New York, p. 152, p. 157.
- Lee, I. K., and O. G. Ingles, 1968. "Strength and Deformation of Soils and Rocks," Chapter 4 of Soil Mechanics Selected Topics, edited by I. K. Lee, Butterworths, London, pp. 195-295.

Lee, S. L., K. W. Lo, F. H. Lee, 1982. "Numerical Model for Crack Propagation in Soils," Proc. Int. Conf. on 'Finite Element Methods,' Aug. (Shanghai, China); New York: Gordon & Breach, Sci. Publ. Inc., Vol. 1, pp. 412-418.

Leonards, G. A., and J. Narain, 1963. "Flexibility of Clay and Cracking of Earth Dams," Proc. ASCE, J. Soil Mech. Found. Div., Vol. 89, SM2, pp. 47-98.

Longwell, C. R., 1928. "Three Common Types of Desert Mud Cracks," Amer. J. of Science, 5th Series, Vol. XV, pp. 136-145.

Means, R. E., and J. V. Parcher, 1963. Physical Properties of Soils, Charles E. Merrill Publishing Co., Columbus, Ohio.

Mitchell, J. K., 1976. Fundamentals of Soil Behavior, John Wiley & Sons, Inc., New York, p.183, p 237.

Mitchell, J. K., 1986. Personal Communications on Desiccation Cracks in a Hydraulic Fill Site at Terminal Island in Los Angeles Harbour.

Moore, C. A., and E. M. Ali, 1982. "Permeability of Cracked Clay Liners," Proc. 8th Annual Research Symp. on Land Disposal of Hazardous Waste, U.S. Environmental Protection Agency, Municipal Environment Res. Lab., Cincinnati, PB82-173022, pp. 174-178.

Muskhelishvili, N. I., 1953. Some Basic Problems of the Mathematical Theory of Elasticity, P. Noordhoff, Groningen, Holland.

Newmark, N. M., 1960. "Failure Hypotheses For Soils," Res. Conf. on Shear Strength of Cohesive Soils, sponsored by ASCE, Soil Mech. Found. Div., Univ. of Colorado, Colorado.

Orowan, E., 1950. "Fundamentals of Brittle Behavior in Metals" Symp. on Fatigue and Fracture of Metals (MIT), John Wiley and Sons, New York.

- Perpich, W. M., R. G. Lukas, and N. B. Clyde, Jr., 1953. "Desiccation of Soil by Trees related to Foundation Settlement," Can. Geotech. J., Vol. 2, No.1, pp. 23-38.
- Peter, P., 1979. "Soil Moisture Suction," Chapter 4 of Footings and Foundations for Small Buildings in Arid Climates with Special Reference to South Australia, edited by P. J. Fargher et al, The Institution of Engineers, South Australia Div. and The Univ. of Adelaide, Australia.
- Picornell, M., and R. L. Lytton, 1987. "Behavior and Design of Vertical Moisture Barriers," Transportation Research Board Annual Meeting, Jan., Washington D.C..
- Picornell, M., 1985. "The Development of Design Criteria to Select the Depth of a Vertical Moisture Barrier," Ph.D. Thesis, Univ. of Texas A & M, Texas, USA.
- Pufahl, D. E., D. G. Fredlund, and H. Rahardjo, 1983. "Lateral Earth Pressure in Expansive Clay Soils," Can. Geotech. J., Vol. 20, No. 2, pp. 228-241.
- Raats, P. A. C., 1984. "Mechanics of Cracking Soils," Proc. Int. Soc. Soil Sci. Symp. on Water and Solute Movement in Heavy Clays Soils, The Netherlands, pp. 23-38.
- Ravina, I., 1984. "The Influence of Vegetation on Moisture and Volume Changes," in The Influence of Vegetation on Clays, The Inst. of Civil Engineers, Thomas Telford Ltd., London, pp. 62-68.
- Ritchie, J. T., and J. E. Adams, 1974. "Field Measurement of Evaporation from Soil Shrinkage Cracks," Proc. Soil Sci. Soc. Amer., Vol. 38, No. 1, pp. 131-134.
- Selim, H. M., and D. Kirkham, 1970. "Soil Temperature and Water Changes During Drying as Influence by Cracks: A Laboratory Experiment," Soil Sci. Soc. of Amer., Proc., Vol. 34, pp. 565-569.
- Sherard, J. L., 1973. "Embankment Dam Cracking," from Embankment Dam Engineering, Casagrande Volume, ed. by R. C. Hirschfeld, and S. J. Poulos, John Wiley & Sons, New York.

- Simpson, W. E., 1936. "Foundation Experiences with Clay in Texas," Civil Eng., Vol. 4, pp. 581-584.
- Skempton, A. W., R. L. Schuster, and D. J. Petley, 1969. "Joints and Fissures in London Clay at Wraysbury and Edgware," Geotechnique, vol. 19, No. 2, pp. 205-217.
- Skempton, A. W., and R. D. Northey, 1952. "The Sensitivity of Clays," Geotechnique, Vol. 3, No. 1, pp. 100-106.
- Spencer, E., 1968. "Effect of Tension Crack on Stability of Embankments," Proc. ASCE, J. Soil Mech. Found. Div., Vol. 94, SM5, pp. 1159-1173.
- Sridharan A., and G. Venkatappa Rao, 1971. "Effective Stress Theory of Shrinkage Phenomena," Can. Geotech. J., Vol. 8, No. 4, pp. 505-513.
- Stirk, G. B., 1954. "Some Aspects of Soil Shrinkage and the Effect of Cracking Upon Water Entry into the Soil," Aust. J. Agric. Res., Vol. 5, No. 2, pp. 281-290.
- Taylor, D. W., 1948. Fundamentals of Soil Mechanics, John Wiley & Sons, Inc., New York.
- Terzaghi, K., 1955. "Influence of Geological factors on the Engineering Properties of Sediments," Economic Geology, Vol. 50, pp. 557-618.
- Terzaghi, K., R. B. Peck, 1967. Soil Mechanics in Engineering Practices, 2nd Ed., John Wiley and Sons, New York.
- Twenhofel, W. H., 1950. Principles of Sedimentation, McGraw-Hill Book Co. Inc., New York, pp. 588-593.
- Wakeling, T. R. M., 1984. Preface of The Influence of Vegetation on Clays, The Inst. of Civil Engineers, Thomas Telford Ltd., London, pp. 1-2.
- Washburn, A. L., 1956. "Classification of Patterned Ground and Review of Suggested Origins," Bull. Geol. Soc. of Amer., Vol. 67, pp. 823-866.

- White, W. A., 1961. "Colloid Phenomena in Sedimentation of Argillaceous Rocks," J. Sedimentary Petrology, Vol. 31, pp. 560-570.
- Willden, R., and D. R. Mabey, 1961. "Giant Desiccation Fissures on the Black Rock and Smoke Creek Deserts, Nevada," Science, Vol. 133, (3461), pp. 1359-1360.
- Williams, A. A. B., and J. T. Pidgeon, J. T., 1983. "Evapo-Transpiration and Heaving Clays in South Africa," Geotechnique, Vol. 23, No. 2, pp. 141-150.
- Winterkorn, H. F., and H. Y. Fang (editors), 1975. Foundation Engineering Handbook, Van Nostrand Reinhold Company.
- Yong, R. N., and B. P. Warkentin, 1966. Introduction to Soil Behavior, The Macmillan Company, New York.
- Zein El Abedine, A., and G. H. Robinson, 1971. "A Study on Cracking in Some Vertisols of the Sudan," Geoderma, 5, pp. 229-241.
- Zienkiewicz, O. C., 1977. The Finite Element Method, 3rd Ed., McGraw-Hill Co., pp. 664-676.

APPENDIX A

Soil Properties of Indian Head Till and Regina Clay.

UNIVERSITY OF SASKATCHEWAN
SOIL MECHANICS LABORATORY
ATTERBERG LIMITS

PROJECT CRACKING IN SOILS

SITE HOLE

SAMPLE CLAY DEPTH

LOCATION

TECHNICIAN J. LAM DATE JAN-87

Liquid Limit

Trial No.	1	2	3		
No. of Blows	29	23	19		
Container No.	4	H	6		
Wt. Sample Wet + Tare	119.23	120.68	154.49		
Wt. Sample Dry + Tare	111.94	112.87	146.79		
Wt. Water	7.29	7.81	7.7		
Tare Container	102.77	103.23	137.45		
Wt. of Dry Soil	9.17	9.64	9.34		
Moisture Content w%	79.5	81.0	82.4		

Average Values

$w_L = 80.5\%$

$w_p = 26.2\%$

$w_s =$

$I_p = 54.3\%$

$I_f =$

$I_t =$

Plastic Limit

Trial No.	1	2	3
Container No.	4	6	12
Wt. Sample Wet + Tare	32.47	41.96	44.30
Wt. Sample Dry + Tare	31.78	41.23	43.50
Wt. Water	0.69	0.73	0.80
Tare Container	29.20	38.41	40.44
Wt. of Dry Soil	2.58	2.82	3.06
Moisture Content %	26.7	25.9	26.1

Shrinkage Limit

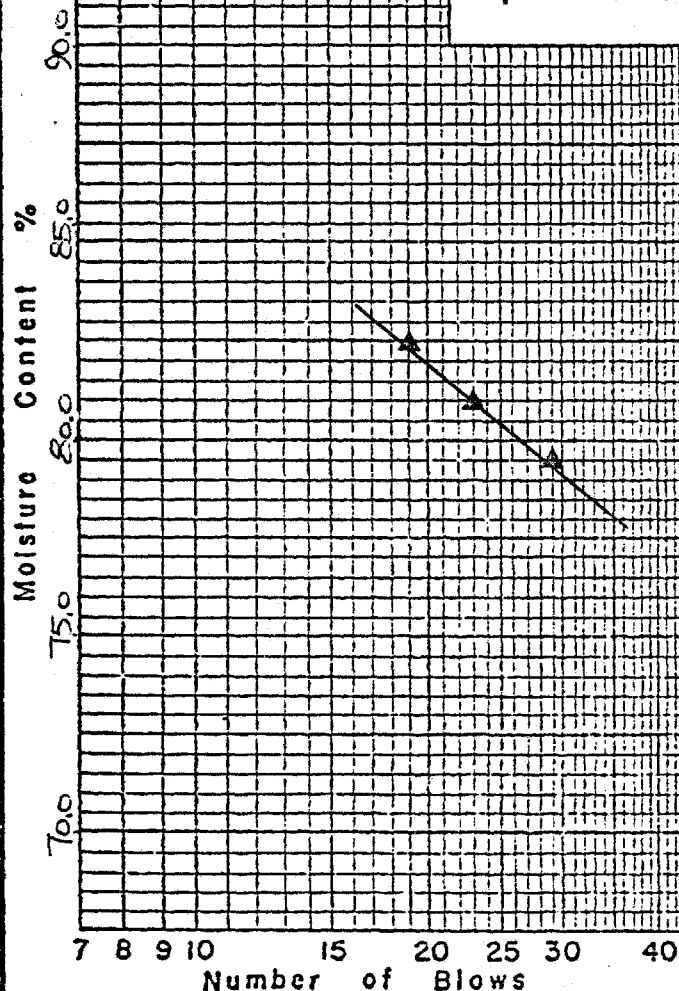
Trial No.			
Container No.			
Wt. Sample Wet + Tare			
Wt. Sample Dry + Tare			
Wt. Water			
Tare Container			
Wt. of Dry Soil W_0			
Moisture Content $w\%$			
Vol. Container V			
Vol. Dry Soil Pat V_0			
Shrinkage Vol. $V - V_0$			
Shrinkage Limit w_s			

$$w_s = w - \left(\frac{V - V_0}{W_0} \times 100 \right)$$

Description of Sample:

REGINA CLAY

Remarks:



UNIVERSITY OF SASKATCHEWAN
SOIL MECHANICS LABORATORY
ATTERBERG LIMITS

PROJECT CRACKING IN SOILS

SITE HOLE

SAMPLE TILL DEPTH

LOCATION

TECHNICIAN J. LAU DATE JAN-87

Liquid Limit

Trial No.	1	2	3			
No. of Blows	21	24	28			
Container No.						
Wt. Sample Wet + Tare	139.89	141.39	144.63			
Wt. Sample Dry + Tare	130.13	131.39	133.89			
Wt. Water	9.76	10.00	10.74			
Tare Container	102.56	102.43	102.05			
Wt. of Dry Soil	27.57	28.96	31.84			
Moisture Content $w\%$	35.4	34.5	33.7			

Average Values

$w_L = 34.3\%$

$w_p = 14.2\%$

$w_s =$

$I_p = 20.1\%$

$I_f =$

$I_t =$

Plastic Limit

Trial No.	1	2	3
Container No.	W3	A1	Z8
Wt. Sample Wet + Tare	27.86	28.27	26.55
Wt. Sample Dry + Tare	26.15	26.61	24.86
Wt. Water	1.71	1.66	1.69
Tare Container	14.09	14.96	12.88
Wt. of Dry Soil	12.06	11.65	11.98
Moisture Content $\%$	14.2	14.2	14.1

Shrinkage Limit

Trial No.			
Container No.			
Wt. Sample Wet + Tare			
Wt. Sample Dry + Tare			
Wt. Water			
Tare Container			
Wt. of Dry Soil W_o			
Moisture Content $w\%$			
Vol. Container V			
Vol. Dry Soil Pat V_o			
Shrinkage Vol. $V - V_o$			
Shrinkage Limit w_s			

$$w_s = w - \left(\frac{V - V_o}{W_o} \times 100 \right)$$

Description of Sample:

INDIAN HEAD TILL

Remarks:

Moisture Content %

Number of Blows

**UNIVERSITY OF SASKATCHEWAN
SOIL MECHANICS LABORATORY
HYDROMETER TEST**

PROJECT CRACKING IN SOILS

SITE _____ HOLE _____

SAMPLE CLAY DEPTH _____

LOCATION _____

TECHNICIAN D.S. DATE JAN/87

Date	Temp.	Time	Elapsed Time	$R_h = \frac{r}{1000(R-1)}$	$r = R_h + c_m$	D m.m.	$r + m_f - c_d$	W %	W % Basis Orig. So.	Remarks
1-6-87	23.0	11:29:00	0							
	23.0	11:29:05	0.1							
	23.0	11:29:15	0.25	32.6		0.07520			97.80	
	23.0	11:29:30	0.5	32.5		0.05330			97.46	
	23.0	11:30:00	1	32.3		0.03780			96.79	
	23.0	11:31:00	2	32.1		0.02680			96.12	
	23.0	11:33:00	4	32.0		0.01890			95.79	
	23.0	11:37:00	8	31.7		0.01340			94.78	
	23.0	11:44:00	15	31.1		0.0099			92.77	
	23.0	11:59:00	30	30.7		0.00767			91.43	
	22.9	12:29:00	60	29.4		0.00510			87.01	
	22.8	1:29:00	120	28.1		0.00368			82.58	
	22.6	3:29:00	240	26.3		0.00267			76.41	
	22.4	8:03:00	514	24.5		0.00187			70.24	
1-7-87	22.5	11:48:00	1459	21.9		0.00114			61.60	
1-8-87	22.4	1:45:00	3016	19.7		0.00082			54.16	
1-9-87	22.4	10:35:00	4266	18.2		0.00070			49.13	

Hydrometer No. _____

Graduate No. _____

$W\% = \frac{100}{W_s} \frac{G_s}{G_s - 1} (r + m_f - c_d) = \text{_____} (r + m_f - c_d)$

Meniscus correction = $c_m = \text{_____}$

Dispersing agent used CALGON Amount _____

Correction for change in density due to addition of dispersing agent = $c_d = \text{_____}$

Specific Gravity of Solids = $G_s = \text{_____}$ $m_f = \text{_____}$

Description of Sample _____
REGINA CLAY

Method of Preparation _____

SIEVE ANALYSIS AFTER HYDROMETER ANALYSIS

	SIEVE NO.	Size of Opening		Weight Retained gms.	Total weight Finer than gms.	Percent Finer than	Per cent Basis orig. sample
		inches	m.m.				
	10	0.075	2.000				
	20	0.0328	0.840				
	40	0.0164	0.420				
	60	0.0097	0.250				
	80	0.0069	0.177				
	100	0.0056	0.149				
	200	0.0029	0.074				
	Pan						

Remarks _____

**UNIVERSITY OF SASKATCHEWAN
SOIL MECHANICS LABORATORY
HYDROMETER TEST**

PROJECT CRACKING IN SOILS

SITE _____ HOLE _____

SAMPLE TILL DEPTH _____

LOCATION _____

TECHNICIAN J. LAU DATE JAN/87

Date	Temp. °C	Time	Elapsed Time Min.	$R'_h =$ $1000(R-1)$	$r =$ $R'_h + c_m$	D m.m.	$r + m_f - c_d$	W %	W % Basis Orig. Sa	Remarks
1-8-87	24.5	9:29:30	0.5	38.7		0.046259			58.27	
	24.5	9:30:00	1	37.0		0.033760			55.50	
	24.5	9:31:00	2	36.0		0.024305			53.88	
	24.5	9:33:00	4	33.0		0.018065			48.99	
	24.4	9:37:00	8	31.0		0.013187			45.71	
	24.4	9:44:00	15	30.3		0.009130			44.57	
	24.4	9:59:00	30	27.1		0.007194			39.36	
	24.3	10:29:00	60	25.2		0.005220			36.23	
	24.3	11:29:00	120	23.5		0.003770			33.47	
	24.1	13:30:00	241	22.1		0.002711			31.12	
	24.0	15:29:00	480	21.0		0.001948			29.39	
	24.7	22:33:00	904	20.0		0.001424			27.92	
1-9-87	24.2	9:29:00	1440	17.9		0.001161			24.32	
1-10-87	24.7	9:29:00	2880	16.3		0.000830			21.90	
1-11-87	24.1	9:29:00	4320	15.0		0.000692			19.57	
1-12-87	24.1	9:29:00	5760	12.3		0.000615			15.17	

Hydrometer No. _____

Graduate No. _____

$W\% = \frac{100}{W_s} \frac{G_s}{G_s - 1} (r + m_f - c_d) = \text{_____} (r + m_f - c_d)$

Meniscus correction = $c_m = \text{_____}$

Dispersing agent used CALSON Amount _____

Correction for change in density due to addition of dispersing agent = $c_d = \text{_____}$

Specific Gravity of Solids = $G_s = \text{_____}$ $m_f = \text{_____}$

Description of Sample _____
INDIAN HEAD TILL

Method of Preparation _____

SIEVE ANALYSIS AFTER HYDROMETER ANALYSIS

	SIEVE NO.	Size of Opening		Weight Retained gms.	Total weight Finer than gms.	Percent Finer than	Per cent Basis orig. sample
		inches	m.m.				
	10	0.075	2.000	0.02	32.78	99.94	99.98
	20	0.0328	0.840	5.64	27.14	82.74	94.08
	40	0.0164	0.420	7.11	20.03	61.07	86.65
	60	0.0097	0.250				
	80	0.0069	0.177	11.22	8.81	26.86	74.91
	100	0.0058	0.149	1.72	7.09	21.62	73.11
	200	0.0029	0.074	6.88	0.21	0.64	65.92
	Pan			0.21	0		

Remarks _____

APPENDIX B

Operation Instructions for Flexible Tube Tensiometer.

2100F

OPERATING INSTRUCTIONS

SOILMOISTURE PROBE

9/83

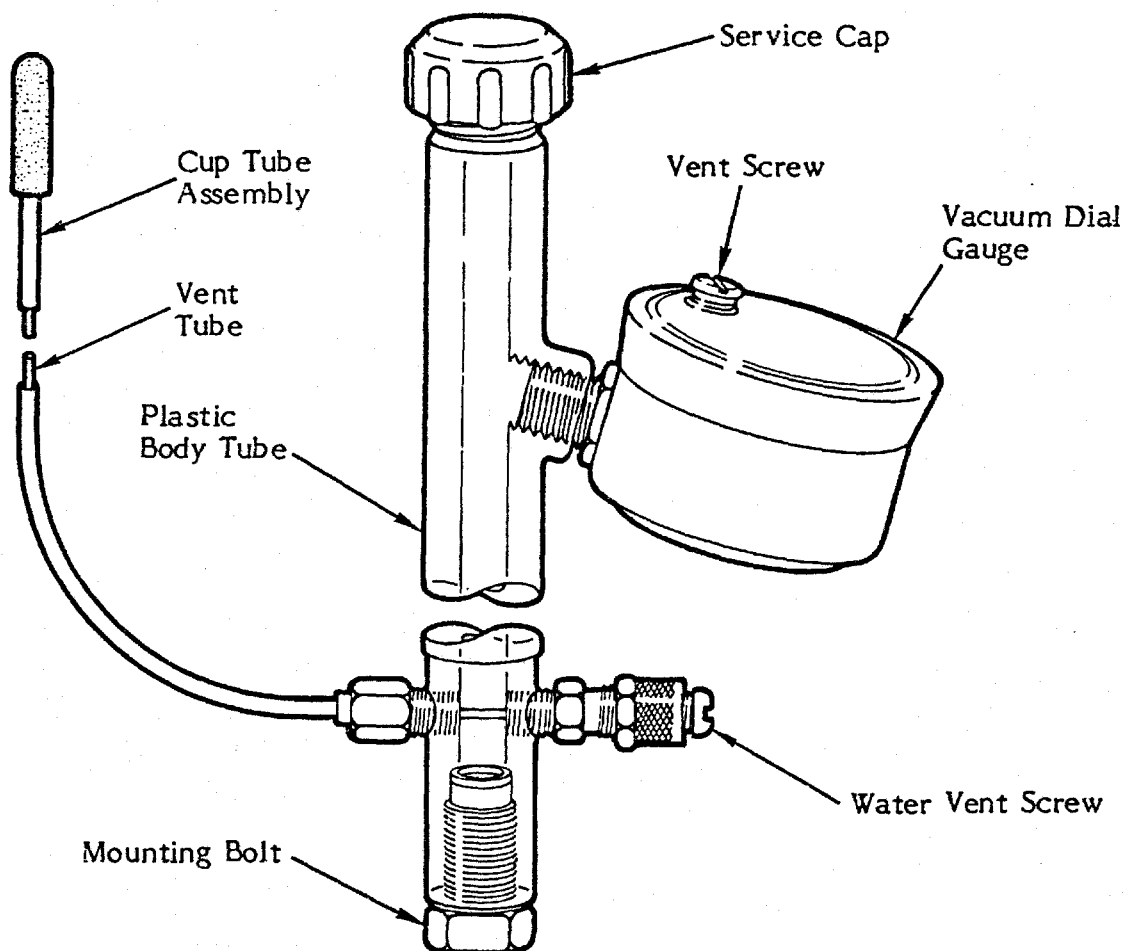


Fig. 1

UNPACKING	Page 1
ACQUAINT YOURSELF WITH THE PARTS	Page 1
INSTALLATION	Page 4
TO REPLACE OR SHORTEN THE CUP TUBE ASSEMBLY	Page 5
GENERAL CARE AND MAINTENANCE	Page 5
MINOR ADJUSTMENTS	Page 6
PRINCIPLES INVOLVED IN THE OPERATION OF A TENSIO-METER TYPE MEASURING INSTRUMENT	Page 6
EFFECTS OF ALTITUDE ON OPERATION OF THE PROBE	Page 8
REPLACEMENT PARTS	Page 9

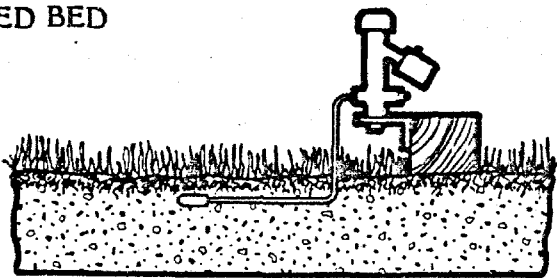
SOILMOISTURE EQUIPMENT CORP.

P. O. Box 30025
Santa Barbara, CA 93105
U.S.A.

Telephone No. (805) 964-3525
Telex No. 65-8424
Cable Address: SOILCORP



SEED BED



SOIL CORE

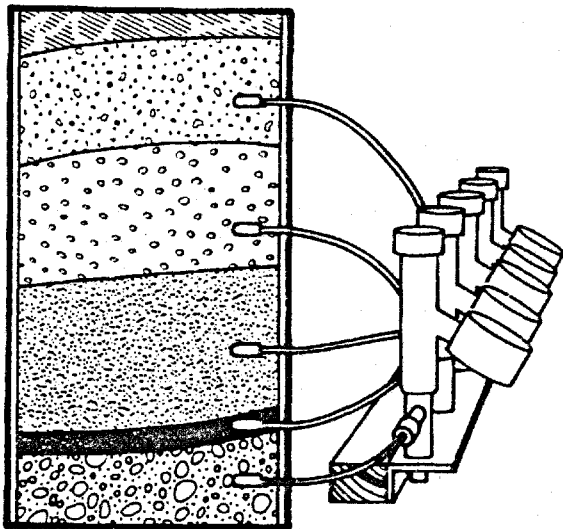


Fig. 2

The Model No. 2100F Soilmoisture Probe is a specialized unit designed for investigation of soil suction in small regimes such as near the soil surface in the region of germinating seeds. The soilmoisture probe also finds excellent application in laboratory work such as for measuring soil suction values at various levels in soil cores subject to experimental treatment, see Fig. 2.

UNPACKING

The Model No. 2100F Soilmoisture Probe shipped to you has been thoroughly tested before shipment. When packed, it was in perfect order. Unpack with care being sure to remove all packing material. Follow the instructions carefully in order to assure long, trouble-free service.

Handle the nylon tubes with care to avoid any "kinking" which will weaken the tubes under vacuum and may cause a restriction to flow of water.

NOTICE: ANY DAMAGE FOUND UPON RECEIPT, SHOULD BE REPORTED IMMEDIATELY TO THE TRANSPORT CARRIER FOR CLAIM. IT IS IMPORTANT THAT YOU

SAVE THE SHIPPING CONTAINER AND ALL EVIDENCE TO SUPPORT YOUR CLAIM.

Be sure to read all operating instructions thoroughly before operating the unit.

ACQUAINT YOURSELF WITH THE PARTS

The vacuum dial gauge was hermetically sealed at the factory at sea level. If you live at a high elevation, the pointer on the dial gauge may be reading higher than zero. This is due to the lower atmospheric pressure at your elevation. Before putting the unit to use, vent the dial gauge by momentarily removing the vent screw in the clear plastic gauge cover, see Fig. 3. Use a small screwdriver for this purpose. After venting, return the vent screw to the gauge cover.

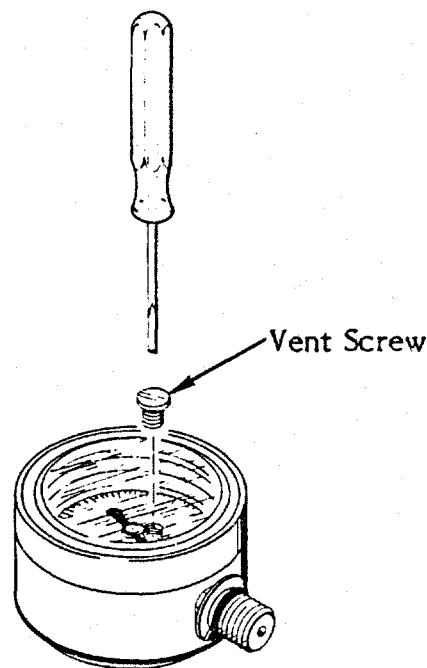


Fig. 3

Fig. 1 and Fig. 4 show the operating parts of the unit. You should become familiar with these parts before proceeding with the preparation of the unit for use.

The vacuum dial gauge is a "Bourdon Tube" type gauge and measures the vacuum in the unit. It is graduated from 0-100 centibars (or 1 Bar) of soil suction.

The porous ceramic cup is made from our 1 Bar Porous Ceramic which has a bubbling pressure of 20-30 psi.

The plastic body tube is of rigid plastic to withstand years of weather abuse.

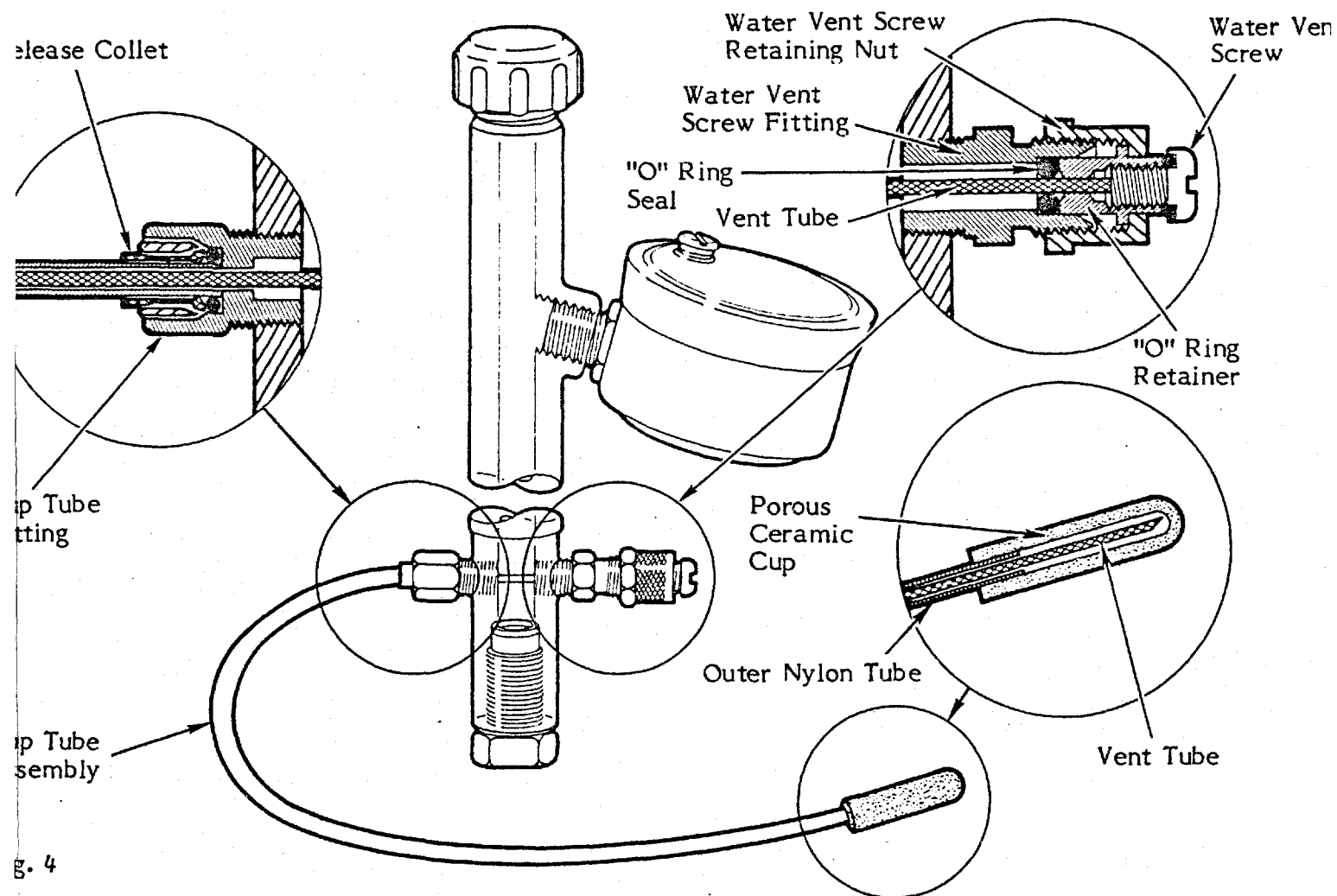


Fig. 4

The mounting bolt is 1/2"-20 X 3/4" long hex head bolt and is used to mount unit in a vertical position.

The Service Cap covers the filler end of the Plastic Body Tube and is used to seal the unit.

PREPARING THE SOILMOISTURE PROBE FOR USE

Before placement of the Soilmoisture Probe in the soil, the unit may be filled with water, if desired. Since the unit is shipped dry, there is a considerable amount of air retained in the walls of the porous ceramic cup and sorbed on the interior walls of the unit. If this air is removed before placement of the unit in the soil, it will have maximum sensitivity with minimum maintenance right from the start.

For the initial filling, it is desirable to use air-free water. This is readily obtained by boiling a quantity of water for several min-

utes and allowing it to cool. It should be used within an hour after cooling. If air-free water is not used it will merely require a longer time for the Soilmoisture Probe to react with maximum sensitivity.

The first step is to immerse the Porous Ceramic Cup in water and to leave it under water for one hour or more to fill the pores with water.

To fill the Soilmoisture Probe with water, use the plastic applicator bottle which is provided. After filling the bottle with air-free water, unscrew the Service Cap on the unit and insert the applicator loosely into the filler end, see Fig. 5. By squeezing the plastic bottle, direct a fine stream of water toward the inner wall of the Plastic Body Tube. Fill the unit slowly so that the water runs down the inside wall. By filling slowly you prevent entrapment of large volumes of air in the tube which requires suction to remove.

Now remove the Water Vent Screw, insert

the stem of the applicator bottle firmly into the filler end so that it makes a seal at the "O" ring, see Fig 5. Squeeze the bottle to force water through the outer nylon tube, to the porous ceramic cup and back through the Vent Tube and out the vent--thus purging air from the system. Continue until a clear flow of water, without air bubbles, comes out the vent. Replace the Water Vent Screw.

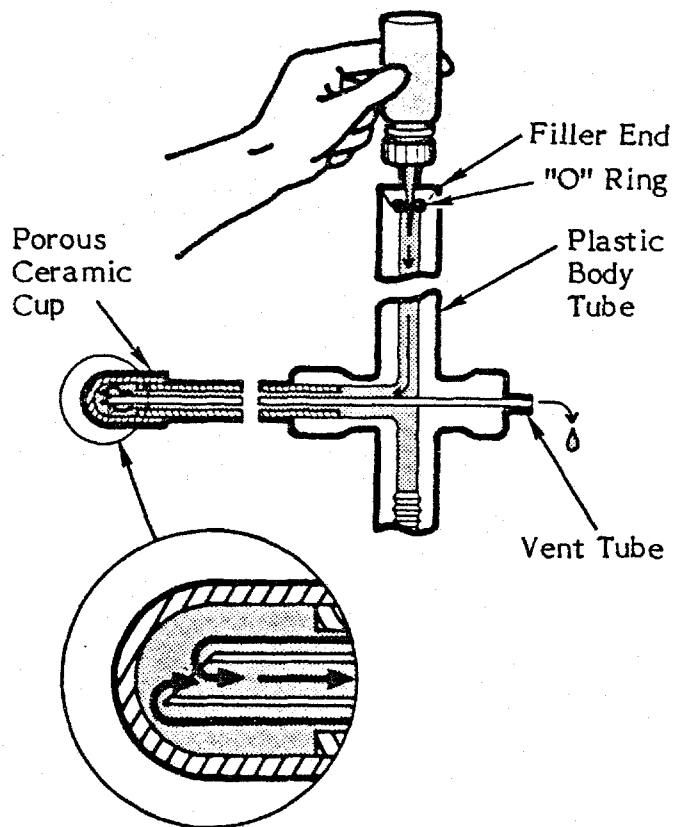


Fig. 5

It is now necessary to apply suction at the filler end to remove air from the bourdon tube in the Vacuum Dial Gauge. Vacuum Hand Pump Model No. 2005G1 may be used for this purpose. Insert the stem of the Vacuum Hand Pump into the filler end of the plastic body tube. The stem should be held firmly against the "O" ring in order to make a seal, see Fig. 6. Now pull out on the Vacuum Hand Pump handle and the vacuum created will cause the Vacuum Dial Gauge reading to rise, and air will be seen to bubble out of the Vacuum Dial Gauge connection inside the unit. Release the stem of the Vacuum Hand Pump slowly from the "O" ring so that the dial gauge reading drops to zero. Add water to keep level above dial gauge connection. Repeat the process several times to remove as much air as possible from the Vacuum Dial Gauge. If laboratory facilities are available, vacuum from the laboratory line may be used

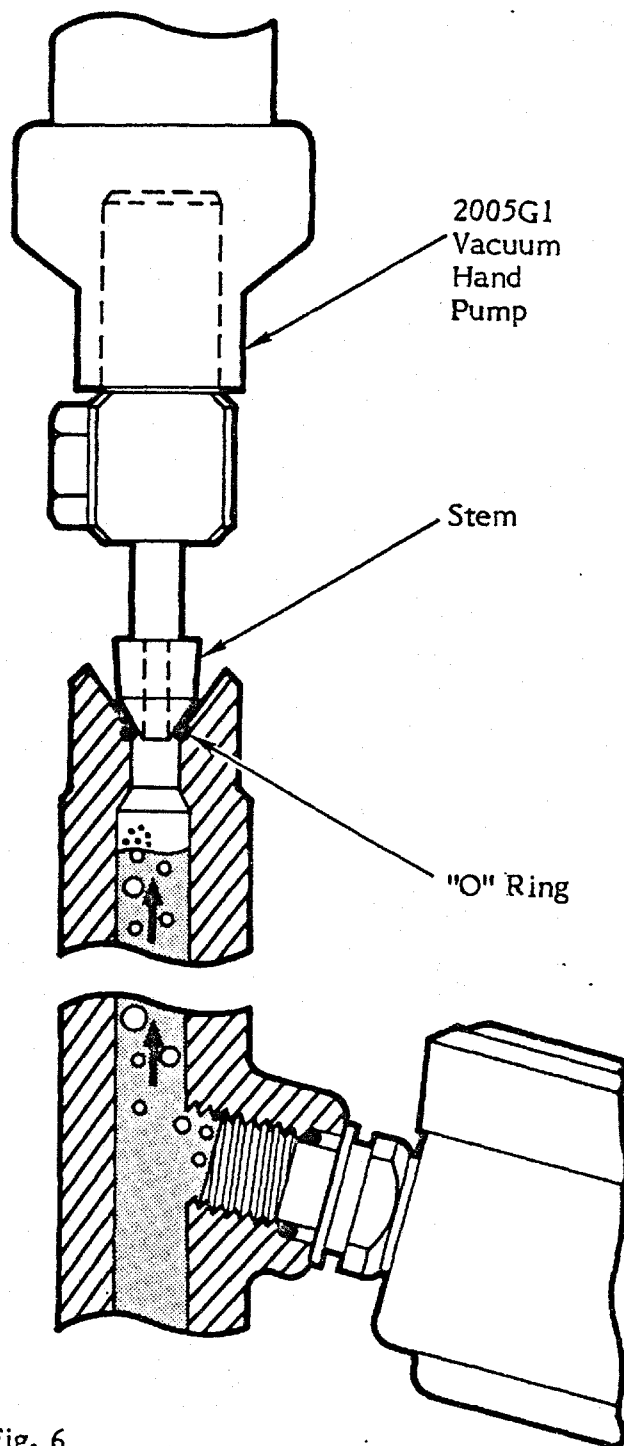
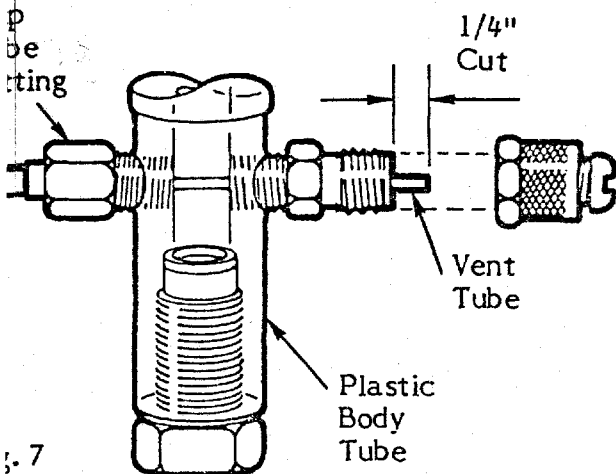


Fig. 6

in place of the Vacuum Hand Pump, or a mechanical vacuum pump can be used. Now, loosen Water Vent Screw, purge water through the nylon tubes again and tighten Water Vent Screw. Be sure Plastic Body Tube is full of water, and then screw Service Cap on snugly. Excess moisture on the porous ceramic cup surface should be removed with absorbent tissue or a clean cloth. Support the plastic body tube in a vertical position and arrange so that moisture is free to evaporate from porous ceramic cup.

As water is evaporated from the cup surface, the dial gauge reading will rise as the vacuum inside the unit increases. As this occurs, trapped air will form in bubbles. After an hour or two, or longer depending on local drying conditions, the dial gauge reading will rise to 60 or more on the scale and there will be a considerable accumulation of air in the probe tubes and in the plastic body tube. This air which has been adsorbed on the inner surfaces of the unit and trapped in the pores of the porous cup. The process of releasing this trapped air is known as outgassing and is characteristic of all vacuum systems. Once this trapped air is removed, it will remain free of air and will be very sensitive to changes in soil suction values.

To remove the accumulated air, first tap the plastic body tube to release as many of the bubbles as possible that cling to the inner wall, then remove the Service Cap. Now, completely remove the Water Vent Screw and push air-free water through the system as was previously. When the Water Vent Screw is removed the Vent Tube will spring out a substantial distance from the end of the vent fitting. This is due to the expansion of the Vent Tube that has taken place as it absorbed water from the system. This inner nylon tube should now be trimmed so that it projects no more than 1/4" beyond the vent fitting, see Fig. 7. A sharp knife or razor blade is used in this operation. After this has been



Completed, replace and tighten the Water Vent Screw. Add water as required to fill the unit and replace the Service Cap. The Soilmoisture Probe is now ready for field installation. If installation is to be delayed for any reason be sure to leave the probe sealed with the porous cup immersed in water to prevent continuing evaporation.

Long term evaporation from the porous ceramic cup should be avoided, since it results in evaporation deposits on the surface of the cup which reduces the sensitivity.

CAUTIONS OR WARNINGS

The Vacuum Dial Gauge has a flexible jacket and is hermetically sealed for maximum gauge life. It is well protected against weathering conditions and can be submerged in water for a limited period without damage. It should be kept in mind, however, that it is a delicate instrument and it should be protected against rough handling and particularly against sharp blows which can damage the integral mechanism. The Vent Screw in the cover of the Vacuum Dial Gauge should always be kept tightly sealed. In the event the dial gauge is damaged, it is easily replaced by unscrewing the gauge from the side port, see Pg. 5.

Be sure to protect the porous ceramic cup from any oil, grease or other materials that will clog pores.

When Soilmoisture Probes are not in use, empty the unit of all water. Do not permit prolonged evaporation from the cup surface. Evaporation deposits on the cup surface can be removed by sanding the surface of the cup with medium grade sandpaper.

Avoid exposing Soilmoisture Probes to freezing conditions.

INSTALLATION

The bottom end of the Plastic Body Tube is threaded with a 1/2"-20 screw thread and a 1/2"-20 by 3/4" long machine bolt is provided with the unit for mounting purposes. The Plastic Body Tube should be mounted in a reasonably vertical position in order to facilitate servicing of the unit. When mounting in confined areas, one should provide adequate clearance for loosening of the Water Vent Screw during a servicing operation.

In handling the nylon probe tubes, care should be taken that they are not bent sharply so as to kink them. Kinking will weaken the tubes under vacuum and may cause a restriction to flow of water.

The porous ceramic cup must be mounted in

the region where soil suction values are required and the cup must be in good contact with the soil. A thin wall 1/4" O.D. tube can be used to core a hole in the soil to accept the porous cup.

After installation is completed the Soil-moisture Probe should be flushed with air-free water; water added to completely fill the Plastic Body Tube; and Service Cap screwed on securely. The unit will now come to equilibrium with the soil and the soil suction in centibars will be read directly on the dial gauge. After an initial installation it requires approximately 24 hours for the Soilmoisture Probe to come to true equilibrium with the soil. The range of operation of the unit is 0-85 centibars. If the porous ceramic cup is exposed to soil suction values much higher than this for an extended time, local drying of the cup will occur and air will enter the cup wall and the dial gauge reading will drop to zero. When this occurs it is necessary to flush the air from the Soil-moisture Probe to make it operative again.

TO REPLACE OR SHORTEN THE CUP TUBE ASSEMBLY

To replace the porous ceramic cup assembly or to shorten the outer nylon tube, the following steps are taken:

Unscrew the Water Vent Screw Retaining Nut completely. This will expose the Vent Tube and "O" Ring Seal, see Fig. 4. On the Cup Tube Fitting, push in the release collet and at

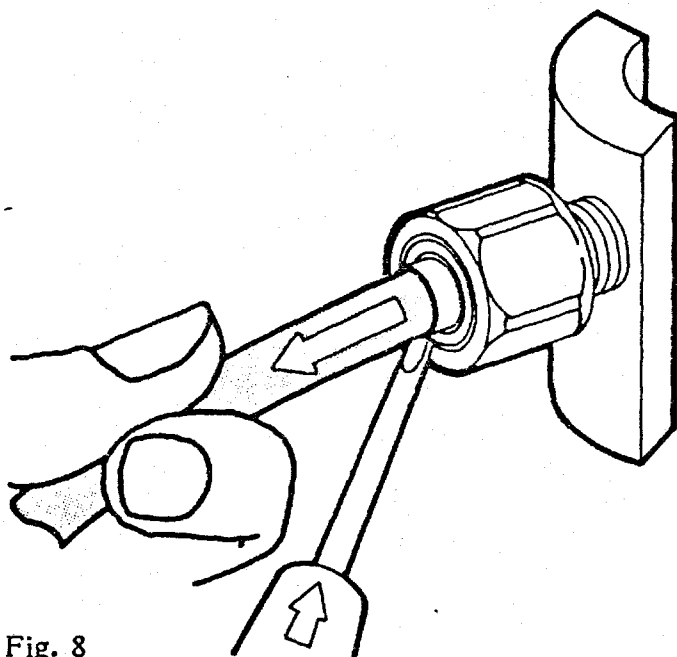


Fig. 8

the same time, pull the outer nylon tube straight out, see Fig. 8. When the outer nylon tube has been pulled free of the Cup Tube Fitting, the Vent Tube can then be pulled out. When the Vent Tube is removed the "O" Ring Seal can then be removed, see Fig. 4. Be careful not to loose this small "O" Ring Seal. To shorten the outer nylon tube, first remove the Vent Tube by pulling it out of the outer nylon tube. Cut the outer nylon tube to the desired length, making sure the end of the outer tube is cut square, with a sharp knife or razor blade. Reinsert the Vent Tube into the outer nylon tube making sure it reaches the bottom of the porous ceramic cup, see Fig. 4. Then insert Vent Tube into the Cup Tube Fitting thru the Plastic Body Tube and out thru the Water Vent Screw Fitting. Insert the outer nylon tube into the Cup Tube Fitting by pushing straight in until the outer nylon tube bottoms out. The Vent Tube can then be trimmed as in Fig. 7. CAUTION: Make sure the Vent Tube still reaches the bottom of the porous ceramic cup, before trimming. After trimming the Vent Tube, install the "O" Ring Seal, pushing it as far back as you can, then screw on the Water Vent Screw Retaining Nut making sure the Vent Tube goes into the "O" Ring Retainer, see Fig. 4. Tighten the Water Vent Screw Retaining Nut finger tight. A wrench is not required.

GENERAL CARE AND MAINTENANCE

Each time soil suction values fall, such as in response to an irrigation, small amounts of air-filled water from the soil enter the soil-moisture probe through the porous ceramic cup. Over a period of time, this air collects and should be removed. A small accumulation of air does not effect the accuracy of the reading, it simply makes the response of the unit somewhat slower.

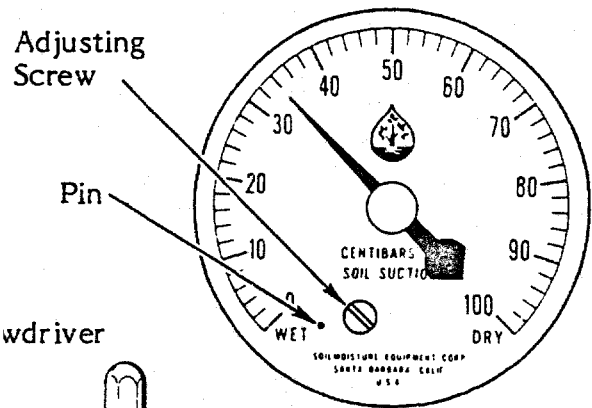
To remove accumulated air, unscrew Service Cap and fill plastic body tube using plastic applicator bottle. Loosen Water Vent Screw, insert stem of applicator bottle into filler end so that it makes a seal at the "O" ring, squeeze bottle to force water through nylon tubes to purge air out through water vent. Tighten Water Vent Screw and add water as required to fill the unit and replace Service Cap making sure that there are no soil particles around sealing area.

OR ADJUSTMENTS

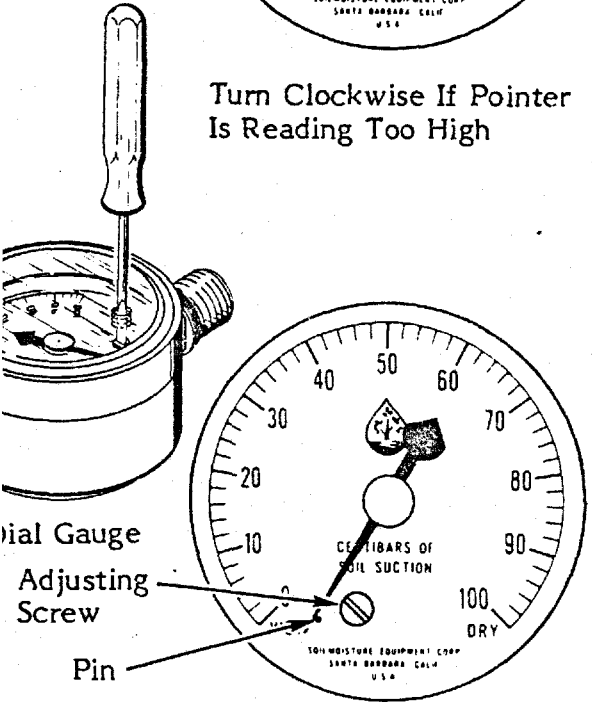
ADJUST THE POINTER

Remove the Vent Screw from the Vacuum Dial Gauge and insert a small screwdriver through the hole in the dial cover to engage the slot in the adjusting screw, see Fig. 9.

If the dial gauge was reading high, turn the screwdriver CLOCKWISE an estimated amount to correct the error.



Turn Clockwise If Pointer Is Reading Too High



Turn Counterclockwise if Pointer is Reading too Low

If the dial gauge was reading low, turn the screwdriver COUNTERCLOCKWISE an estimated amount to correct the error.

Repeat the process if necessary until the pointer is on the zero position.

TO REPLACE VACUUM DIAL GAUGE

To remove Vacuum Dial Gauge, grasp the dial gauge firmly and turn counter-clockwise. When replacing, be sure threads on stem of dial gauge line up with threads in Plastic Body Tube and enter easily, see Fig. 10. Screw dial gauge in clockwise, until backup washer on stem touches body tube and then unscrew dial gauge a portion of a turn until desired orientation is obtained. Do not over-tighten dial gauge in body tube -- the "O" ring on the stem of the dial gauge makes the vacuum seal, not the threads.

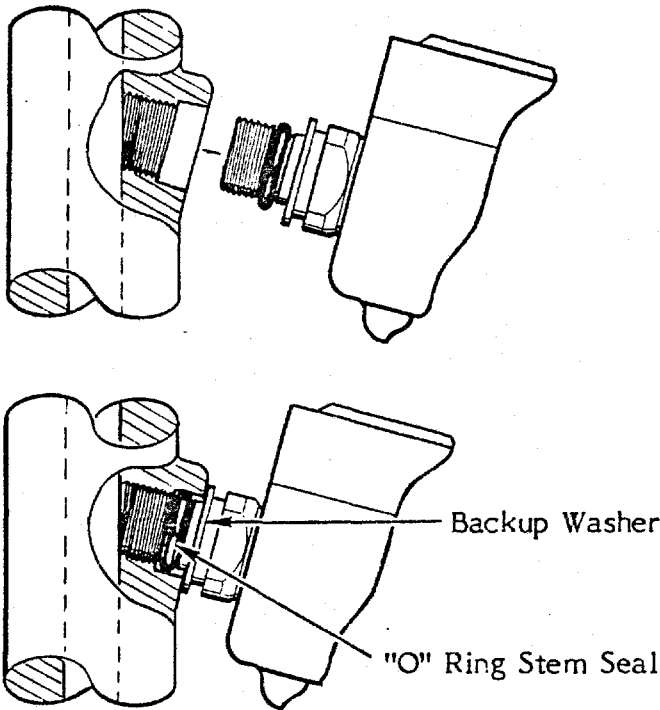


Fig. 10

PRINCIPLES INVOLVED IN THE OPERATION OF A TENSIO-METER TYPE MEASURING INSTRUMENT

The illustration below, Fig. 11, shows a section view of a tensiometer in place in the soil. When the unit is first filled with water and the cap sealed, the vacuum dial gauge will read zero. However, the dry soil in contact with the porous ceramic cup will immediately start to "suck" water from the unit--through the porous ceramic cup and out into the soil. The action is much the same as a dry sponge soaking up water.

The insert shows a magnified view of the porous ceramic cup in contact with the soil particles. The special thing about the porous ceramic cup is the size of the pores. These

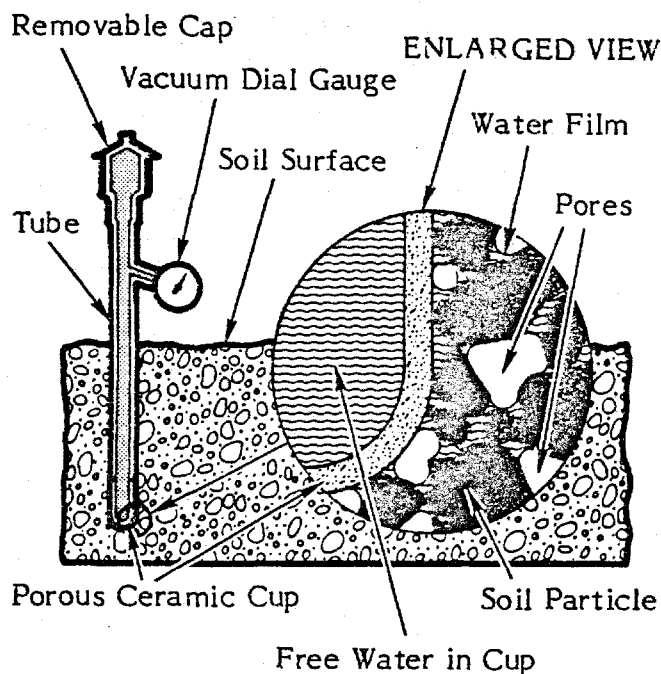


Fig. 11

cups are carefully manufactured so that the pores are reasonably uniform and of controlled maximum size. When the wall of the porous ceramic cup is wetted and the pores filled with water, the surface tension of the water at the air-water interface, at each of the pores, seals the pores. Water can flow through the pores but the water film at each pore acts like a thin rubber diaphragm and will not let air pass, throughout the working range of the tensiometer.

The insert also shows the water film which surrounds each soil particle. These films of water are bound to each of the soil particles by strong molecular forces. As soil dries out, these water films become thinner and more tightly bound. It is actually the "tension" thus produced within these water films that cause the water to be sucked from the porous ceramic cup. These same strong molecular forces make it increasingly difficult for plants to suck moisture from the soil as the soil dries out.

As water is sucked from the porous ceramic cup by the soil, a partial vacuum is created in the tensiometer since it is completely sealed except for the porous ceramic cup. As more water is removed, the vacuum inside the unit becomes higher. The amount of the vacuum is registered on the vacuum dial gauge. Water is sucked from the tensiometer by the soil until such time as the vacuum created inside the tensiometer is just sufficient to overcome the suction of the soil. At this

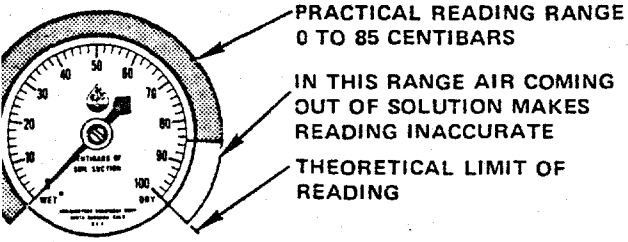
point an equilibrium is reached and water ceases to flow from the cup. The vacuum dial gauge then reads directly the amount of "soil suction". As the soil moisture is depleted through evaporation, drainage or the action of plant roots, the soil suction increases. Consequently more water is sucked from the tensiometer until the vacuum in the unit is increased and a new equilibrium point reached.

When water is added to the soil from rainfall or irrigation, the soil suction is reduced. Then the high vacuum in the tensiometer causes soil moisture to be drawn from the soil, through the walls of the porous ceramic cup and into the unit. This flow of water back into the tensiometer reduces the vacuum. The flow continues until the vacuum in the unit drops to the value where it is just balanced by the soil suction. If water is added to the soil until the soil is completely saturated, then the vacuum dial gauge on the tensiometer will drop until it reads zero.

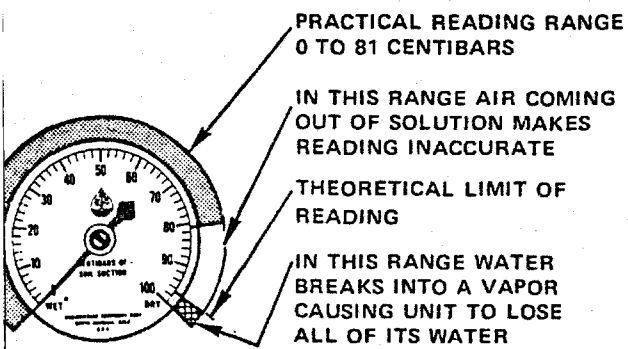
As outlined above, the tensiometer, after initial installation, is always in balance with the soil suction and the vacuum dial gauge on the unit indicates at all times the value of the suction at the porous ceramic cup.

All tensiometers are graduated so that they read directly in bars of soil suction. On the bourdon vacuum gauge type units, the scale is graduated 0-100. Full scale represents 100 centibars (or 1 bar) of soil suction. Due to the physical properties of free water, all tensiometers can be used reliably only in the 0-85 centibar range of soil suction. Knowing that plants can survive and extract moisture from soils even when the soil suction is as high as 15 bars (approximate permanent wilting point for plants) it would appear that the tensiometer is very limited in its application. However, this 0-85 centibar range of soil suction represents the range in which virtually all soil moisture movement takes place and it is the range of optimum growth for most commercial plants.

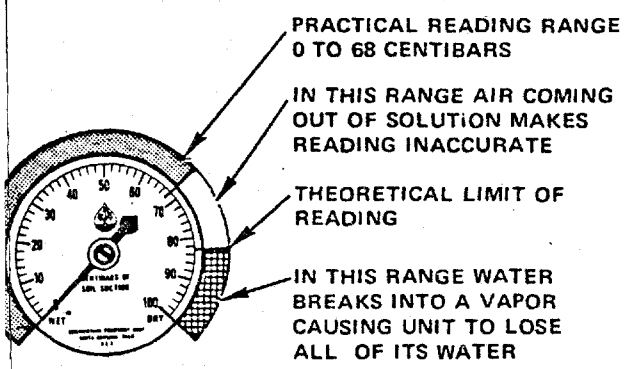
**EFFECTS OF ALTITUDE ON OPERATION
OF THE PROBE**



At Sea Level



1000 Ft. above Sea Level



5000 Ft. above Sea Level

The Reading Range is Reduced Approximately 3.5 Centibars for Each 1000 Ft. Increase in Elevation

APPENDIX C

Tabulated Values on the Predicted Crack Depth Obtained

From

Elastic Equilibrium Analysis and

Plastic Equilibrium Analysis.

Table C.01: Prediction of crack depth using elastic analysis matrix suction profile "A" (i.e., matrix suction varies with depth), $F_w = 1.0$, soil unit weight = 18.5 kN/m^3 .

E/H	Poisson's ratio, μ					
	0.20	0.25	0.30	0.35	0.40	0.45
0.02	0.050Dw	0.041Dw	0.034Dw	0.029Dw	0.026Dw	0.023Dw
0.04	0.096Dw	0.078Dw	0.066Dw	0.057Dw	0.050Dw	0.045Dw
0.06	0.137Dw	0.113Dw	0.096Dw	0.083Dw	0.074Dw	0.066Dw
0.08	0.175Dw	0.145Dw	0.124Dw	0.108Dw	0.096Dw	0.086Dw
0.10	0.210Dw	0.175Dw	0.150Dw	0.132Dw	0.117Dw	0.105Dw
0.12	0.241Dw	0.203Dw	0.175Dw	0.154Dw	0.137Dw	0.124Dw
0.14	0.271Dw	0.229Dw	0.198Dw	0.175Dw	0.157Dw	0.142Dw
0.16	0.298Dw	0.253Dw	0.220Dw	0.195Dw	0.175Dw	0.159Dw
0.18	0.323Dw	0.276Dw	0.241Dw	0.214Dw	0.193Dw	0.175Dw
0.20	0.347Dw	0.298Dw	0.261Dw	0.233Dw	0.210Dw	0.191Dw
0.22	0.368Dw	0.318Dw	0.280Dw	0.250Dw	0.226Dw	0.206Dw
0.24	0.389Dw	0.337Dw	0.298Dw	0.267Dw	0.241Dw	0.220Dw
0.26	0.408Dw	0.355Dw	0.315Dw	0.283Dw	0.256Dw	0.235Dw
0.28	0.426Dw	0.373Dw	0.331Dw	0.298Dw	0.271Dw	0.248Dw
0.30	0.443Dw	0.389Dw	0.347Dw	0.312Dw	0.285Dw	0.261Dw

Where F_w = matrix suction profile factor.

E = elastic modulus with respect to total stress.

H = elastic modulus with respect to matrix suction.

μ = Poisson's ratio.

Dw = depth to water table.

Table C.02: Prediction of crack depth using elastic Equilibrium analysis matric suction profile "A" (i.e., matric suction varies with depth), $F_w = 1.5$, soil unit weight = 18.5 kN/m^3 .

E/H	Poisson's ratio, μ					
	0.20	0.25	0.30	0.35	0.40	0.45
0.02	0.074Dw	0.060Dw	0.050Dw	0.043Dw	0.038Dw	0.034Dw
0.04	0.137Dw	0.113Dw	0.096Dw	0.083Dw	0.074Dw	0.066Dw
0.06	0.193Dw	0.160Dw	0.137Dw	0.120Dw	0.107Dw	0.096Dw
0.08	0.241Dw	0.203Dw	0.175Dw	0.154Dw	0.137Dw	0.124Dw
0.10	0.285Dw	0.241Dw	0.210Dw	0.185Dw	0.166Dw	0.150Dw
0.12	0.323Dw	0.276Dw	0.241Dw	0.214Dw	0.193Dw	0.175Dw
0.14	0.358Dw	0.308Dw	0.271Dw	0.241Dw	0.218Dw	0.198Dw
0.16	0.389Dw	0.337Dw	0.298Dw	0.267Dw	0.241Dw	0.220Dw
0.18	0.417Dw	0.364Dw	0.323Dw	0.290Dw	0.264Dw	0.241Dw
0.20	0.443Dw	0.389Dw	0.347Dw	0.312Dw	0.285Dw	0.261Dw
0.22	0.467Dw	0.412Dw	0.368Dw	0.333Dw	0.304Dw	0.280Dw
0.24	0.488Dw	0.433Dw	0.389Dw	0.353Dw	0.323Dw	0.298Dw
0.26	0.508Dw	0.453Dw	0.408Dw	0.371Dw	0.341Dw	0.315Dw
0.28	0.527Dw	0.471Dw	0.426Dw	0.389Dw	0.358Dw	0.331Dw
0.30	0.544Dw	0.488Dw	0.443Dw	0.405Dw	0.374Dw	0.347Dw

Where F_w = matric suction profile factor.

E = elastic modulus with respect to total stress.

H = elastic modulus with respect to matric suction.

μ = Poisson's ratio.

Dw = depth to water table.

Table C.03: Prediction of crack depth using elastic equilibrium analysis matrix suction profile "A" (i.e., matrix suction varies with depth), $F_w = 2.0$, soil unit weight = 18.5 kN/m^3 .

E/H	Poisson's ratio, μ					
	0.20	0.25	0.30	0.35	0.40	0.45
0.02	0.096Dw	0.078Dw	0.066Dw	0.057Dw	0.050Dw	0.045Dw
0.04	0.175Dw	0.145Dw	0.124Dw	0.108Dw	0.096Dw	0.086Dw
0.06	0.241Dw	0.203Dw	0.175Dw	0.154Dw	0.137Dw	0.124Dw
0.08	0.298Dw	0.253Dw	0.220Dw	0.195Dw	0.175Dw	0.159Dw
0.10	0.347Dw	0.298Dw	0.261Dw	0.233Dw	0.210Dw	0.191Dw
0.12	0.389Dw	0.337Dw	0.298Dw	0.267Dw	0.241Dw	0.220Dw
0.14	0.426Dw	0.373Dw	0.331Dw	0.298Dw	0.271Dw	0.248Dw
0.16	0.459Dw	0.404Dw	0.361Dw	0.327Dw	0.298Dw	0.274Dw
0.18	0.488Dw	0.433Dw	0.389Dw	0.353Dw	0.323Dw	0.298Dw
0.20	0.515Dw	0.459Dw	0.414Dw	0.377Dw	0.347Dw	0.320Dw
0.22	0.538Dw	0.483Dw	0.437Dw	0.400Dw	0.368Dw	0.341Dw
0.24	0.560Dw	0.504Dw	0.459Dw	0.421Dw	0.389Dw	0.361Dw
0.26	0.580Dw	0.524Dw	0.479Dw	0.441Dw	0.408Dw	0.380Dw
0.28	0.598Dw	0.543Dw	0.497Dw	0.459Dw	0.426Dw	0.398Dw
0.30	0.614Dw	0.560Dw	0.515Dw	0.476Dw	0.443Dw	0.414Dw

Where F_w = matrix suction profile factor.

E = elastic modulus with respect to total stress.

H = elastic modulus with respect to matrix suction.

μ = Poisson's ratio.

D_w = depth to water table.

Table C.04: Prediction of crack depth using elastic equilibrium analysis matric suction profile "B" (i.e., matric suction is constant with depth), $F_w = 1.0$, soil unit weight = 18.5 kN/m^3 .

E/H	Poisson's ratio					
	0.20	0.25	0.30	0.35	0.40	0.45
0.02	0.053Dw	0.042Dw	0.035Dw	0.030Dw	0.027Dw	0.024Dw
0.04	0.106Dw	0.085Dw	0.071Dw	0.061Dw	0.053Dw	0.047Dw
0.06	0.159Dw	0.127Dw	0.106Dw	0.091Dw	0.080Dw	0.071Dw
0.08	0.212Dw	0.170Dw	0.141Dw	0.121Dw	0.106Dw	0.094Dw
0.10	0.265Dw	0.212Dw	0.177Dw	0.152Dw	0.133Dw	0.118Dw
0.12	0.318Dw	0.255Dw	0.212Dw	0.182Dw	0.159Dw	0.141Dw
0.14	0.371Dw	0.297Dw	0.247Dw	0.212Dw	0.186Dw	0.165Dw
0.16	0.424Dw	0.339Dw	0.283Dw	0.242Dw	0.212Dw	0.189Dw
0.18	0.477Dw	0.382Dw	0.318Dw	0.273Dw	0.239Dw	0.212Dw
0.20	0.530Dw	0.424Dw	0.354Dw	0.303Dw	0.265Dw	0.236Dw
0.22	0.583Dw	0.467Dw	0.389Dw	0.333Dw	0.292Dw	0.259Dw
0.24	0.636Dw	0.509Dw	0.424Dw	0.364Dw	0.318Dw	0.283Dw
0.26	0.689Dw	0.551Dw	0.460Dw	0.394Dw	0.345Dw	0.306Dw
0.28	0.742Dw	0.594Dw	0.495Dw	0.424Dw	0.371Dw	0.330Dw
0.30	0.795Dw	0.636Dw	0.530Dw	0.455Dw	0.398Dw	0.354Dw

Where F_w = matric suction profile factor.

E = elastic modulus with respect to total stress.

H = elastic modulus with respect to matric suction.

μ = Poisson's ratio.

D_w = depth to water table.

Table C.05: Prediction of crack depth using plastic equilibrium analysis matric suction profile "A" (i.e., matric suction varies with depth).

$$F_t = 0.2500, Q_u/\sigma_t = 4.0, \text{Min. X Term} = 1.22489$$

ϕ_b	Fw=0.5		Fw=1.0		Fw=1.5		Fw=2.0	
	$c'=0$	$c'=10$	$c'=0$	$c'=10$	$c'=0$	$c'=10$	$c'=0$	$c'=10$
	kPa		kPa		kPa		kPa	
	*		*		*		*	
0	0.000Dw	0.83m	0.000Dw	0.83m	0.000Dw	0.83m	0.000Dw	0.83m
2	0.014Dw	0.82m	0.028Dw	0.81m	0.041Dw	0.80m	0.054Dw	0.79m
4	0.028Dw	0.81m	0.054Dw	0.79m	0.079Dw	0.77m	0.102Dw	0.75m
6	0.041Dw	0.80m	0.079Dw	0.77m	0.114Dw	0.74m	0.146Dw	0.71m
8	0.054Dw	0.79m	0.103Dw	0.75m	0.147Dw	0.71m	0.187Dw	0.68m
10	0.067Dw	0.78m	0.126Dw	0.73m	0.178Dw	0.68m	0.224Dw	0.65m
12	0.080Dw	0.77m	0.148Dw	0.71m	0.207Dw	0.66m	0.258Dw	0.62m
14	0.092Dw	0.76m	0.169Dw	0.69m	0.234Dw	0.64m	0.289Dw	0.59m
16	0.105Dw	0.75m	0.190Dw	0.67m	0.260Dw	0.62m	0.319Dw	0.57m
18	0.117Dw	0.73m	0.210Dw	0.66m	0.285Dw	0.60m	0.347Dw	0.54m
20	0.129Dw	0.72m	0.229Dw	0.64m	0.308Dw	0.58m	0.373Dw	0.52m
22	0.142Dw	0.71m	0.248Dw	0.63m	0.331Dw	0.56m	0.397Dw	0.50m
24	0.154Dw	0.70m	0.267Dw	0.61m	0.353Dw	0.54m	0.421Dw	0.48m
26	0.166Dw	0.69m	0.285Dw	0.60m	0.374Dw	0.52m	0.443Dw	0.46m
28	0.178Dw	0.68m	0.303Dw	0.58m	0.394Dw	0.50m	0.465Dw	0.45m
30	0.191Dw	0.67m	0.320Dw	0.57m	0.414Dw	0.49m	0.485Dw	0.43m

* Note: These columns give the increase in crack depth in meter when $c' = 10$ kPa.

Where Fw = matric suction profile factor.

F_t = ratio of tensile strength to compressive strength.
(i.e., σ_t/Q_u).

Q_u = unconfined compressive strength.

σ_t = tensile strength.

Dw = depth to water table.

c' = cohesion intercept when $(\sigma - u_a)$ and $(u_a - u_w)$ are equal to zero.

ϕ_b = friction angle with respect to $(u_a - u_w)$.

Table C.06: Prediction of crack depth using plastic equilibrium analysis, matric suction profile "A" (i.e., matric suction varies with depth).

$$F_t = 0.1667, Q_u/\sigma_t = 6.0, \text{Min. X Term} = 1.00011$$

ϕ_b	Fw=0.5		Fw=1.0		Fw=1.5		Fw=2.0	
	$c'=0$	$c'=10$	$c'=0$	$c'=10$	$c'=0$	$c'=10$	$c'=0$	$c'=10$
		kPa		kPa		kPa		kPa
		*		*		*		*
0	0.000Dw	1.02m	0.000Dw	1.02m	0.000Dw	1.02m	0.000Dw	1.02m
2	0.017Dw	1.00m	0.034Dw	0.98m	0.050Dw	0.97m	0.065Dw	0.95m
4	0.034Dw	0.98m	0.065Dw	0.95m	0.095Dw	0.92m	0.123Dw	0.89m
6	0.050Dw	0.97m	0.095Dw	0.92m	0.136Dw	0.88m	0.174Dw	0.84m
8	0.066Dw	0.95m	0.123Dw	0.89m	0.174Dw	0.84m	0.219Dw	0.80m
10	0.081Dw	0.94m	0.150Dw	0.87m	0.209Dw	0.81m	0.261Dw	0.75m
12	0.096Dw	0.92m	0.175Dw	0.84m	0.242Dw	0.77m	0.298Dw	0.72m
14	0.111Dw	0.91m	0.200Dw	0.82m	0.272Dw	0.74m	0.333Dw	0.68m
16	0.125Dw	0.89m	0.223Dw	0.79m	0.301Dw	0.71m	0.364Dw	0.65m
18	0.140Dw	0.88m	0.245Dw	0.77m	0.328Dw	0.69m	0.394Dw	0.62m
20	0.154Dw	0.86m	0.267Dw	0.75m	0.353Dw	0.66m	0.421Dw	0.59m
22	0.168Dw	0.85m	0.288Dw	0.73m	0.377Dw	0.63m	0.447Dw	0.56m
24	0.182Dw	0.83m	0.308Dw	0.71m	0.400Dw	0.61m	0.471Dw	0.54m
26	0.196Dw	0.82m	0.328Dw	0.69m	0.422Dw	0.59m	0.494Dw	0.52m
28	0.210Dw	0.81m	0.347Dw	0.67m	0.444Dw	0.57m	0.515Dw	0.49m
30	0.224Dw	0.79m	0.366Dw	0.65m	0.464Dw	0.55m	0.536Dw	0.47m

* Note: These columns give the increase in crack depth in meter when $c' = 10$ kPa.

Where Fw = matric suction profile factor.

F_t = ratio of tensile strength to compressive strength.
(i.e., σ_t/Q_u).

Q_u = unconfined compressive strength.

σ_t = tensile strength.

Dw = depth to water table.

c' = cohesion intercept when $(\sigma - u_a)$ and $(u_a - u_w)$ are equal to zero.

ϕ_b = friction angle with respect to $(u_a - u_w)$.

Table C.07: Prediction of crack depth using plastic equilibrium analysis, matric suction profile "A" (i.e., matric suction varies with depth).

$$F_t = 0.1250, Q_u/\sigma_t = 8.0, \text{Min. X Term} = 0.85512$$

ϕ_b	Fw=0.5		Fw=1.0		Fw=1.5		Fw=2.0	
	$c'=0$	$c'=10$ kPa	$c'=0$	$c'=10$ kPa	$c'=0$	$c'=10$ kPa	$c'=0$	$c'=10$ kPa
		*		*		*		*
0	0.000Dw	1.18m	0.000Dw	1.18m	0.000Dw	1.18m	0.000Dw	1.18m
2	0.020Dw	1.15m	0.039Dw	1.13m	0.057Dw	1.11m	0.075Dw	1.09m
4	0.039Dw	1.13m	0.075Dw	1.09m	0.108Dw	1.05m	0.139Dw	1.01m
6	0.057Dw	1.11m	0.108Dw	1.05m	0.154Dw	1.00m	0.195Dw	0.95m
8	0.075Dw	1.09m	0.140Dw	1.01m	0.196Dw	0.95m	0.245Dw	0.89m
10	0.092Dw	1.07m	0.169Dw	0.98m	0.234Dw	0.90m	0.289Dw	0.84m
12	0.109Dw	1.05m	0.197Dw	0.95m	0.269Dw	0.86m	0.329Dw	0.79m
14	0.126Dw	1.03m	0.224Dw	0.91m	0.302Dw	0.82m	0.365Dw	0.75m
16	0.142Dw	1.01m	0.249Dw	0.88m	0.332Dw	0.79m	0.398Dw	0.71m
18	0.158Dw	0.99m	0.273Dw	0.86m	0.360Dw	0.75m	0.429Dw	0.67m
20	0.174Dw	0.97m	0.296Dw	0.83m	0.387Dw	0.72m	0.457Dw	0.64m
22	0.189Dw	0.95m	0.318Dw	0.80m	0.412Dw	0.69m	0.483Dw	0.61m
24	0.204Dw	0.94m	0.340Dw	0.78m	0.435Dw	0.66m	0.507Dw	0.58m
26	0.220Dw	0.92m	0.360Dw	0.75m	0.458Dw	0.64m	0.530Dw	0.55m
28	0.235Dw	0.90m	0.380Dw	0.73m	0.479Dw	0.61m	0.551Dw	0.53m
30	0.250Dw	0.88m	0.400Dw	0.71m	0.500Dw	0.59m	0.571Dw	0.50m

* Note: These columns give the increase in crack depth in meter when $c' = 10$ kPa.

Where Fw = matric suction profile factor.

F_t = ratio of tensile strength to compressive strength.
(i.e., σ_t/Q_u).

Q_u = unconfined compressive strength.

σ_t = tensile strength.

Dw = depth to water table.

c' = cohesion intercept when $(\sigma - u_a)$ and $(u_a - u_w)$ are equal to zero.

ϕ_b = friction angle with respect to $(u_a - u_w)$.

Table C.08: Prediction of crack depth using plastic equilibrium analysis, matric suction profile "A" (i.e., matric suction varies with depth).

$$F_t = 0.1000, Q_u/\sigma_t = 10.0, \text{Min. X Term} = 0.77468$$

ϕ_b	Fw=0.5		Fw=1.0		Fw=1.5		Fw=2.0	
	$c'=0$	$c'=10$	$c'=0$	$c'=10$	$c'=0$	$c'=10$	$c'=0$	$c'=10$
	kPa		kPa		kPa		kPa	
	*		*		*		*	
0	0.000Dw	1.32m	0.000Dw	1.32m	0.000Dw	1.32m	0.000Dw	1.32m
2	0.022Dw	1.29m	0.043Dw	1.26m	0.063Dw	1.23m	0.083Dw	1.21m
4	0.043Dw	1.26m	0.083Dw	1.21m	0.119Dw	1.16m	0.153Dw	1.11m
6	0.064Dw	1.23m	0.119Dw	1.16m	0.169Dw	1.09m	0.213Dw	1.04m
8	0.083Dw	1.21m	0.154Dw	1.11m	0.214Dw	1.03m	0.266Dw	0.97m
10	0.102Dw	1.18m	0.185Dw	1.07m	0.255Dw	0.98m	0.313Dw	0.90m
12	0.121Dw	1.16m	0.215Dw	1.03m	0.292Dw	0.93m	0.354Dw	0.85m
14	0.139Dw	1.13m	0.243Dw	1.00m	0.326Dw	0.89m	0.392Dw	0.80m
16	0.156Dw	1.11m	0.270Dw	0.96m	0.357Dw	0.85m	0.425Dw	0.76m
18	0.173Dw	1.09m	0.295Dw	0.93m	0.386Dw	0.81m	0.456Dw	0.72m
20	0.190Dw	1.07m	0.320Dw	0.90m	0.413Dw	0.77m	0.484Dw	0.68m
22	0.207Dw	1.04m	0.343Dw	0.86m	0.439Dw	0.74m	0.511Dw	0.64m
24	0.223Dw	1.02m	0.365Dw	0.84m	0.463Dw	0.71m	0.535Dw	0.61m
26	0.239Dw	1.00m	0.386Dw	0.81m	0.486Dw	0.68m	0.557Dw	0.58m
28	0.255Dw	0.98m	0.407Dw	0.78m	0.507Dw	0.65m	0.579Dw	0.55m
30	0.271Dw	0.96m	0.427Dw	0.75m	0.528Dw	0.62m	0.598Dw	0.53m

* Note: These columns give the increase in crack depth in meter when $c' = 10$ kPa.

Where Fw = matric suction profile factor.

F_t = ratio of tensile strength to compressive strength.
(i.e., σ_t/Q_u).

Q_u = unconfined compressive strength.

σ_t = tensile strength.

Dw = depth to water table.

c' = cohesion intercept when $(\sigma - u_a)$ and $(u_a - u_w)$ are equal to zero.

ϕ_b = friction angle with respect to $(u_a - u_w)$.

Table C.09: Prediction of crack depth using plastic equilibrium analysis, matric suction profile "A" (i.e., matric suction varies with depth).

$$F_t = 0.0833, Q_u/\sigma_t = 12.0, \text{Min. X Term} = 0.70719$$

ϕ_b	Fw=0.5		Fw=1.0		Fw=1.5		Fw=2.0	
	$c'=0$	$c'=10$	$c'=0$	$c'=10$	$c'=0$	$c'=10$	$c'=0$	$c'=10$
		kPa		kPa		kPa		kPa
		*		*		*		*
0	0.000Dw	1.44m	0.000Dw	1.44m	0.000Dw	1.44m	0.000Dw	1.44m
2	0.024Dw	1.41m	0.047Dw	1.37m	0.069Dw	1.34m	0.090Dw	1.31m
4	0.047Dw	1.37m	0.090Dw	1.31m	0.129Dw	1.26m	0.165Dw	1.20m
6	0.069Dw	1.34m	0.129Dw	1.25m	0.182Dw	1.18m	0.229Dw	1.11m
8	0.090Dw	1.31m	0.166Dw	1.20m	0.230Dw	1.11m	0.284Dw	1.03m
10	0.111Dw	1.28m	0.200Dw	1.15m	0.272Dw	1.05m	0.333Dw	0.96m
12	0.131Dw	1.25m	0.231Dw	1.11m	0.311Dw	0.99m	0.375Dw	0.90m
14	0.150Dw	1.23m	0.261Dw	1.07m	0.346Dw	0.94m	0.414Dw	0.85m
16	0.169Dw	1.20m	0.288Dw	1.03m	0.378Dw	0.90m	0.448Dw	0.80m
18	0.187Dw	1.17m	0.315Dw	0.99m	0.408Dw	0.85m	0.479Dw	0.75m
20	0.205Dw	1.15m	0.340Dw	0.95m	0.436Dw	0.81m	0.507Dw	0.71m
22	0.222Dw	1.12m	0.364Dw	0.92m	0.461Dw	0.78m	0.533Dw	0.67m
24	0.239Dw	1.10m	0.386Dw	0.88m	0.486Dw	0.74m	0.557Dw	0.64m
26	0.256Dw	1.07m	0.408Dw	0.85m	0.508Dw	0.71m	0.580Dw	0.61m
28	0.273Dw	1.05m	0.429Dw	0.82m	0.530Dw	0.68m	0.601Dw	0.58m
30	0.290Dw	1.02m	0.449Dw	0.79m	0.550Dw	0.65m	0.620Dw	0.55m

* Note: These columns give the increase in crack depth in meters when $c' = 10$ kPa.

Where Fw = matric suction profile factor.

F_t = ratio of tensile strength to compressive strength.
(i.e., σ_t/Q_u).

Q_u = unconfined compressive strength.

σ_t = tensile strength.

Dw = depth to water table.

c' = cohesion intercept when $(\sigma - u_a)$ and $(u_a - u_w)$ are equal to zero.

ϕ_b = friction angle with respect to $(u_a - u_w)$.

Table C.10: Prediction of crack depth using plastic equilibrium analysis, matric suction profile "A" (i.e., matric suction varies with depth).

$$F_t = 0.0714, Q_u/\sigma_t = 14.0, \text{Min. X Term} = 0.65473$$

ϕ_b	Fw=0.5		Fw=1.0		Fw=1.5		Fw=2.0	
	$c'=0$	$c'=10$	$c'=0$	$c'=10$	$c'=0$	$c'=10$	$c'=0$	$c'=10$
	kPa		kPa		kPa		kPa	
	*		*		*		*	
0	0.000Dw	1.56m	0.000Dw	1.56m	0.000Dw	1.56m	0.000Dw	1.56m
2	0.026Dw	1.52m	0.051Dw	1.48m	0.074Dw	1.44m	0.096Dw	1.41m
4	0.051Dw	1.48m	0.096Dw	1.41m	0.138Dw	1.34m	0.176Dw	1.28m
6	0.074Dw	1.44m	0.138Dw	1.34m	0.194Dw	1.25m	0.243Dw	1.18m
8	0.097Dw	1.41m	0.177Dw	1.28m	0.244Dw	1.18m	0.300Dw	1.09m
10	0.119Dw	1.37m	0.212Dw	1.23m	0.288Dw	1.11m	0.350Dw	1.01m
12	0.140Dw	1.34m	0.245Dw	1.18m	0.327Dw	1.05m	0.394Dw	0.94m
14	0.160Dw	1.31m	0.276Dw	1.13m	0.364Dw	0.99m	0.432Dw	0.88m
16	0.180Dw	1.28m	0.305Dw	1.08m	0.396Dw	0.94m	0.467Dw	0.83m
18	0.199Dw	1.25m	0.332Dw	1.04m	0.427Dw	0.89m	0.498Dw	0.78m
20	0.217Dw	1.22m	0.357Dw	1.00m	0.455Dw	0.85m	0.526Dw	0.74m
22	0.236Dw	1.19m	0.382Dw	0.96m	0.481Dw	0.81m	0.552Dw	0.70m
24	0.254Dw	1.16m	0.405Dw	0.93m	0.505Dw	0.77m	0.576Dw	0.66m
26	0.271Dw	1.13m	0.427Dw	0.89m	0.528Dw	0.74m	0.598Dw	0.63m
28	0.289Dw	1.11m	0.448Dw	0.86m	0.549Dw	0.70m	0.619Dw	0.59m
30	0.306Dw	1.08m	0.469Dw	0.83m	0.569Dw	0.67m	0.638Dw	0.56m

* Note: These columns give the increase in crack depth in meters when $c' = 10$ kPa.

Where Fw = matric suction profile factor.

F_t = ratio of tensile strength to compressive strength.
(i.e., σ_t/Q_u).

Q_u = unconfined compressive strength.

σ_t = tensile strength.

Dw = depth to water table.

c' = cohesion intercept when $(\sigma - u_a)$ and $(u_a - u_w)$ are equal to zero.

ϕ_b = friction angle with respect to $(u_a - u_w)$.

Table C.11: Prediction of crack depth using plastic equilibrium analysis, matric suction profile "B" (i.e., matric suction is constant with depth).

$$F_w = 1.0$$

$F_t = 0.250$	$Q_u/\sigma_t = 4.0$	Max. Y term = 0.7698
$F_t = 0.167$	$Q_u/\sigma_t = 6.0$	Max. Y term = 0.9427
$F_t = 0.125$	$Q_u/\sigma_t = 8.0$	Max. Y term = 1.0887

ϕ_b	$Q_u/\sigma_t = 4.0$		$Q_u/\sigma_t = 6.0$		$Q_u/\sigma_t = 8.0$	
	$c' = 0$	$c' = 10$	$c' = 0$	$c' = 10$	$c' = 0$	$c' = 10$
	kPa		kPa		kPa	
	*		*		*	
0	0.000Dw	0.83m	0.000Dw	1.02m	0.000Dw	1.18m
2	0.029Dw	0.83m	0.035Dw	1.02m	0.040Dw	1.18m
4	0.057Dw	0.83m	0.070Dw	1.02m	0.081Dw	1.18m
6	0.086Dw	0.83m	0.105Dw	1.02m	0.121Dw	1.18m
8	0.115Dw	0.83m	0.141Dw	1.02m	0.162Dw	1.18m
10	0.144Dw	0.83m	0.176Dw	1.02m	0.204Dw	1.18m
12	0.174Dw	0.83m	0.213Dw	1.02m	0.245Dw	1.18m
14	0.204Dw	0.83m	0.249Dw	1.02m	0.288Dw	1.18m
16	0.234Dw	0.83m	0.287Dw	1.02m	0.331Dw	1.18m
18	0.265Dw	0.83m	0.325Dw	1.02m	0.375Dw	1.18m
20	0.297Dw	0.83m	0.364Dw	1.02m	0.420Dw	1.18m
22	0.330Dw	0.83m	0.404Dw	1.02m	0.466Dw	1.18m
24	0.363Dw	0.83m	0.445Dw	1.02m	0.514Dw	1.18m
26	0.398Dw	0.83m	0.488Dw	1.02m	0.563Dw	1.18m
28	0.434Dw	0.83m	0.532Dw	1.02m	0.614Dw	1.18m
30	0.471Dw	0.83m	0.577Dw	1.02m	0.667Dw	1.18m

* Note: These columns give the increase in crack depth in meters when $c' = 10$ kPa.

Where F_w = matric suction profile factor.

F_t = ratio of tensile strength to compressive strength.
(i.e., σ_t/Q_u).

Q_u = unconfined compressive strength.

σ_t = tensile strength.

D_w = depth to water table.

c' = cohesion intercept when $(\sigma - u_a)$ and $(u_a - u_w)$ are equal to zero.

ϕ_b = friction angle with respect to $(u_a - u_w)$.

Table C.12: Prediction of crack depth using plastic equilibrium analysis, matric suction profile "B" (i.e., matric suction is constant with depth),

$$F_w = 1.0$$

$F_t = 0.100$	$Q_u/\sigma_t = 10.0$	Max. Y term = 1.2172
$F_t = 0.083$	$Q_u/\sigma_t = 12.0$	Max. Y term = 1.3336
$F_t = 0.071$	$Q_u/\sigma_t = 14.0$	Max. Y term = 1.4404

ϕ_b	$Q_u/\sigma_t = 10.0$		$Q_u/\sigma_t = 12.0$		$Q_u/\sigma_t = 14.0$	
	$c' = 0$	$c' = 10$	$c' = 0$	$c' = 10$	$c' = 0$	$c' = 10$
	kPa		kPa		kPa	
	*		*		*	
0	0.000Dw	1.32m	0.000Dw	1.44m	0.000Dw	1.56m
2	0.045Dw	1.32m	0.049Dw	1.44m	0.053Dw	1.56m
4	0.090Dw	1.32m	0.099Dw	1.44m	0.107Dw	1.56m
6	0.136Dw	1.32m	0.149Dw	1.44m	0.161Dw	1.56m
8	0.181Dw	1.32m	0.199Dw	1.44m	0.215Dw	1.56m
10	0.228Dw	1.32m	0.249Dw	1.44m	0.269Dw	1.56m
12	0.274Dw	1.32m	0.301Dw	1.44m	0.325Dw	1.56m
14	0.322Dw	1.32m	0.353Dw	1.44m	0.381Dw	1.56m
16	0.370Dw	1.32m	0.406Dw	1.44m	0.438Dw	1.56m
18	0.419Dw	1.32m	0.460Dw	1.44m	0.496Dw	1.56m
20	0.470Dw	1.32m	0.515Dw	1.44m	0.556Dw	1.56m
22	0.522Dw	1.32m	0.571Dw	1.44m	0.617Dw	1.56m
24	0.575Dw	1.32m	0.630Dw	1.44m	0.680Dw	1.56m
26	0.630Dw	1.32m	0.690Dw	1.44m	0.745Dw	1.56m
28	0.686Dw	1.32m	0.752Dw	1.44m	0.812Dw	1.56m
30	0.745Dw	1.32m	0.817Dw	1.44m	0.882Dw	1.56m

* Note: These columns give the increase in crack depth in meters when $c' = 10$ kPa.

Where F_w = matric suction profile factor.

F_t = ratio of tensile strength to compressive strength.
(i.e., σ_t/Q_u).

Q_u = unconfined compressive strength.

σ_t = tensile strength.

Dw = depth to water table.

c' = cohesion intercept when $(\sigma - u_a)$ and $(u_a - u_w)$ are equal to zero.

ϕ_b = friction angle with respect to $(u_a - u_w)$.

APPENDIX D

Experimental Results on Shrinkage Tests and Cracking Tests.

UNIVERSITY OF SASKATCHEWAN, DEP. OF CIVIL ENGINEERING.

SHRINKAGE TEST RESULT

Test no. : S01

Date started : 11/25/86

Page no. : 2 of 3

Soil type : Indian Head Till

Conducted by : J. Lau

TIME hr.		Gross Wt gram	Dia. mm	Ht. ctr. mm	Ht. edg mm	Ht. mm	H-Strain	V-Strain	Net Wt. gram	Vol. cu. mm	w %	Spe. Vol. 100cc/g
1/26/85		A 413.46	62.50	21.75	22.30	22.03	-0.01730	-0.11010	133.31	67572.01	27.57	64.66
8:00 a.m.	17.50	B 413.16	62.50	21.85	22.25	22.05	-0.01652	-0.10909	133.72	67648.71	28.36	64.94
		C 413.14	62.50	21.75	22.30	22.03	-0.01730	-0.11010	132.80	67572.01	27.65	64.95
						Ave.	-0.01704	-0.10976		Ave.	27.86	64.85
		A 412.24	61.95	21.65	22.30	21.98	-0.02594	-0.11212	132.09	66237.27	26.40	53.38
0:05 a.m.	19.35	B 411.91	61.95	21.75	22.25	22.00	-0.02518	-0.11111	132.47	66312.62	27.16	63.65
		C 411.82	61.95	21.70	22.20	21.95	-0.02594	-0.11313	131.48	66161.91	26.38	63.60
						Ave.	-0.02569	-0.11212		Ave.	26.65	63.54
		A 411.18	61.50	21.45	22.30	21.88	-0.03302	-0.11616	131.03	64981.42	25.39	62.18
2:00 p.m.	21.50	B 410.83	61.50	21.75	22.15	21.95	-0.03226	-0.11313	131.39	65204.21	26.12	62.59
		C 410.73	61.50	21.65	22.10	21.88	-0.03302	-0.11616	130.39	64981.42	25.34	62.46
						Ave.	-0.03277	-0.11515		Ave.	25.61	62.41
		A 408.82	60.75	21.35	22.15	21.75	-0.04481	-0.12121	128.67	63043.85	23.13	60.33
4:00 p.m.	25.50	B 408.50	60.75	21.35	21.95	21.65	-0.04406	-0.12525	129.06	62753.99	23.88	60.24
		C 408.44	60.75	21.25	21.85	21.55	-0.04481	-0.12929	128.10	62464.14	23.13	60.04
						Ave.	-0.04456	-0.12525		Ave.	23.38	60.20
		A 405.65	59.85	20.75	21.75	21.25	-0.05896	-0.14141	125.50	59783.06	20.09	57.21
9:30 p.m.	31.00	B 405.25	59.85	20.85	21.75	21.30	-0.05822	-0.13939	125.81	59923.73	20.76	57.52
		C 404.96	59.85	20.75	21.75	21.25	-0.05896	-0.14141	124.62	59783.06	19.79	57.47
						Ave.	-0.05872	-0.14074		Ave.	20.22	57.40
1/27/86		A 403.23	59.30	20.55	21.55	21.10	-0.06761	-0.14747	123.14	58275.06	17.84	55.76
2:45 a.m.	35.25	B 402.92	59.30	20.65	21.60	21.13	-0.06688	-0.14646	123.48	58344.11	18.53	56.00
		C 402.55	59.30	20.55	21.55	21.05	-0.06761	-0.14949	122.21	58136.97	17.47	55.88
						Ave.	-0.06737	-0.14781		Ave.	17.95	55.88
		A 399.91	58.40	20.25	21.35	20.80	-0.08176	-0.15960	119.76	55716.00	14.60	53.32
9:30 a.m.	43.00	B 399.52	58.40	20.25	21.25	20.75	-0.08104	-0.16162	120.08	55582.07	15.26	53.35
		C 399.17	58.05	20.35	21.35	20.85	-0.08726	-0.15758	118.83	55182.50	14.22	53.04
						Ave.	-0.08335	-0.15960		Ave.	14.70	53.24
		A 398.75	58.20	20.15	21.15	20.65	-0.08491	-0.16566	118.61	54935.99	13.50	52.57
1:30 a.m.	45.00	B 398.38	58.15	20.20	21.15	20.68	-0.08497	-0.16465	118.94	54908.03	14.17	52.71
		C 398.75	57.95	20.15	21.15	20.65	-0.08684	-0.16566	118.41	54465.04	13.82	52.35
						Ave.	-0.08624	-0.16532		Ave.	13.83	52.54
		A 397.76	58.10	20.15	21.05	20.60	-0.08648	-0.16768	117.61	54614.80	12.54	52.26
1:45 p.m.	47.25	B 397.42	58.05	20.20	21.05	20.63	-0.08653	-0.16657	117.98	54587.01	13.25	52.40
		C 397.06	57.85	20.05	21.05	20.55	-0.09041	-0.16970	116.72	54014.39	12.20	51.92
						Ave.	-0.08781	-0.16801		Ave.	12.66	52.19
		A 395.60	58.00	20.05	21.05	20.55	-0.08805	-0.16970	115.45	54294.86	10.48	51.96
7:05 p.m.	54.58	B 395.01	57.85	20.15	20.95	20.55	-0.08969	-0.16970	115.57	54014.39	10.93	51.85
		C 394.96	57.80	20.05	21.05	20.55	-0.09119	-0.16970	114.62	53921.06	10.18	51.83
						Ave.	-0.08965	-0.16970		Ave.	10.53	51.88

UNIVERSITY OF SASKATCHEWAN, DEP. OF CIVIL ENGINEERING.

SHRINKAGE TEST RESULT

Test no. : S01

Date started : 11/25/86

Page no. : 3 of 3

Soil type : Indian Head Till

Conducted by : J. Lau

TIME		Gross Wt	Dia.	Ht. ctr.	Ht. edg	Ht.	H-Strain	V-Strain	Net Wt.	Vol.	w	Spe. Vol.
hr.		gram	mm	mm	mm	mm			gram	cu. mm	%	100cc/g
1/28/86		A 393.29	57.75	19.95	20.95	20.45	-0.09198	-0.17374	113.14	53555.87	8.27	51.25
1:00 a.m.	63.50	B 392.59	57.75	20.00	20.95	20.46	-0.09127	-0.17273	113.15	53631.35	8.61	51.46
		C 392.75	57.75	20.05	21.05	20.55	-0.09198	-0.16970	112.41	53827.81	8.05	51.74
						Ave.	-0.09174	-0.17205		Ave.	8.31	51.49
		A 392.33	57.70	19.95	20.95	20.45	-0.09277	-0.17374	112.18	53473.16	7.35	51.17
1:15 a.m.	67.75	B 391.57	57.80	20.00	20.90	20.45	-0.09048	-0.17374	112.13	53658.67	7.63	51.51
		C 391.81	57.70	20.05	21.00	20.53	-0.09277	-0.17071	111.47	53559.27	7.15	51.59
						Ave.	-0.09200	-0.17273		Ave.	7.38	51.42
		A 391.43	57.70	19.95	20.95	20.45	-0.09277	-0.17374	111.28	53473.16	6.49	51.17
1:10 p.m.	72.67	B 390.59	57.70	20.00	20.90	20.45	-0.09205	-0.17374	111.15	53473.16	6.69	51.33
		C 390.93	57.70	20.05	21.00	20.53	-0.09277	-0.17071	110.59	53559.27	6.30	51.59
						Ave.	-0.09253	-0.17273		Ave.	6.49	51.36
		A 390.57	57.70	19.95	20.95	20.45	-0.09277	-0.17374	110.52	53473.16	5.76	51.17
1:40 p.m.	76.17	B 389.81	57.70	20.00	20.90	20.45	-0.09205	-0.17374	110.37	53473.16	5.94	51.33
		C 390.19	57.70	20.05	21.00	20.53	-0.09277	-0.17071	109.85	53559.27	5.59	51.59
						Ave.	-0.09253	-0.17273		Ave.	5.76	51.36
1:01/86 *		A 384.65	57.70	19.95	20.85	20.40	-0.09277	-0.17576	104.50	53342.42	0.00	51.04
1:15 a.m.	126.75	B 383.62	57.70	20.00	20.85	20.43	-0.09205	-0.17475	104.18	53407.79	0.00	51.27
		C 384.37	57.70	20.05	20.75	20.40	-0.09277	-0.17576	104.03	53342.42	0.00	51.27
						Ave.	-0.09253	-0.17542		Ave.	0.00	51.19

NOTES: * Samples were oven dried.

** End of Test S01 **

UNIVERSITY OF SASKATCHEWAN, DEP. OF CIVIL ENGINEERING.

SHRINKAGE TEST RESULT

Test no. : 502

Date started : 12/15/85

Page no. : 1 of 3

Soil type : Indian Head Till

Conducted by : J. Lau

Initial Conditions				
	Tare	Gross Wt.	w	Net Dry Wt.
	gram	gram	%	gram
Brass Container A :	280.17	427.31	31.15	112.19
Brass Container B :	279.45	425.89	30.98	112.57
Brass Container C :	280.36	425.82	30.81	111.95

TIME		Gross Wt.	Dia.	Ht. ctr.	Ht. edg.	Ht.	H-Strain	V-Strain	Net Wt.	Vol.	w	Spe. Vol.
hr.		gram	mm	mm	mm	mm			gram	cu. mm	%	100cc/g
1/15/86		A 427.31	53.50	24.75	24.75	24.75	0.00000	0.00000	147.14	78528.55	31.15	70.08
1:00 a.m.	0.00	B 425.89	53.55	24.75	24.75	24.75	0.00000	0.00000	147.44	78504.93	30.98	69.74
		C 425.82	53.50	24.75	24.75	24.75	0.00000	0.00000	145.45	78528.55	30.81	70.23
						Ave.	0.00000	0.00000		Ave.	30.98	70.02
1:00 a.m.	1.00	A 425.55	53.50	24.55	24.55	24.55	0.00000	-0.00808	145.39	77593.18	30.48	69.52
		B 425.18	53.55	24.55	24.55	24.55	0.00000	-0.00808	145.73	77870.50	30.35	69.18
		C 425.04	53.50	24.55	24.55	24.55	0.00000	-0.00808	145.58	77593.18	30.11	69.55
						Ave.	0.00000	-0.00808		Ave.	30.31	69.45
1:00 noon	2.00	A 425.74	53.50	24.15	24.45	24.30	0.00000	-0.01818	145.57	77198.95	29.75	68.81
		B 425.42	53.55	24.15	24.45	24.30	0.00000	-0.01818	145.97	77077.62	29.57	68.47
		C 425.23	53.50	24.15	24.40	24.28	0.00000	-0.01919	144.87	77119.53	29.39	68.88
						Ave.	0.00000	-0.01852		Ave.	29.50	68.72
1:00 p.m.	3.00	A 424.92	53.25	23.85	24.35	24.10	-0.00550	-0.02525	144.75	75723.21	29.02	67.49
		B 424.63	53.30	23.90	24.30	24.10	-0.00393	-0.02525	145.18	75842.97	28.97	67.38
		C 424.33	53.25	23.85	24.30	24.08	-0.00550	-0.02727	143.97	75644.55	28.59	67.55
						Ave.	-0.00498	-0.02550		Ave.	28.85	67.48
2:00 p.m.	4.00	A 424.09	53.10	23.70	24.25	23.98	-0.00765	-0.03131	143.92	74973.58	28.28	65.83
		B 423.83	53.00	23.75	24.25	24.00	-0.00855	-0.03030	144.38	74814.05	28.25	65.46
		C 423.54	53.00	23.70	24.25	23.98	-0.00943	-0.03131	143.18	74735.13	27.88	65.75
						Ave.	-0.00855	-0.03098		Ave.	28.14	65.58
3:00 p.m.	5.00	A 423.19	52.85	23.55	24.15	23.85	-0.01179	-0.03535	143.02	73992.87	27.43	65.95
		B 422.99	52.70	23.65	24.20	23.93	-0.01335	-0.03333	143.54	73871.67	27.52	65.52
		C 422.64	52.80	23.55	24.15	23.85	-0.01253	-0.03535	142.28	73875.18	27.08	65.98
						Ave.	-0.01258	-0.03535		Ave.	27.35	65.85
4:00 p.m.	6.00	A 422.41	52.45	23.40	24.05	23.73	-0.01808	-0.04141	142.24	72571.15	25.78	64.77
		B 422.21	52.40	23.50	24.05	23.78	-0.01810	-0.03939	142.75	72707.73	25.52	64.59
		C 421.84	52.45	23.45	24.05	23.75	-0.01808	-0.04040	141.48	72747.72	25.35	64.97
						Ave.	-0.01809	-0.04040		Ave.	25.55	64.78
5:00 p.m.	7.00	A 421.59	52.10	23.25	24.00	23.63	-0.02358	-0.04545	141.42	71555.98	25.05	63.78
		B 421.35	52.10	23.40	24.00	23.70	-0.02282	-0.04242	141.91	71783.14	25.07	63.77
		C 420.93	52.10	23.25	24.00	23.63	-0.02358	-0.04545	140.57	71555.98	25.55	63.91
						Ave.	-0.02333	-0.04444		Ave.	25.69	63.82
6:15 p.m.	9.25	A 419.98	51.55	23.05	23.55	23.50	-0.03055	-0.05051	139.81	70149.55	24.62	62.53
		B 419.79	51.55	23.15	23.55	23.55	-0.02990	-0.04848	140.34	70298.81	24.67	62.45
		C 419.33	51.55	23.05	23.55	23.50	-0.03055	-0.05051	138.97	70149.55	24.12	62.55
						Ave.	-0.03041	-0.04983		Ave.	24.47	62.54

UNIVERSITY OF SASKATCHEWAN, DEP. OF CIVIL ENGINEERING.

SHRINKAGE TEST RESULT

Test no. : S02

Date started : 12/16/86

Page no. : 2 of 3

Soil type : Indian Head Till

Conducted by : J. Lau

TIME hr.		Gross Wt gram	Dia. mm	Ht. ctr. mm	Ht. edg mm	Ht. mm	H-Strain	V-Strain	Net Wt. gram	Vol. cu. mm	w %	Spe. Vol. 100cc/g
/16/86		A 418.69	61.50	22.85	23.80	23.33	-0.03302	-0.05758	138.52	69288.75	23.47	61.76
1:00 p.m.	11.00	B 418.53	61.50	22.90	23.80	23.35	-0.03226	-0.05657	139.08	69363.02	23.55	61.62
		C 417.97	61.50	22.85	23.85	23.35	-0.03302	-0.05657	137.61	69363.02	22.91	61.95
						Ave.	-0.03277	-0.05690		Ave.	23.31	61.78
		A 417.22	61.00	22.65	23.65	23.15	-0.04088	-0.05465	137.05	67655.26	22.16	60.30
1:00 p.m.	13.00	B 417.09	61.00	22.65	23.65	23.15	-0.04013	-0.05465	137.64	67655.26	22.27	60.10
		C 416.59	61.00	22.60	23.75	23.18	-0.04088	-0.05354	136.23	67728.32	21.67	60.49
						Ave.	-0.04063	-0.05431		Ave.	22.03	60.30
/17/86		A 415.37	60.50	22.45	23.55	23.00	-0.04874	-0.07071	135.20	66119.49	20.51	58.33
1:00 a.m.	16.00	B 415.28	60.40	22.45	23.45	22.95	-0.04957	-0.07273	135.83	65757.83	20.67	58.42
		C 414.78	60.50	22.45	23.50	22.98	-0.04874	-0.07172	134.42	66047.62	20.06	58.59
						Ave.	-0.04902	-0.07172		Ave.	20.41	58.78
		A 413.45	60.00	22.30	23.25	22.78	-0.05660	-0.07980	133.28	64394.95	18.80	57.40
1:00 a.m.	19.00	B 413.47	60.00	22.25	23.25	22.75	-0.05586	-0.08081	134.02	64324.26	19.06	57.14
		C 412.91	60.00	22.30	23.25	22.78	-0.05660	-0.07980	132.55	64394.95	18.39	57.51
						Ave.	-0.05636	-0.08013		Ave.	18.75	57.35
		A 412.02	59.40	22.15	23.15	22.65	-0.06604	-0.08485	131.85	62767.09	17.52	55.95
1:30 a.m.	21.50	B 411.93	59.40	22.20	23.10	22.65	-0.06530	-0.08485	132.48	62767.09	17.69	55.76
		C 411.28	59.40	22.15	23.10	22.63	-0.06604	-0.08596	130.92	62697.81	16.93	56.00
						Ave.	-0.06579	-0.08519		Ave.	17.38	55.90
		A 409.53	58.75	21.90	22.85	22.38	-0.07626	-0.09596	129.36	60655.43	15.30	54.06
1:00 a.m.	25.00	B 409.45	58.80	21.95	22.90	22.43	-0.07474	-0.09394	130.00	60894.49	15.49	54.10
		C 408.86	58.90	21.95	22.95	22.45	-0.07390	-0.09293	128.50	61169.91	14.77	54.63
						Ave.	-0.07497	-0.09428		Ave.	15.19	54.26
		A 407.50	58.40	21.75	22.55	22.15	-0.08176	-0.10505	127.33	59232.18	13.49	52.88
1:00 p.m.	28.00	B 407.49	58.55	21.80	22.70	22.25	-0.07868	-0.10101	128.04	59906.61	13.75	53.22
		C 406.92	58.55	21.80	22.75	22.28	-0.07940	-0.10000	126.56	59973.92	13.04	53.57
						Ave.	-0.07995	-0.10202		Ave.	13.42	53.22
		A 406.34	58.40	21.70	22.50	22.10	-0.08176	-0.10707	125.17	59198.25	12.46	52.77
1:00 p.m.	30.00	B 406.23	58.40	21.70	22.65	22.18	-0.08104	-0.10404	125.78	59399.15	12.53	52.77
		C 405.77	58.40	21.80	22.70	22.25	-0.08176	-0.10101	125.41	59500.05	12.01	53.23
						Ave.	-0.08152	-0.10404		Ave.	12.35	52.92
		A 404.90	58.35	21.65	22.55	22.10	-0.08255	-0.10707	124.73	59095.93	11.18	52.67
1:45 p.m.	32.75	B 404.74	58.30	21.65	22.65	22.15	-0.08261	-0.10505	125.29	59129.16	11.30	52.53
		C 404.41	58.40	21.75	22.60	22.18	-0.08176	-0.10404	124.05	59399.15	10.79	53.05
						Ave.	-0.08231	-0.10539		Ave.	11.09	52.75
/18/86		A 402.38	58.20	21.60	22.45	22.03	-0.08491	-0.11010	122.21	58593.95	8.93	52.23
1:30 a.m.	40.50	B 402.17	58.20	21.65	22.45	22.05	-0.08419	-0.10909	122.72	58650.46	9.02	52.11
		C 402.04	58.30	21.65	22.45	22.05	-0.08333	-0.10909	121.69	58862.21	8.68	52.57
						Ave.	-0.08414	-0.10943		Ave.	8.88	52.30

UNIVERSITY OF SASKATCHEWAN, DEP. OF CIVIL ENGINEERING.

SHRINKAGE TEST RESULT

Test no. : S02

Date started : 11/25/86

Page no. : 3 of 3

Soil type : Indian Head Till

Conducted by : J. Lau

	TIME		Gross Wt	Dia.	Ht. ctr.	Ht. edg	Ht.	H-Strain	V-Strain	Net Wt.	Vol.	w	Spe. Vol.
	hr.		gram	mm	mm	mm	mm			gram	cu. mm	%	100cc/g
1/18/86		A	400.69	58.10	21.60	22.45	22.03	-0.08548	-0.11010	120.52	58392.77	7.42	52.05
1:00 a.m.	48.00	B	400.50	58.10	21.65	22.45	22.05	-0.08576	-0.10909	121.05	58459.05	7.54	51.93
		C	400.42	58.20	21.65	22.45	22.05	-0.08491	-0.10909	120.06	58660.46	7.23	52.39
							Ave.	-0.08571	-0.10943		Ave.	7.40	52.12
		A	399.68	58.00	21.60	22.45	22.03	-0.08805	-0.11010	119.51	58191.94	6.52	51.87
1:00 p.m.	54.00	B	399.45	58.00	21.60	22.45	22.03	-0.08733	-0.11010	120.00	58191.94	6.60	51.70
		C	399.44	58.10	21.65	22.45	22.05	-0.08548	-0.10909	119.08	58459.05	6.35	52.21
							Ave.	-0.08729	-0.10976		Ave.	6.49	51.93
1/23/86 *		A	392.36	57.80	21.60	22.40	22.00	-0.09119	-0.11111	112.19	57725.71	0.00	51.45
1:15 a.m.	167.25	B	392.02	57.80	21.60	22.35	21.98	-0.09048	-0.11212	112.57	57560.11	0.00	51.22
		C	392.32	58.00	21.65	22.35	22.00	-0.08805	-0.11111	111.96	58125.88	0.00	51.91
							Ave.	-0.08991	-0.11145		Ave.	0.00	51.53

* Samples were oven-dried.

** End of Test no. S02 **

UNIVERSITY OF SASKATCHEWAN, DEP. OF CIVIL ENGINEERING.

SHRINKAGE TEST RESULT

Test no. : 503
Soil type : Regina Clay

Date started : 01/20/87

Page no. : 1 of 4
Conducted by : J. Lau

Initial Conditions

	Tare	Gross Wt.	w	Net Dry Wt.
	gram	gram	%	gram
Brass Container A :	280.17	400.06	79.50	55.79
Brass Container B :	279.46	400.45	80.07	57.19
Brass Container C :	280.35	400.24	80.39	55.46

TIME		Gross Wt.	Dia.	Ht. ctr.	Ht. edg.	Ht.	H-Strain	V-Strain	Net Wt.	Vol.	w	Spe. Vol.
hr.		gram	mm	mm	mm	mm			gram	cu. mm	%	100cc/g
1/20/87		A 400.06	53.60	24.75	24.75	24.75	0.00000	0.00000	119.89	78528.55	79.50	117.72
1:30 a.m.	0.00	B 400.45	53.55	24.75	24.75	24.75	0.00000	0.00000	120.99	78504.98	80.07	115.84
		C 400.24	53.60	24.75	24.75	24.75	0.00000	0.00000	119.89	78528.56	80.39	118.31
						Ave.	0.00000	0.00000		Ave.	79.99	117.62
2:30 p.m.	1.00	A 399.44	53.60	24.35	24.40	24.38	0.00000	-0.01515	119.27	77437.22	78.57	115.94
		B 399.65	53.55	24.55	24.55	24.55	0.00000	-0.00808	120.39	77870.60	79.18	115.90
		C 399.64	53.60	24.40	24.40	24.40	0.00000	-0.01414	119.29	77516.64	79.49	115.63
						Ave.	0.00000	-0.01245		Ave.	79.08	115.16
1:30 p.m.	2.00	A 398.73	53.60	24.25	24.15	24.20	0.00000	-0.02222	118.55	76881.26	77.51	115.11
		B 399.18	53.55	24.30	24.40	24.35	0.00000	-0.01515	119.72	77235.21	78.18	114.95
		C 398.94	53.60	24.10	24.25	24.18	0.00000	-0.02323	118.59	76801.84	78.43	115.55
						Ave.	0.00000	-0.02054		Ave.	78.04	115.21
2:30 p.m.	3.00	A 397.98	53.60	23.75	23.95	23.85	0.00000	-0.03535	117.81	75769.34	76.39	113.44
		B 398.41	53.55	23.85	24.00	23.93	0.00000	-0.03333	118.95	75888.15	77.03	112.94
		C 398.09	53.60	23.70	23.95	23.83	0.00000	-0.03737	117.74	75589.92	77.13	113.89
						Ave.	0.00000	-0.03569		Ave.	76.85	113.42
3:30 p.m.	4.00	A 397.08	53.60	23.65	23.20	23.43	0.00000	-0.05354	116.91	74419.15	75.04	111.42
		B 397.56	53.55	23.55	23.70	23.63	0.00000	-0.04545	118.10	74935.57	75.77	111.53
		C 397.22	53.60	23.35	23.65	23.50	0.00000	-0.05051	116.87	74657.42	75.85	112.33
						Ave.	0.00000	-0.04983		Ave.	75.55	111.76
4:30 p.m.	5.00	A 396.38	53.30	22.95	23.35	23.15	-0.00472	-0.05465	116.21	72853.31	73.99	109.08
		B 396.96	53.30	23.25	23.15	23.25	-0.00393	-0.06061	117.50	73168.02	74.88	108.90
		C 396.55	53.30	23.15	23.35	23.25	-0.00472	-0.05051	115.21	73168.02	74.85	110.09
						Ave.	-0.00446	-0.05195		Ave.	74.57	109.35
5:30 p.m.	7.00	A 394.98	52.20	22.85	23.25	23.05	-0.02201	-0.05869	114.81	70039.43	71.89	104.86
		B 395.53	52.60	23.20	23.45	23.33	-0.01495	-0.05756	116.07	71789.55	72.75	106.84
		C 395.10	52.60	23.00	23.65	23.13	-0.01572	-0.06566	114.75	71173.99	72.66	107.09
						Ave.	-0.01755	-0.06397		Ave.	72.43	106.27
6:30 p.m.	9.00	A 393.44	52.40	22.55	23.15	22.90	-0.01837	-0.07475	113.27	70031.84	69.59	104.85
		B 394.10	52.40	23.00	23.35	23.18	-0.01810	-0.06364	114.64	70872.84	70.62	105.48
		C 393.77	52.40	22.90	23.15	23.03	-0.01837	-0.06970	113.42	70414.11	70.55	105.95
						Ave.	-0.01861	-0.06935		Ave.	70.29	105.43
1/21/87		A 390.74	51.45	22.30	22.85	22.58	-0.03381	-0.08788	110.57	65951.83	65.55	100.24
2:30 a.m.	13.00	B 391.50	51.45	22.65	23.15	22.90	-0.03304	-0.07475	112.04	67915.70	66.75	101.08
		C 391.05	51.45	22.55	22.85	22.70	-0.03381	-0.08283	110.70	67322.55	66.56	101.30
						Ave.	-0.03355	-0.08182		Ave.	66.29	100.87

UNIVERSITY OF SASKATCHEWAN, DEP. OF CIVIL ENGINEERING.

SHRINKAGE TEST RESULT

Test no. : 503

Date started : 01/21/87

Page no. : 2 of 4

Soil type : Regina Clay

Conducted by : J. Lau

TIME		Gross Wt	Dia.	Ht. ctr.	Ht. edg	Ht.	H-Strain	V-Strain	Net Wt.	Vol.	w	Spe. Vol.
hr.		gram	mm	mm	mm	mm			gram	cu. mm	%	100cc/g
1/21/87		A 388.74	60.80	21.95	22.65	22.30	-0.04403	-0.09899	108.57	64744.51	62.55	96.94
3:45 a.m.	16.25	B 389.56	60.80	22.35	22.85	22.60	-0.04327	-0.08687	110.10	65615.51	63.66	97.66
		C 389.04	60.80	22.20	22.65	22.43	-0.04403	-0.09394	108.69	65107.42	63.54	97.96
						Ave.	-0.04377	-0.09327		Ave.	63.32	97.52
7:00 a.m.	19.50	A 366.76	60.30	21.65	22.40	22.03	-0.05189	-0.11010	106.59	62898.67	59.59	94.17
		B 387.64	60.30	22.05	22.70	22.38	-0.05114	-0.09596	108.18	63858.19	61.00	95.10
		C 387.12	60.30	21.95	22.45	22.20	-0.05189	-0.10303	106.77	63393.43	60.65	95.39
						Ave.	-0.05164	-0.10303		Ave.	60.41	94.89
9:00 a.m.	21.50	A 385.34	59.75	21.45	22.25	21.85	-0.05053	-0.11717	105.17	61655.81	57.46	91.73
		B 386.31	59.75	21.85	22.55	22.20	-0.05580	-0.10303	106.85	62247.18	59.03	92.64
		C 385.70	59.75	21.75	22.35	22.05	-0.06053	-0.10909	105.35	61826.59	58.51	93.03
						Ave.	-0.06029	-0.10976		Ave.	58.33	92.47
11:00 a.m.	23.50	A 383.84	59.20	21.20	22.00	21.60	-0.06918	-0.12727	103.67	59454.96	55.22	89.02
		B 384.82	59.20	21.65	22.50	22.08	-0.06845	-0.10808	105.36	60762.41	56.81	90.43
		C 384.35	59.20	21.50	22.15	21.83	-0.06918	-0.11818	104.00	60074.28	56.48	90.39
						Ave.	-0.06894	-0.11785		Ave.	56.17	89.95
1:00 p.m.	25.50	A 382.34	58.55	21.00	21.95	21.48	-0.07940	-0.12232	102.17	57819.97	52.97	86.57
		B 383.40	58.55	21.45	22.40	21.93	-0.07868	-0.11414	103.94	59031.57	54.69	87.86
		C 382.99	58.55	21.30	22.05	21.68	-0.07940	-0.12424	102.64	58358.46	54.44	87.81
						Ave.	-0.07916	-0.12357		Ave.	54.03	87.41
3:00 p.m.	27.50	A 381.06	58.30	20.85	21.85	21.35	-0.08333	-0.13737	100.89	56993.57	51.05	85.33
		B 382.13	58.45	21.20	22.25	21.78	-0.08025	-0.12020	102.67	58427.61	52.80	86.96
		C 381.73	58.45	21.15	21.85	21.50	-0.08097	-0.13131	101.38	57589.71	52.54	86.80
						Ave.	-0.08152	-0.12953		Ave.	52.13	86.36
5:00 p.m.	29.50	A 379.70	57.70	20.70	21.70	21.20	-0.09277	-0.14343	99.53	55434.28	49.02	83.00
		B 380.80	57.70	21.20	22.15	21.68	-0.09205	-0.12424	101.34	56575.32	50.82	84.35
		C 380.27	57.70	20.90	21.75	21.33	-0.09277	-0.13838	99.92	55761.13	50.34	83.90
						Ave.	-0.09253	-0.13535		Ave.	50.06	83.75
7:15 p.m.	31.75	A 378.42	57.15	20.45	21.40	20.93	-0.10142	-0.15455	98.25	53577.07	47.10	80.37
		B 379.45	57.15	20.95	22.00	21.48	-0.10071	-0.13232	99.99	55087.94	48.82	81.99
		C 378.94	57.15	20.70	21.60	21.15	-0.10142	-0.14545	98.59	54254.25	48.34	81.53
						Ave.	-0.10118	-0.14411		Ave.	48.09	81.33
9:45 p.m.	34.25	A 376.97	56.60	20.30	21.35	20.83	-0.11006	-0.15859	96.80	52397.28	44.93	78.45
		B 377.96	56.60	20.70	21.90	21.30	-0.10936	-0.13939	98.50	53592.42	46.60	79.76
		C 377.49	56.60	20.30	21.35	20.83	-0.11006	-0.15859	97.14	52397.28	45.16	78.64
						Ave.	-0.10983	-0.15219		Ave.	45.90	79.02
1/22/87		A 375.63	55.35	20.15	21.15	20.65	-0.11399	-0.16566	95.46	51499.00	42.92	77.10
1:15 a.m.	35.75	B 376.63	55.35	20.55	21.65	21.10	-0.11330	-0.14747	97.17	52521.25	44.62	78.32
		C 376.11	55.35	20.30	21.25	20.78	-0.11399	-0.16061	95.75	51610.74	44.08	77.96
						Ave.	-0.11376	-0.15791		Ave.	43.83	77.79

UNIVERSITY OF SASKATCHEWAN, DEP. OF CIVIL ENGINEERING.

SHRINKAGE TEST RESULT

Test no. : 903

Date started : 01/20/87

Page no. : 3 of 4

Soil type : Regina Clay

Conducted by : J. Lau

TIME hr.		Gross Wt gram	Dia. mm	Ht. ctr. mm	Ht. edg mm	Ht. mm	H-Strain	V-Strain	Net Wt. gram	Vol. cu. mm	w %	Spe. Vol. 100cc/g
1/22/87		A 373.65	55.50	19.90	20.80	20.35	-0.12736	-0.17778	93.48	49231.30	39.96	73.71
4:30 a.m.	41.00	B 374.49	55.50	20.25	21.35	20.80	-0.12667	-0.15960	95.03	50319.95	41.43	74.89
		C 373.99	55.50	20.05	21.05	20.55	-0.12736	-0.16970	93.64	49715.14	40.89	74.80
						Ave.	-0.12713	-0.16902		Ave.	40.76	74.47
		A 371.87	54.70	19.65	20.65	20.15	-0.13994	-0.18586	91.70	47352.25	37.29	70.90
8:00 a.m.	44.50	B 372.69	54.70	20.05	21.20	20.63	-0.13926	-0.16667	93.23	48458.49	38.75	72.14
		C 372.10	54.70	19.85	20.95	20.40	-0.13994	-0.17576	91.75	47939.74	38.05	72.13
						Ave.	-0.13971	-0.17609		Ave.	38.03	71.72
		A 370.72	54.30	19.50	20.50	20.00	-0.14623	-0.19192	90.55	45314.88	35.57	69.34
0:00 a.m.	46.50	B 371.50	54.30	19.95	21.05	20.50	-0.14555	-0.17172	92.04	47472.75	36.98	70.65
		C 370.96	54.30	19.65	20.65	20.15	-0.14623	-0.18586	90.51	46562.24	35.33	70.21
						Ave.	-0.14600	-0.18316		Ave.	36.30	70.07
		A 369.15	53.95	19.35	20.35	19.85	-0.15173	-0.19798	88.98	45376.85	33.22	67.94
1:00 p.m.	49.50	B 369.91	53.95	19.70	20.80	20.25	-0.15106	-0.18182	90.45	46291.24	34.62	68.90
		C 369.39	53.95	19.45	20.45	19.95	-0.15173	-0.19394	89.04	45605.44	33.97	68.62
						Ave.	-0.15151	-0.19125		Ave.	33.94	68.48
		A 367.57	53.00	19.15	20.05	19.60	-0.16657	-0.20808	87.40	43241.30	30.86	64.74
5:00 p.m.	52.50	B 368.27	53.00	19.50	20.75	20.13	-0.16601	-0.18687	88.81	44399.55	32.18	66.08
		C 367.80	53.00	19.35	20.35	19.85	-0.16667	-0.19798	87.45	43792.84	31.58	65.89
						Ave.	-0.16645	-0.19764		Ave.	31.54	65.57
		A 365.67	52.10	18.90	20.00	19.45	-0.18082	-0.21414	85.50	41455.41	28.01	62.08
8:00 p.m.	55.50	B 366.27	52.10	19.35	20.35	19.85	-0.18017	-0.19798	85.81	42318.17	29.20	62.98
		C 365.91	52.10	19.10	20.05	19.58	-0.18082	-0.20909	85.55	41731.90	28.74	62.79
						Ave.	-0.18060	-0.20707		Ave.	28.65	62.62
1/23/87		A 363.22	51.35	18.55	19.35	18.95	-0.19261	-0.23434	83.05	39244.70	24.34	58.76
9:15 a.m.	62.75	B 363.74	51.35	18.95	19.95	19.45	-0.19197	-0.21414	84.28	40280.18	25.43	59.95
		C 363.42	51.35	18.95	19.55	19.25	-0.19261	-0.22222	83.07	39855.93	24.99	59.98
						Ave.	-0.19240	-0.22357		Ave.	24.92	59.56
		A 362.29	51.00	18.40	19.25	18.83	-0.19811	-0.23939	82.12	38456.19	22.95	57.58
5:00 a.m.	65.50	B 362.72	51.00	18.85	19.75	19.30	-0.19748	-0.22020	83.26	39425.53	23.92	58.58
		C 362.45	51.00	18.65	19.35	19.10	-0.19811	-0.22828	82.10	39017.97	23.53	58.71
						Ave.	-0.19790	-0.22929		Ave.	23.47	58.32
		A 361.19	50.40	18.20	19.20	18.70	-0.20755	-0.24444	81.02	37307.28	21.30	56.86
9:30 a.m.	69.00	B 361.54	50.40	18.65	19.20	18.93	-0.20692	-0.23535	82.03	37755.16	22.16	56.19
		C 361.29	50.40	18.55	19.35	18.95	-0.20755	-0.23434	80.94	37806.04	21.78	56.88
						Ave.	-0.20734	-0.23805		Ave.	21.75	56.31
		A 360.21	50.30	18.15	19.15	18.65	-0.20912	-0.24646	80.04	37060.02	19.84	55.49
1:00 a.m.	71.50	B 360.50	50.30	18.35	19.05	18.70	-0.20350	-0.24444	81.04	37159.38	20.61	55.30
		C 360.25	50.30	18.40	19.10	18.75	-0.20912	-0.24242	79.91	37258.74	20.23	55.06
						Ave.	-0.20891	-0.24444		Ave.	20.23	55.62

UNIVERSITY OF SASKATCHEWAN, DEP. OF CIVIL ENGINEERING.

SHRINKAGE TEST RESULT

Test no. : S03

Date started : 01/21/87

Page no. : 4 of 4

Soil type : Regina Clay

Conducted by : J. Lau

	TIME hr.		Gross Wt gram	Dia. mm	Ht. ctr. mm	Ht. edg mm	Ht. mm	H-Strain	V-Strain	Net Wt. gram	Vol. cu. mm	w %	Spe. Vol. 100cc/g
1/23/87		A	358.30	50.20	17.85	18.85	18.35	-0.21069	-0.25859	78.13	36319.04	16.98	54.38
4:30 p.m.	77.00	B	358.40	50.20	18.25	19.05	18.65	-0.21007	-0.24645	78.94	36912.82	17.49	54.94
		C	358.15	50.20	18.05	18.65	18.35	-0.21059	-0.25859	77.80	36319.04	17.06	54.65
							Ave.	-0.21048	-0.25455		Ave.	17.17	54.65
		A	357.21	50.00	17.75	18.40	18.08	-0.21384	-0.25970	77.04	35490.25	15.34	53.14
9:00 p.m.	81.50	B	357.17	50.00	18.05	18.95	18.50	-0.21322	-0.25253	77.71	36324.75	15.66	54.06
		C	357.05	50.00	18.00	18.65	18.33	-0.21384	-0.25960	75.71	35981.14	15.42	54.14
							Ave.	-0.21363	-0.25061		Ave.	15.47	53.78
1/24/87		A	355.20	49.90	17.55	18.35	17.95	-0.21541	-0.27475	75.03	35103.99	12.34	52.56
7:30 a.m.	92.00	B	355.07	49.90	17.95	18.55	18.25	-0.21479	-0.25253	75.61	35590.68	12.53	53.12
		C	355.05	49.90	17.85	18.25	18.05	-0.21541	-0.27071	74.70	35299.55	12.40	53.11
							Ave.	-0.21520	-0.26936		Ave.	12.42	52.93
		A	353.31	49.90	17.55	18.25	17.90	-0.21541	-0.27677	73.14	35006.20	9.51	52.41
8:45 p.m.	105.25	B	353.04	49.90	17.75	18.45	18.10	-0.21479	-0.25869	73.58	35397.33	9.51	52.68
		C	353.16	49.90	17.75	18.10	17.93	-0.21541	-0.27576	72.81	35055.10	9.55	52.74
							Ave.	-0.21520	-0.27374		Ave.	9.52	52.61
1/25/87		A	352.45	49.90	17.55	18.25	17.90	-0.21541	-0.27677	72.28	35006.20	8.22	52.41
8:00 a.m.	115.50	B	352.16	49.90	17.75	18.40	18.08	-0.21479	-0.26970	72.70	35348.44	8.20	52.61
		C	352.27	49.90	17.75	18.10	17.93	-0.21541	-0.27576	71.92	35055.10	8.21	52.74
							Ave.	-0.21520	-0.27407		Ave.	8.21	52.59
		A	351.73	49.90	17.55	18.25	17.90	-0.21541	-0.27677	71.55	35006.20	7.14	52.41
5:00 p.m.	125.50	B	351.52	49.90	17.75	18.40	18.08	-0.21479	-0.26970	72.06	35348.44	7.25	52.61
		C	351.65	49.90	17.75	18.10	17.93	-0.21541	-0.27576	71.30	35055.10	7.28	52.74
							Ave.	-0.21520	-0.27407		Ave.	7.22	52.59
1/26/87		A	351.13	49.90	17.55	18.25	17.90	-0.21541	-0.27677	70.96	35006.20	6.24	52.41
0:30 a.m.	143.00	B	350.50	49.90	17.75	18.40	18.08	-0.21479	-0.26970	71.44	35348.44	6.32	52.61
		C	351.03	49.90	17.75	18.10	17.93	-0.21541	-0.27576	70.68	35055.10	6.35	52.74
							Ave.	-0.21520	-0.27407		Ave.	6.30	52.59
1/27/87		A	346.96	49.50	17.45	18.05	17.75	-0.22170	-0.28283	66.79	34158.57	0.00	51.14
0:30 a.m.	*157.00	B	346.65	49.50	17.65	18.25	17.95	-0.22109	-0.27475	67.19	34543.45	0.00	51.41
		C	346.81	49.40	17.65	18.05	17.85	-0.22327	-0.27879	66.46	34212.35	0.00	51.48
							Ave.	-0.22202	-0.27879		Ave.	0.00	51.34

* Samples were oven-dried.

** End of Test no. S03 **

UNIVERSITY OF SASKATCHEWAN, DEP. OF CIVIL ENGINEERING.

SHRINKAGE TEST RESULT

Test no. : 501
Soil type : Indian Head Till

Date started : 11/25/86

Page no. : 1 of 3
Conducted by : J. Lau

Initial Conditions

	Tare	Gross Wt.	w	Net Dry Wt.
	gram	gram	%	gram
Brass Container A :	280.15	424.07	37.72	104.50
Brass Container B :	279.44	423.03	37.83	104.18
Brass Container C :	280.34	423.53	37.64	104.03

TIME		Gross Wt.	Dia.	Ht. ctr.	Ht. edg	Ht.	H-Strain	V-Strain	Net Wt.	Vol.	w	Spe. Vol.
hr.		gram	mm	mm	mm	mm			gram	cu. mm	%	100cc/g
1/25/86		A 424.07	63.60	24.75	24.75	24.75	0.00000	0.00000	143.92	78628.56	37.72	75.24
2:30 p.m.	0.00	B 423.03	63.55	24.75	24.75	24.75	0.00000	0.00000	143.59	78504.98	37.83	75.36
		C 423.53	63.60	24.75	24.75	24.75	0.00000	0.00000	143.19	78628.56	37.64	75.58
						Ave.	0.00000	0.00000		Ave.	37.73	75.39
3:45 p.m.	1.25	A 423.56	63.60	24.60	24.60	24.60	0.00000	-0.00606	143.41	78152.02	37.23	74.79
		B 422.54	63.55	24.60	24.60	24.60	0.00000	-0.00606	143.10	78029.19	37.36	74.90
		C 422.90	63.60	24.60	24.60	24.60	0.00000	-0.00606	142.56	78152.02	37.03	75.12
						Ave.	0.00000	-0.00606		Ave.	37.21	74.94
4:45 p.m.	2.25	A 422.94	63.60	24.45	24.55	24.50	0.00000	-0.01010	142.79	77834.33	36.64	74.48
		B 421.97	63.55	24.45	24.45	24.45	0.00000	-0.01212	142.53	77553.40	36.81	74.44
		C 422.26	63.60	24.35	24.40	24.38	0.00000	-0.01515	141.92	77437.22	36.42	74.44
						Ave.	0.00000	-0.01245		Ave.	36.62	74.45
7:05 p.m.	4.58	A 421.43	63.60	23.55	24.05	23.85	0.00000	-0.03636	141.28	75769.34	35.19	72.51
		B 420.57	63.55	23.75	24.05	23.90	0.00000	-0.03434	141.13	75808.85	35.47	72.77
		C 420.85	63.60	23.75	24.05	23.90	0.00000	-0.03434	140.51	75928.19	35.06	72.99
						Ave.	0.00000	-0.03502		Ave.	35.24	72.75
9:40 p.m.	7.17	A 419.78	63.60	23.25	23.55	22.40	0.00000	-0.05455	139.63	74339.73	33.61	71.14
		B 419.13	63.55	23.35	23.55	23.45	0.00000	-0.05253	139.69	74381.49	34.09	71.40
		C 419.31	63.60	23.25	23.45	23.35	0.00000	-0.05657	138.97	74180.89	33.58	71.31
						Ave.	0.00000	-0.05455		Ave.	33.76	71.28
1:00 p.m.	8.50	A 418.50	63.60	23.10	23.25	23.18	0.00000	-0.06354	138.75	73624.93	32.77	70.45
		B 418.35	63.55	23.15	23.45	23.30	0.00000	-0.05859	138.92	73905.70	33.35	70.94
		C 418.46	63.60	23.00	23.35	23.18	0.00000	-0.06364	138.12	73624.93	32.77	70.77
						Ave.	0.00000	-0.06195		Ave.	32.96	70.72
1/25/86		A 418.06	63.60	22.85	23.03	22.94	0.00000	-0.07313	137.91	72878.35	31.97	69.74
2:20 a.m.	9.83	B 417.59	63.55	22.85	23.05	22.95	0.00000	-0.07273	138.15	72795.53	32.61	69.88
		C 417.65	63.60	22.75	23.05	22.90	0.00000	-0.07475	137.31	72751.28	31.99	69.93
						Ave.	0.00000	-0.07354		Ave.	32.19	69.85
3:05 a.m.	11.58	A 417.06	63.50	22.35	22.85	22.60	-0.00157	-0.08687	136.91	71576.60	31.01	68.49
		B 416.65	63.55	22.40	22.85	22.63	0.00000	-0.08586	137.22	71754.65	31.72	68.89
		C 416.70	63.60	22.25	22.75	22.50	0.00000	-0.09091	136.36	71480.51	31.07	68.71
						Ave.	-0.00052	-0.08788		Ave.	31.27	68.70
5:05 a.m.	13.58	A 415.86	63.00	21.85	22.35	22.10	-0.00943	-0.10707	135.71	68891.28	29.66	65.92
		B 415.49	63.00	22.05	22.35	22.20	-0.00855	-0.10303	136.05	69203.01	30.59	66.43
		C 415.51	63.00	21.95	22.35	22.15	-0.00943	-0.10505	135.17	69047.15	29.93	66.37
						Ave.	-0.00917	-0.10505		Ave.	30.13	66.24

UNIVERSITY OF SASKATCHEWAN, DEP. OF CIVIL ENGINEERING.

CRACKING TEST RESULT

Test no. : T01 Date started : 11/25/86 Page no. : 1 of 1
 Soil : Indian Head Till Conducted by : J. Lau

Initial Soil Thickness (mm)

at ref. #1 : 58.00
 at ref. #2 : 58.65
 at ref. #3 : 60.73
 at ref. #4 : 57.99

Time hr.	Suction				Vertical Shrinkage				Vertical Strain				Average Strain
	#1 kPa	#2 kPa	#3 kPa	#4 kPa	#1 mm	#2 mm	#3 mm	#4 mm	#1	#2	#3	#4	
0.00	0.0	0.0	0.0	0.0	0.00	0.00	0.00	0.00	0.00000	0.00000	0.00000	0.00000	0.00000
2.25	0.0	0.0	0.0	0.0	-0.20	-0.20	-0.38	-0.38	-0.00345	-0.00341	-0.00627	-0.00627	-0.00485
4.58	0.0	0.0	0.0	0.0	-0.30	-0.30	-0.56	-0.51	-0.00517	-0.00512	-0.00920	-0.00836	-0.00696
7.17	0.0	0.0	0.0	0.0	-0.50	-0.30	-0.84	-0.51	-0.00862	-0.00512	-0.01380	-0.00836	-0.00898
8.50	0.5	0.3	0.8	0.2	-0.80	-0.70	-1.02	-1.02	-0.01379	-0.01194	-0.01673	-0.01673	-0.01480
9.83	0.8	0.5	0.9	0.2	-0.82	-0.72	-1.07	-1.02	-0.01414	-0.01228	-0.01757	-0.01673	-0.01518
11.58	0.8	0.5	1.0	0.2	-1.00	-1.00	-1.24	-1.09	-0.01724	-0.01705	-0.02049	-0.01798	-0.01819
13.58	1.0	0.8	1.2	0.4	-1.10	-1.25	-1.42	-1.27	-0.01897	-0.02131	-0.02342	-0.02091	-0.02115
17.50	1.2	1.0	1.6	0.6	-1.50	-1.50	-1.78	-1.52	-0.02586	-0.02558	-0.02928	-0.02509	-0.02645
19.35	1.5	1.2	1.8	0.9	-1.70	-1.75	-2.03	-1.78	-0.02931	-0.02984	-0.03346	-0.02928	-0.03047
21.50	1.8	1.6	1.9	1.0	-1.90	-1.85	-2.29	-2.03	-0.03276	-0.03154	-0.03764	-0.03346	-0.03385
25.50	2.2	1.8	2.0	1.2	-2.40	-2.20	-2.79	-2.34	-0.04138	-0.03751	-0.04601	-0.03848	-0.04084
31.00	3.0	1.9	2.4	1.8	-2.95	-2.80	-3.43	-2.92	-0.05086	-0.04774	-0.05646	-0.04810	-0.05079
36.25	3.3	2.5	3.0	2.2	-3.25	-3.05	-3.81	-3.18	-0.05603	-0.05200	-0.06274	-0.05228	-0.05576
*43.00	4.5	3.1	3.8	3.0	-3.70	-3.50	-4.19	-3.56	-0.06379	-0.05968	-0.06901	-0.05855	-0.06276
45.00	4.5	3.1	4.0	3.8	-3.90	-3.55	-4.45	-3.68	-0.06724	-0.06053	-0.07319	-0.06065	-0.06540
47.25	4.5	3.2	4.2	3.8	-4.05	-3.80	-4.57	-3.81	-0.06983	-0.06479	-0.07528	-0.06274	-0.06816
54.58	6.2	3.8	4.0	3.0	-4.30	-4.40	-4.83	-3.94	-0.07414	-0.07502	-0.07947	-0.06483	-0.07336
63.50	9.0	6.0	5.8	4.8	-4.55	-4.75	-5.08	-4.06	-0.07845	-0.08099	-0.08365	-0.06692	-0.07750
67.75	11.8	7.1	7.5	6.0	-4.75	-4.90	-5.44	-4.57	-0.08190	-0.08355	-0.08950	-0.07528	-0.08256
72.67	14.5	8.5	9.5	7.5	-5.15	-5.05	-5.72	-4.83	-0.08879	-0.08610	-0.09411	-0.07947	-0.08712
78.17	17.9	10.1	11.5	9.0	-5.40	-5.25	-6.05	-4.98	-0.09310	-0.08951	-0.09954	-0.08198	-0.09103
91.50	24.5	14.2	16.5	13.0	-5.90	-5.75	-6.58	-5.41	-0.10172	-0.09804	-0.10833	-0.08909	-0.09929
113.25	49.5	26.5	43.5	26.5	-6.70	-6.50	-7.37	-6.10	-0.11552	-0.11083	-0.12129	-0.10038	-0.11200
123.50	77.0	36.5	65.0	36.2	-7.05	-6.80	-7.75	-6.60	-0.12155	-0.11594	-0.12756	-0.10874	-0.11845
138.75	+86.0	55.0	68.0	54.0	-7.50	-7.25	-8.13	-6.99	-0.12931	-0.12361	-0.13384	-0.11502	-0.12545

** End of Test T01 **

NOTES: * Soils sample started to crack at the locations where suction sensors were installed.
 All suction sensors were installed horizontally, with 150 mm embedment in the soils,
 from the container sidewalls.

UNIVERSITY OF SASKATCHEWAN, DEP. OF CIVIL ENGINEERING.

MOISTURE CONTENT TEST RESULTS

Test no. : T01 Date started : 11/25/86 Page no. : 1 of 1
 Soil type : Indian Head Till Conducted by : J. Lau
 Total sample thickness : 60.0 mm approx.

TIME	SAMPLE	JAR #	TARE	GROSS	GROSS	NET	MOISTURE	REMARKS	
hr.	DEPTH			WET WT.	DRY WT.	DRY WT.	CONTENT		
	mm		gram	gram	gram	gram	%		
11/25/86	0.00	Bulk	X1	102.13	215.99	184.73	82.60	37.85	Initial w%
2:30 p.m.		Bulk	X2	102.60	222.76	189.83	87.23	37.75	
11/26/86	18.00	0.0-12.0	D	102.08	113.26	110.43	8.35	33.89	
8:30 a.m.		12.0-24.0	J7	102.23	112.62	109.94	7.71	34.76	
		24.0-36.0	11	103.13	113.47	110.78	7.65	35.16	
		36.0-48.0	12	102.20	110.67	108.45	6.25	35.52	
		48.0-60.0	13	102.33	107.03	105.81	3.48	35.06	
11/27/86	43.60	0.0-12.0	L1	103.01	117.66	114.10	11.09	32.10	Soil cracked
10:10 a.m.		12.0-24.0	F5	135.72	149.91	146.43	10.71	32.49	
		24.0-36.0	J6	102.31	111.09	108.89	6.58	33.43	
		36.0-48.0	R7	136.17	148.10	144.96	8.79	35.72	
		48.0-60.0	X10	99.18	108.88	106.43	7.25	33.79	
11/28/86	63.50	0.0-12.0	X2	103.13	120.62	116.79	13.66	28.04	
6:00 a.m.		12.0-24.0	L3	99.46	115.12	111.61	12.15	28.89	
		24.0-36.0	T12	101.95	114.27	111.48	9.53	29.28	
		36.0-48.0	V31	100.06	112.32	109.53	9.47	29.46	
		48.0-60.0	6E8	102.46	119.05	115.24	12.78	29.81	
12/1/86	126.75	0.0-12.0	D	102.07	142.18	134.58	32.51	23.38	End of test
9:15 a.m.		12.0-24.0	J7	102.24	127.47	122.68	20.44	23.43	
		24.0-36.0	11	103.13	128.61	123.72	20.59	23.75	
		36.0-48.0	13	102.33	137.68	130.84	28.51	23.99	
		48.0-60.0	V33	101.79	125.36	120.83	19.04	23.79	

** End of Test T01 **

UNIVERSITY OF SASKATCHEWAN, DEP. OF CIVIL ENGINEERING.

CRACKING TEST RESULT

Test no. : T02 Date started : 12/03/85 Page no. : 1 of 2
Soil type : Indian Head Till Conducted by : J. Lau

Initial Soil Thickness (mm)

at ref. #1 : 53.88
at ref. #2 : 54.57
at ref. #3 : 53.75
at ref. #4 : 54.35

Time	Suction				Shrinkage				Strain				Average
hr.	#1 kPa	#2 kPa	#3 kPa	#4 kPa	#1 mm	#2 mm	#3 mm	#4 mm	#1	#2	#3	#4	Strain
0.00	0.0	0.0	0.0	0.0	0.00	0.00	0.00	0.00	0.00000	0.00000	0.00000	0.00000	0.00000
2.25	0.0	0.0	0.0	0.0	-0.50	-0.48	-0.48	-0.48	-0.00928	-0.00880	-0.00898	-0.00898	-0.00901
6.50	0.0	0.0	0.0	0.0	-1.05	-1.05	-1.07	-1.02	-0.01949	-0.01924	-0.01955	-0.01890	-0.01937
7.50	0.0	0.0	0.0	0.0	-1.25	-1.20	-1.14	-1.02	-0.02320	-0.02199	-0.02127	-0.01890	-0.02134
12.17	0.0	0.0	0.0	0.0	-1.65	-1.70	-1.52	-1.50	-0.03062	-0.03115	-0.02835	-0.02977	-0.02998
21.50	1.0	1.0	0.9	0.8	-2.42	-2.40	-2.03	-2.11	-0.04431	-0.04398	-0.03780	-0.03922	-0.04148
25.00	1.8	1.8	1.9	1.8	-2.65	-2.75	-2.41	-2.54	-0.04918	-0.05039	-0.04489	-0.04726	-0.04793
28.00	2.3	2.3	2.5	2.2	-2.93	-3.10	-2.59	-2.62	-0.05428	-0.05581	-0.04820	-0.04867	-0.05202
30.00	2.9	2.8	3.0	2.8	-3.00	-3.15	-2.87	-3.05	-0.05568	-0.05772	-0.05340	-0.05571	-0.05588
31.50	3.0	3.0	3.2	3.0	-3.20	-3.30	-3.05	-3.18	-0.05939	-0.06047	-0.05571	-0.05907	-0.05891
*34.50	3.5	3.5	3.9	3.5	-3.45	-3.55	-3.18	-3.43	-0.06403	-0.06505	-0.05907	-0.06380	-0.06299
35.50	4.0	4.0	4.8	4.2	-3.55	-3.70	-3.45	-3.56	-0.06589	-0.06780	-0.06427	-0.06515	-0.06503
38.50	4.2	4.5	5.0	4.5	-3.60	-3.70	-3.45	-3.68	-0.06682	-0.06780	-0.06427	-0.06552	-0.06585
40.50	4.5	4.8	5.5	4.8	-3.75	-3.90	-3.55	-3.81	-0.06960	-0.07147	-0.06516	-0.07088	-0.06953
42.50	5.0	5.0	5.8	5.0	-3.88	-4.00	-3.58	-3.81	-0.07201	-0.07320	-0.06852	-0.07088	-0.07118
45.00	5.5	5.5	6.0	5.2	-3.97	-4.05	-3.68	-3.94	-0.07368	-0.07482	-0.06852	-0.07325	-0.07242
47.00	6.2	6.0	6.5	5.5	-4.10	-4.35	-4.06	-4.06	-0.07510	-0.07971	-0.07551	-0.07551	-0.07676
49.00	6.5	6.5	7.5	6.1	-4.30	-4.35	-4.24	-4.32	-0.07581	-0.07971	-0.07892	-0.08033	-0.07959
51.33	6.0	7.2	8.1	5.5	-4.30	-4.55	-4.32	-4.32	-0.07581	-0.08338	-0.08033	-0.08033	-0.08095
53.00	6.5	7.8	8.8	5.5	-4.30	-4.55	-4.45	-4.32	-0.07581	-0.08338	-0.08270	-0.08033	-0.08155
54.50	7.4	8.3	9.0	6.0	-4.45	-4.63	-4.45	-4.32	-0.08259	-0.08485	-0.08270	-0.08033	-0.08262
60.50	9.5	9.5	11.0	7.8	-4.55	-4.75	-4.57	-4.32	-0.08445	-0.08704	-0.08505	-0.08033	-0.08422
71.50	15.0	12.5	15.0	12.5	-4.65	-5.45	-5.08	-4.45	-0.09001	-0.09587	-0.09451	-0.08270	-0.09177
73.50	15.5	12.0	15.8	14.1	-4.95	-5.55	-5.08	-4.57	-0.09187	-0.10170	-0.09451	-0.08505	-0.09329
78.50	19.8	14.0	20.0	17.2	-5.10	-5.60	-5.33	-4.57	-0.09465	-0.10262	-0.09524	-0.08505	-0.09539
80.50	21.0	15.0	21.5	18.0	-5.30	-5.60	-5.33	-4.70	-0.09651	-0.10262	-0.09524	-0.08742	-0.09545
84.50	23.0	17.0	22.0	20.2	-5.45	-5.60	-5.45	-4.75	-0.10115	-0.10262	-0.10160	-0.08837	-0.09943
94.25	27.5	24.2	32.2	25.2	-5.45	-5.60	-5.45	-4.83	-0.10115	-0.10262	-0.10160	-0.08979	-0.09879
102.75	40.0	32.5	46.0	35.5	-5.70	-5.75	-5.59	-4.95	-0.10579	-0.10537	-0.10395	-0.09215	-0.10182
108.50	47.5	37.5	54.2	44.0	-5.80	-5.80	-5.72	-5.03	-0.10765	-0.10629	-0.10633	-0.09357	-0.10246

NOTES: * Soils sample started to crack at the locations where suction sensors were installed.
All suction sensors were installed vertically from the bottom, with about 35mm soil embedment

UNIVERSITY OF SASKATCHEWAN, DEP. OF CIVIL ENGINEERING.

CRACKING TEST RESULT

Test no. : T02 Date started : 12/03/86 Page no. : 2 of 2
Soil type : Indian Head Till Conducted by : J. Lau

Time hr.	Suction				Shrinkage				Strain				Average Strain
	#1 kPa	#2 kPa	#3 kPa	#4 kPa	#1 mm	#2 mm	#3 mm	#4 mm	#1	#2	#3	#4	
119.50	71.0	49.5	69.0	60.2	-5.95	-6.10	-5.46	-4.95	-0.11043	-0.11178	-0.10160	-0.09215	-0.10399
124.00	77.5	53.0	73.0	59.0	-6.00	-6.14	-5.46	-5.33	-0.11136	-0.11252	-0.10160	-0.09924	-0.10618
126.50	81.0	55.0	75.5	72.2	-6.10	-6.15	-5.46	-5.59	-0.11321	-0.11270	-0.10160	-0.10396	-0.10787
133.50	86.0	59.5	80.0	75.0	-6.10	-6.20	-5.46	-5.46	-0.11321	-0.11362	-0.10160	-0.10160	-0.10751
144.00	89.0	63.0	83.5	75.0	-6.20	-	-	-5.66	-0.11507	-	-	-0.10538	-0.11023
147.75	+90.0	62.5	84.5	-	-6.30	-	-	-5.66	-0.11507	-	-	-0.10538	-0.11023
149.75	-	62.0	85.0	-	-6.22	-	-	-5.72	-0.11544	-	-	-0.10633	-0.11088
168.25	-	+62.0	+86.0	-	-6.40	-	-	-5.82	-0.11878	-	-	-0.10822	-0.11350
173.50	-	-	-	-	-6.50	-	-	-5.89	-0.12064	-	-	-0.10953	-0.11514
191.50	-	-	-	-	-6.90	-	-	-6.35	-0.12806	-	-	-0.11814	-0.12310
198.25	-	-	-	-	-7.18	-	-	-6.45	-0.13326	-	-	-0.12002	-0.12654
216.00	-	-	-	-	-7.42	-	-	-6.60	-0.13771	-	-	-0.12287	-0.13029

** End of Test T02 **

UNIVERSITY OF SASKATCHEWAN, DEP. OF CIVIL ENGINEERING.

MOISTURE CONTENT TEST RESULTS

Test no. : T02 Date started : 12/03/86 Page no. : 1 of 2
 Soil type : Indian Head Till Conducted by : J. Lau
 Total sample thickness : 55.0 mm approx.

	TIME	SAMPLE DEPTH	JAR #	TARE	GROSS WET WT.	GROSS DRY WT.	NET DRY WT.	MOISTURE CONTENT	REMARKS
	hr.	mm		gram	gram	gram	gram	%	
12/03/86	0.00	BULK	V31	100.04	170.82	151.25	51.21	38.22	Initial w%
9.30 a.m.		BULK	W20	103.16	192.44	167.83	64.67	38.05	
12/04/86	34.50	0.0-11.0	L1	103.10	125.01	119.64	16.54	32.47	Soil Cracked
8.00 p.m.		11.0-22.0	L3	99.46	118.52	113.82	14.36	32.73	
		22.0-33.0	T12	101.95	126.93	120.71	18.76	33.16	
		33.0-44.0	F5	135.70	155.22	150.30	14.60	33.70	
		44.0-55.0	V33	101.79	122.29	117.10	15.31	33.90	
12/05/86	42.50	0.0-11.0	D	102.07	128.32	122.06	19.99	31.32	
4:00 a.m.		11.0-22.0	W4	99.44	117.96	113.50	14.06	31.72	
		22.0-33.0	11	103.13	125.61	120.16	17.03	32.00	
		33.0-44.0	T12	101.96	116.11	112.67	10.71	32.12	
		44.0-55.0	13	102.34	120.52	116.08	13.74	32.31	
12/06/86	71.50	0.0-11.0	L1-2	101.95	124.52	119.67	17.72	27.37	
9:00 a.m.		11.0-22.0	L1-5	103.19	118.25	114.94	11.75	28.17	
		22.0-33.0	F-5	135.71	155.80	151.34	15.63	28.53	
		33.0-44.0	L1-6	101.74	119.31	115.38	13.64	28.81	
		44.0-55.0	137	137.75	155.70	151.69	13.94	28.77	
12/07/86	94.25	0.0-11.0	L1	103.01	127.56	122.53	19.52	25.77	
7:45 a.m.		11.0-22.0	C2	102.61	121.45	117.51	14.90	26.44	
		22.0-33.0	L3	103.42	126.85	121.81	18.39	27.41	
		33.0-44.0	J7	102.24	118.96	115.35	13.11	27.54	
		44.0-55.0	12	102.21	125.88	120.82	18.61	27.19	
12/08/86	119.50	0.0-11.0	D	102.06	129.99	124.91	22.85	22.23	
9:00 a.m.		11.0-22.0	L3	99.42	129.13	123.64	24.22	22.67	
		22.0-33.0	T12	101.95	134.10	127.95	26.00	23.65	
		33.0-44.0	13	102.33	120.86	117.27	14.94	24.03	
		44.0-55.0	V31	100.04	123.02	118.58	18.54	23.95	

UNIVERSITY OF SASKATCHEWAN, DEP. OF CIVIL ENGINEERING.

MOISTURE CONTENT TEST RESULTS

Test no. : T02 Date started : 12/03/86 Page no. : 2 of 2
 Soil type : Indian Head Till Conducted by : J. Lau
 Total sample thickness : 55.0 mm approx.

TIME	SAMPLE	JAR #	TARE	GROSS	GROSS	NET	MOISTURE	REMARKS
hr.	DEPTH			WET WT.	DRY WT.	DRY WT.	CONTENT	
	mm		gram	gram	gram	gram	%	
12/09/86	129.50	0.0-11.0	J1	103.38	133.90	129.19	25.81	18.25
3:00 p.m.		11.0-22.0	1	102.14	134.17	129.11	26.97	18.76
		22.0-33.0	L1	102.91	133.25	128.28	25.37	19.59
		33.0-44.0	11	103.13	121.07	118.11	14.98	19.76
		44.0-55.0	X20	103.13	127.86	123.83	20.70	19.47
12/12/86	217.50	0.0-11.0	L1	102.69	136.29	134.03	31.34	7.21 At Crack
11:00 a.m.		11.0-22.0	L3	103.14	130.50	127.96	24.82	10.23 face
		22.0-33.0	W1	135.55	153.78	151.87	16.32	11.70
		33.0-44.0	J6	102.31	123.60	121.26	18.95	12.35
		44.0-55.0	X10	99.81	122.01	119.45	19.64	13.03
12/12/86	217.50	0.0-11.0	C2	102.61	146.93	142.33	39.72	11.58 At Centre
11:00 a.m.		11.0-22.0	L2	101.95	170.08	162.07	60.12	13.32 of soil ped
		22.0-33.0	F5	135.72	196.39	188.93	53.21	14.02
		33.0-44.0	L6	101.75	149.70	143.72	41.97	14.25
		44.0-55.0	12	102.20	158.54	151.55	49.35	14.16

** End of Test T02 **

UNIVERSITY OF SASKATCHEWAN, DEP. OF CIVIL ENGINEERING.

CRACKING TEST RESULT

Test no. : T03 Date started : 12/15/86 Page no. : 1 of 1
Soil type : Indian Head Till Conducted by : J. Lau

Initial Soil Thickness (mm)
at ref. #1 : 61.33
at ref. #2 : 59.35
at ref. #3 : 61.96
at ref. #4 : 58.95

Time hr.	Suction				Shrinkage				Strain				Average Strain
	#1 kPa	#2 kPa	#3 kPa	#4 kPa	#1 mm	#2 mm	#3 mm	#4 mm	#1	#2	#3	#4	
0.00	0.6	0.8	1.5	0.9	0.00	0.00	0.00	-	0.00000	0.00000	0.00000	-	0.00000
2.00	1.0	1.0	1.9	1.2	-0.25	-0.27	-0.25	-	-0.00408	-0.00455	-0.00403	-	-0.00422
3.00	1.4	1.4	2.0	1.5	-0.50	-0.45	-0.40	-	-0.00815	-0.00758	-0.00545	-	-0.00740
*4.00	1.5	1.6	2.2	2.0	-0.50	-0.50	-0.50	-	-0.00978	-0.01011	-0.00958	-	-0.00955
5.00	1.6	1.8	2.4	2.4	-0.90	-0.90	-0.85	-	-0.01467	-0.01515	-0.01372	-	-0.01452
6.00	1.9	1.9	2.8	2.5	-1.00	-1.00	-1.00	-	-0.01631	-0.01685	-0.01614	-	-0.01643
7.00	2.0	2.2	3.0	3.0	-1.10	-1.10	-1.00	-	-0.01794	-0.01853	-0.01614	-	-0.01754
9.25	2.2	2.9	3.2	3.6	-1.35	-1.30	-1.30	-	-0.02201	-0.02190	-0.02098	-	-0.02163
11.00	2.4	3.1	3.5	4.4	-1.70	-1.55	-1.35	-	-0.02772	-0.02512	-0.02173	-	-0.02521
13.00	3.0	3.5	3.8	4.2	-1.90	-1.75	-1.55	-	-0.03098	-0.02949	-0.02502	-	-0.02849
16.00	3.6	3.5	3.8	4.2	-2.20	-2.00	-1.70	-	-0.03537	-0.03370	-0.02744	-	-0.03234
19.00	5.0	5.2	5.8	5.8	-2.30	-2.20	-1.90	-	-0.03750	-0.03707	-0.03056	-	-0.03508
21.50	6.2	6.5	6.5	7.0	-2.45	-2.30	-2.00	-	-0.03995	-0.03875	-0.03228	-	-0.03599
25.00	8.0	7.8	9.0	8.5	-2.70	-2.50	-2.20	-	-0.04402	-0.04381	-0.03551	-	-0.04111
28.00	10.4	9.5	11.0	11.0	-2.80	-2.80	-2.45	-	-0.04555	-0.04718	-0.03954	-	-0.04412
30.00	11.6	10.5	11.5	11.2	-2.95	-2.85	-2.59	-	-0.04810	-0.04802	-0.04180	-	-0.04597
32.75	13.5	12.5	15.0	14.5	-3.10	-3.00	-2.70	-	-0.05055	-0.05055	-0.04358	-	-0.04822
40.50	19.2	16.0	21.0	18.5	-3.50	-3.50	-3.15	-	-0.05707	-0.05697	-0.05084	-	-0.05563
48.00	29.0	22.8	29.0	25.2	-3.75	-3.80	-3.45	-	-0.05114	-0.05403	-0.05558	-	-0.05028
54.00	37.5	26.0	37.0	31.5	-4.03	-4.15	-3.75	-	-0.05571	-0.05592	-0.05052	-	-0.05539
59.00	44.4	33.0	44.0	37.0	-4.15	-4.32	-3.90	-	-0.05767	-0.07279	-0.06294	-	-0.05780
71.00	64.2	47.0	60.5	52.0	-4.45	-4.60	-4.25	-	-0.07255	-0.08068	-0.06859	-	-0.07401
75.00	63.5	51.3	64.5	57.0	-4.54	-4.95	-4.40	-	-0.07403	-0.08340	-0.07101	-	-0.07515
79.00	70.0	58.2	70.0	64.0	-4.65	-5.15	-4.50	-	-0.07582	-0.08677	-0.07263	-	-0.07641
94.75	+30.0	75.0	+30.0	77.5	-4.95	-5.55	-4.80	-	-0.08071	-0.09351	-0.07747	-	-0.08390
101.00	-	78.2	-	+30.0	-5.05	-5.59	-4.91	-	-0.08234	-0.09587	-0.07924	-	-0.08582
128.50	-	+30.0	-	-	-5.50	-5.00	-5.45	-	-0.09131	-0.10110	-0.08812	-	-0.09351
144.00	-	-	-	-	-5.95	-6.35	-5.78	-	-0.09702	-0.10599	-0.09329	-	-0.09910
150.00	-	-	-	-	-6.00	-6.45	-5.95	-	-0.09783	-0.10358	-0.09619	-	-0.10090
167.25	-	-	-	-	-6.14	-6.62	-6.04	-	-0.10011	-0.11154	-0.09748	-	-0.10305
192.00	-	-	-	-	-6.30	-6.85	-6.16	-	-0.10272	-0.11542	-0.09942	-	-0.10585
216.50	-	-	-	-	-6.58	-6.90	-5.95	-	-0.10532	-0.11525	-0.09619	-	-0.10712

*Notes : Soil sample cracked at location between sensor # 1 and sensor # 2.

** End of Test T03 **

UNIVERSITY OF SASKATCHEWAN, DEP. OF CIVIL ENGINEERING.

MOISTURE CONTENT TEST RESULTS

Test no. : T03

Date started : 12/16/86

Page no. : 1 of 1

Soil type : Indian Head Till

Conducted by : J. Lau

Total sample thickness : 55.0 mm approx.

TIME	SAMPLE DEPTH	JAR #	TARE	GROSS WET WT.	GROSS DRY WT.	NET DRY WT.	MOISTURE CONTENT	REMARKS	
	mm		gram	gram	gram	gram	%		
12/16/86	0.00	BULK	L1	102.69	172.59	155.89	53.20	31.39	Initial w%
10:00 a.m.		BULK	L3	103.14	193.92	172.51	69.37	30.86	
12/16/86	5.00	0.0-11.0	L1	99.71	120.74	116.07	16.36	28.55	1 hr. after soil cracked
3:00 p.m.		11.0-22.0	J6	102.31	123.06	118.39	16.08	29.04	
		22.0-33.0	X10	99.17	115.71	111.89	12.72	30.03	
		33.0-44.0	137	137.74	155.89	151.68	13.94	30.20	
		44.0-55.0	GEB	102.45	130.10	123.63	21.18	30.55	
12/17/86	25.00	0.0-11.0	J1	103.37	133.40	126.94	23.57	27.41	
11:00 a.m.		11.0-22.0	W4	99.43	132.07	124.84	25.41	28.45	
		22.0-33.0	L1	101.74	134.37	126.99	25.25	29.23	
		33.0-44.0	V33	101.79	129.83	123.40	21.61	29.75	
		44.0-55.0	W20	103.13	138.04	130.10	26.97	29.44	
12/18/86	59.00	0.0-11.0	L1	102.92	143.04	135.35	32.43	23.71	
9:00 p.m.		11.0-22.0	K1	102.19	130.11	124.61	22.42	24.53	
		22.0-33.0	11	103.14	137.57	130.77	27.63	24.61	
		33.0-44.0	T11	102.35	128.80	123.57	21.22	24.65	
		44.0-55.0	13	102.34	134.75	128.22	25.88	25.23	
12/20/86	65.25	0.0-11.0	D	102.07	131.72	126.95	24.88	19.17	
3:15 p.m.		11.0-22.0	L1	101.76	126.56	122.56	20.80	19.23	
		22.0-33.0	L2	101.95	133.88	128.55	26.60	20.04	
		33.0-44.0	V31	100.06	128.36	123.49	23.43	20.79	
		44.0-55.0	J101	103.20	134.12	128.73	25.53	21.11	
12/24/86	193.00	0.0-11.0	L1	103.00	139.89	135.75	32.75	12.64	
11:00 a.m.		11.0-22.0	L3	103.14	139.38	135.05	31.91	13.57	
		22.0-33.0	F5	135.72	180.21	174.70	38.98	14.14	
		33.0-44.0	J6	102.31	147.33	141.66	39.35	14.41	
		44.0-55.0	V30	99.71	136.83	132.13	32.42	14.50	
12/30/86	337.00	0.0-11.0	J1	103.38	141.15	139.93	36.55	3.34	End of test
11:00 a.m.		11.0-22.0	L3	99.44	138.21	136.48	37.04	4.67	
		22.0-33.0	13	102.33	148.08	145.52	43.19	5.93	
		33.0-44.0	V31	100.06	118.14	117.30	17.24	4.87	
		44.0-55.0	D	102.07	154.15	151.15	49.08	6.11	

UNIVERSITY OF SASKATCHEWAN, DEP. OF CIVIL ENGINEERING.

CRACKING TEST RESULT

Test no. : T04 Date started : 01/06/87 Page no. : 1 of 2
Soil type : Indian Head Till Conducted by : J. Lau

Initial Soil Thickness (mm)

at ref. #1 : 32.50

at ref. #2 : 33.15

at ref. #3 : 33.30

at ref. #4 : 35.75

Time hr.	Suction				Vertical Shrinkage				Vertical Strain				Average Strain
	#1 kPa	#2 kPa	#3 kPa	#4 kPa	#1 mm	#2 mm	#3 mm	#4 mm	#1	#2	#3	#4	
0.00	0.0	0.0	0.0	0.0	0.00	0.00	0.00	0.00	0.00000	0.00000	0.00000	0.00000	0.00000
1.00	0.0	0.0	0.0	0.0	-0.20	-0.15	-0.15	-0.20	-0.00515	-0.00452	-0.00450	-0.00501	-0.00530
2.00	0.0	0.0	0.0	0.2	-0.50	-0.30	-0.20	-0.30	-0.01538	-0.00905	-0.00601	-0.00901	-0.00926
4.00	0.3	0.3	0.3	0.8	-0.70	-0.50	-0.55	-0.50	-0.02154	-0.01508	-0.01652	-0.01502	-0.01704
5.00	0.8	0.5	0.8	1.0	-0.80	-0.50	-0.60	-0.50	-0.02462	-0.01810	-0.01802	-0.01502	-0.01834
6.00	1.0	0.5	1.0	1.0	-1.00	-0.75	-0.70	-0.85	-0.03077	-0.02252	-0.02102	-0.02553	-0.02499
7.00	1.2	1.0	1.2	1.2	-1.00	-0.75	-0.70	-0.85	-0.03077	-0.02252	-0.02102	-0.02553	-0.02499
8.00	1.3	1.1	1.3	1.5	-1.25	-1.00	-0.90	-1.00	-0.03846	-0.03017	-0.02703	-0.03003	-0.03142
9.50	1.8	1.4	1.5	1.8	-1.40	-1.20	-1.05	-1.05	-0.04308	-0.03620	-0.03153	-0.03153	-0.03558
10.50	2.1	1.8	1.9	2.1	-1.55	-1.40	-1.15	-1.40	-0.04759	-0.04223	-0.03453	-0.04204	-0.04163
11.50	2.5	1.9	2.0	2.2	-1.55	-1.40	-1.15	-1.50	-0.04769	-0.04223	-0.03453	-0.04505	-0.04238
12.50	2.6	2.1	2.1	2.5	-1.75	-1.45	-1.20	-1.60	-0.05385	-0.04374	-0.02604	-0.04805	-0.04542
13.50	3.0	2.3	2.3	2.9	-1.85	-1.50	-1.35	-1.65	-0.05592	-0.04525	-0.04054	-0.04955	-0.04807
14.50	3.2	2.5	2.6	3.0	-2.00	-1.65	-1.45	-1.75	-0.06154	-0.04977	-0.04354	-0.05255	-0.05185
17.50	3.9	3.3	3.2	3.5	-2.25	-1.75	-1.65	-2.00	-0.06923	-0.05279	-0.04955	-0.06005	-0.05791
*22.50	5.0	4.5	4.2	4.1	-2.65	-2.10	-2.00	-2.30	-0.08154	-0.06335	-0.06006	-0.06907	-0.06850
23.50	5.9	5.4	5.0	4.8	-2.65	-2.20	-2.15	-2.35	-0.08154	-0.06637	-0.06455	-0.07057	-0.07075
24.50	6.5	5.5	5.3	5.1	-2.85	-2.30	-2.20	-2.45	-0.08769	-0.06938	-0.06507	-0.07357	-0.07418
25.50	7.0	5.6	5.8	5.4	-2.90	-2.35	-2.35	-2.60	-0.08923	-0.07089	-0.07057	-0.07808	-0.07719
27.50	6.8	5.8	6.0	6.0	-3.10	-2.60	-2.50	-2.65	-0.09538	-0.07843	-0.07508	-0.07958	-0.08212
28.50	6.2	5.2	5.0	5.2	-3.10	-2.65	-2.60	-2.80	-0.09538	-0.07594	-0.07308	-0.08408	-0.08437
30.00	6.8	7.1	5.0	7.0	-3.30	-2.80	-2.80	-2.95	-0.10154	-0.08446	-0.08408	-0.08859	-0.08957
31.50	7.8	7.8	6.8	7.9	-3.40	-2.90	-2.90	-3.05	-0.10462	-0.08748	-0.08709	-0.09159	-0.09269
33.50	8.5	8.5	7.2	8.8	-3.50	-2.90	-2.90	-3.05	-0.10769	-0.08748	-0.08709	-0.09159	-0.09346
35.75	10.0	9.9	8.8	10.2	-3.65	-3.20	-3.05	-3.25	-0.11231	-0.09652	-0.09159	-0.09760	-0.09551
41.50	11.8	11.2	10.0	12.1	-3.90	-3.25	-3.20	-3.50	-0.12000	-0.09804	-0.09510	-0.10511	-0.10481
47.00	12.5	14.8	11.0	12.8	-3.90	-3.45	-3.40	-3.50	-0.12000	-0.10407	-0.10210	-0.10811	-0.10857
48.50	14.5	15.8	12.0	14.5	-3.90	-3.70	-3.50	-3.70	-0.12000	-0.11161	-0.10811	-0.11111	-0.11271
50.00	15.8	15.8	12.8	15.2	-3.95	-3.80	-3.85	-3.65	-0.12154	-0.11463	-0.11562	-0.11562	-0.11685
52.25	18.2	18.0	13.8	17.2	-3.95	-3.90	-3.90	-3.95	-0.12154	-0.11765	-0.11712	-0.11852	-0.11873

NOTES: * Soils sample started to crack at the locations where suction sensors were installed.
All suction sensors were installed horizontally from the container side wall,
with about 35 mm soil embedment.

UNIVERSITY OF SASKATCHEWAN, DEP. OF CIVIL ENGINEERING.

CRACKING TEST RESULT

Test no. : T04 Date started : 01/06/87 Page no. : 2 of 2
 Soil type : Indian Head Till Conducted by : J. Lau

Time hr.	Suction				Vertical Shrinkage				Vertical Strain				Average Strain
	#1 kPa	#2 kPa	#3 kPa	#4 kPa	#1 mm	#2 mm	#3 mm	#4 mm	#1	#2	#3	#4	
54.00	20.8	19.8	15.6	19.0	-3.95	-4.00	-3.90	-4.10	-0.12154	-0.12066	-0.11712	-0.12312	-0.12061
56.50	23.8	21.5	17.2	21.8	-4.00	-4.10	-4.10	-4.30	-0.12308	-0.12368	-0.12312	-0.12913	-0.12475
61.75	31.2	25.8	23.0	23.5	-4.00	-4.15	-4.35	-4.55	-0.12308	-0.12519	-0.13063	-0.13664	-0.12888
70.50	41.9	36.9	31.0	31.0	-4.10	-4.25	-4.45	-4.70	-0.12615	-0.12821	-0.13363	-0.14114	-0.13228
74.50	49.8	44.8	38.5	38.5	-4.10	-4.30	-4.50	-4.80	-0.12615	-0.12971	-0.13514	-0.14414	-0.13379
85.00	70.0	68.8	62.0	64.5	-4.10	-4.40	-4.50	-4.85	-0.12615	-0.13273	-0.13514	-0.14565	-0.13492
93.25	77.0	72.2	72.5	77.8	-4.10	-4.40	-4.60	-4.90	-0.12615	-0.13273	-0.13814	-0.14715	-0.13604
105.25	+80.0	+80.0	+80.0	+80.0	-4.30	-4.40	-4.50	-4.95	-0.13231	-0.13273	-0.13514	-0.14865	-0.13721
126.75	-	-	-	-	-4.50	-4.50	-4.55	-5.00	-0.13846	-0.13575	-0.13664	-0.15015	-0.14025
145.00	-	-	-	-	-4.60	-4.50	-4.60	-5.10	-0.14154	-0.13575	-0.13814	-0.15315	-0.14214
163.25	-	-	-	-	-4.82	-4.55	-4.70	-5.25	-0.14831	-0.13725	-0.14114	-0.15766	-0.14609
192.00	-	-	-	-	-4.90	-4.55	-4.70	-5.35	-0.15077	-0.13725	-0.14114	-0.16066	-0.14746

** End of Test T04 **

UNIVERSITY OF SASKATCHEWAN, DEP. OF CIVIL ENGINEERING.

MOISTURE CONTENT TEST RESULTS

Test no. : T04

Date started : 01/06/87

Page no. : 1 of 1

Soil type : Indian Head Till

Conducted by : J. Lau

Total sample thickness : 33.0 mm approx.

TIME	SAMPLE DEPTH mm	JAR #	TARE gram	GROSS WET WT. gram	GROSS DRY WT. gram	NET DRY WT. gram	MOISTURE CONTENT %	REMARKS
01/06/87 09:30 a.m.	0.00 BULK	V31	100.07	137.29	127.02	26.95	38.11	Initial w%
01/07/87 8:30 a.m.	25.00 0.0-11.0	L1	103.01	126.37	120.62	17.61	32.65	Soil cracked
	11.0-22.0	F5	135.72	149.65	146.16	10.44	33.43	
	22.0-33.0	J6	102.31	116.85	113.22	10.91	33.27	
01/08/87 8:30 a.m.	47.00 0.0-11.0	J1	103.38	114.37	111.93	8.55	28.54	
	11.0-22.0	K1	102.19	114.18	111.49	9.30	28.92	
	22.0-33.0	L3	99.44	107.79	105.89	6.45	29.46	
01/08/87 6:00 p.m.	56.50 0.0-11.0	C2	102.61	117.71	114.54	11.93	26.57	
	11.0-22.0	11	103.13	120.87	117.04	13.91	27.53	
	22.0-33.0	13	102.33	114.31	111.72	9.39	27.58	
01/10/87 6:45 a.m.	69.25 0.0-11.0	1	102.14	121.05	117.59	15.45	22.39	
	11.0-22.0	L1	99.72	118.06	114.71	14.99	22.35	
	22.0-33.0	12	102.21	126.42	122.02	19.81	22.21	
01/14/87 10:00 a.m.	240.50 0.0-11.0	L1-3	103.15	160.37	157.27	54.12	5.73	End of test
	11.0-22.0	L1-6	101.75	135.64	132.98	31.23	8.52	
	22.0-33.0	GEB	102.46	127.87	125.94	23.48	8.22	

UNIVERSITY OF SASKATCHEWAN, DEP. OF CIVIL ENGINEERING.

CRACKING TEST RESULT

Test no. : T05 Date started : 01/20/87 Page no. : 1 of 2
Soil type : Regina Clay Conducted by : J. Lau

Initial Soil Thickness (mm)

at ref. #1 : 59.80
at ref. #2 : 57.35
at ref. #3 : 51.00
at ref. #4 : 50.60

Time hr.	Suction				Shrinkage				Strain				Average Strain
	#1 kPa	#2 kPa	#3 kPa	#4 kPa	#1 mm	#2 mm	#3 mm	#4 mm	#1	#2	#3	#4	
0.00	0.0	0.0	0.0	0.0	0.00	0.00	0.00	0.00	0.00000	0.00000	0.00000	0.00000	0.00000
1.00	0.1	0.5	1.0	0.4	-0.05	-0.05	-0.05	0.00	-0.00084	-0.00087	-0.00082	0.00000	-0.00063
2.00	0.2	0.5	1.2	0.8	-0.10	-0.10	-0.10	-0.10	-0.00167	-0.00174	-0.00164	-0.00164	-0.00167
3.00	0.4	0.8	1.3	0.8	-0.10	-0.20	-0.20	-0.20	-0.00167	-0.00349	-0.00328	-0.00328	-0.00293
4.00	0.5	0.8	1.5	0.8	-0.10	-0.30	-0.25	-0.20	-0.00167	-0.00523	-0.00410	-0.00328	-0.00357
5.00	0.6	0.9	1.5	0.9	-0.15	-0.30	-0.25	-0.20	-0.00251	-0.00523	-0.00410	-0.00328	-0.00378
7.00	0.8	1.0	1.6	1.0	-0.40	-0.40	-0.35	-0.35	-0.00669	-0.00697	-0.00674	-0.00674	-0.00628
9.00	1.0	1.0	1.8	1.0	-0.40	-0.40	-0.50	-0.35	-0.00669	-0.00697	-0.00820	-0.00674	-0.00690
13.00	1.0	1.2	1.9	1.2	-0.50	-0.55	-0.65	-0.50	-0.00836	-0.00959	-0.01066	-0.00820	-0.00920
15.25	1.0	1.2	1.9	1.2	-0.60	-0.70	-0.70	-0.50	-0.01003	-0.01221	-0.01148	-0.00820	-0.01048
19.50	1.0	1.4	1.9	1.4	-0.75	-0.85	-0.80	-0.65	-0.01254	-0.01482	-0.01311	-0.01066	-0.01273
21.50	1.4	1.6	1.9	1.8	-0.90	-0.95	-0.95	-0.65	-0.01505	-0.01655	-0.01557	-0.01393	-0.01528
23.50	1.4	1.8	2.0	1.9	-1.05	-1.05	-1.05	-1.00	-0.01755	-0.01831	-0.01721	-0.01639	-0.01737
25.50	1.9	2.0	2.2	2.0	-1.15	-1.15	-1.20	-1.05	-0.01923	-0.02005	-0.01967	-0.01721	-0.01904
27.50	2.0	2.1	2.3	2.1	-1.35	-1.35	-1.40	-1.20	-0.02090	-0.02354	-0.02295	-0.01967	-0.02177
29.50	2.1	2.2	2.3	2.2	-1.40	-1.45	-1.50	-1.30	-0.02341	-0.02528	-0.02459	-0.02131	-0.02355
31.75	2.5	2.5	3.0	2.5	-1.60	-1.70	-1.70	-1.60	-0.02576	-0.02954	-0.02787	-0.02623	-0.02752
34.25	3.0	3.0	3.2	3.0	-1.75	-1.85	-1.75	-1.65	-0.02925	-0.03226	-0.02869	-0.02705	-0.02931
36.75	3.2	3.2	3.3	3.5	-1.80	-1.95	-1.85	-1.70	-0.03010	-0.03400	-0.03033	-0.02787	-0.03057
41.00	3.8	3.8	3.9	3.8	-2.00	-2.15	-1.95	-1.80	-0.03344	-0.03749	-0.03197	-0.02951	-0.03310
44.50	4.0	4.0	4.3	4.2	-2.15	-2.25	-2.15	-2.10	-0.03595	-0.03923	-0.03525	-0.03443	-0.03521
46.50	4.2	4.8	5.0	4.5	-2.20	-2.45	-2.35	-2.25	-0.03679	-0.04272	-0.03852	-0.03689	-0.03873
49.30	5.0	5.2	5.2	5.0	-2.45	-2.65	-2.55	-2.40	-0.04057	-0.04621	-0.04180	-0.03934	-0.04208
52.50	5.8	5.8	6.0	5.8	-2.70	-2.80	-2.65	-2.65	-0.04515	-0.04882	-0.04344	-0.04344	-0.04521
*55.50	6.4	6.4	6.0	5.8	-2.80	-2.90	-2.70	-2.30	-0.04682	-0.05057	-0.04425	-0.04590	-0.04689
#52.75	7.2	7.2	6.2	5.8	-3.00	-3.05	-2.75	-2.20	-0.05017	-0.05318	-0.04508	-0.05246	-0.05022
^55.50	6.2	8.0	7.0	6.0	-3.15	-3.10	-2.80	-3.20	-0.05258	-0.05405	-0.04590	-0.05246	-0.05127
59.00	6.5	8.9	6.0	6.2	-3.15	-3.15	-2.65	-3.20	-0.05263	-0.05493	-0.04572	-0.05246	-0.05170
71.50	7.2	9.5	7.0	7.0	-3.20	-3.20	-2.85	-3.30	-0.05351	-0.05580	-0.04572	-0.05410	-0.05253

Note: * First crack occurred at sensor # 3.

Crack occurred at sensor # 4.

^ Crack occurred at sensor # 1.

UNIVERSITY OF SASKATCHEWAN, DEP. OF CIVIL ENGINEERING.

CRACKING TEST RESULT

Test no. : T05 Date started : 01/20/87 Page no. : 2 of 2
Soil type : Regina Clay Conducted by : J. Lau

Time hr.	Suction				Shrinkage				Strain				Average Strain
	#1 kPa	#2 kPa	#3 kPa	#4 kPa	#1 mm	#2 mm	#3 mm	#4 mm	#1	#2	#3	#4	
77.00	9.2	10.2	8.8	8.5	-3.25	-3.30	-2.90	-3.35	-0.05435	-0.05754	-0.04754	-0.05492	-0.05359
81.50	10.2	11.5	10.0	10.0	-3.40	-3.40	-3.00	-3.40	-0.05685	-0.05929	-0.04918	-0.05574	-0.05526
92.00	11.0	13.2	12.5	12.5	-3.45	-3.80	-3.00	-3.45	-0.05769	-0.06626	-0.04918	-0.05555	-0.05742
105.25	24.5	15.2	17.9	16.2	-3.65	-4.50	-3.20	-3.50	-0.06104	-0.07847	-0.05246	-0.05738	-0.06233
116.50	31.8	15.8	22.0	19.9	-3.75	-4.50	-3.20	-3.70	-0.06271	-0.07847	-0.05246	-0.06066	-0.06357
125.50	40.8	18.5	26.5	25.0	-3.85	-4.70	-3.50	-	-0.06438	-0.08155	-0.05738	-	-0.06790
143.00	58.8	29.0	38.0	34.8	-4.10	-5.05	-3.55	-	-0.06856	-0.08806	-0.05934	-	-0.07215
155.00	60.8	42.5	48.0	47.8	-4.50	-5.45	-4.05	-	-0.07525	-0.09503	-0.06539	-	-0.07889
189.25	62.2	53.2	60.2	60.2	-5.20	-5.95	-4.70	-	-0.08595	-0.10375	-0.07705	-	-0.08925
213.50	66.2	76.2	65.0	70.0	-6.05	-6.60	-5.40	-	-0.10117	-0.11508	-0.08852	-	-0.10159
237.00	68.0	78.2	+80.0	72.1	-6.49	-7.12	-5.65	-	-0.10853	-0.12415	-0.09262	-	-0.10843
259.50	71.0	79.8	-	+80.0	-7.14	-7.97	-5.70	-	-0.11940	-0.13897	-0.09344	-	-0.11727
286.75	+80.0	+80.0	-	-	-7.55	-8.10	-6.95	-	-0.12625	-0.14124	-0.11393	-	-0.12714
313.50	-	-	-	-	-8.05	-8.50	-7.50	-	-0.13462	-0.14821	-0.12295	-	-0.13526
334.50	-	-	-	-	-8.50	-	-	-	-0.14381	-	-	-	-0.14381
358.00	-	-	-	-	-8.50	-	-	-	-0.14381	-	-	-	-0.14381

** End of Test T05 **

Note: \$ Crack occurred at sensor # 2.

UNIVERSITY OF SASKATCHEWAN, DEP. OF CIVIL ENGINEERING.

MOISTURE CONTENT TEST RESULTS

Test no. : T05

Date started : 01/20/87

Page no. : 1 of 1

Soil type : Regina Clay

Conducted by : J. Lau

Total sample thickness : 60.0 mm approx.

	TIME	SAMPLE DEPTH	JAR #	TARE	GROSS WET WT.	GROSS DRY WT.	NET DRY WT.	MOISTURE CONTENT	REMARKS
	hr.	mm		gram	gram	gram	gram	%	
1/20/87	0.00	BULK	C2	103.37	154.74	131.53	28.16	82.42	Initial w%
11:30 a.m.		BULK	W20	102.61	164.72	136.60	33.99	82.73	
1/22/87	56.50	0.0-12.0	L1	101.76	119.53	112.15	10.39	71.03	Soil cracked
8:00 p.m.		12.0-24.0	K1	102.20	118.51	111.67	9.47	72.23	
		24.0-36.0	6	137.45	153.09	146.46	9.01	73.58	
		36.0-48.0	T12	101.96	114.89	109.35	7.39	74.97	
		48.0-60.0	I3	102.34	115.84	110.01	7.67	76.01	
1/24/87	92.50	0.0-12.0	D	102.08	118.75	112.08	10.00	66.70	
8:00 a.m.		12.0-24.0	L1	102.70	120.07	113.00	10.30	68.64	
		24.0-36.0	8	102.60	112.44	108.40	5.80	69.66	
		36.0-48.0	C11	102.29	108.99	106.25	3.96	69.19	
		48.0-60.0	C12	137.75	149.15	144.52	6.77	68.39	
1/25/87	116.50	0.0-12.0	J1	103.38	124.55	116.48	13.10	61.60	
8:00 a.m.		12.0-24.0	C2	102.62	122.67	114.96	12.34	62.48	
		24.0-36.0	L1	103.14	117.52	111.94	8.80	63.41	
		36.0-48.0	T11	102.36	115.10	110.11	7.75	64.39	
		48.0-60.0	12	102.20	116.62	111.00	8.80	63.86	
1/28/87	189.50	0.0-12.0	L1-2	101.95	125.62	117.51	15.56	52.12	
9:00 a.m.		12.0-24.0	F5	135.71	159.08	150.90	15.19	53.85	
		24.0-36.0	L1-6	101.74	120.80	114.04	12.30	54.96	
		36.0-48.0	J6	102.31	122.58	115.30	12.99	56.04	
		48.0-60.0	J101	103.19	127.16	118.54	15.35	56.16	
1/31/87	259.50	0.0-12.0	1	102.14	132.57	123.10	20.96	45.18	
7:00 a.m.		12.0-24.0	L1	103.00	124.16	117.39	14.39	47.05	
		24.0-36.0	V3	101.69	131.03	121.40	19.71	48.86	
		36.0-48.0	W4	99.44	120.29	113.39	13.95	49.46	
		48.0-60.0	X10	99.18	126.36	117.22	18.04	50.67	
2/05/87	383.00	0.0-12.0	D	102.07	155.07	144.99	42.92	23.49	End of Test
10:30 a.m.		12.0-24.0	L1	102.69	138.46	130.85	28.16	27.02	
		24.0-36.0	K1	102.19	129.50	123.38	21.19	28.88	
		36.0-48.0	C12	137.75	172.09	164.13	26.38	30.17	
		48.0-60.0	T12	101.95	134.79	127.06	25.11	30.78	

UNIVERSITY OF SASKATCHEWAN, DEP. OF CIVIL ENGINEERING.

CRACKING TEST RESULT

Test no. : T06 Date started : 02/14/87 Page no. : 1 of 2
Soil type : Indian Head Till Conducted by : J. Lau

Initial Soil Thickness (mm)

at ref. #1 : 60.45
at ref. #2 : 61.25
at ref. #3 : 60.20
at ref. #4 : 61.45

Time hr.	Suction				Vertical Shrinkage				Vertical Strain				Average Strain
	#1 kPa	#2 kPa	#3 kPa	#4 kPa	#1 mm	#2 mm	#3 mm	#4 mm	#1	#2	#3	#4	
0.00	0.0	0.0	0.0	0.0	0.00	0.00	0.00	0.00	0.00000	0.00000	0.00000	0.00000	0.00000
1.00	0.0	0.0	0.0	0.0	-0.10	-0.10	-0.10	-0.20	-0.00165	-0.00163	-0.00166	-0.00332	-0.00207
2.00	0.0	0.0	0.0	0.0	-0.30	-0.35	-0.30	-0.40	-0.00495	-0.00571	-0.00498	-0.00654	-0.00558
3.00	0.0	0.0	0.0	0.0	-0.50	-0.50	-0.50	-0.55	-0.00827	-0.00816	-0.00831	-0.00914	-0.00847
4.00	0.0	0.0	0.0	0.0	-0.60	-0.55	-0.60	-0.75	-0.00993	-0.00898	-0.00997	-0.01246	-0.01033
5.00	0.0	0.0	0.0	0.0	-0.65	-0.65	-0.65	-0.80	-0.01075	-0.01051	-0.01080	-0.01329	-0.01135
6.00	0.0	0.0	0.0	0.0	-0.70	-0.75	-0.80	-0.95	-0.01158	-0.01224	-0.01329	-0.01578	-0.01322
7.00	0.0	0.0	0.0	0.0	-0.75	-0.80	-0.85	-1.10	-0.01241	-0.01306	-0.01412	-0.01827	-0.01447
11.00	0.0	0.0	0.0	0.0	-1.05	-1.15	-1.05	-1.30	-0.01737	-0.01878	-0.01744	-0.02159	-0.01880
15.50	0.0	0.0	0.0	0.0	-1.30	-1.50	-1.35	-1.75	-0.02151	-0.02449	-0.02243	-0.02907	-0.02437
21.50	0.1	0.1	0.1	0.1	-1.50	-1.70	-1.50	-2.00	-0.02481	-0.02776	-0.02492	-0.03322	-0.02758
27.25	0.5	0.5	0.4	0.5	-1.95	-2.10	-2.00	-2.50	-0.03226	-0.03429	-0.03322	-0.04153	-0.03532
32.00	1.0	1.0	0.9	1.0	-2.20	-2.40	-2.30	-2.80	-0.03539	-0.03918	-0.03821	-0.04651	-0.04007
37.50	1.9	1.9	1.8	1.9	-2.60	-2.75	-2.65	-3.15	-0.04301	-0.04490	-0.04402	-0.05233	-0.04606
41.00	2.2	2.2	2.0	2.2	-2.70	-3.00	-2.75	-3.30	-0.04467	-0.04898	-0.04568	-0.05482	-0.04854
45.50	2.9	2.9	2.3	2.9	-3.10	-3.25	-3.05	-3.70	-0.05129	-0.05305	-0.05065	-0.06146	-0.05412
48.00	3.5	3.5	3.2	3.5	-3.35	-3.40	-3.20	-3.80	-0.05542	-0.05551	-0.05316	-0.06312	-0.05680
51.00	4.0	4.0	3.8	4.0	-3.60	-3.65	-3.50	-4.00	-0.05955	-0.05959	-0.05814	-0.06545	-0.05993
54.00	4.8	4.8	4.2	4.8	-3.80	-3.85	-3.70	-4.20	-0.06285	-0.06285	-0.06146	-0.06977	-0.06424
57.50	5.5	5.5	5.0	5.5	-4.00	-4.10	-3.90	-4.60	-0.06517	-0.06594	-0.06478	-0.07641	-0.06958
61.50	6.5	6.5	6.0	6.5	-4.30	-4.35	-4.15	-4.90	-0.07113	-0.07102	-0.06894	-0.08140	-0.07312
68.00	8.2	7.9	7.9	7.9	-4.50	-4.70	-4.50	-5.20	-0.07444	-0.07573	-0.07475	-0.08533	-0.07808
70.50	9.1	8.5	8.5	9.1	-4.86	-5.03	-4.80	-5.53	-0.08040	-0.08212	-0.07973	-0.09186	-0.08353
73.50	10.2	10.2	9.9	10.0	-5.09	-5.44	-4.98	-5.74	-0.08420	-0.08882	-0.08272	-0.09535	-0.08777
78.50	12.0	12.1	11.2	12.0	-5.27	-5.70	-5.23	-6.04	-0.08718	-0.09306	-0.08586	-0.10033	-0.09165
*81.50	9.0	13.3	12.1	13.1	-5.40	-5.70	-5.30	-6.10	-0.08933	-0.09306	-0.08804	-0.10133	-0.09294
88.50	12.0	13.2	14.5	15.5	-5.50	-5.60	-5.55	-6.30	-0.09098	-0.09469	-0.09219	-0.10465	-0.09563

Note: Container sidewalls were lined with waxpaper and aluminum foil.

All suction sensors were installed vertically from the bottom of the container.

! No sign of cracking, but the soil sample pulled away from
container side wall by 6 mm.

* Soil cracked at sensor # 1.

UNIVERSITY OF SASKATCHEWAN, DEP. OF CIVIL ENGINEERING.

CRACKING TEST RESULT

Test no. : T06 Date started : 02/14/87 Page no. : 2 of 2
 Soil type : Indian Head Till Conducted by : J. Lau

Time hr.	Section				Vertical Shrinkage				Vertical Strain				Average Strain
	#1 kPa	#2 kPa	#3 kPa	#4 kPa	#1 mm	#2 mm	#3 mm	#4 mm	#1	#2	#3	#4	
96.00	15.5	16.5	17.2	13.8	-5.80	-6.10	-5.85	-6.45	-0.09595	-0.09959	-0.09718	-0.10714	-0.09996
98.50	17.2	18.2	18.5	15.9	-5.65	-6.20	-5.95	-6.55	-0.09677	-0.10122	-0.09884	-0.10880	-0.10141
101.50	19.2	20.2	20.1	18.0	-6.05	-6.25	-6.05	-6.60	-0.10008	-0.10204	-0.10050	-0.10963	-0.10306
107.50	22.1	24.5	23.0	22.8	-6.15	-6.60	-6.35	-6.75	-0.10174	-0.10776	-0.10548	-0.11213	-0.10678
119.00	29.5	32.5	29.0	31.8	-6.20	-6.90	-6.55	-7.00	-0.10255	-0.11255	-0.10880	-0.11628	-0.11008
122.25	33.0	36.8	32.0	35.2	-6.25	-7.10	-6.70	-7.05	-0.10339	-0.11592	-0.11130	-0.11711	-0.11193
127.00	36.8	39.5	32.50	39.5	-6.25	-7.25	-6.70	-7.10	-0.10339	-0.11837	-0.11130	-0.11794	-0.11275
132.75	43.0	45.9	35.5	42.9	-6.25	-7.35	-6.70	-7.15	-0.10339	-0.12000	-0.11130	-0.11877	-0.11336
142.75	54.8	57.8	49.20	53.8	-6.30	-7.60	-6.70	-7.30	-0.10422	-0.12403	-0.11130	-0.12126	-0.11521
147.00	62.5	63.2	57.00	60.5	-6.30	-7.70	-6.70	-7.35	-0.10422	-0.12571	-0.11130	-0.12209	-0.11583
151.00	68.5	68.0	63.00	65.8	-6.35	-7.80	-6.70	-7.40	-0.10505	-0.12735	-0.11130	-0.12292	-0.11665
157.25	+80.0	+80.0	+80.0	+80.0	-6.55	-8.00	-6.80	-7.70	-0.10835	-0.13051	-0.11295	-0.12791	-0.11996
174.00	-	-	-	-	-6.75	-8.15	-6.90	-7.85	-0.11166	-0.13305	-0.11462	-0.13040	-0.12244
199.00	-	-	-	-	-7.10	-8.15	-7.20	-8.25	-0.11745	-0.13306	-0.11960	-0.13704	-0.12579
216.00	-	-	-	-	-7.55	-8.20	-7.45	-8.55	-0.12490	-0.13388	-0.12375	-0.14203	-0.13114
241.00	-	-	-	-	-8.10	-8.20	-7.70	-8.90	-0.13400	-0.13388	-0.12791	-0.14784	-0.13591
257.00	-	-	-	-	-8.30	-8.30	-8.00	-9.10	-0.13730	-0.13551	-0.13289	-0.15116	-0.13922
291.00	-	-	-	-	-8.35	-8.30	-8.00	-9.10	-0.13813	-0.13551	-0.13289	-0.15116	-0.13942

Note: 3 Soil cracked at sensor # 4.

^ Soil cracked at sensor # 3.

** End of Test T06 **

UNIVERSITY OF SASKATCHEWAN, DEP. OF CIVIL ENGINEERING.

MOISTURE CONTENT TEST RESULTS

Test no. : T05

Date started : 02/14/87

Page no. : 1 of 1

Soil type : Indian Head Till

Conducted by : J. Lau

Total sample thickness : 51.0 mm approx.

TIME	SAMPLE DEPTH	JAR #	TARE	GROSS WET WT.	GROSS DRY WT.	NET DRY WT.	MOISTURE CONTENT	REMARKS	
hr.	mm		gram	gram	gram	gram	%		
02/14/87	0.00	BULK	V12	102.20	171.05	152.27	50.07	37.51	Initial wx
10:00 a.m.		BULK	V20	103.13	170.39	152.02	48.89	37.57	
02/17/87	55.00	0.0-12.0	L1	102.70	130.58	124.30	21.60	29.54	
6:00 a.m.		12.0-24.0	K1	102.20	129.48	123.22	21.02	29.73	
		24.0-35.0	C12	137.76	172.35	164.34	26.58	30.14	
		35.0-48.0	T11	102.36	137.72	129.34	26.98	31.06	
		48.0-51.0	BEB	102.47	128.85	122.57	20.10	31.24	
02/17/87	81.50	0.0-12.0	D	102.06	123.85	119.17	17.11	27.35	Soil cracked
7:30 p.m.		12.0-24.0	J1	103.37	129.13	123.51	20.14	27.50	
		24.0-35.0	C11	102.29	128.14	122.33	20.04	28.99	
		35.0-48.0	T12	101.95	117.03	113.62	11.67	29.22	
		48.0-51.0	I3	102.32	119.92	115.98	13.66	28.84	
02/19/87	115.00	0.0-12.0	6	137.45	166.41	160.54	23.09	25.42	
9:00 a.m.		12.0-24.0	L17	102.92	129.99	124.44	21.52	25.79	
		24.0-35.0	8	102.60	127.00	121.93	19.33	26.23	
		35.0-48.0	J22	102.96	128.97	123.50	20.54	26.53	
		48.0-51.0	J30	102.42	133.81	127.20	24.78	26.57	
02/21/87	171.00	0.0-12.0	L1	103.01	135.06	129.38	26.37	21.54	
1:00 p.m.		12.0-24.0	L13	103.13	126.75	122.50	19.37	21.94	
		24.0-35.0	L3	99.44	126.54	121.67	22.23	22.35	
		35.0-48.0	X10	99.18	123.58	119.19	20.01	21.94	
		48.0-51.0	J101	103.19	137.39	131.25	28.07	21.84	
02/25/87	291.00	0.0-12.0	J1	103.38	140.65	135.16	34.78	7.16	
1:00 p.m.		12.0-24.0	L11	102.70	139.36	135.04	33.34	9.95	
		24.0-35.0	K1	102.19	144.65	140.30	38.11	11.41	
		35.0-48.0	T11	102.36	140.65	136.51	34.25	11.80	
		48.0-51.0	T12	101.95	140.68	135.40	34.45	12.42	End of test